NASA CONTRACTOR REPORT

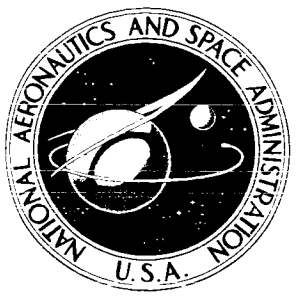

NASA CR-43

NASA CR-43

DEVELOPMENT OF THE DUAL MEMBRANE FUEL CELL AND THE OSMOTIC STILL

Prepared under Contract No. NAS 3-2551 *by*
THOMPSON RAMO WOOLDRIDGE, INC.
Cleveland, Ohio
for

NATIONAL AERONAUTICS AND SPACE ADMINISTRATION • WASHINGTON, D. C. • MAY 1964

DEVELOPMENT OF THE DUAL MEMBRANE FUEL CELL AND THE OSMOTIC STILL

Prepared under Contract No. NAS 3-2551 by
THOMPSON RAMO WOOLDRIDGE, INC.
Cleveland, Ohio

NATIONAL AERONAUTICS AND SPACE ADMINISTRATION

For sale by the Office of Technical Services, Department of Commerce, Washington, D.C. 20230 -- Price $3.50

FOREWORD

This is the Final Report on Contract NAS-3-2551 covering the period from 30 June 1962 through 15 December 1963. The work performed under this contract was administered under direction of the NASA Lewis Research Center's Solar and Chemical Power Branch. Mr. Harvey J. Schwartz, Head, Electrochemical Technology Section was the Program Manager for NASA. The report covers the work performed by the prime contractor, Thompson Ramo Wooldridge Inc., Electromechanical Division, New Product Research Department and Ionics, Inc. as a major subcontractor to TRW. Mr. William J. Leovic was the TRW Program Manager and Mr. Thomas H. Hacha was the Project Engineer and major author of Part II of the report. The work performed by Ionics Inc. was under the technical direction of Dr. Werner Glass, Assistant Director of Research. Mr. Frank B. Leitz was the lead engineer at Ionics and was co-author of Part I of the report. Dr. Richard A. Wynveen of TRW served as a technical consultant to program management and contributed in part to the preparation of this report.

ABSTRACT

21252

Fuel cell components satisfactory for service in 6 N H_2SO_4 at temperatures up to 95°C were determined. Critical components selected included the Ionic 61-AZG cation membrane and niobium current collectors. Ultimately a 10-cell battery was constructed according to results obtained on five 5-cell batteries. The 10-cell battery performance was characterized by 7.8 volts at 24 amp/ft^2 (a 15% increase over the design goal), a specific conductance of 360 mhos/ft^2/cell and a peak power density of 64 watts/ft^2/cell. Increasing the operating temperature increased the performance. Electrolyte normality, N_e, gas flow-rates and small changes in pressure levels (5 to 15 psig) had no noticeable effect on performance. The liquid transport rate across the H_2 - side membrane, however, was $\propto N_e^2$ while the transport across the O_2 - side membrane was $\propto N_m^{-2}$, where N_m is "membrane" normality. A conservative 2 KW fuel cell battery was designed.

In addition, a number of commercially available membranes were evaluated for use in an osmotic water separating still. The American Machine and Foundry C-60 membrane was determined to be most suitable for this application. A "2 KW Osmotic Still" was designed and fabricated. This "Osmotic Still" utilized multiple C-60 membranes and completed a 100 hour test. The design water extraction rate of 2 lbs/hr of pH 5 or above from 6 N H_2SO_4 at 195°F was obtained during this test.

Author

TABLE OF CONTENTS

TABLE OF CONTENTS (Cont'd)

TABLE OF CONTENTS (Cont'd)

TABLE OF CONTENTS (Cont'd)

TABLE OF CONTENTS (Cont'd)

TABLE OF CONTENTS (Cont'd)

PART I

LIST OF FIGURES

LIST OF FIGURES (Cont'd)

PART II

LIST OF FIGURES

PART I

LIST OF TABLES

APPENDIX TO PART I

LIST OF TABLES

PART II

LIST OF TABLES

I.0 INTRODUCTION

This report summarizes the results of a two part experimental development program on the dual membrane fuel cell system using an osmotic still to separate product water from an acid electrolyte. The program has been a joint effort by Thompson Ramo Wooldridge Inc. and Ionics, Inc. as a subcontractor. TRW has been responsible for overall program management and the development of the osmotic water separating still. Ionics has conducted the work relating to the designing and testing of the low pressure, non-regenerative, dual membrane hydrogen-oxygen fuel cell.

Continuous operation of H_2 - O_2 fuel cells require that the heat and water generated in the cells be removed. Figure I-1 shows a schematic of the space power system utilizing the dual membrane fuel cell and osmotic still. Continuous operation is accomplished by circulating the electrolyte through the fuel cells to absorb the heat and moisture, into an osmotic still to remove water and through a heat exchanger to remove heat. It was the purpose of the present program to develop the osmotic still and to improve the performance characteristics of the dual membrane fuel cell.

This report is organized into two separate parts. Each part is complete with its own introduction, summary, description of the work completed, and recommendations.

Part I covers the development of the dual membrane fuel cell which terminated in the delivery to NASA-Lewis of a 10-cell battery and a detailed engineering design of a 2 KW battery.

Part II describes the developmental program leading to the successful 100 hour operation of an osmotic still capable of handling all the water formed by a 2 KW, H_2 - O_2 fuel cell. The 2 KW osmotic still was also delivered to NASA-Lewis

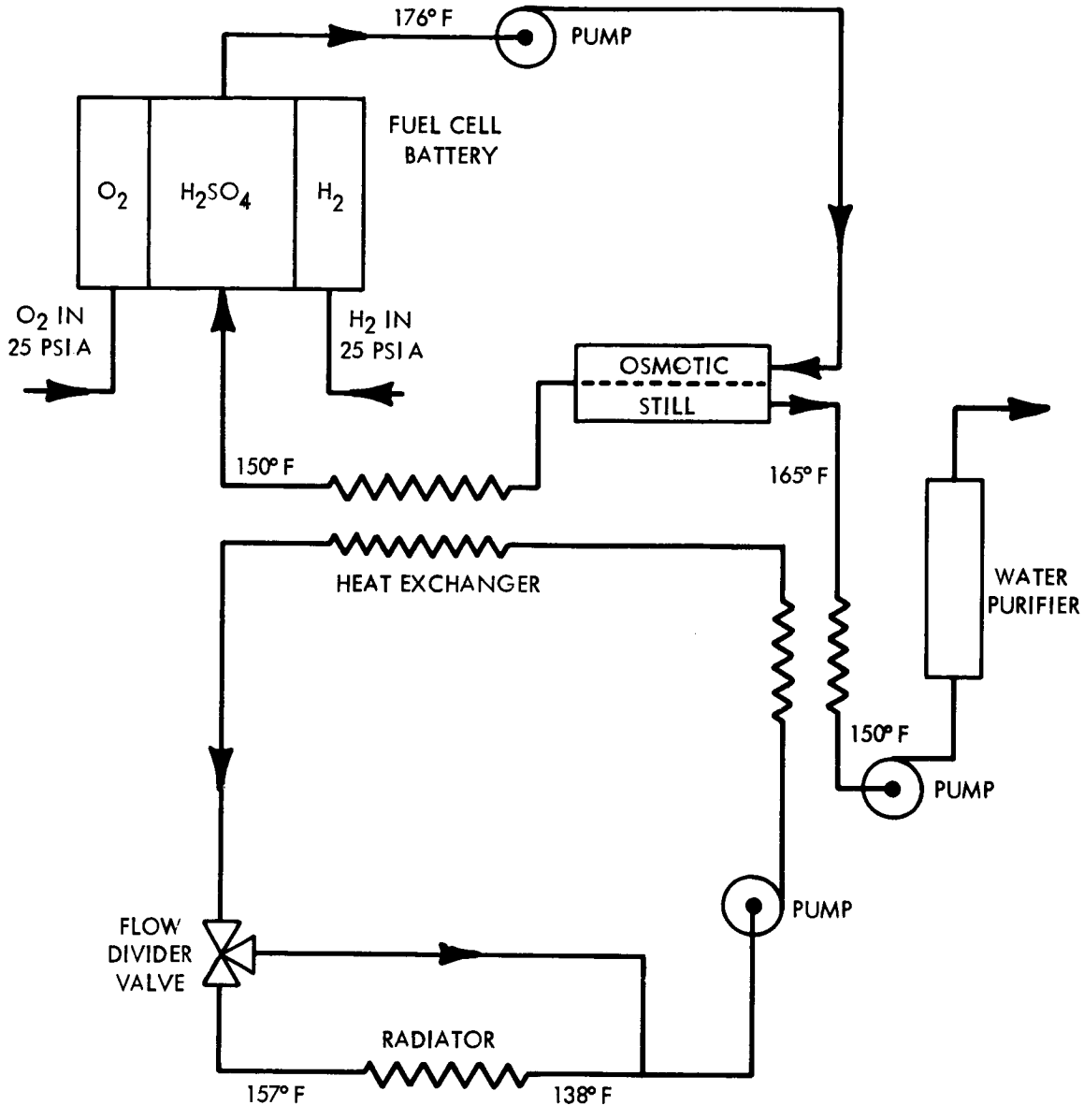

Figure I-1 Electrolyte Circulation System

II. SUMMARY

The developmental work on the dual membrane fuel cell led to the selection of the optimum materials for fuel cell components. The effect of changes in cell configuration and electrode manufacture were investigated in single cells and then favorable combinations were further tested in a series of five 5-cell batteries. All of the 5 cell batteries passed the qualification test by running for 100 hours at greater than 3.4 volts while at a current density of 24 amps/ ft^2.

A 10-cell battery was then constructed using components of the type found to give the best performance in the 5-cell assemblies. The resulting battery averaged 7.78 volts at 24 amps/sq. ft. during its qualification run. This was considerably above the program design goal of 6.8 volts at 24 amps/sq. ft.

The program was completed with the detailed engineering design of a 2 KW battery. In order to minimize scale-up problems the design has retained the overall component size and materials of the successful 10-cell battery. This means, however, that the design has not been optimized.

Under Part II of the program, a series of commercially available ion-exchange membranes were evaluated for use in a osmotic water separting still. The AMF C-60 cation membrane was determined to be the most suitable membrane for use in a 2 KW "Osmotic Still"

PART I

DUAL MEMBRANE FUEL CELL DEVELOPMENT

1.0 Introduction

This part of the report covers all efforts directed toward performance improvement of the dual membrane fuel cell. These investigations had three major objectives:

1. Continue the development of the Ionics Dual-Membrane H_2/O_2 Fuel Cell
2. Deliver a 10-cell Battery with 1/4 ft^2 of active area per cell; this battery to be capable of maintaining at least 6.8 volts at a current of 6 amps or 24 amps/ft^2.
3. Furnish a detailed engineering design of a 2-KW (net) Ionics Dual-Membrane H_2/O_2 Fuel Cell Battery.

Previous work at Ionics had led to development of the Dual-Membrane fuel cell where the "separator" between the H_2 and O_2 compartments consists of two ion-exchange membranes sandwiched around a layer of liquid electrolyte. The electrolyte, an aqueous solution of H_2SO_4, is circulated through the cell and serves not only as electrolyte but also as coolant and as membrane moisture controller.

Waste heat is removed from the cell by the circulating electrolyte. The continuous contact between the ion-exchange membranes and the liquid electrolyte keeps the membranes adequately moist at all times, no matter what current load is being drawn from the cell. As the membranes are thus kept moist by the electrolyte they will not dry out and crack, a fairly common phenomenon with single-membrane H_2/O_2 fuel cells.

Section 3.0 of this part of the report describes the experimental apparatus and procedures used during the development phases of the work which are covered in Section 4.0. The single cell tests covered in Section 5, provided the information necessary to design, construct, and test the five 5-cell batteries. The basis for the design and construction of the 10-cell battery is brought out in Section 7.0 which covers the five 5-cell battery tests. The actual construction and testing of the 10-cell battery is described in Section 8.0. The process

design basis for the 2-KW Battery is developed mainly in Section 6.0, Parametric Evaluation. The detailed design is given in Section 9.0, 2-KW Battery.

2.0 Summary

Development work was continued on the Ionics Dual-Membrane H_2/O_2 fuel cell. A 10 Cell Battery was constructed, tested and delivered on schedule. A detailed engineering design of a 2-KW Battery was prepared.

The development phase of the study included a materials testing program carried out both at Ionics and under subcontract by A. D. Little, Inc. The materials testing program, along with the other experimental work led to the selection of the following materials for fuel cell components:

1.	Membranes:	Ionics cation resin 61-AZG
2.	Electrodes:	Platinum and Teflon
3.	Pusher and Collector Plates:	Niobium
4.	Compartment Frames:	Teflon or Penton
5.	Elastomers:	Dacron-backed Viton A and Butyl Rubber
6.	Spacer Mesh:	Trilok 6027-1-1 (polypropylene and saran)

The effects of changes in cell configuration, electrode manufacture, membrane backing and the like were investigated in individual fuel cells. The favorable variations were further tested in multiple-cell batteries. Extended runs were achieved in both single-cell and battery test programs under either constant or variable load. Over 1000 hours were accumulated during the single cell tests.

The construction of the 10-Cell Battery was preceded by the construction and testing of five 5-Cell Batteries as prescribed in the statement of work of this contract. All five 5-Cell batteries passed the qualification test of running for 100 hours at more than 3.4 volts while at a current density of 24 amps/ft^2. The 10-Cell Battery averaged 7.78 volts at 24 amps/ft^2 during its qualification run.

The process design of the 2-KW Battery was based on the data obtained from a study of the effect of operating parameters on the performance of 5-cell batteries.

Performance at 60°C of a battery containing niobium metallics can be characterized by an average voltage of 0.78 volts/cell at 24 amps/ft^2, a specific

conductance of 360 mhos/ft^2/cell and a peak power density of 64 watts/ft^2/cell. Variations existed between cells presumed to be primarily due to oxygen electrode variations. With judicious selection of oxygen electrodes, the average cell voltage should be raised to at least 0.8 volts/cell at 24 amps/ft^2

Decreasing temperature lowers the voltage attainable at a given current density and decreases the specific conductance. Lowering the temperature from 60°C to 20°C decreases the specific conductance by as much as 50 mhos/ft^2 and lowers the extrapolated zero current voltage by 10 to 20 mv.

Electrolyte normality, gas flow rates and small changes in pressure level (5 to 15 psig) have no noticeable effect on battery electric performance. Gas pressure drops can be kept low, on the order of 25 mm H_2O, without adversely affecting gas distribution among the cells of a battery.

Electrolyte normality has a pronounced effect on the amount of liquid transported across the ion-exchange membranes. At 20°C, the quantities involved are given by the relations:

$$\text{Liquid transported across } H_2\text{-side membrane} = 0.0022\ N_e^2 \text{ gms/amp-hr-cell}$$
$$\text{Liquid transported across } O_2\text{-side membrane} = 2.9\ N_m^{-2} \text{ gms/amp-hr-cell}$$

where N_e is the electrolyte normality and N_m is the "membrane" normality, i.e., the geometric mean of the liquid normalities on either side of the oxygen-side membrane. Increasing the temperature from 20°C to 60°C approximately doubled these liquid rates.

The engineering details of most of the components for the 2-KW Battery design were taken from the successful components developed for the 10-Cell Battery to minimize any possible scale-up problems.

3.0 Experimental Apparatus & Procedures

3.1 Overall Experimental Program

The experimental aspects of this study can be divided into five categories as follows:

1. Materials Testing - screening materials to find those suitable for use in Dual-Membrane Fuel Cells, i.e., able to resist 6 N H_2SO_4 at temperatures up to 90°C.

2. Single Cell Testing - screening various cell configurations and components to find those permitting long term favorable electrical performance.

3. Parametric Evaluation - determining the effect of operating parameters on Fuel Cell performance to permit a rational design of a 2 KW battery.

4. Five-Cell Battery Testing - assembling 5-cell batteries of various components and investigating their performance in 100-hour runs.

5. Ten-Cell Battery Testing - assembling a 10-cell battery, following its performance during a 100-hour run and delivering it to the prime contractor, New Products Research, Thompson Ramo Wooldridge Inc.

The experimental apparatus and procedures involved will be dealt with below.

3.2 Materials Testing

Experimentation consisted of immersing suitable duplicate weighed samples in 6 N H_2SO_4 and determining weight change after a given time at the temperature of interest. Part of the work was carried out at Ionics, the rest under subcontract at A.D. Little, Inc. Further details are given in Section 4.0 of this part of the report.

3.3 Single Cell Testing

Testing involved assembling a cell, hooking it up to the required flow streams and monitoring the voltage produced as it ran at a given current density. Periodic determinations of the voltage-current characteristics of the cell were made.

Two sizes of dual-membrane fuel cells were used in the course of this program: "small" cells, with an active area of 4 in^2, and "large" cells with 36 in^2. The 4 in^2 cells were used to screen components where tests in the large cells would be unduly expensive, where components of large size were not readily available or when the flow control systems on the test rig for the large cells were not acting reliably.

3.3.1 Description of Small Cells

An exploded schematic of a small cell is shown in Figure 3.1. It consists essentially of a "stack" of components assembled between lucite end blocks. The stack is held together by means of end frames consisting of metal pipe flanges and four corner tie bolts.

Gas is fed to the cell by suitable fittings screwed into the end blocks. Between the end blocks there are three compartments (hydrogen, electrolyte, oxygen) each consisting of a 0.5 inch thick lucite slab with a 2" x 2" hole cut out of the middle. The electrolyte compartment is separated from the gas compartments by ion exchange membranes. Two holes are drilled in the top of the electrolyte compartment to permit ready filling with electrolyte. A suitable electrode is placed in each gas compartment and held tightly against the ion exchange membrane by a perforated lucite pusher plate. These plates are grooved on the electrode side to give gas ready access to the electrode. A force is applied to the back of the pusher plate by means of a pushing screw turned into the lucite end block. The membranes are supported on the side away from the electrode by a piece of expanded metal set into a rim cut into the lucite electrolyte compartment.

The electrodes usually consisted of 2" x 4" strips of platinum gauze, the bottom half of which (2" x 2") was coated with platinum black catalyst. The uncoated

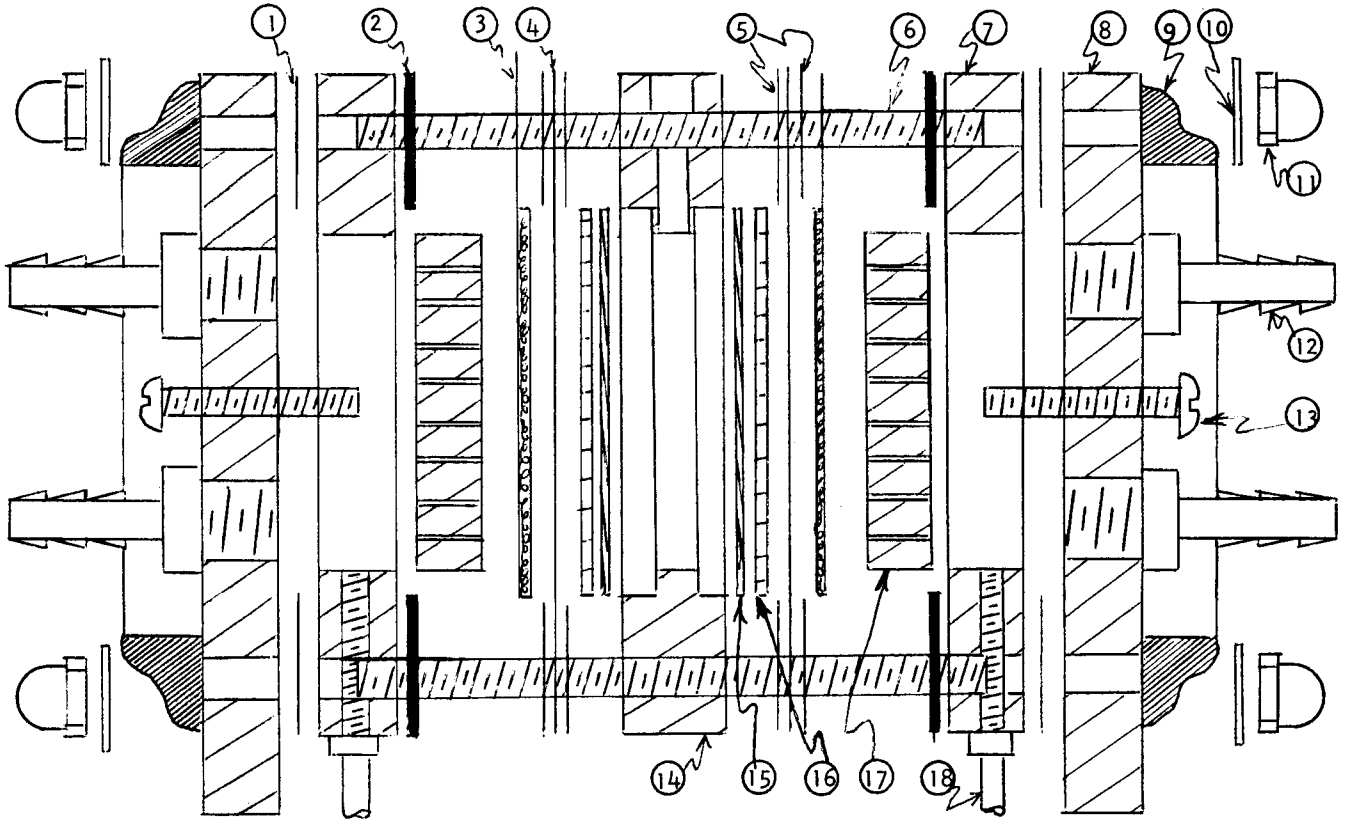

1. Light Gasket
2. Heavy Gasket
3. Electrode
4. Membrane
5. Membrane Gaskets
6. Tie Bolt
7. Spacer Block
8. End Block
9. Retainer Plate
10. Washer
11. Nut
12. Gas Connection
13. Compression Bolt
14. Center Block
15. Supporting Grid
16. Plastic Mesh
17. Compression Block
18. Drainage Taps

Figure 3.1 4 Sq. In. Dual-Membrane Fuel Cell

end protruded out of the top of the cell and served as an electrical lead for the load resistor and for the current and voltage measurements. Thin rubber gaskets were used to eliminate gas or electrolyte leaks from the cell.

3.3.2 Operation of Small Cells

Operation was at ambient pressure and temperature. Feed gases were passed through bubblers before entering the cell. These bubblers served to help humidify the gases and also acted as rough flow meters.

Most cells were run steadily either at 16 amps/ft^2 or at 16 ma/cm^2 (14.8 amps/ft^2) except when polarization curves were obtained. This consisted of measuring the potential difference between the electrodes at cell current densities of 0, 4, 8, 16, 24, 32, 40, etc. amps/ft^2 (or ma/cm^2) until a steady potential could no longer be obtained. The specific conductance of the cell (mhos/ft^2) was calculated from the slope of the polarization curve.

For many cells the measured potential difference between the electrodes was further broken down by the use of a standard calomel electrode inserted into the electrolyte compartment. The voltage between the calomel electrode and the hydrogen electrode was reported as the "H_2 Half Cell Voltage" and the voltage between the calomel and oxygen electrodes as the "O_2 Half Cell Voltage".

3.3.3 Description of Large Cells

An exploded schematic of a large (36 in^2) cell is shown in Figure 3.2. It differs from the small 4 in^2 cell (other than in area) primarily by the fact that electrolyte is continuously pumped through the electrolyte compartment. Other differences become apparent in the description below.

The end plates of 3/8" stainless steel combine some of the functions of end block and end frame. These end plates hold the 1/4" swagelock tubing fittings carrying gases and electrolyte in and out of the cell. In addition, they distribute the compressive forces generated by the twelve edge-located tie bolts over the entire gasket area. Manifold headers were used to lead the gases and electrolyte in and out of the appropriate compartments. The gas and electrolyte

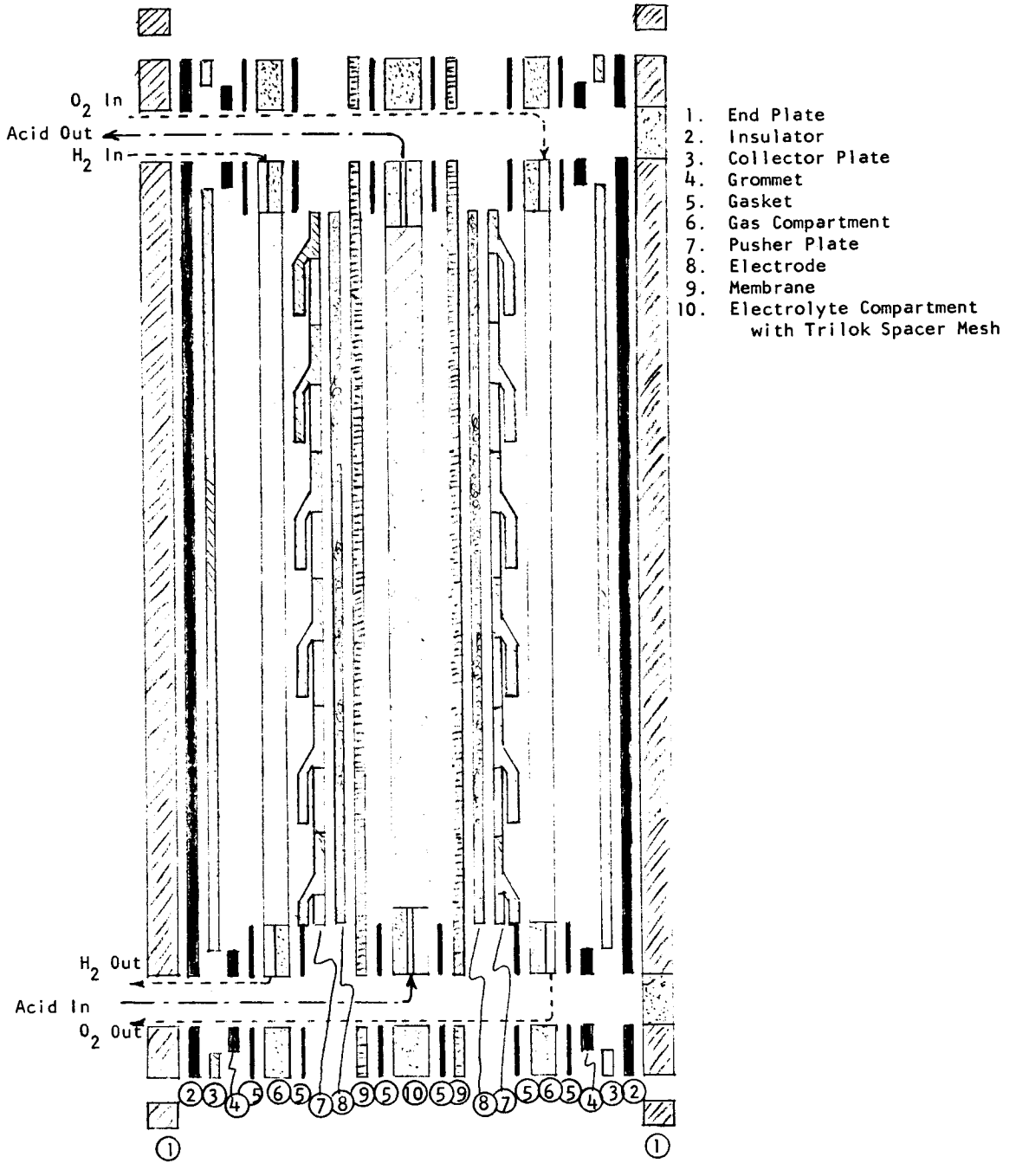

Figure 3.2 Schematic of 36 Sq. In. Dual-Membrane Cell

compartments were made of various plastic materials ranging from 40 to 125 mils thickness. The electrodes consisted of platinum black catalyst on platinum screen. Metallic "pusher plates" pressed the electrodes against the ion-exchange membranes which formed the walls of the electrolyte compartment. These pusher plates were stamped out of flat stock. Numerous tabs were slotted out of the material and formed into springy "fingers" protruding on one side of the stock. The remaining flat side was placed against the electrode and the "fingers" came in contact with a flat metallic "collector plate". Current could thus flow from the electrode through the pusher plate to the collector plate. The collector plates had a small tab protruding from the side of the cell to serve as electrical lead for the load current and for voltage and current measurements. The collector plates were insulated from the steel end plates by rubber insulators. A springly woven plastic filler material was placed in the electrolyte compartment between the membranes to serve as a membrane support. The gas compartments were slightly larger in internal dimensions than the electrolyte compartment. This was to prevent the sharp edge of the pusher plate from shearing through the membrane. Thin rubber gaskets were used to prevent leakage from the cell.

Pressure gages were provided in the gas and electrolyte lines leading to the cell. A pressure sensitive relay monitored the electrolyte feed pressure. If this pressure moved outside a set range (presumably indicative of a ruptured membrane or external electrolyte line failure), the relay activated solenoids which cut off the gas feed to the cell.

For operation at other than ambient temperature, the cell was immersed in a suitably temperature controlled water bath up to the collector plate tabs which provided the electrical load leads.

3.3.4 Operation of Large Cells

After assembly of a cell, suitable connections to the gas and electrolyte inlet and outlet lines were made. Electrolyte was then pumped through the electrolyte compartment entering from the bottom and leaving out of the top. The electrolyte gradually swept out trapped gas bubbles from the electrolyte compartment. After about 20 minutes, gases were admitted to the cell. Pressure level in

the cell gas compartments was adjusted by controlling the gas supply pressure and restricting the outlet flow by means of a constriction in the outlet line.

The single large cells were normally run at 16 amps/ft^2 except when a polarization curve was obtained. For some of the large cells "half cell potentials" were measured as described in Section 3.3.3 for the small cells. However the calomel electrode was immersed in the electrolyte stream leaving the cell rather than in the electrolyte compartment itself.

3.4 Parametric Evaluation

Most of the data used to determine the effect of operating variables on fuel cell performance were obtained in a multiple-cell battery. This was done for three major reasons:

1. The larger flow rates associated with multiple-cell batteries could be more accurately determined. This was especially true for such dependent variables as the liquid accumulation rate in the gas streams leaving the battery.

2. Multiple-cell batteries performed better than the single cells. It is felt that this resulted from better electrode-membrane contact due to the greater elasticity or "give" of a stack of five or more cells each with two "springy" pusher plates and with a woven plastic mesh spacer.

3. End effects could be eliminated by obtaining electrical performance data only from the central cells of the battery.

The multiple-cell battery used was assembled out of components paralleling those used during the single-cell tests. The collector plates, here, performed the additional function of separating the hydrogen compartment of one cell from the oxygen compartment of the next cell.

Gas and electrolyte flow rates to the battery were measured by calibrated rotameters. The electrolyte feed was brought to temperature by passing it through a long coil immersed in the same water bath as the battery. The temperature

of the electrolyte entering and leaving the battery was measured for some runs. The normality of the circulating electrolyte was followed. The incoming gas streams were humidified in bubblers (containing 3 $\underline{N}$ H_2SO_4) which were also kept in the same bath as the battery itself. The gas streams leaving the battery were passed through collector bottles also maintained at the bath temperature. The amount of liquid collected over finite stretches of time was noted and the samples obtained were titrated to determine the H_2SO_4 normality. Runs were made at various current densities (0 to 80 amps/ft^2). The effect of gas and electrolyte flow rates at various electrolyte concentrations (approximately 3 $\underline{N}$ to 9 $\underline{N}$) and 20°C and 60°C was deduced from runs made on other multiple cell batteries. All carefully controlled data were obtained at close to 5 psig.

3.5 Multiple Cell Batteries

All the 5 and 10-cell batteries were assembled out of components identical to those used for the large (36 in^2) single cells. The gas and electrolyte flow streams were metered. Except for the initial 5-cell battery runs, the gas feed streams were humidified. Operation was at 30°C or 60°C (bath temperature) and close to 5 psig. In addition to the pressure level, the hydrogen, oxygen and electrolyte pressure differentials across the battery were measured. A steady current of 6 amps (corresponding to 24 amps/ft^2) was drawn over the extent of most of the runs. Some polarization curves were obtained. Gas leak tests were made by immersing the entire battery below the bath water level and noting any bubbles that escaped.

4.0 Materials Testing

4.1 Introduction

The objective of this investigation was to determine what materials could be used satisfactorily in the Ionics' Dual Membrane Fuel Cell, i.e., have the ability to withstand attack by sulfuric acid in concentrations around 6 N at temperatures up to 95°C.

4.2 Experimental Procedure and Results

Five types of materials are needed:

1. An ionic conductor, presumably metallic, for collector and pusher plates. This must also withstand galvanic corrosion in intimate contact with platinum;
2. A cationic ion-exchange membrane;
3. An elastomer for gaskets, grommets and insulators;
4. A fairly rigid machineable plastic for compartments; and
5. A mesh material, presumably plastic, for maintaining pressure on membranes.

Part of the materials testing was carried out at Ionics and part was performed under subcontract at Arthur D. Little Inc. (ADL). Materials at Ionics were tested at 30°C, 60°C and 95°C. These materials are described in Table 4.1. Duplicate samples were weighed before immersion in individual specimen bottles containing 6 N sulfuric acid. After a period of time at temperature, usually 550 hours, the samples were weighed and visual observations noted. The weight changes are averages of two measured values.

The results of the tests are tabulated in Tables 4.2 (30°C), 4.3 (60°C) and 4.4 (95°C).

TABLE 4.1

Materials Tested at Ionics and ADL

Material	Composition	Appearance
Metallic Materials		
Titanium-HS7-40	commercial titanium	gray rectangular sheet; 10 ml thickness
Platinized* titanium	-	dark gray rectangular sheet; 10 ml thickness
Monel Alloy 400	-	gray rectangular sheet; 10 ml thickness
Gold plated** titanium (200 micro inches)	-	gold rectangular sheet; 10 ml thickness
Gold plated titanium (300 micro inches)	-	gold rectangular sheet; 10 ml thickness
Gold plated titanium (400 micro inches)	-	gold rectangular sheet; 10 ml thickness
Gold plated titanium (500-600 micro inches)	-	gold rectangular sheet; 10 ml thickness
Non-metallic Materials		
ION EXCHANGE MEMBRANE		
Ionics 61-AZG	sulfonated polystyrene	tan rectangle
GASKETING		
Buna-N on Nylon	butadiene and acrylonitrite copolymer	black rectangle 6 mil thick
COMPARTMENT		
Epoxy fiberglass	-	green rectangle; 60 ml thick
Teflon	fluorocarbon polymer	white rectangle
Halon TVS 300	fluorohalocarbon polymer	white rectangle
Kel-F	copolymer of chlorotrifluoro-ethylene and vinylidene fluoride	white rectangle

TABLE 4.1 (Cont'd)

Materials Tested at Ionics and ADL

Material	Composition	Appearance
	Non-metallic Materials (Cont'd)	
SPACER MESH		
Trilok 6001-1-1	64% saran and 36% polyethylene	black woven square
Trilok 6027-1-1	73% polypropylene and 27% polyethylene	black woven square

* by thermal decomposition of chloroplatinic acid

** by American Electroplating Co., Cambridge, Mass.

The work at ADL was all performed at 95°C. Twelve different metals or alloys were tested. The composition of the alloys is given in Table 4.5. Since the metals were to be in contact with metallic platinum, the effect of galvanic currents which may be set up by the two metals had to be examined. Consequently most of the samples were tested with and without a piece of platinum wire wrapped around the specimen. Data on the corrosion of metals and alloys are tabulated in Table 4.6. The symbol "+ Pt" after the material indicates tests done with platinum wire in contact with the specimen.

The non-metallic materials investigated are tabulated in Table 4.7. These include four membranes, five elastomers, fifteen plastics for compartments and one spacer mesh. The results of the immersion tests on these materials are given in Table 4.8.

TABLE 4.2

Behavior of Materials in 6 N H_2SO_4 at 30°C

Material	Test Duration Hours	Percentage Weight Less	Observations
Titanium	550	-40.0	surface badly attacked
Platinized titanium	550	- 0.4	no change
Ionics 61-AZG Membrane	550	- 3.0	no change
Buna-N on nylon	550	-12.1	specimen slightly warped
Epoxy fiberglass	550	0.0	slight whitening
Teflon	550	- 0.8	no change
Trilok 6001-1-1	550	- 0.2	no change

TABLE 4.3

Behavior of Materials in 6 N H_2SO_4 at 60°C

Material	Test Duration Hours	Percentage Weight Less or Gain	Observations
Titanium	550	-100	specimen disintegrated
Platinized titanium	550	- 11.0	platinum coating loosened
Gold plated titanium (200 micro inches)	140	-100	titanium completely dissolved
Gold plated titanium (400 micro inches)	650	- 2.1	no change
Monel alloy 400	530	- 1.5	surface became copper colored
Ionics 61-AZG Membrane	550	- 12.7	turned reddish brown
Buna-N on nylon	550	- 5.5	solution yellowish; specimen warped
Epoxy fiberglass	550	+ 8.4	no change
Teflon	550	- 0.8	no change
Halon TVS 300	580	0.0	no change
Kel-F	580	0.0	no change
Trilok 6001-1-1	550	- 0.3	loss of springiness

TABLE 4.4

Behavior of Materials in 6 N H_2SO_4 at 95°C

Material	Test Duration Hours	Percentage Weight Less or Gain	Observations
Gold plated titanium (400 micro inches)	50	-100	titanium completely dissolved
Gold plated titanium (500-600 micro inches)	410	-100	titanium completely dissolved
Monel Alloy 40C	550	- 3.0	blackening of surface
Ionics 61-AZG Membrane	580	+ 2.0	surface became dark brown
Buna-N on nylon	530	+ 20.6	loss of elasticity specimen became easy to tear
Epoxy fiberglass	580	+ 15.0	whitening of surface material became brittle
Teflon	450	- 0.7	no change
Halon TVS 300	580	0.0	no change
Kel-F	580	+ 6.5	no change
Trilok 6027-I-1	580	+ 6.5	no change

TABLE 4.5

Nominal Composition of Alloys

Alloy	Composition								
	Ni	Fe	Al	Cu	Ma	Cr	C	Mo	Other
Ampco #8		1.5	7	91.5					
Ampco #755	10	1.25		88.4	0.4				
Ampco #702	30	0.5		68.9	0.6				
Monel	67	1.5		30	1				
Carpenter-20	29	46		3	1	20	1		
Hastelloy B-1	62	6						32	
Ti (MST-40)		0.25							commercial Ti
Ti (0.2% Pd)									0.2% Pd alloy

TABLE 4.6

Corrosion of Metals and Alloys in 6 N H_2SO_4 at 95°C

Material	Specific Gravity	Thickness of Sheet mils	Approximate Electrical Resistivity microhm-cm room temp.	Test Duration Hours	Corrosion Rate mils/year
Ta	16.6	32	15.5	350	0
Ta + Pt				350	0
Nb	8.4	40 mil wire	20	350	5.0
Nb + Pt				350	5.4
Zr	6.5	30	41	350	1.26
Zr + Pt				350	1.28
Ampco #8	7.78	123	10	137	9.6
Ampco #8 + Pt				137	18
Ampco #755	8.50	45		137	43
Ampco #755 + Pt				137	38
Ampco #702	8.40	48	37	137	47
Ampco #702 + Pt				137	51
Monel CG-S	8.90	60	48	98	67
Monel CG-S + Pt				98	58
Carpenter 20-3	8.00	57	130	306	21
Carpenter 20-3 + Pt				306	22
Hastelloy B-1	9.24	190	135	297	9
Hastelloy B-1 + Pt				297	12
Cu	8.94	5	2	22	55
Ti (MST-40)		12	3	24	>1000
Ti (.27% Pd)		3		24	>1000

TABLE 4.7

Description of Non-Metallic Materials

Material	Composition	Color & Shape
Ion-Exchange Membranes		
Ionics, 61-AZG	sulfonated polystyrene	tan rectangle
AMF, C-313	sulfonated polystyrene	clear, rect. sheet
AMF, C-60	sulfonated polystyrene	brown, rect. sheet
Gelman Acropor	PVC acrylonitrile	white, rect. sheet
Gasketing		
Red Silicone	silicone rubber	red, rect. sheet
Gray Silicone	silicone rubber	gray, rect. sheet
Buna-N	butadiene & acrylonitrile copolymer	black, rect. sheet
Butyl Rubber	butyl rubber	black, tri. sheet
Viton-A	fluorinated hydrocarbon	black, rect. sheet
Compartment Frame		
Teflon	fluorocarbon resin	white, rectangle
Kel-F	copolymer of chlorotrifluoro-ethylene and vinylidene fluoride	clear, rect. sheet
Penton	chlorinated polyether	green, square
Halon TVS	fluorohalocarbon resin	white, rectangle
Epoxy Fiberglass	epoxy fiberglass	green, rectangles: 100-125 mil thick
Polyster Fiberglass	isophthalic polyester	green, rectangles: 100-125 mil thick
ADM Aropol 7250	chemically resistant polyester	yellow, rectangles: 100-125 mil thick
DAP	Dapon-35 in diallyphthalate monomer	tan, rectangles: 100-125 mil thick
Hetron 92	polyester	yellow, rectangles: 100-125 mil thick
Buton	hydrocarbon resin	clear, rectangles: 100-125 mil thick
Laminac 4173	chemically resistant polyester	yellow, rectangles: 100-125 mil thick
Stypol 2012	flexible polyester resin	yellow, rectangles: 100-125 mil thick
Nypol 4050	acrylic modified chemically resistant polyester	yellow, rectangles: 100-125 mil thick
Atlac 382	chemically resistant polyester	yellow, rectangles: 100-125 mil thick
Laminac W/G/255	laminac with glass reinforcement	gray, rectangles: 100-125 mil thick
Spacer Mesh		
Trilok 6001-1-1	36% polyethylene & 64% saran mesh	black, square

TABLE 4.8

Behavior of Non-Metallic Materials in 6 N H_2SO_4 at 95°C

Materials	Test Duration Hours	Percent Weight Loss or Gain	Observations
Ion Exchange Membranes			
Ionics, 61-AZG	308	-15.2	no change
AMF, C-313	353	2.35	slight darkening, shriveled
AMF, C-60	353	17.4	extreme darkening
Gelman Acropor	48	--	fell apart
Gasketing			
Red Silicone	281	-19.0	cracked, disintegrated
Gray Silicone	611	-11.65	flaky
Buna-N	114	18.9	disintegrated
Butyl Rubber	285	0.07	slight disintegration
Viton-A	285	1.73	no change
Compartment Frame			
Teflon	611	0.0	no change
Kel-F	611	0.53	curled
Penton	447	- 0.37	no change
Halon TVS	308	0.03	no change
Epoxy Fiberglass	611	37.2	extreme darkening, brittle
Polyester Fiberglass	611	22.3	yellow, brittle, swollen
ADM Aropol 7250	471	0.17	no change
DAP	471	- 1.34	charred
Hetron 92	471	0.28	very slight darkening
Buton	471	- 0.94	considerable darkening
Laminac 4173	471	0.32	slight darkening
Stypol 2012	471	-35.5	darkened, cracked, brittle
Nypol 4050	471	- 0.88	no change
Atlac 382	471	- 0.74	no change
Laminac W/G/255	471	0.0	considerable darkening
Spacer Mesh			
Trilok 6001-1-1	611	- 2.70	no change

4.3 Conclusions

At least one, and sometimes more than one, material was found for each of the fuel cell requirements. The materials which are satisfactory from the point of resistance to 6N sulfuric acid at temperatures up to 95°C are:

1. Metallic - Tantalum, zirconium, niobium (in that order)
2. Membrane - Ionics 61-AZG
3. Elastomer - Viton-A and bytyl rubber
4. Compartment Plastic - Teflon, Kel-F, Penton, Halon TVS-500, ADM Aropol-7250, Hetron 92, Hypol 4050 and Atlac 382.
5. Spacer Mesh - Trilok 6027-1-1.

No difficulties are therefore expected in meeting the materials requirements of the Dual Membrane Fuel Cell design.

5.0 Single Cell Tests

More than 50 single H_2/O_2 cells were assembled and tested during this phase of the work. As detailed in Section 3.0 of this report, testing consisted primarily of running a cell at a steady current density and periodically determining the cell current-voltage relation ("polarization curve"). The variation primarily investigated were:

1. Effect of electrode variations
2. Effect of membrane variations

Some cells were used to check a specific point; the origin of liquid in the gas compartments.

5.1 Electrode Manufacturing Technique

5.1.1 Introduction

The most critical components in the fuel cell are the electrodes. Considerable effort was expended on screening different types of electrodes and on varying parameters in the method of manufacturing the electrodes.

The problem of making a good electrode is a complex one. There must be an active catalyst, presumably but not necessarily platinum, spread out evenly over the electrode surface. This catalyst must adhere strongly to the electrode to prevent its being washed off by the flow of fluids through the gas chamber. If this is accomplished by an adhesive, the adhesive must not cover the active sites to the extent that the reaction rate is impeded. The catalyst must be in contact with the electrolyte which may or may not mean intimate contact with the ion-exchange membrane. The electrode and catalyst layer must be sufficiently porous to allow easy approach of the reactant gases to the reaction sites. Finally the electrode must be a good electronic conductor to make the internal resistance of the cell as small as possible.

These desirable properties are not always compatible. Good adhesion usually precludes porosity. Three-phase contact is difficult to obtain in a relatively static system. Porosity implies stagnant layers and stagnant layers lead to

slow diffusion-controlled processes. Active catalysts frequently do not have long lives. The result is that the electrode is a bundle of compromises.

Most of the electrode screening tests were carried out in small 4 sq. inch cells rather than in large 36 square inch cells. This was done partly for reasons of economy and partly because the control systems for the large-cell test racks functioned erratically at the start of this work.

The electrode screening tests fall into three categories:

1. Comparison of "paste" and "sintered" electrodes
2. Evaluation of the manufacture of sintered electrodes
3. Evaluation of electrodes made by radically different techniques

5.1.2 Comparison of Paste and Sintered Electrodes

At the beginning of the program, the conventional electrode was the Ionics "paste" electrode. This was manufactured as follows:

> For a 4 inch^2 electrode mix one gram of platinum black* with enough distilled or deionized water to make a thick paste. Other size electrodes, pro rata. Spread the material evenly on 90% platinum - 10% rhodium screen, 80 mesh, 3 mil wire.* Dry the electrode for five (5) minutes in a 110^{o}C oven. Spray both sides of the electrode with teflon dispersion.** Place the electrode in a hydraulic press and subject it to 500 psi for one minute. When assembling the cell, place the side of the electrode on which the platinum was spread against the membrane.

---

* J. Bishop & Company, Malvern, Pennsylvania; supplier

** Oil - Es-Oil, supplied by American Durafilm Company, Newton Lower Falls, Massachusetts

During the first month of the contract, the paste electrode was compared to the Ionics "sintered" teflon electrode. The recipe for this is:

> For a 4 inch^2 electrode mix two grams of platinum black* with 0.14 grams teflon dispersion*** and 0.2 grams reagent grade magnesium oxide.**** Add distilled or deionized water to make spreadable paste. Spread mixture on platinum gauze as before. Dry electrode and place between sheets of aluminum foil dusted with magnesium oxide. Place in press at 4000 psi and 600°F for 5 minutes. Leach magnesium oxide from electrode in boiling 6 N sulfuric acid for 15 minutes. Rinse in water and dry. Again, place the coated side of the gauze against the membrane.
>
> The first comparison between paste and sintered electrodes, reported in the first Monthly Report, showed a sintered electrode considerably better than a paste electrode (0.79 vs 0.68 volts at 16 amps/ft^2). This comparison was made in 4 inch^2 cells run at ambient (25°C) temperature.
>
> Several large (36 in^2) cells were assembled to permit comparison of these two types of electrodes at two different temperatures. These cells were selected because, other than electrodes, they were similar in construction and the runs lasted long enough (5 to 40 days) to be significant.

Platinized titanium metallics and 61-AZG membranes were used and the gas and electrolyte pressure were 15 and 20 psig respectively. The results obtained at 30°C are shown in Figure 5.1. The cell with the paste electrode gave slightly more erratic results but no significant difference between the two types can be seen.

Figure 5.2 shows the results obtained at 60°C. Both cells declined markedly in performance with time. It is not known whether this was due to actual

---

*** Teflon Dispersion #852-201, American Durafilm Company

**** Baker & Adamson Lot V331 used during this contract

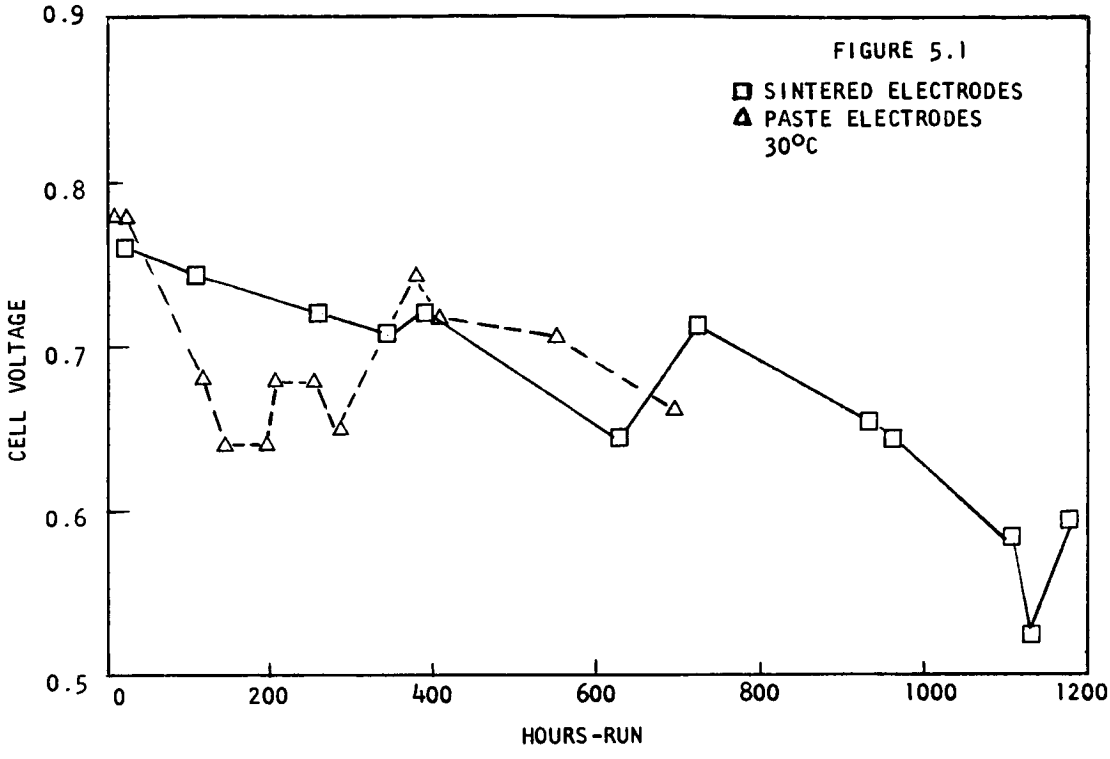

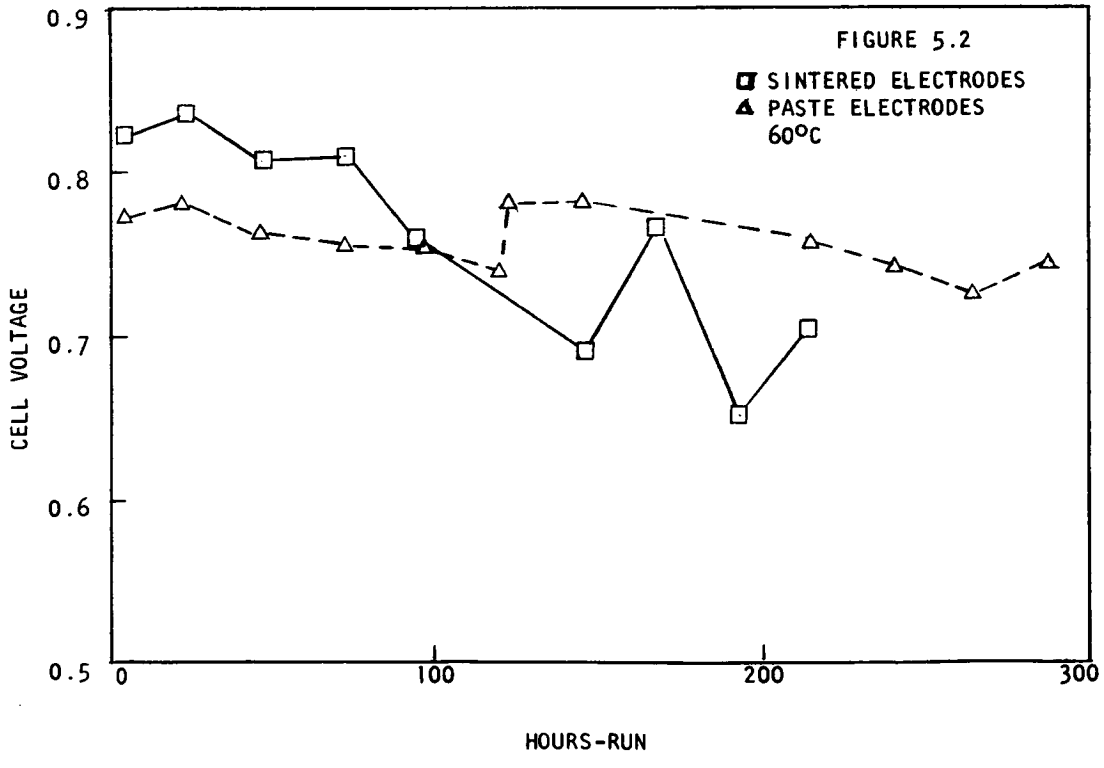

Figures 5.1 & 5.2 Comparison of Sintered and Paste Electrodes

deterioration of the cells or just gradual cell flooding. No adequate provisions had been made at that time to assure liquid removal from the gas side of the cells. The sintered electrode cell was about 60-100 mv. better at 16 amps/ft^2 than the paste electrode cell.

Based solely on electrical performance, the sintered electrode had at best a slim edge. Physically, however, the sintered electrodes were much more resistant to handling. The platinum black was bound far more tightly to the supporting screen. They should thus have higher resistance to shock and vibration. The sintered electrodes were therefore the preferred ones - primarily because of their greater inherent toughness.

5.1.3 Manufacturing Variations for Sintered Electrodes

The variation studied involved:

1. Use of Kel-F in lieu of teflon
2. Varying amounts of teflon
3. Use of no MgO or light-weight MgO in lieu of standard MgO

5.1.3.1 Kel-F Vs. Teflon

The use of Kel-F instead of teflon as a wet-proofing agent was investigated in both small and large cells. This change would cause a considerable simplification in manufacturing since Kel-F sinters at a lower temperature (475°F) and pressure (700 psig) than teflon (600°F and 4000 psig). Tests run in the 4 square inch cells included one in which the MgO was left out of the electrode formulation. (See Table 5.1)

Both cells with Kel-F electrodes were poorer than the Teflon cell. The unusual feature of these data was that the Kel-F electrodes with MgO performed notably poorer than those without. There has been no satisfactory explanation for this.

At the time when comparison runs were being made in the large single cells, operation of these cells was generally not very stable. Consequently a really clean-cut comparison between the two types of electrodes could not be made. However, the three runs tabulated below were among the more steady. The conclusions drawn from these runs agree, in general, with the results of the small

Table 5.1

Comparison of Kel-F and Teflon Sintered Electrodes

(4 Sq. In. Electrodes)

Cell No.	Electrode Contents, Gms			Cell Performance	
	Kel-F Dispersion	Teflon Dispersion	MgO	Volts @ 16 Amps/Ft^2	Specific Conductance Mhos/Ft^2
D9708	----	0.26	0.4	0.71	135
E1308	0.28	----	----	0.63	145
E1312	0.28	----	0.4	0.54	67

* The polarization curves from which these data were taken appear in Figure 5.3.

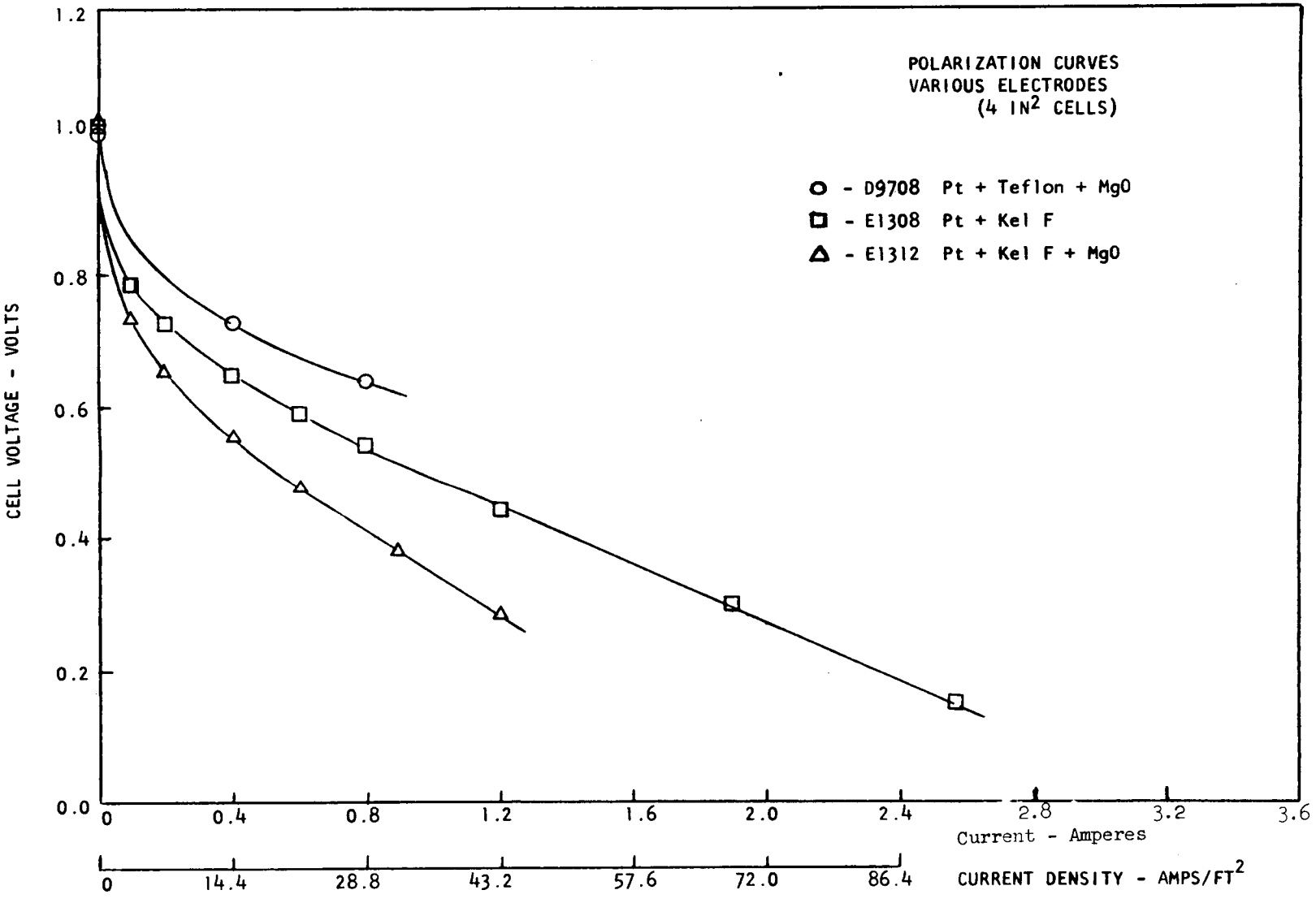

Figure 5.3 Polarization Curves - Various Electrodes

cell tests above. (See Table 5.2)

The 60°C Kel-F cell, E1279, performed poorly. Only for a brief period did it produce a voltage over 0.7 volts at 16 amps/ft^2, and the specific conductance averaged about 75 mhos/ft^2. For the first 48 hours the 30°C Kel-F cell, E1292, performed better than the 30°C teflon cell, D9723. However, the balance of its performance was poorer. Consequently the teflon cell which maintained a voltage over 0.7 volts for much longer than 100 hours was the more desirable.

5.1.3.2 Varying Amount of Teflon

The standard sintered electrodes were made up with 0.26 grams teflon dispersion per 4 square inches electrode. Cells were run where the amount of teflon dispersion was varied from 0.13 grams to 2.00 grams per 4 square inches electrode. A reference electrode was placed in the electrolyte chamber of the cell to permit the determination of the specific conductance of each half of the cell as well as of the cell itself. (See Table 5.3)

Varying the amount of teflon from 0.13 to 1.06 grams dispersion per 4 square inches electrode has relatively little effect on cell performance. The cells containing 0.13 and 0.26 grams dispersion/electrode had somewhat higher specific conductances than those with more teflon. This trend was emphasized by Cell E1320 containing 2.00 grams dispersion/electrode which showed poor output voltage as well as low specific conductance. It is likely that the great quantity of teflon in the electrodes of this cell completely enveloped some of the catalyst platinum black.

The conclusion can be drawn that the quantity of teflon dispersion used is not critical as long as there is enough to give good adhesion of the catalyst to the electrode screen and not so much as to envelope the catalyst completely. A range of 0.1 to 1.0 grams/4 square inches appears acceptable with 0.26 grams/4 square inches the preferred value.

5.1.3.3 Varying MgO Content

The MgO was present in the formulation so that its removal by leaching after sintering would leave a more porous structure. To find out whether this

Table 5.2

Comparison of Kel-F and Teflon Electrodes in Large Cells

Cell No.	Type of Electrode	Bath Temp.	Pressure Gas	Pressure Electrolyte	Time of Run (Hours)	Voltage @ 16 Amps/Ft^2	Spec. Cond. Mhos/Ft^2
E1279	Sintered Kel-F	60°C	16 psig	16 psig	4	0.548	84
					24	0.602	105
					48	0.602	84
					66	0.712	70
					87	0.570	42
E1292	Sintered Kel-F	30°C	16 psig	16 psig	4	0.762	121
					24	0.780	160
					48	0.702	125
					72	0.598	52
					144	0.638	65
D9723	Sintered Teflon	30°C	15 psig	20 psig	10	0.762	--
					34	0.71	--
					41	0.712	100
					84	0.768	114
					108	0.756	110
					252	0.718	--
					396	0.723	99

* 2.3 gms of Kel-F for 42 in^2. Pressed at 720 psi and 475°F.

Table 5.3

Effect of Varying Amount of Teflon

Cell No.	Gms Teflon Dispersion	Cell Performance			
		Voltage	Specific Conductance, Mhos/Ft^2		
		@ 16 Amps/Ft^2	Total Cell	O_2 Side	H_2 Side
E1313	0.13	0.68	135	200	400
D9708	0.26	0.71	135	200	400
E1314	0.52	0.65	100	180	230
E1315	1.06	0.70	125	200	320
E1320	2.00	0.39	64	100	145

Polarization curves for these runs appear in Figures 5.4 & 5.5.

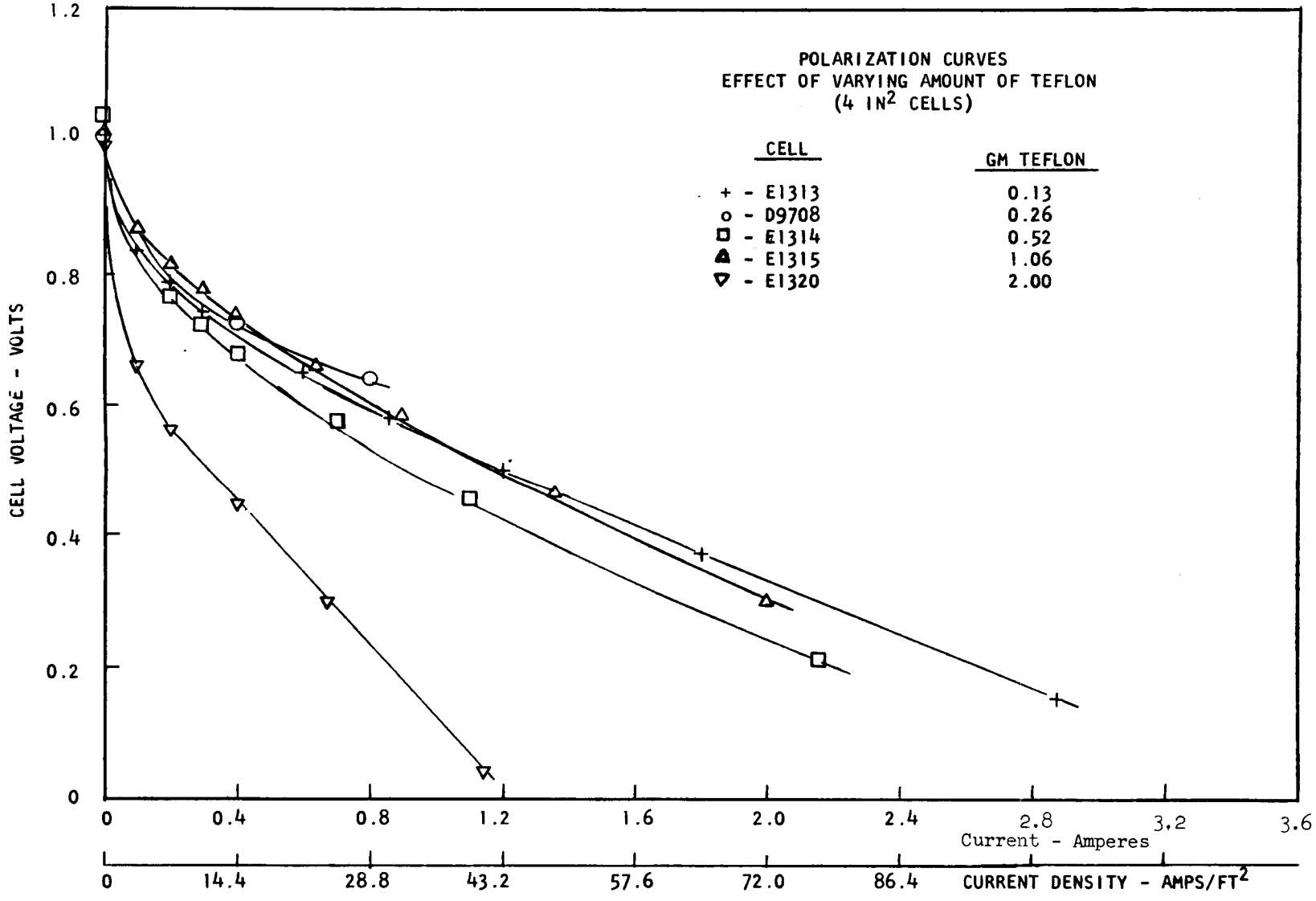

Figure 5.4 Polarization Curves - Varying Amounts of Teflon

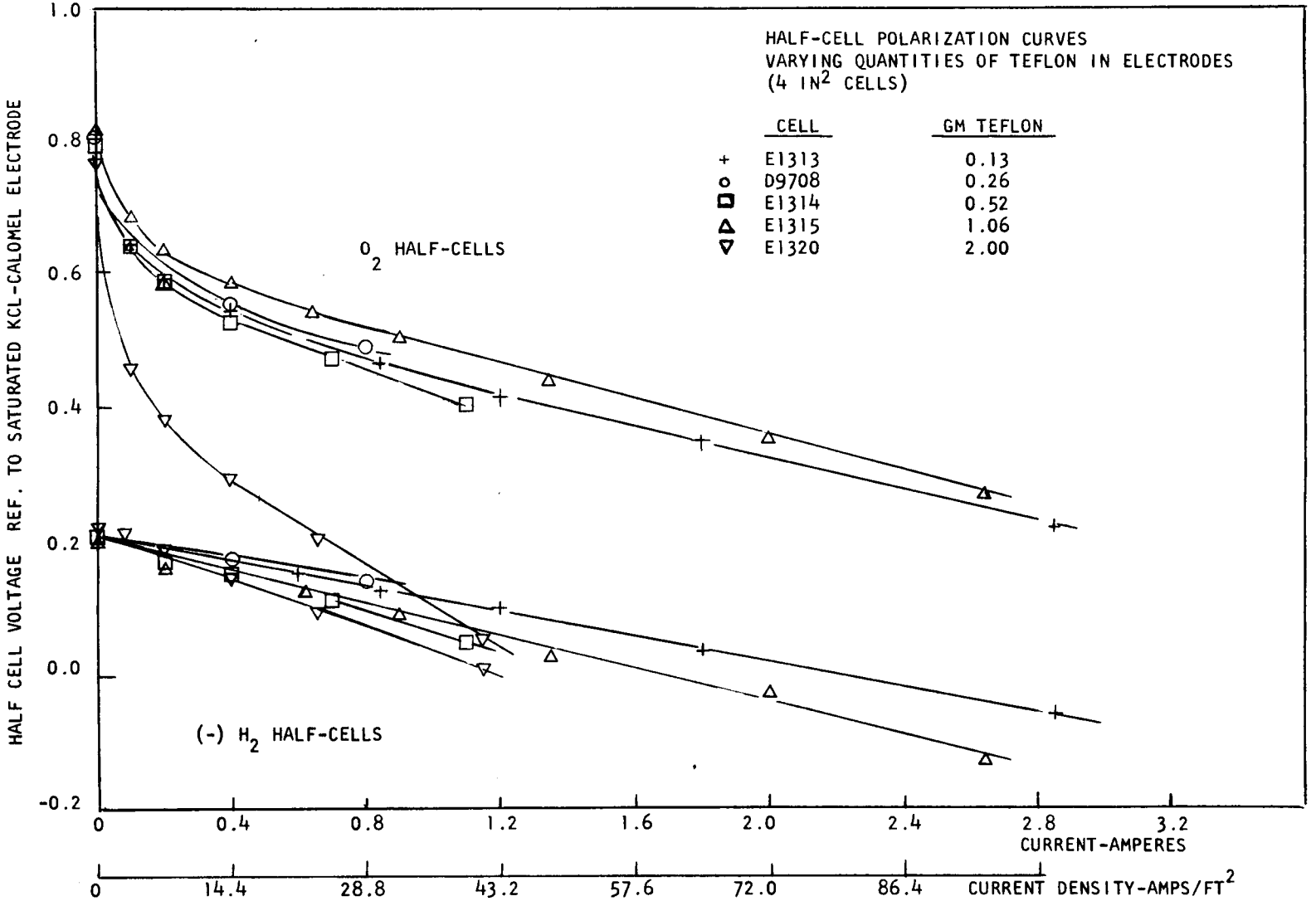

Figure 5.5 Half-Cell Polarization Curve - Varying Quantities of Teflon in Electrodes

artificially induced porosity actually helped electrode performance, some cells were made up using electrodes that had been made without MgO. In addition, a cell was made up using electrodes manufactured by the Clevite Corporation using a special "light-weight" fluffy MgO and a sintering pressure of 10,000 psi instead of the usual 4,000 psi. (See Table 5.4)

The cell whose electrodes had been made up using standard MgO showed somewhat better performance than the cell whose electrodes had been made without MgO. The poor performance of the cell using light-weight MgO was very possibly due to the higher sintering pressure used. The effect of using more MgO than 0.4 gm/4 sq. in. was not investigated during this study.

5.1.4 Radically Different Techniques

The sintered and past electrodes investigated represent only a small part of the spectrum of solutions to the electrode problem. Several studies and screening tests were made of different approaches.

Four approaches were considered by Arthur D. Little and four were tested at Ionics.

5.1.4.1 Imprinted Electrodes (ADL)

It appeared first that a technique of imprinting the membrane with Pt black would improve the catalyst-membrane contact as experiments of this type had been performed by Gregor[1], [2] with some success. Series 100 AMF membranes had been subjected to 60,000 psi and 115°C to imbed Pt black and had performed well in single membrane cells with no free electrolyte. However, further experiments reported by Perry[3] in which imprinted cation membranes were used in a dual membrane alkaline cell gave polarization curves no higher than those reported by Lurie et al[4] for similar cells with unimprinted Ionics membranes. Attempts to imprint both Ionics and AMF membranes at lower temperatures (to prevent membrane drying) had proved unsuccessful and were discontinued in the light of Perry's report.

Table 5.4

Effect of Varying MgO Content

Cell No.	MgO Content		Sintering Pressure psi	Cell Performance	
	Type	Gms/4 in^2		@ 16 amps/ft^2	Specific Conductance Mhos/ft^2
D9708	Std.	0.4	4,000	0.71	135
E1318	None	0.0	4,000	0.67	115
E1324	Lt.Wt.	0.4	10,000	0.40	100

Polarization curves for these runs appear in Figure 5.6

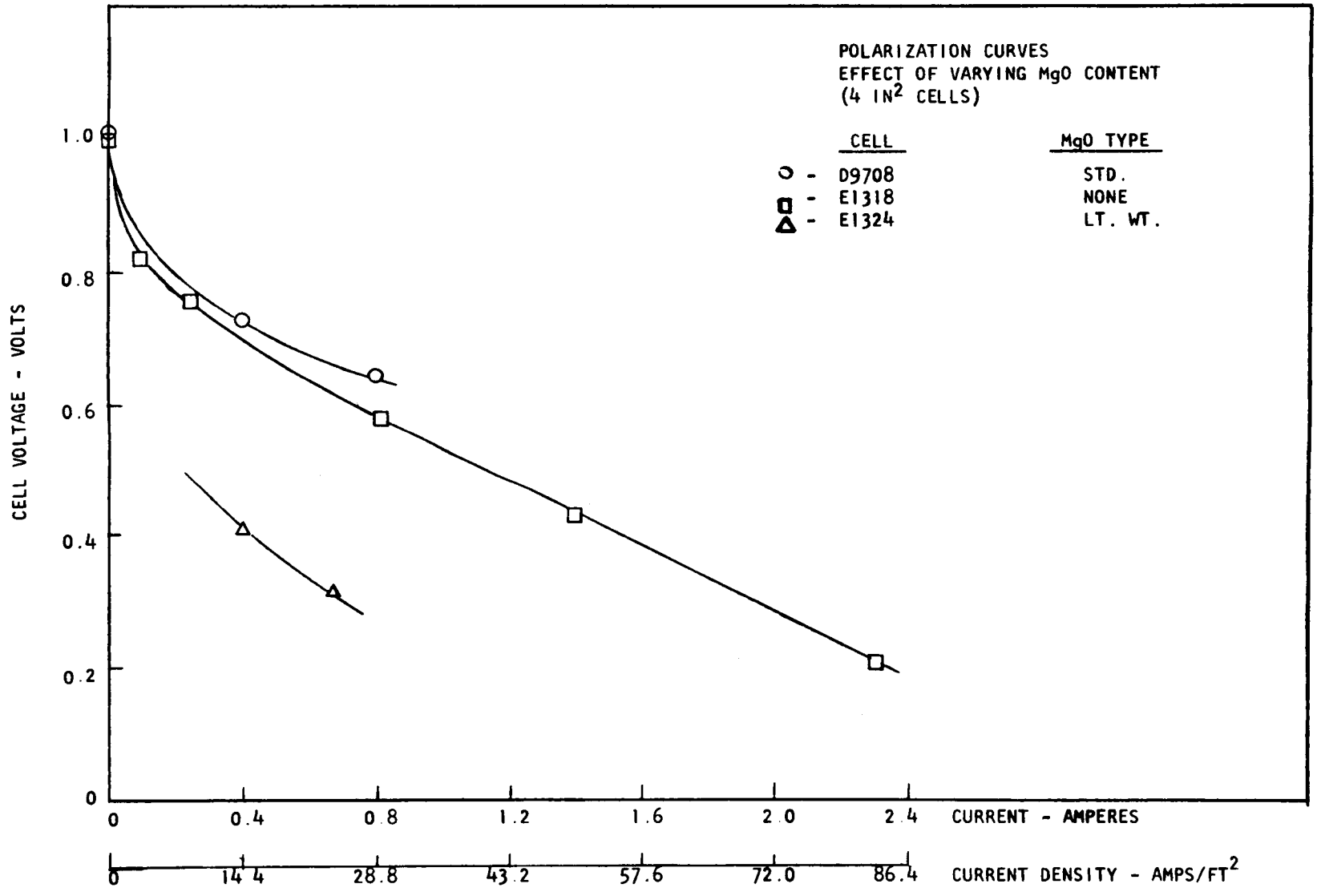

Figure 5.6 Polarization Curves - Effect of Varying MgO Content

5.1.4.2 Deposited Electrodes (ADL)

Chemical reduction of platinum compounds to metal in and on the membrane was attempted in an effort to put more active catalyst in intimate contact with the membrane. The soluble Pt (NH_3) Cl_2 complex was prepared by treating a chloroplatinic acid solution with excess ammonia and the membrane surface washed with this solution. The membrane was then flushed with a basic solution of sodium borohydride, reducing the complex to finely-divided platinum and various soluble salts. While a darkening of the membrane was observed which could be attributed to the presence of platinum, it was not possible to build up any appreciable concentration at the surface of the membrane, the only area in which it would be accessible to gaseous H_2 and so useful as a catalyst.

An attempt was also made to use this impregnated membrane as a cathode and deposit upon it electrochemically Pt black from standard platinizing solutions. This also proved unsatisfactory as no significant current density could be obtained, showing that even with reduced platinum present, the surface of the membrane was still not the electronic conductor required for this technique.

5.1.4.3 Pure Platinum Electrodes (ADL and Ionics)

The presence of teflon in the Pt paste seemed a possible source of trouble as it placed an electrically insulating material in the electrode-catalyst region. Taschek and Wynn[5] report that it may introduce as much as 70 mv additional polarization when used as wet-proofing material in place of the more common but less durable paraffin. A fuel cell was prepared in which a thin layer of pure Pt black was sandwiched between membranes and electrodes, the electrodes having been well coated with Pt black electrochemically. Sintered teflon-free platinum electrodes were also prepared by Mott Metallurgical Corp., Hartford, Connecticut. Conditions of manufacture were proprietary. The electrodes were tested in Cell E1332 at Ionics. (See Table 5.5)

The performance of the Mott cell was very poor, presumably due to sintering of any constituent platinum black. The performance of the ADL cell without any wet-proofing agent whatever was only 50 mv better at 16 amps/ft^2 than that of a cell with standard sintered teflon electrodes. The presence of the teflon thus does not account for very much of the 520 mv. difference between the

Table 5.5

Performance of Pure Platinum Electrodes

Cell Number	Electrode Description	Cell Performance	
		@ 16 amps/ft^2	Specific Conductance Mhos/ft^2
PADL-2	Pure Pt. Black (ADL)	0.75	95
E1332	Pure Sintered Pt. (MOTT)	0.44	95
ADL-1	Std. Sintered Teflon (IONICS)	0.71	135

Polarization curves for these runs appear in Figure 5.7

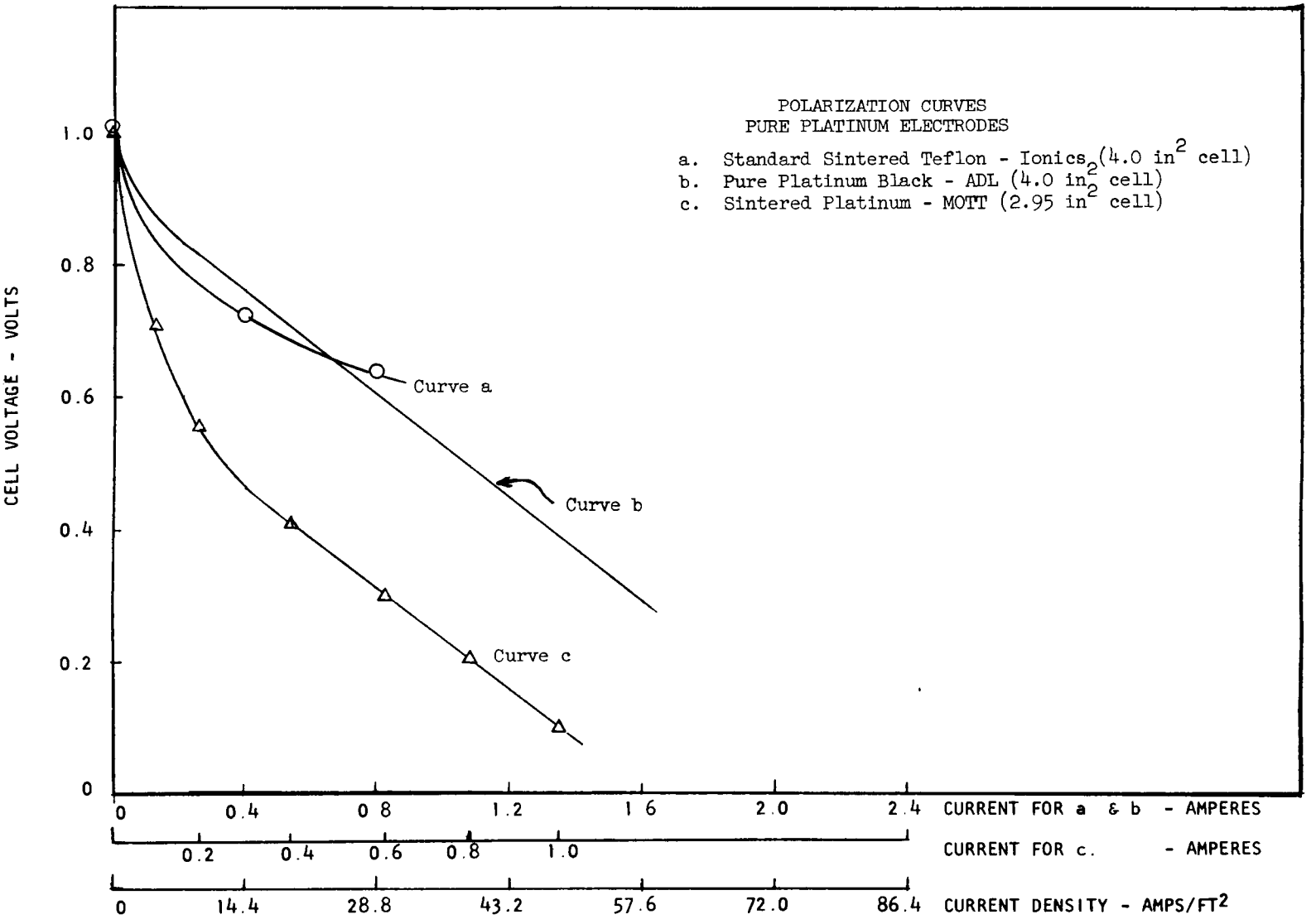

Figure 5.7 Polarization Curves - Pure Platinum Electrodes

thermodynamically possible 1.23 volts and the 0.71 volts obtained. A better catalyst is needed.

5.1.4.4 Platinized Carbon Electrodes(ADL)

As one step toward investigation of the catalysis problem, a pair of platinized carbon electrodes were prepared according to the method of Taschek and Wynn[5]. Two 2" x 2" x 3/32" pieces of PC 57 manufactured by the Stackpole Carbon Company were chosen. This material has a porosity of 1.07 cc/g and surface area of about 300 M^2/g. Pores range from 3 to 7 microns in diameter. These blocks were wet-proofed by soaking in a solution of 2 grams paraffin in 100 ml petroleum ether, dried, and heated to 200°C for two hours. While still hot, they were painted with a 10% solution of H_2PtCl_4, using enough solution for a coverage of 2 mg Pt/cm^2. They were then dried in an oven at 100°C for several hours and transferred to a vacuum oven at 150°C for five more hours to decompose the platinum compound.

The prepared carbon was put into the cell with the treated surface against the membrane and electrical contact was made by platinum gauze pressed against the back of the carbon. Resistance of the assembled cell was 0.4 ohm, measured with a Kiethley Model 502 Multiohmeter. The cell produced a voltage of only 0.30 volts at 16 amps/ft^2 compared to the 0.71 volts of the standard sintered electrode. These platinized carbon electrodes were evidently not the answer to the catalysis problem.

5.1.4.5 Bibliography for ADL Electrode Study

1. H. P. Gregor, "Fuel Cell Materials", Fifth Quarterly Progress Report, Contract No. DA-36-039 SC-85384.

2. H. P. Gregor, "Fuel Cell Materials", Final Report, Contract No. DA-36-039 SC-85384.

3. J. Perry, Jr., Proceedings 16th Annual Power Sources Conf. (1962).

4. R. M. Lurie, C. Berger and R. J. Schuman, "Fuel Cells", Vol. 11, Reinhold, p. 143 (1963).

5. W. G. Taschek and J. E. Wynn, Proceedings 16th Annual Power Sources Conf. (1962).

5.1.4.6 Pt Black Sprayed on Gauze

Cell E0223 - The electrodes were made by spraying a mixture of 5 grams platinum black and 10 ml of 1% polyethylene solution in benzene on platinum gauze. Since the mixture is not a stable suspension, the proportion of platinum to polyethylene is not necessarily the same as in the original mixture. An average of 0.29 grams of material was deposited on each 2 inch by 4 inch gauze. The performance of these electrodes and of those detailed in the following three paragraphs are given in Table 5.6 and Figure 5.8.

5.1.4.7 Pt Black Sprayed on Membranes

Cell E1305 - The same mixture was sprayed on one side on CR-61-AZG membranes. When the cell was assembled a platinum gauze was pressed into the platinum plus polyethylene mixture on the membranes. Since the membranes were kept wet no weight was recorded.

5.1.4.8 Platinized Carbon Sprayed on Gauze

Cell E1310 - The electrodes were made by spraying a mixture of 5 grams of 30% platinized carbon* and 30 ml of 1% polyethylene in benzene on platinum gauze.

5.1.4.9 Electro-Platinized Gauze

Cell E1302 - The electrodes were electro-platinized gauze. The plating solution was 4% aqueous platinic chloride with 0.04% lead acetate.

The electrodes were plated for 20 minutes at a current density of 0.5 amps/sq. in.

---

* J. Bishop & Company

Table 5.6

Performance of Radically Different Electrodes

Cell No.	Electrode Description	Cell Performance	
		@ 16 amps/ft^2	Specific Conductance Mhos/ft^2
E0223	Pt. Black Sprayed on Gauze	0.68	95
E1305	Pt. Black Sprayed on Membrane	0.63	105
E1310	Platinized Carbon Sprayed on Gauze	0.39	55
E1302	Electro-Platinized Gauze	0.35	-
D9708	Std. Sintered Teflon	0.71	135

Polarization curves for these runs appear in Figure 5.8

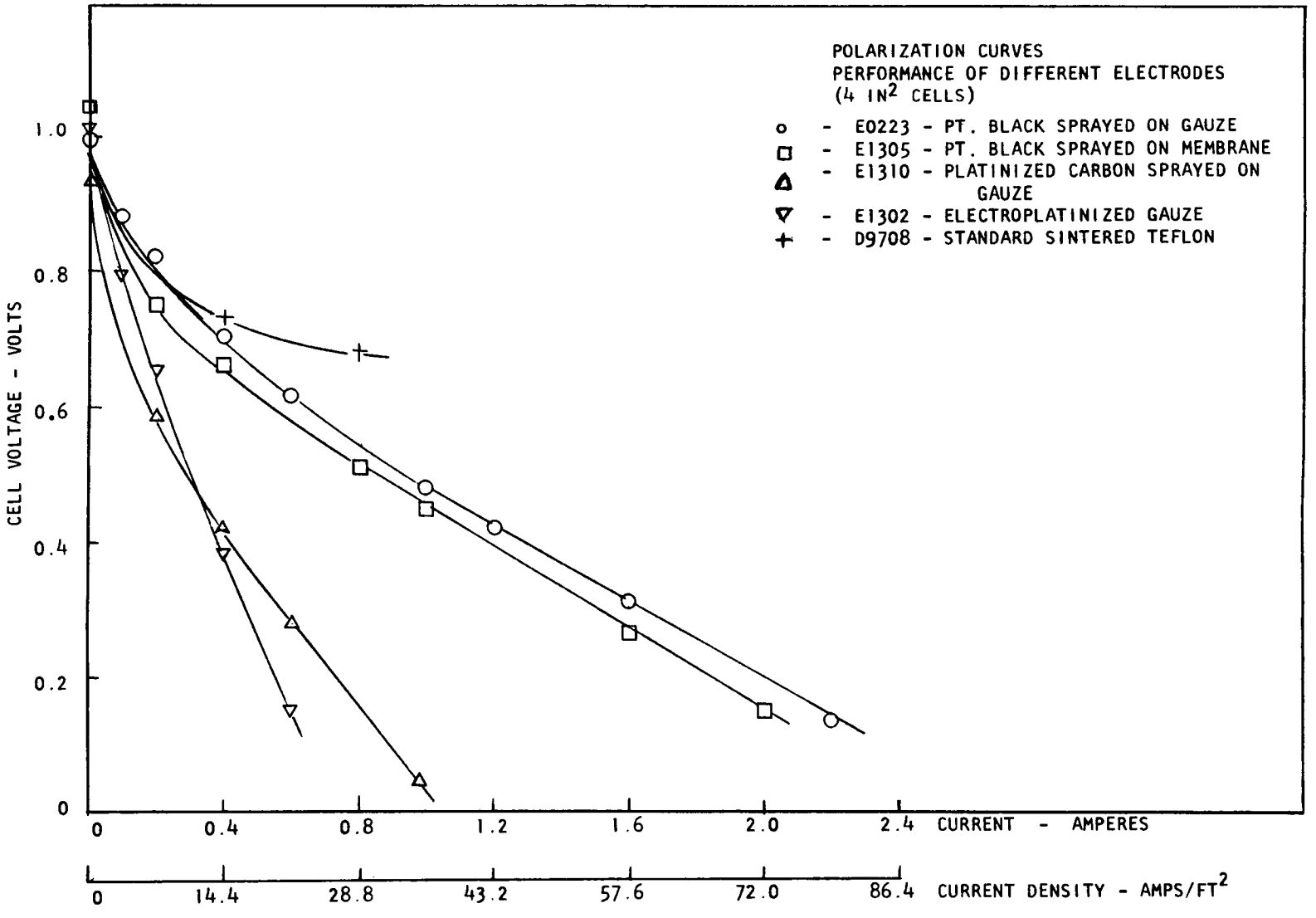

Figure 5.8 Polarization Curves - Performance of Different Electrodes

None of the radically different electrodes was an improvement on the standard sintered teflon electrodes. The electrodes in cell E0223 are within the range of interest and might be worth following up.

5.2 Membrane Study

Membranes used in ion-exchange fuel cells should have a low ionic resistance, thus permitting the construction of cells with high specific conductances. The membranes should also be unaffected by their surroundings for long periods of time and be dimensionally stable. Five types of Ionics cation membranes were tested:

61-AZG - standard resin	802 glass backing
61-DYG - resin variation	806 glass backing
61-AZL-4 - standard resin	402 dynel backing
61-AZL-8 - standard resin	802 dynel backing
61-AZL-15 - standard resin	1502 dynel backing

The AMF-C-60 and AMF-C-313 membranes were also investigated.

Ionics 61-AZG and 61-DYG membranes were compared in the large cells. These cells used sintered Kel-F electrodes.

The specific conductance figures which are averages of values measured over the runs strongly favor the standard resin membranes. The measured voltages support this judgment. Cell D9749 averaged about 0.5 volts with a maximum of 0.56 volts and Cell D9750 averaged 0.6 volts with a high reading of 0.65 volts. By contrast the cell with standard 61-AZG membranes, E1292, averaged 0.67 with a maximum voltage of 0.78 volts. (See Table 5.7)

All other single cell membrane evaluation was performed using 4 sq. in. cells. At the time when these tests were made, these cells were more stable and reproducible than the larger cells. They also used considerably smaller pieces of membrane. These tests were performed at Ionics and, as part of a subcontract, at Arthur D. Little Inc. (ADL). (See Table 5.8)

Table 5.7

Membrane Study - 36 Square Inch Cells - 30°C

Cell No.	Membrane	Cell Specific Conductance Mhos/ft^2	Average Cell Voltage @ 16 amps/ft^2
D9749	61-DYG	40	0.5
D9750	61-DYG	68	0.6
E1292	61-AZG	104	0.67

Table 5.8

Membrane Study - 4 Square Inch Cells - 25°C

Cell No.	Membrane Type	Cell Specific Conductance Mhos/Ft^2
E0224	61-AZG	116
ADL-11	61-AZG	135
E1325	61-DYG	80
E1327	61-AZL-4	138
E1330	61-AZL-8	95
E1326	61-AZL-15	80
ADL-13	AMF-C-60	95
E1331	AMF-C-313	109
ADL-12	AMF-C-313	104

All cells were run at a current of 400 ma (14.8 amps/ft^2) except when polarization curves were taken. Cell conductances were calculated from the slopes of the polarization curves. Cell containing 61-AZL-4 and 61-AZG membranes showed the highest specific conductances: 138 and 116 to 135 mhos/ft^2. Cells with AMF, 61-AZL-8 and 61-AZL-15 membranes showed 80-109 mhos/ft^2.

The 61-AZG and 61-AZL-4 appear the most desirable membranes. The AMF membranes had previously shown considerably poorer stability than 61-AZG or 61-AZL on continued exposure to 6 N sulfuric acid at elevated temperatures.

The final evaluation of membranes, the choice between 61-AZG and 61-AZL-4, was made in the five cell battery tests. Results are given in Section 7.0. The conclusion from those tests was that the 61-AZG membrane was preferred.

5.3 Other Single Cells

Two cells, E1279 and E1652, were constructed to check on possible mechanical leakages. These are discussed in Section 6.3.2.1. Additional cells were occasionally assembled for other special purposes. These are all listed in Appendix Table A1.

6.0 Parametric Evaluation

6.1 Introduction

The effect of various operating variables on battery performance must be known before a rational 2-KW battery design can be made. An extended study of a special 5 cell battery was carried out in order to obtain that part of the needed information which would not be obtained during the 5-cell battery study described in Section 7.0. A multi-cell battery was used rather than a single cell for three major reasons as detailed in Section 3.4. Briefly these reasons were:

1. Multiple-cell batteries perform better.
2. Liquid accumulation rates could be determined more accurately.
3. End-effects could be eliminated by determining electrical performance data from central cells only.

The battery used had Ionics 61-AZG membranes, penton compartments and tantalum pusher and collector plates.

6.2 Variables Considered

6.2.1 Independent Variables

The independent operating variables and their ranges considered during the parametric evaluation were:

1. Temperature: 20-60°C
2. Electrolyte Normality: 3 $\frac{N}{2}$ to 9 $\frac{N}{2}$
3. Current density: 0 to 80 amps/ft^2

Other independent variables, such as gas and liquid flow rates, were not considered for the following reasons:

1. Gas flow rate: Runs 1A, 1B and 1C of the 5-cell batteries (Section 7.3.1) show that varying the gas rate over a four-fold range had no effect on the electrical performance of

the battery as long as the manifold pressure drop was high enough (more than 20 mm H_2O) to assure adequate gas distribution. Tests run on the single cell D9228 also showed that wide variations in gas rate had no effect on the cell performance.

2. Liquid flow rate: The major effect of varying liquid rate is to vary the percentage of the dissipated heat carried out of the cell by the electrolyte. (The rest of the heat is lost to the surroundings). This effect is best studied as an effect of operating temperature. Liquid rate will affect the mass transfer rate between the membrane and the electrolyte. The amount of material transferred, however, is so small relative to the bulk flow of acid that no "concentration polarization" can be expected.

3. Pressure Level: Doubling the pressure level from 20 psia to 40 psia would double hydrogen and oxygen activities and thus lead to a very slight increase in the theoretical open-circuit voltage. It was not felt worthwhile at this time to check whether a comparable gain would be obtained at operation current densities. As the cells are not concentration polarized on the gas side, no other benefits would be expected.

6.2.2 Dependent Variables

The dependent variables followed during the parametric evaluation were:

1. Cell voltage. Obtained by measuring and averaging the potential developed across each of the central three cells.

2. Gas side liquid accumulation rate and normality. Obtained by separating and collecting the liquid for definite time periods.

6.3 Test Results

The special battery was run for 1500 hours to provide information for parametric evaluation. The first 475 hours were run at ambient external temperature; the primary concern was to tie down the effect of current density and

electrolyte normality on gas-side liquid collection rates. Bath temperature was then added as a variable and the remaining one thousand hours included periods at bath temperatures up to 60°C. A log of cell electrical performance is given in Table 6.1.

6.3.1 Effect of Variables on Electrical Performance

6.3.1.1 Effect of Electrolyte Normality on Cell Voltage

For the first 475 hours the electrolyte to the battery was at ambient temperature and the battery itself was also exposed to the laboratory atmosphere. The average cell voltages obtained during this period are shown plotted versus electrolyte normality in Figure 6.1. It can be seen that, within the repeatability of the data, electrolyte normality has no effect on cell voltage. This is not surprising as the electrical resistance of the electrolyte is very low and does not vary much with composition in the normality range covered.

6.3.1.2 Effect of Time on Cell Voltage

As pointed out in Section 6.3.1.1, electrolyte normality has no noticeable effect on cell voltage. The remaining independent variables, as far as cell voltage is concerned, are then temperature, current density, and possibly time. Figure 6.2 presents a plot of cell voltage vs, time with current density and temperature as parameters.

It can be seen that some abrupt changes in cell behavior occurred at around 600 hours and again somewhere between 1250 and 1450 hours. During the interval between these two abrupt changes, the cell performed consistently better than either before the first or after the second change. Neither the nature of, nor the cause for, these two changes is known at present. Two modes of cell behavior can be delineated: Mode I during 0-600 and 1350-1500 hours; Mode II during 600-1350 hrs. During each of these periods cell performance remained reasonably constant. There was thus no noticeable degradation with time.

6.3.1.3 Effect of Current Density and Temperature on Cell Performance

As seen in Figure 6.2, within each mode, decreasing current density or increasing

Table 6.1

Effect of Operating Variables on Electrical Performance

Run Hours	Current Density Amp/Ft^2	Electrolyte Temp., ^{o}C		Electrolyte Normality	Average Voltage Per Cell
		In	Out		
0	24	24	--	6.00	0.798
4	24	19	--	5.78	0.777
20	24	16	--	5.22	0.740
24	24	15	--	5.25	0.737
25	40	16	--	6.00	0.674
40	40	18	--	5.22	0.679
68	40	20	--	4.20	0.692
87	60	20	--	4.6	0.619
91	60	22	--	4.5	0.632
95	60	22	--	5.0	0.628
111	60	20	--	4.38	0.623
112	80	20	--	4.35	0.537
112	40	20	--	4.32	0.705
113	24	20	--	4.3	0.775
120	24	23	--	4.3	0.760
135	24	20	--	4.0	0.786
199	12	18	--	5.55	0.855
208	12	18	--	5.4	0.852
214	12	17	--	5.25	0.856
230	12	17	--	5.0	0.838
258	12	22	--	8.7	0.817
279	12	22	--	8.0	0.803
285	12	22	--	7.9	0.812
308	24	21	--	8.0	0.756
326	24	21	--	7.5	0.747
332	60	21	--	7.9	0.651
333	60	21	--	7.5	0.678
335	24	22	--	6.1	0.792

Table 6.1 (continued)

Effect of Operating Variables on Electrical Performance.

Run Hours	Current Density Amp/Ft^2	Electrolyte Temp., ^{o}C		Electrolyte Normality	Average Voltage Per Cell
		In	Out		
351	24	22	--	5.5	0.787
378	24	23	--	2.95	0.762
401	60	25	--	3.25	0.631
422	12	25	--	3.05	0.816
447	12	25	--	3.00	0.798
454	24	31	37	5.1	0.762
471	24	26	33	5.5	0.770
478	60	45	--	6.3	0.707
503	60	52	--	5.25	0.633
520	24	56	--	5.8	0.782
524	24	59	60	5.65	0.839
534	24	59	60	6.15	0.818
544	24	59	60	5.80	0.785
549	12	60	61	6.35	0.835
552	12	61	61	6.30	0.820
553	12	61	61	6.30	0.862
593	60	57	67	6.35	0.703
596	60	54	62	6.05	0.693
648	24	26	31	7.7	0.843
663	24	21	26	7.1	0.822
688	24	18	23	6.1	0.812
693	24	17	24	5.6	0.811
713	24	17	24	5.1	0.811
741	24	22	29	4.35	0.822
758	24	22	29	4.9	0.808
766	24	57	58	6.8	0.857
783	24	60	61	6.85	0.846
790	60	59	63	6.68	0.746
807	24	59	60	6.65	0.829

Table 6.1 (continued)

Effect of Operating Variables on Electrical Performance

Run Hours	Current Density Amp/Ft^2	Electrolyte Temp., ^{o}C		Electrolyte Normality	Average Voltage Per Cell
		In	Out		
809	12	59	59	6.35	0.880
816	12	59	59	6.30	0.868
832	12	59	59	4.05	0.868
834	12	59	59	7.88	0.854
859	12	59	59	6.11	0.888
903	12	32	32	7.05	0.860
909	12	58	58	7.18	0.890
928	12	61	61	7.65	0.882
988	12	58	58	----	0.880
999	12	36	36	----	0.856
1006	12	60	60	----	0.878
1246	24	43	45	3.35	0.837
1246	40	43	46	3.35	0.803
1465	24	20	21	----	0.762
1486	24	20	21	----	0.770

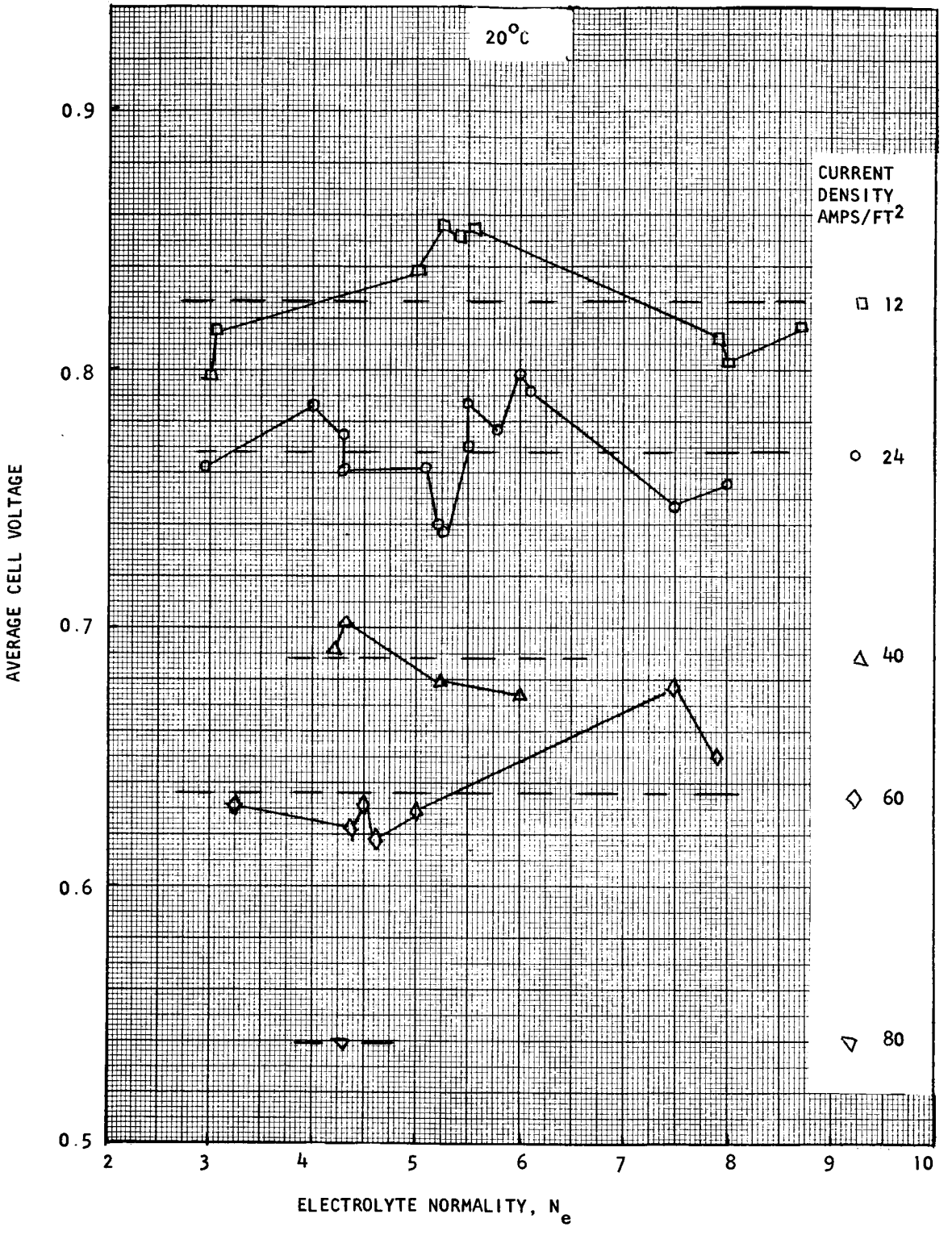

Figure 6.1 Effect of Electrolyte Normality on Voltage

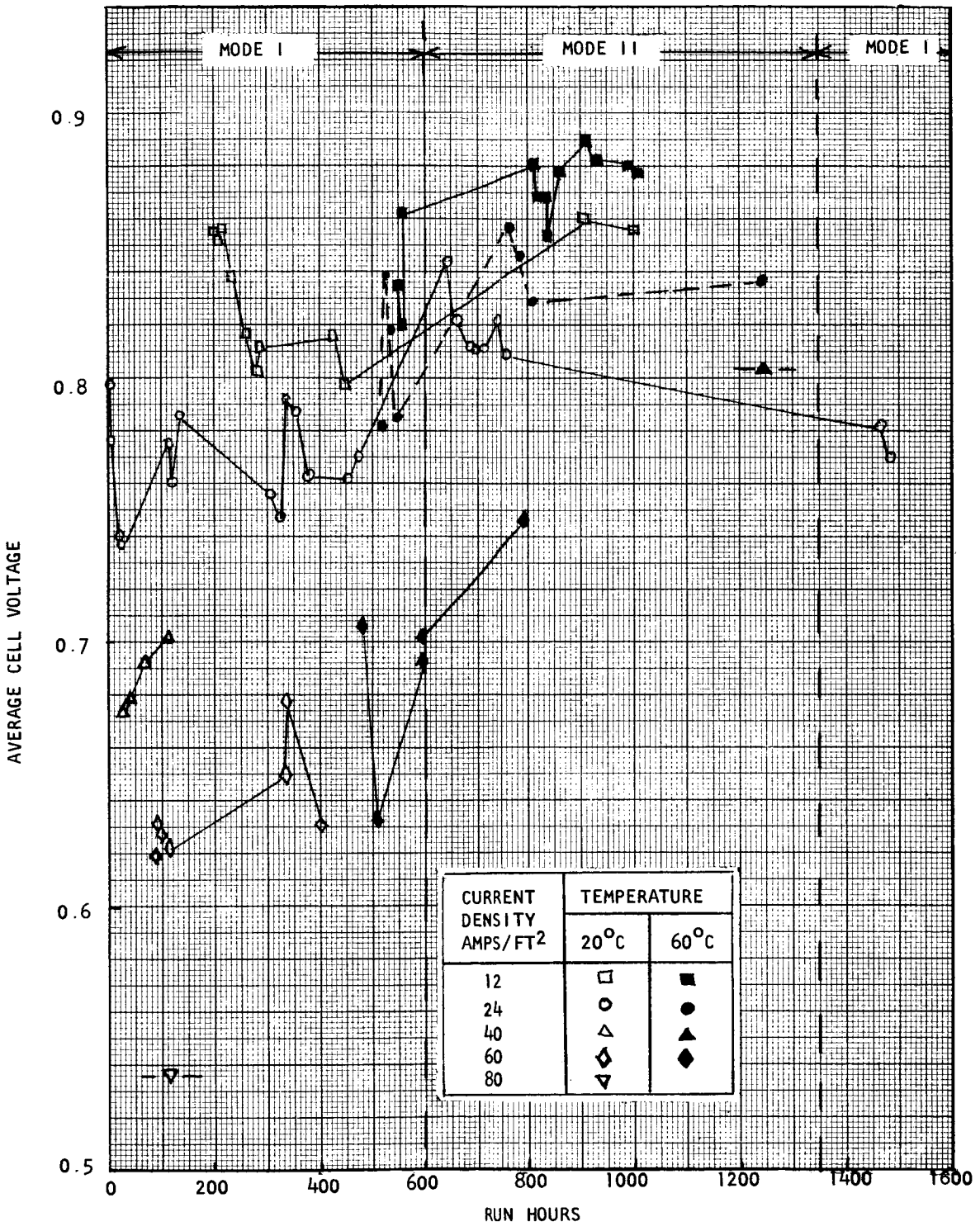

Figure 6.2 Average Cell Voltage Vs. Time

temperature increases the cell voltage. The direction of these effects is as expected. In order to focus on the quantitative aspects involved, the points corresponding to a given current density were averaged for each mode of operation.

In light of the scatter of the data, temperature was treated as only a two-level variable. The results are given in Table 6.2 and plotted in Figures 6.3 and 6.4.

The lines drawn in Figures 6.3 and 6.4 permit the calculation of the specific cell conductance (expressed in mhos/ft^2) and of the extrapolated zero-current voltage for a cell. The results are listed in Table 6.3.

Both the values of specific conductance and of extrapolated zero-current voltage increase with temperature. Operation at 60°C rather than 20°C thus appears desirable from an electrical view-point alone.

The specific conductances obtained at 60°C (305 mhos/ft^2 for Mode I, 375 for Mode II) can be compared to the 369 mhos/ft^2 obtained after Run 3A for Battery 3 (See Section 7.0). That battery had niobium metallics rather than the tantalum metallics used here. Niobium metallics have given better performance than tantalum wherever the two have been compared. A specific conductance of 360 mhos/ft^2 at 60°C with niobium metallics thus appears to be an achievable value even if the cells are not in the improved state characterized as "Mode II".

6.3.2 Effect of Variables on Liquid Transfer

Some liquid always appears in the gas streams leaving a dual-membrane fuel cell. Possible sources for this liquid are:

1. Mechanical leaks between electrolyte stream and gas streams. This would include leaks through the membranes and leaks between the respective manifolds.

2. Transfer of liquid across the membrane due to other than mechanical causes.

Table 6.2

Effect of Variables on Cell Voltage

Mode	Average Cell Voltage			
	I		II	
Temperature**	Lo	Hi	Lo	Hi
Current Density amps/ft^2				
12	0.827	0.838	0.858	0.876
24	0.768	0.806	0.818	0.842
40	0.688	-	-	0.803
60	0.637	0.684	-	0.746
80	0.537	-	-	-

* Mode I: 0-600; 1350-1500 hours
Mode II: 600-1350 hours

** Lo: approximately 20°C
Hi: approximately 60°C

Table 6.3

Effect of Variables on Electrical Performance(1)

Mode(2)	Temperature(3)	Cell Specific Conductance Mhos/ft^2	Extrap. Zero-Current Voltage, Volts
I	Lo	250	0.867
I	Hi	305	0.880
II	Lo	360(4)	0.883(4)
II	Hi	375	0.906

(1) For cells with tantalum metallics, niobium metallics expected to increase conductance by about 60 mhos/ft^2.

(2) Mode I and Mode II: same as in Table 6.2, above.

(3) Lo = approximately 20°C; Hi = approximately 60°C.

(4) Based on only two points on polarization curve.

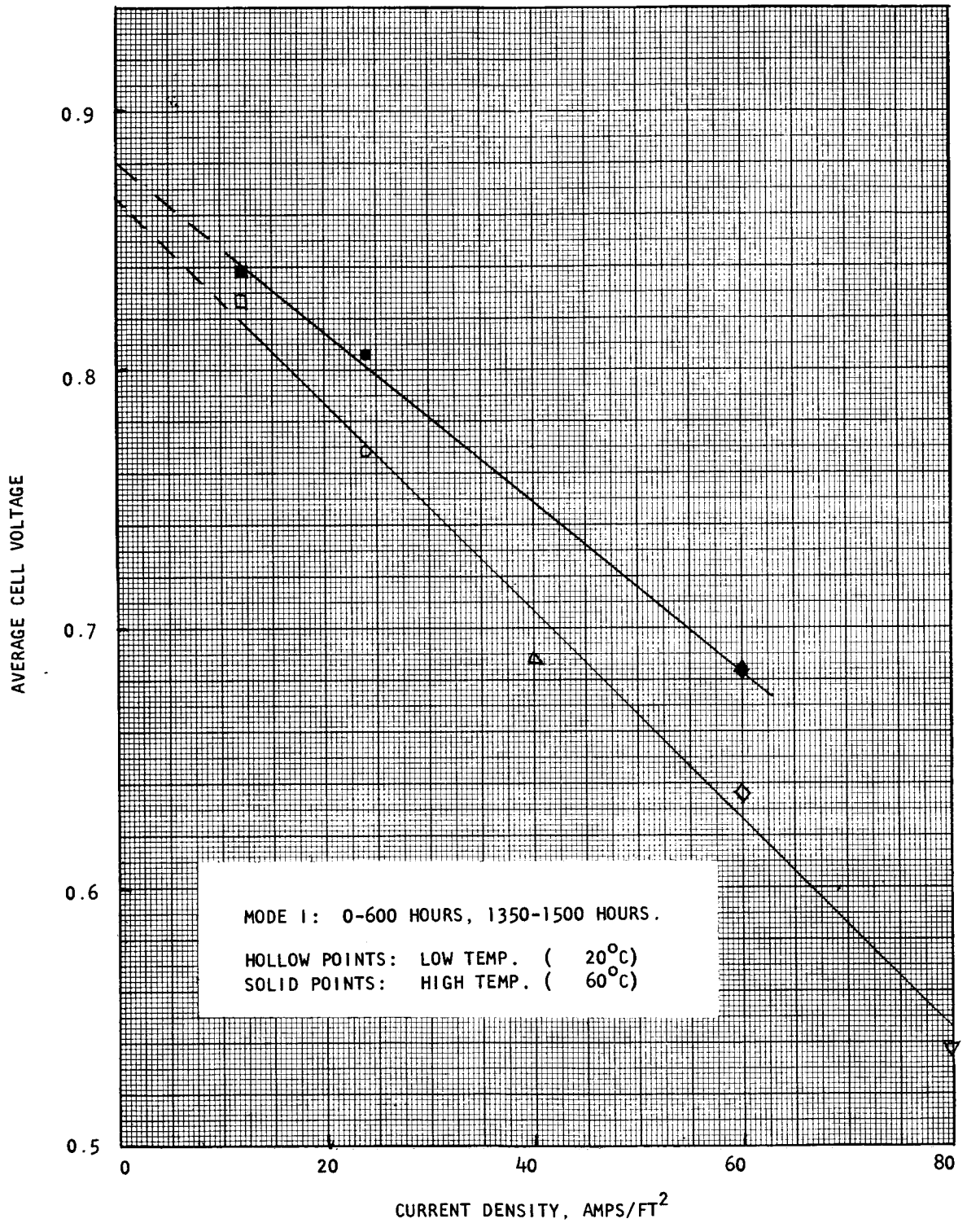

Figure 6.3 Average Cell Voltage Vs. Current Density

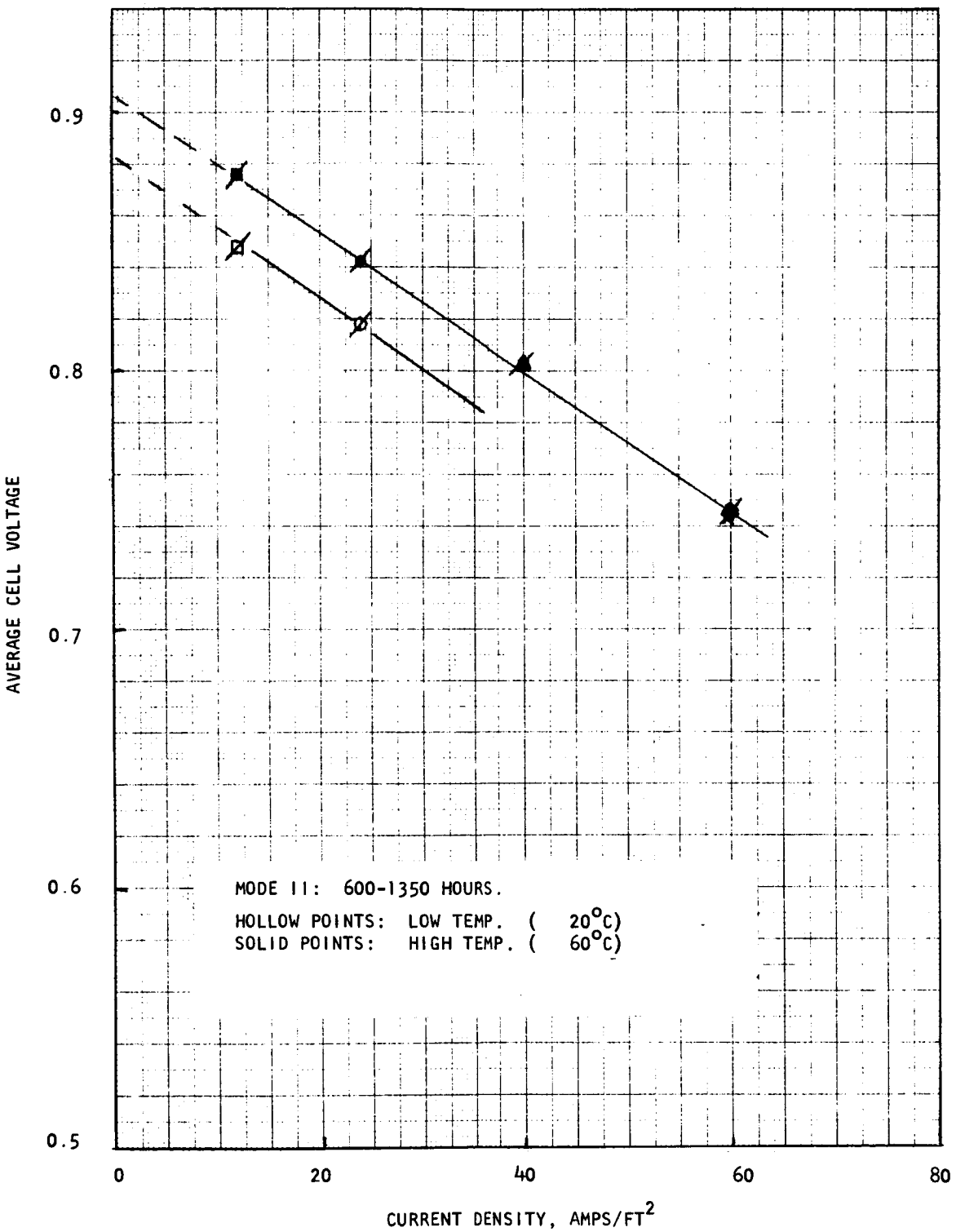

Figure 6.4 Average Cell Voltage Vs. Current Density

3. Chemical reaction: $H_2 + \frac{1}{2}O_2 \rightarrow H_2O(l)$

4. Condensation, whenever the collector bottle is at a considerably lower temperature than the gas leaving the battery.

6.3.2.1 Check for Mechanical Leakage

To see whether mechanical leakage was responsible for the liquid appearing in the gas stream, two special single cells were constructed: Cell E1279 and Cell E1652. The first of these, Cell E1279, had ion-impermeable rubber sheets in lieu of ion-exchange membranes. Aside from this use of rubber "membranes", this cell was constructed normally, i.e., with electrolyte fed to and removed from the electrolyte compartment via manifold ports leading to headers which passed through various other cell components. The second cell, Cell E1652, used regular ion-exchange membranes but was built without manifold-headers. Instead, the electrolyte entered and left the electrolyte compartment directly through holes drilled down through the electrolyte compartment wall.

The cell with rubber membranes showed no noticeable liquid accumulation in the gas compartments after having been "run" for several weeks. There was thus no mechanical leakage from the electrolyte manifold to the gas manifold.

The cell without manifold headers but with ion-exchange membranes consistently had liquid leaving with the gas streams. The amount of liquid was not affected by changes in the differential pressure between the electrolyte compartment and the gas compartments. The liquid showing up in the gas streams thus had come through the membranes but by mechanisms other than mechanical "pin-hole" leakage.

(It is possible to obtain "pin-hole" type leakage through the membranes if the electrolyte normality is increased above 11 $\underline{N}$ H_2SO_4. At that concentration, the H_2SO_4 dehydrates the membranes to such an extent that macropores open up and very high leakage rates result. These leakage rates are then dependent on the pressure differential maintained. When the normality is again lowered below 11 $\underline{N}$ H_2SO_4, the ion-exchange resin re-solvates, the macropores close up and the mechanical integrity of the membrane is restored.)

6.3.2.2 Hydrogen-Side Liquid

Liquid was collected from both the hydrogen and the oxygen leaving dual-membrane cells. The data obtained from each of the two gas streams will be considered separately, as the effect of the operating variables are quite different.

The data considered in this section were obtained from the same special 5-cell battery used to determine the effect of operating variables on electrical performance as detailed in Section 6.3.1. The data are listed in Table 6.4 which is included in Section 6.3.2.3.

The normality of the hydrogen-side liquid collected during the low temperature runs is plotted versus the electrolyte normality in Figure 6.5 for current densities of 12 to 60 amps/ft^2. No liquid was obtained at 0 amps/ft^2. It can be seen that, within the scatter of the data, the hydrogen side liquid has the same normality as the electrolyte itself. One source of scatter is a possible slight temperature imbalance will lead to condensation or evaporation of liquid. Although at first glance the equal normality of the electrolyte and of the collected liquid may suggest a mechanical leak, it is felt that no such mechanical leakage is involved. The reasons for this belief appear when we consider the rate at which hydrogen-side liquid is accumulated.

Figure 6.6 shows a plot of liquid rate (plotted as gms/amp-hr-cell)versus electrolyte normality for these same runs. A single curve adequately represent the data. This says that the amount of liquid collected from a cell was proportional to the amount of current passing through the cell. This could hardly be ascribed to any "mechanical" leakage.

The reaction theoretically occurring at the hydrogen electrode is $H_2 \rightarrow 2H^+ + 2e^-$ with the H^+ ions going <u>from</u> the electrode in the H_2 compartment through the membrane <u>into</u> the electrolyte compartment. Yet a flow of electrolyte exists <u>from</u> the electrolyte compartment <u>to</u> the H_2 compartment. The most probably explanation is that, although the majority of the current is carried by the H^+ cations, some of the current is carried by sulfate or bisulfate anions. These anions are well solvated and thus their effect is to carry electrolyte

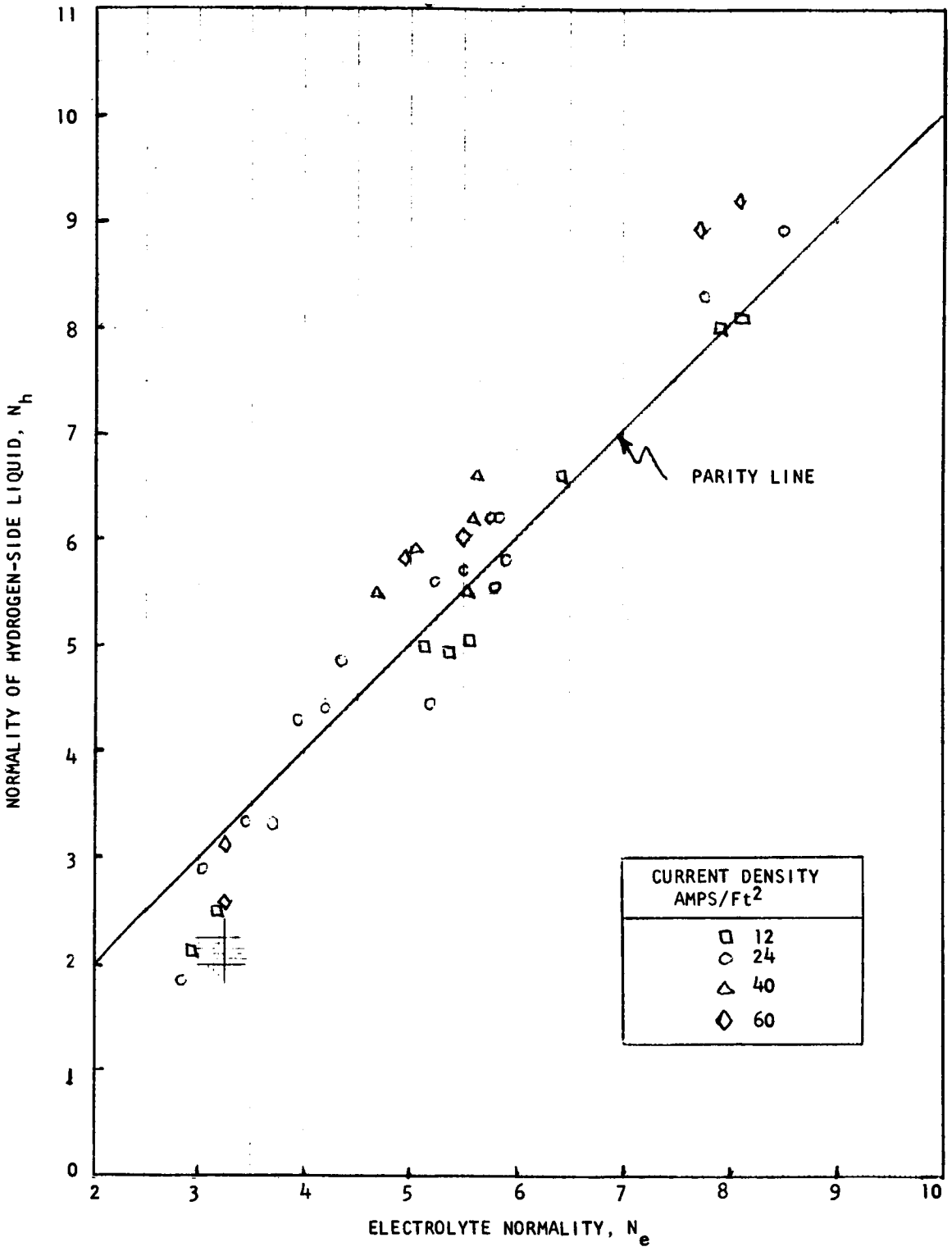

Figure 6.5 Hydrogen-Side Liquid Normality Vs. Electrolyte Normality

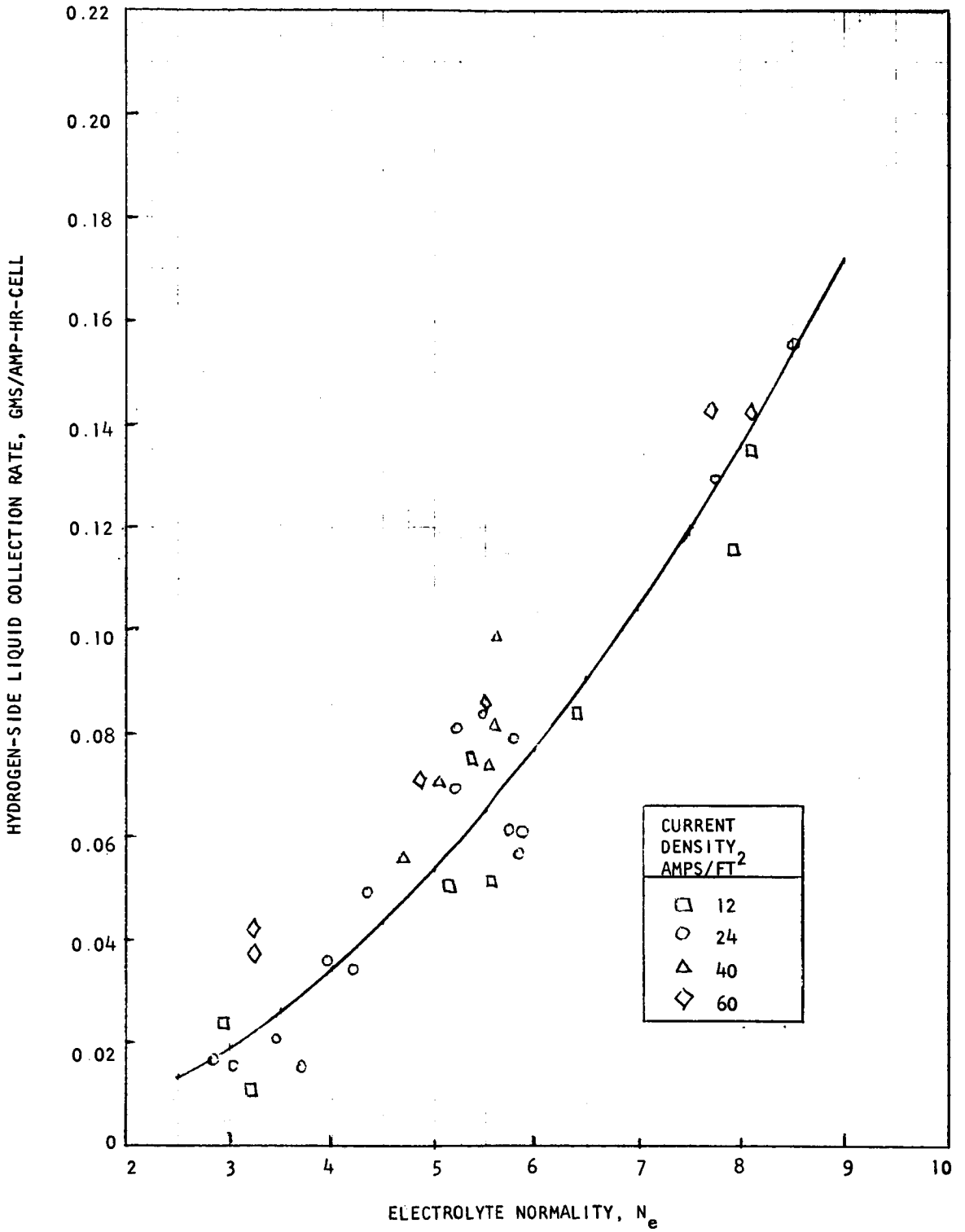

Figure 6.6 Hydrogen-Side Liquid Rate Vs. Electrolyte Normality

out into the gas compartment. (It must be remembered that at the electrolyte concentration involved - 3N to 9N H_2SO_4 - the bound anionic charges on the membrane resin are no longer completely effective at screening out other anions). Figure 6.7 shows the same data as Figure 6.6, i.e., hydrogen-side liquid rate (gms/amp-hr-cell) versus electrolyte normality but plotted on logarithmic paper. It can be seen that the rate is proportional to about the square of the electrolyte normality. (Some high temperature data (60°C) which will be discussed later in this section are also shown).

Figure 6.8 again presents the same hydrogen-side liquid collection rate data, but this time expressed as equivalents of H_2SO_4 collected per cell per electrochemical equivalent of current, i.e., per faraday. It can be seen that this ratio is a strong function of electrolyte normality: it increases approximately as N_e^3. The absolute value, however, remains quite small. When the electrolyte is 6N, the H_2SO_4 collected represents only about 1% of the faradays passed.

High temperature data (60°C) were also taken to delineate the effect of temperature on hydrogen-side liquid. The data were somewhat clouded by the difficulty of preventing condensation or evaporation in the cell or the collector bottles due to variations in the temperature and humidity of the gas stream when leaving the humidifier, passing through the cell and leaving the collector bottles. The data obtained at approximately a constant electrolyte normality averaging 6.8N were broken down into grams H_2O/ft^2-hr-cell and grams H_2SO_4/ft^2-hr-cell, each of which was plotted separately against current density (see Figure 6.9). Each was found to form a straight line but having a positive intercept at zero current density. This rate at zero current density was accounted for by hypothesizing that some water condensed in the cell and then drew some H_2SO_4 electrolyte out by osmotic or diffusion forces.) The slopes of the two lines in Figure 6.9 give the incremental collection rates in gms/amp-hr-cell, one for the H_2SO_4 component and one for the H_2O. The sum of these two quantities, 0.163 grams of liquid/amp-hr-cell, represents the best estimate of the hydrogen-side collection rate at 60°C and at this electrolyte normality of 6.8N and is plotted on Figure 6.7. The rate of 0.163 gms/amp-hr-cell obtained at 60°C is higher than the 0.1 gms/amp-hr-cell expected at this normality at 20°C.

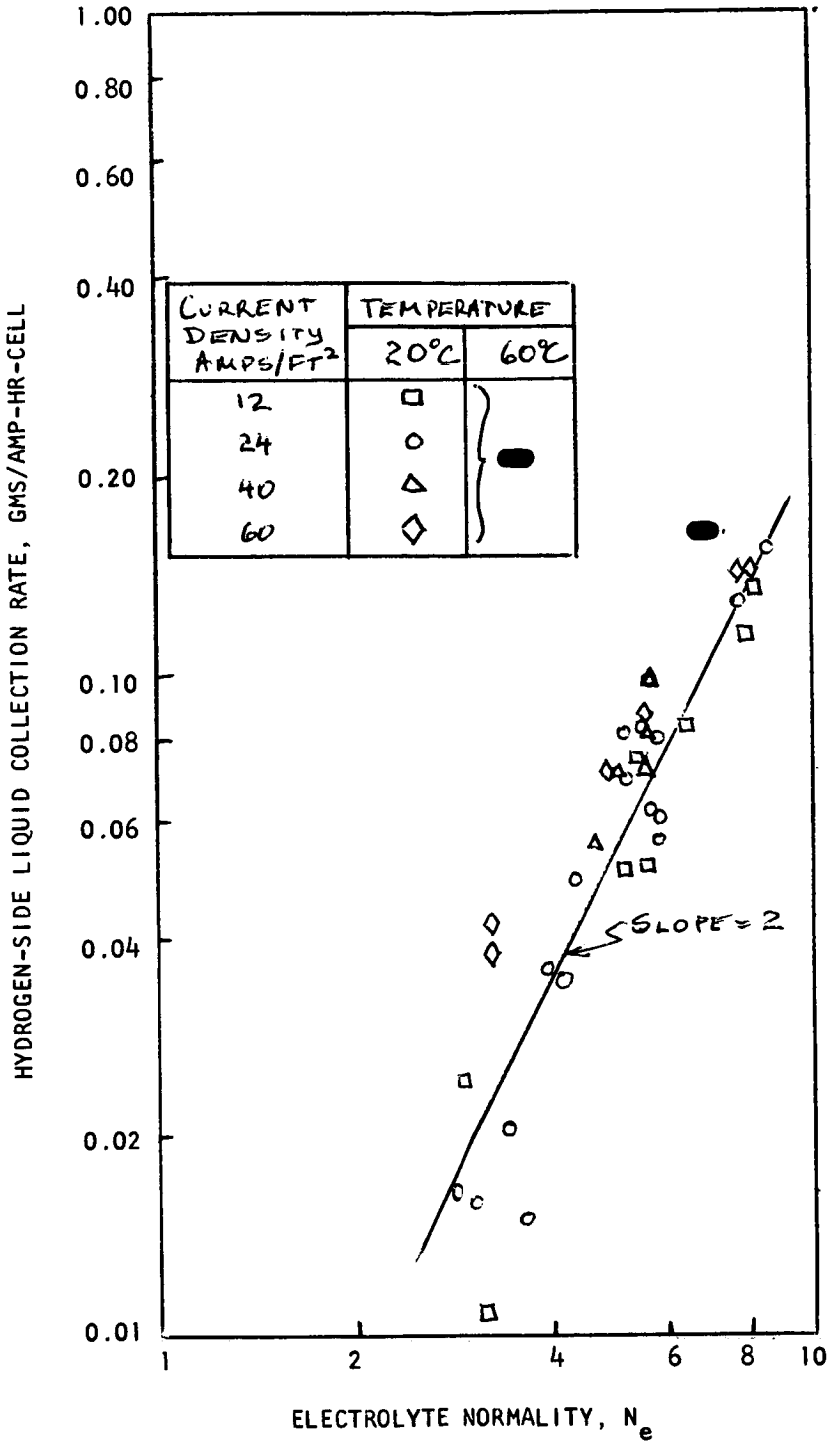

Figure 6.7 Hydrogen-Side Liquid Rate Vs. Electrolyte Normality

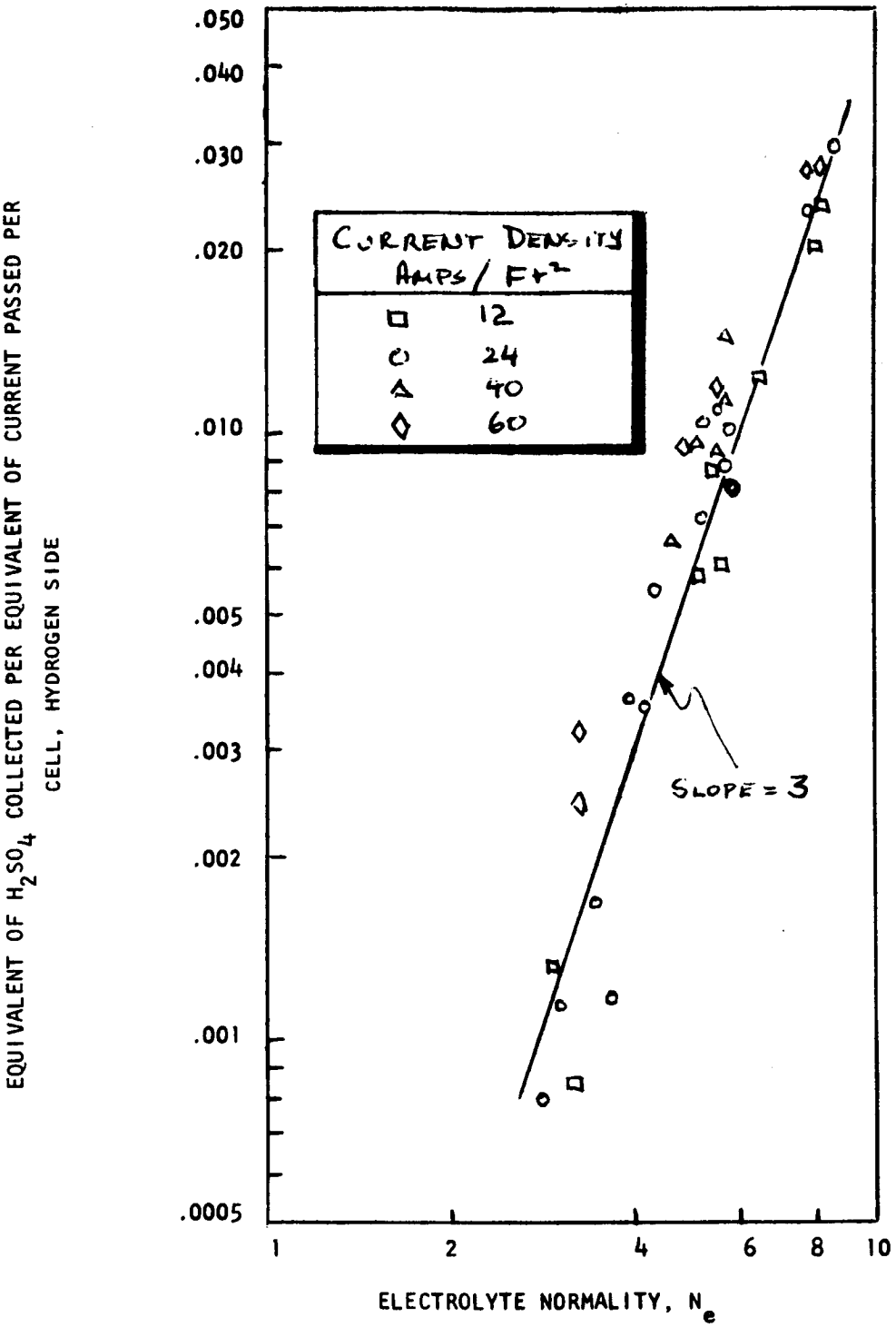

Figure 6.8 Hydrogen-Side Equivalents

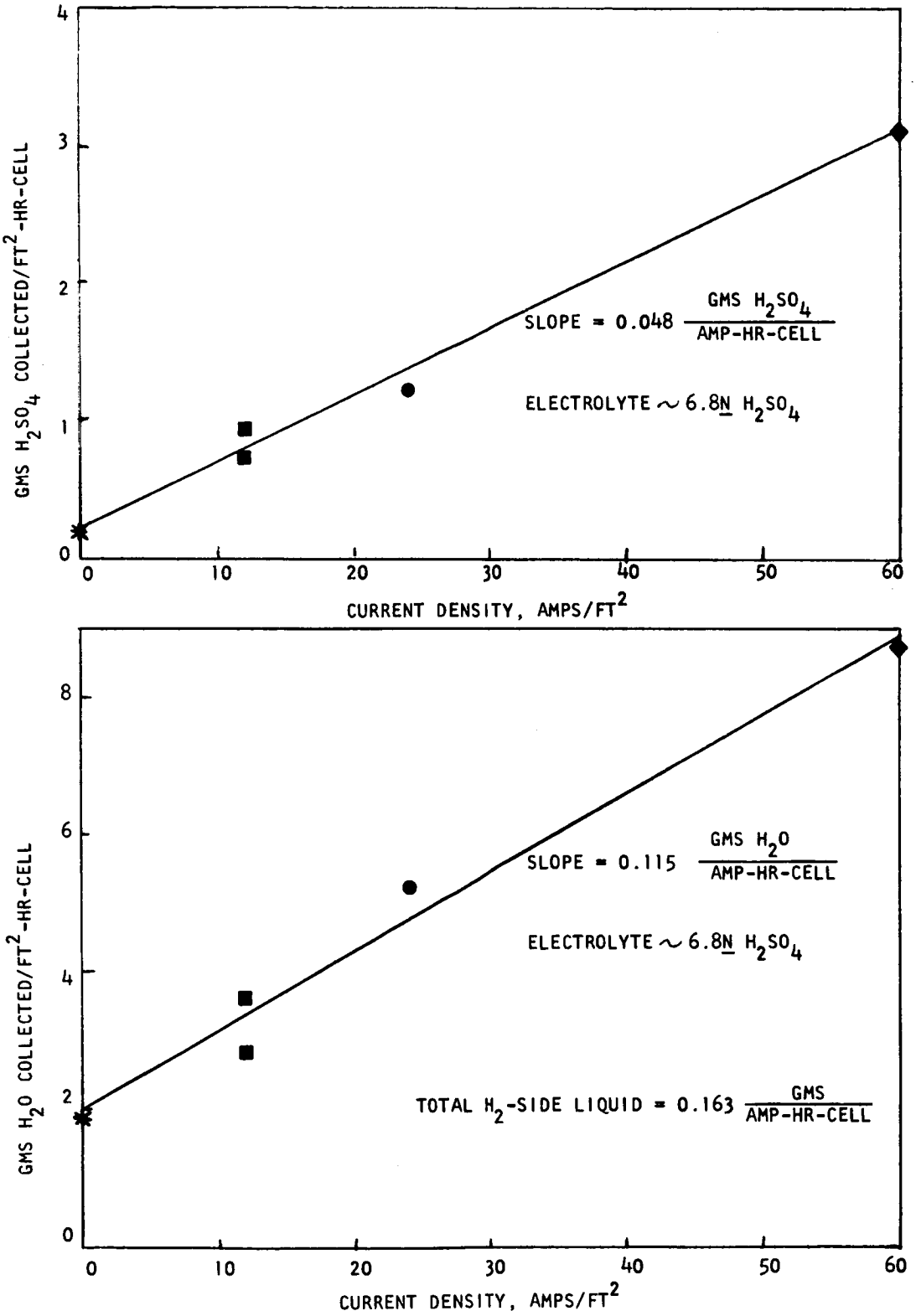

Figure 6.9 Hydrogen-Side Liquid Collection at 60°C

6.3.2.3 Oxygen-Side Liquid

Water is the product of the chemical reaction occurring in an H_2-O_2 fuel cell. For dual-membrane cells using acid electrolyte, the water is formed at the O_2 electrode where:

$$2H^+ + 2e^- + \tfrac{1}{2}O_2 \rightarrow H_2O(l)$$

In addition to this water formed by chemical reactions, the H^+ ions passing through the membrane do so in a solvated form and thus effectively bring with them some of the highly acid liquid of solvation present in the membrane. To complicate the picture further, H_2O has a low activity coefficient in the concentrated H_2SO_4 present in the electrolyte compartment and thus H_2O tends to diffuse from the membrane-electrode interface back into the electrolyte compartment.

The net oxygen side liquid collection rate depends (aside from condensation effects) on a balance between:

1. Rate of water formation by reaction
2. Rate of solvation-liquid transfer
3. Rate of back diffusion of water

Figure 6.10 shows that at a given electrolyte normality, the oxygen-side normality goes down as the current density is increased. This is due to the fact that an increase in current density implies an increase in the water produced at the oxygen-side electrode by reaction of H_2 and O_2. The additional water results in a lower acid concentration at the electrode. The oxygen-side membrane is in contact with the oxygen-side liquid of normality N_o on one side and the electrolyte of normality N_e on the other. The net effect of this can often be described as saying the membrane is in contact with a liquid of normality N_m, the "membrane normality", where N_m is the geometric mean of N_e and N_o, i.e., $N_m = \sqrt{N_o N_e}$. Figure 6.11 presents a plot of oxygen-side liquid collection rate at 20°C, expressed as gms/amp-hr-cell, versus N_m. The data fall reasonably closely together. The same data are plotted logarithmically in Figure 6.12. The rate of liquid collection falls off with increasing membrane normality- the more concentrated H_2SO_4 "sucks" the product water back into the

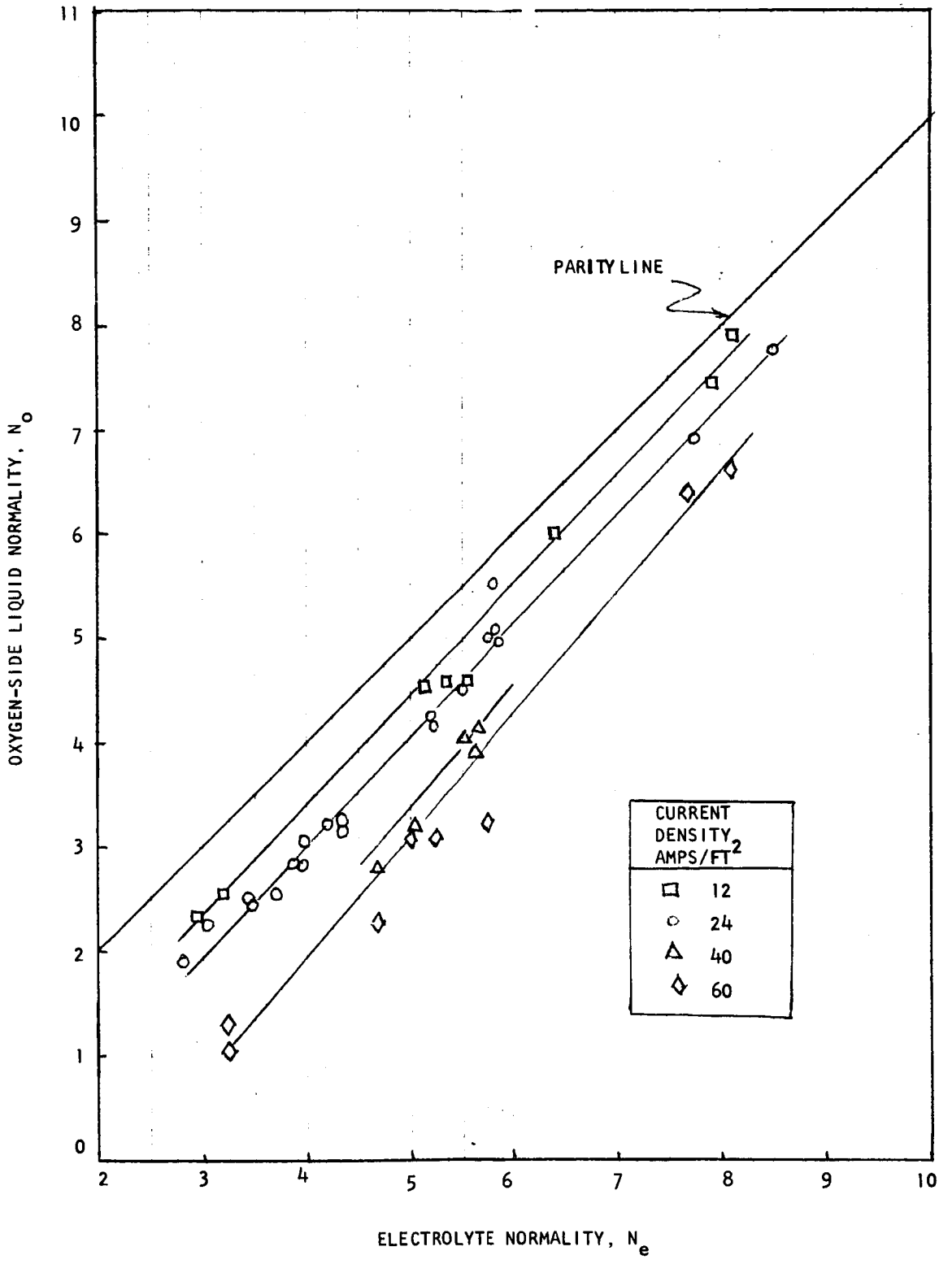

Figure 6.10 Oxygen-Side Liquid Normality Vs. Electrolyte Normality

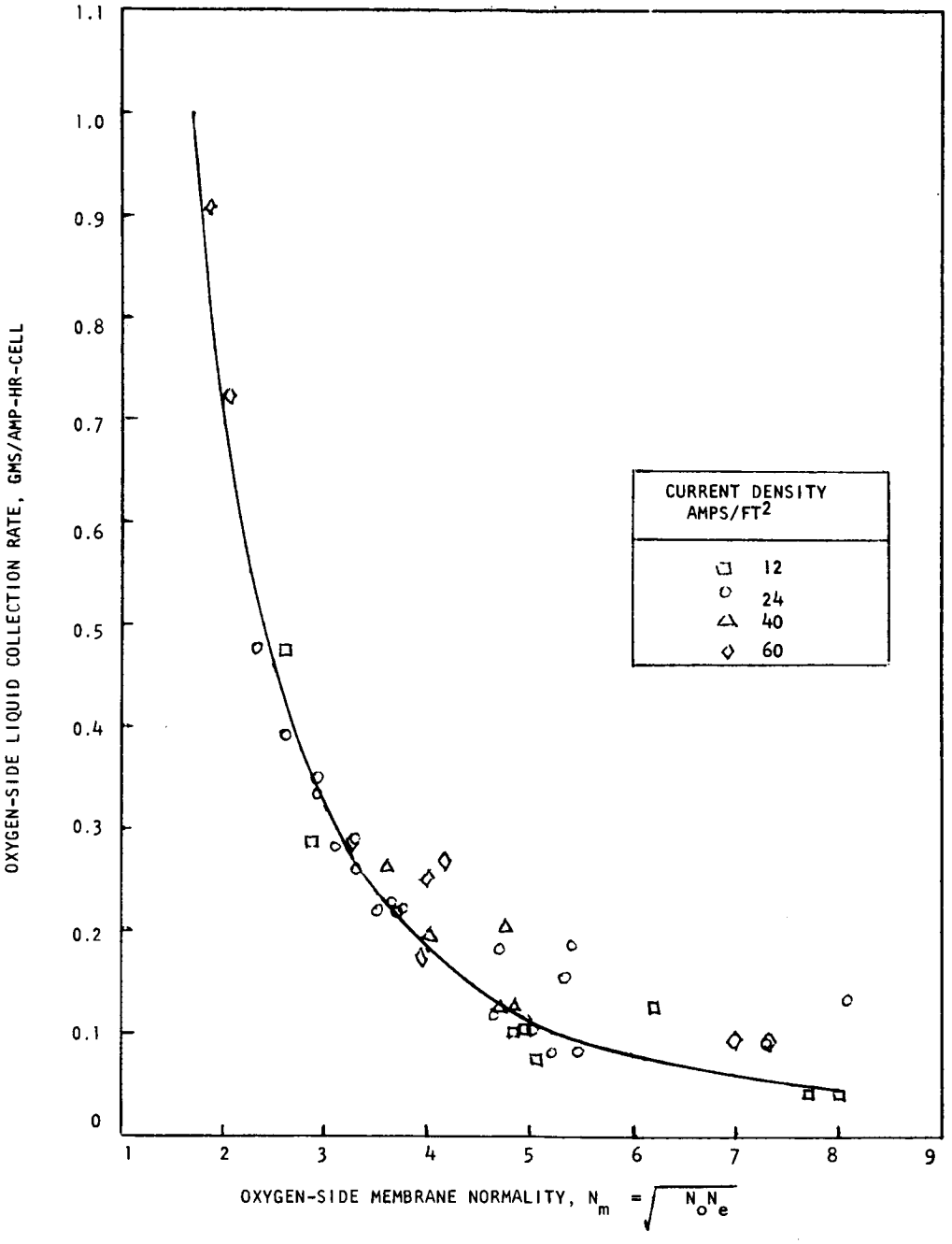

Figure 6.11 Oxygen-Side Liquid Rate

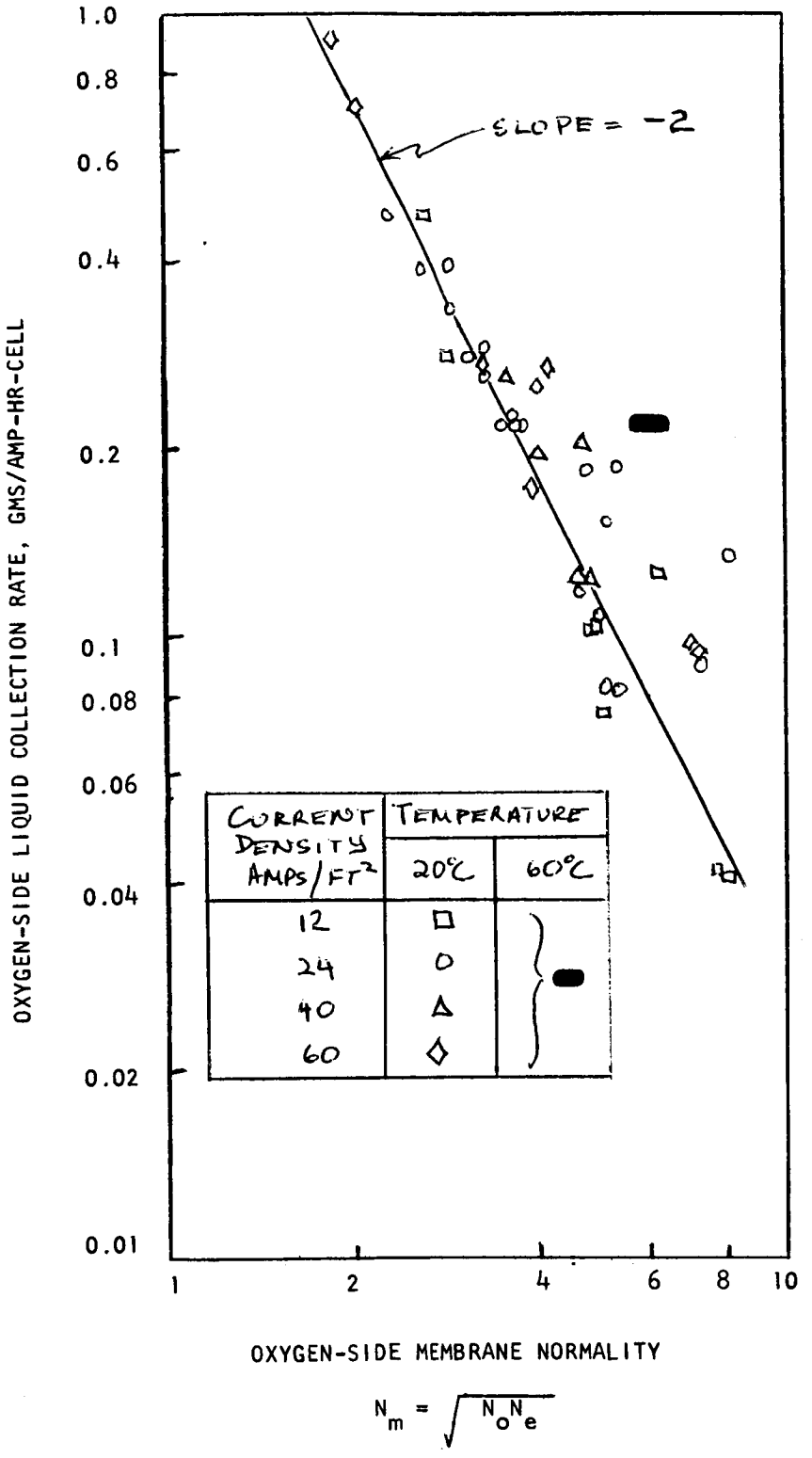

Figure 6.12 Oxygen-Side Liquid Rate Vs. Membrane Normality

electrolyte compartment. The oxygen-side collection rate is approximately proportional to N_m^{-2}. The relevant data are listed in Table 6.4.

Oxygen-side liquid collection data obtained at 60°C were treated exactly as the 60°C hydrogen-side data discussed in 6.3.2.2. The resulting plots are shown in Figure 6.13. (The 60°C liquid collection data are summarized in Table 6.5). The oxygen-side rate of 0.221 gms/amp-hr-cell determined from Figure 6.13 is also shown on Figure 6.12. It is seen that the collection rate is higher than the 0.08 gms/amp-hr-cell expected for a membrane normality of 6.0N at 20°C.

6.4 Summarized Effect of Variables

The parametric evaluation showed that electrolyte normality has no effect on cell voltage but does have a strong effect on the rate at which liquid is transported into the gas compartments. The collection rates are proportional to the current passed. Increasing electrolyte normality increases the rate of liquid collection on the hydrogen side and decreases the collection rate on the oxygen side. Figures 6.5 through 6.13 show the correlations obtained.

Increasing temperature raises the cell voltage, lowers cell resistance and increases the gas-side liquid collection rates as shown in Figures 6.3, 6.4, 6.7 and 6.12. Time, per se, does not seem to have a deleterious effect on the cell; however an unexplained increase in performance persisted for a 750 hour span during a 1500 hour run. This is shown in Figures 6.2 through 6.4.

Variations in gas and liquid flow rates and in pressure level have only minor effects, if any, on cell performance as detailed primarily in Sections 5.0 and 7.0 of this part of the report.

Table 6.4

Gas-Side Liquid Collection Rate Data

($20^{o}C$)

Current Density Amp/ft^2	Normalities				Liq. Collection Rate Gms/Amp-Hr-Cell		Equiv. H_2SO_4/ Faraday
	Electrolyte N_e	H_2-Side N_h	O_2-Side N_o	Membrane $N_m = \sqrt{N_o N_e}$	O_2-Side	H_2-Side	H_2-Side
12	8.1	8.1	7.9	8.0	.041	.135	.0237
	7.9	8.0	7.45	7.7	.042	.116	.0202
	6.4	6.6	6.0	6.2	.128	.0838	.0123
	5.55	5.05	4.6	5.05	.075	.0512	.00605
	5.35	4.95	4.6	4.95	.104	.075	.0087
	5.12	5.0	4.55	4.85	.102	.0504	.0059
	3.18	2.5	2.55	2.85	.288	.0108	.00074
	2.92	2.15	2.35	2.60	.474	.0240	.00133
24	8.5	8.9	7.75	8.1	.134	.1555	.0294
	7.75	8.3	6.90	7.3	.090	.1295	.0233
	4.35	---	3.15	3.7	.218	-----	-----
	4.35	4.85	3.25	3.75	.220	.0488	.00555
	4.20	4.4	3.20	3.65	.228	.0340	.00353
	3.98	---	3.05	3.5	.218	-----	-----
	3.92	4.3	2.80	3.3	.206	.0357	.00364
	3.88	---	2.85	3.3	.290	-----	-----
	3.7	3.3	2.55	3.1	.284	.0149	.00120
	3.48	---	2.45	2.9	.334	-----	-----
	3.42	3.35	2.50	2.9	.349	.0204	.00167
	5.88	5.8	4.95	5.4	.187	.0606	.0081
	5.50	5.7	4.55	5.0	.104	.0840	.0109
	5.22	5.6	4.15	4.65	.120	.0812	.0104
	5.85	6.2	5.1	5.45	.081	.0562	.00782
	5.75	6.2	5.0	5.35	.152	.0607	.00845

Table 6.4 (continued)

Gas-Side Liquid Collection Rate Data

($20^{o}C$)

Current Density Amp/ft^2	Normalities				Liq. Collection Rate Gms/Amp-Hr-Cell		Equiv. H_2SO_4 Faraday^2
	Electrolyte N_e	H_2-Side N_h	O_2-Side N_o	Membrane $N_m = \sqrt{N_o N_e}$	O_2-Side	H_2-Side	H_2-Side
24	3.02	2.9	2.25	2.6	.390	.0159	.00114
	2.82	1.85	1.9	2.3	.475	.0164	.00077
	5.2	4.45	4.25	4.7	.186	.0690	.0072
	5.8	5.55	4.65	5.2	.082	.0798	.0101
40	5.62	6.6	3.9	4.7	.125	.0985	.0145
	4.68	5.5	2.8	3.6	.264	.0556	.00695
	5.65	6.2	4.15	4.85	.128	.081	.01135
	5.52	5.5	4.05	4.75	.210	.0736	.0092
	5.05	5.9	3.2	4.0	.198	.0708	.0096
60	5.75	---	3.2	4.17	.273	----	----
	5.25	6.05	3.05	4.0	.254	.0865	.01195
	5.0	---	3.1	3.93	.174	----	----
	4.7	5.85	2.3	3.3	.287	.0718	.0096
	3.25	2.6	1.05	1.85	.908	.038	.00248
	3.25	3.15	1.3	2.05	.726	.042	.00325
	8.1	9.2	6.65	7.3	.094	.1428	.0275
	7.7	8.95	6.4	7.0	.099	.1424	.0272

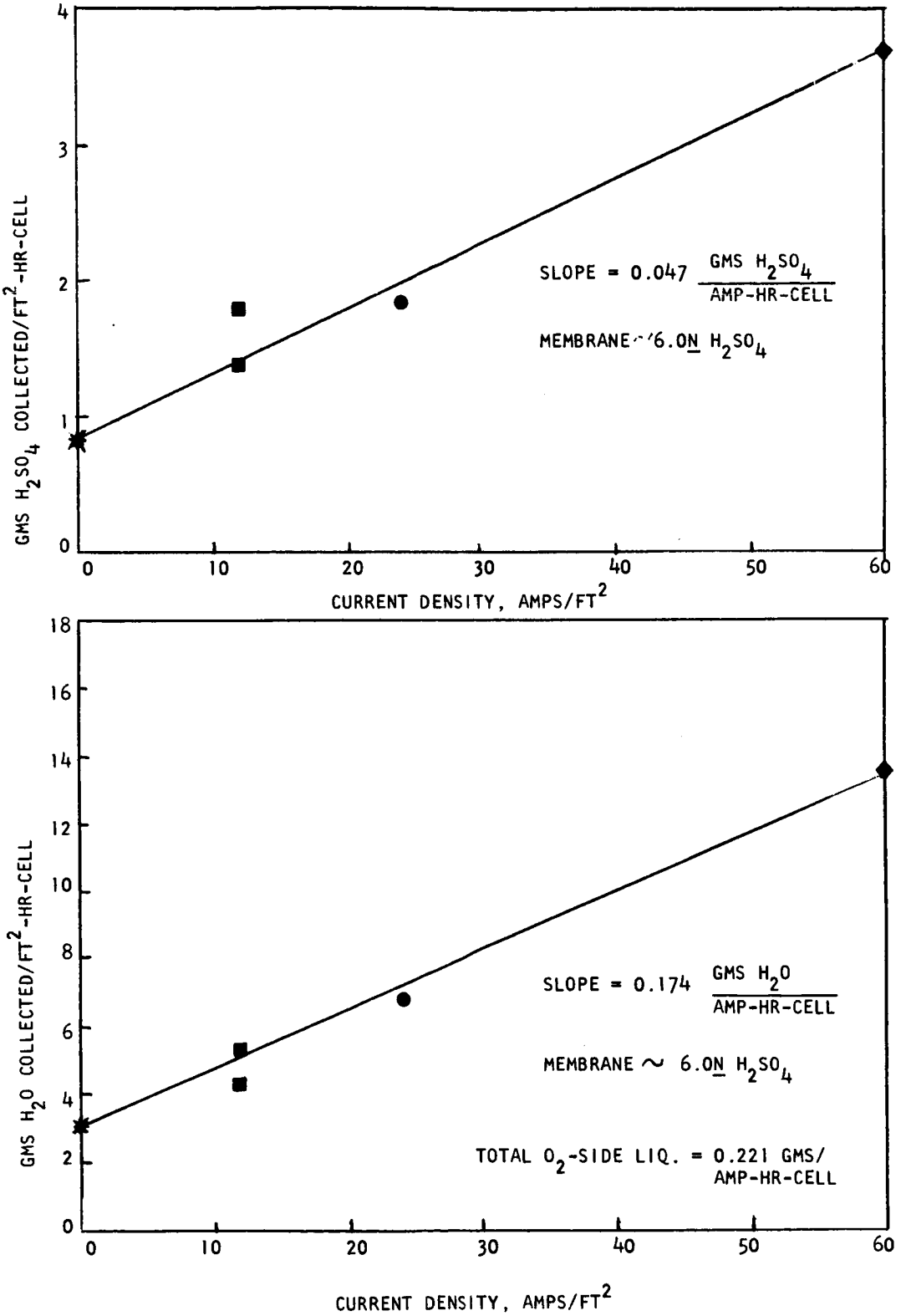

Figure 6.13 Oxygen-Side Liquid Collection at 60°C

Table 6.5

Gas-Side Liquid Collection Rate Data

($60^{o}C$)

Current Density, Amps/Ft^2	Normalities				Gross Liquid Rates, Gms/Ft^2-Hr-Cell			
					H_2-Side		O_2-Side	
	Electrolyte N_e	H_2-Side N_h	O_2-Side N_o	Membrane $N_m = \sqrt{N_e N_o}$	H_2SO_4	H_2O	H_2SO_4	H_2O
0	6.55	2.15	4.75	5.6	0.200	1.84	0.856	3.30
12	7.4	4.9	5.7	6.5	0.744	2.81	1.344	4.28
12	7.1	5.0	6.2	6.6	0.976	3.62	1.832	5.28
24	6.6	4.45	5.0	5.75	1.228	5.12	1.84	6.82
60	6.7	6.35	5.0	5.8	3.104	8.76	3.68	13.6

	Net Rates, Gms/Amp-Hr-Cell	
	H_2-Side	O_2-Side
H_2SO_4	0.048	0.074
H_2O	0.115	0.174
Total	0.163	0.221

7.0 Five-Cell Battery Tests

The test rig was modified to permit handling several 5-cell batteries simultaneously. Techniques for assembling and filling the batteries were tested and finalized. Two batteries were assembled during the month of March, 1963 and subjected to 100-hour performance tests at the prescribed current density of 24 amps/ft^2. The effect of varying some of the flow parameters was also investigated. Three additional batteries were constructed and run successfully for over 100-hours each during the month of April. A total of 893 hours at 24 amps/ft^2 was logged on these 5- cell batteries.

7.1 Assembling and Filling 5-Cell Batteries

Forms and systems were devised and employed to provide multiple quality assurance checks during the assembly of the batteries. All compartments and electrodes were individually identified and their correct emplacement with regard to location, direction and right or left handedness within the battery stack was verified and recorded.

The electrolyte compartments were filled by sucking 6N H_2SO_4 up through the acid inlet manifold with the aid of a slight vacuum (13.2 psia) applied to the acid exit manifold. The filling rate was adjusted by means of a variable constriction in the acid inlet line to about 20 ml/min. Prior tests with a dummy electrolyte compartment faced with a lucite cover plate showed that this technique would result in bubble-free filling of the electrolyte compartments.

The work with this dummy compartment also suggested a modification in the design of the top (exit end) of electrolyte compartments. A slight "cathedral ceiling" (mid-point raised 3/16" above the horizontal)would facilitate the removal of any gas bubbles that might otherwise remain in the compartment. Such a modification in the design of electrolyte compartments has been adopted and implemented.

After filling a battery, the inlet acid manifold was closed and the vacuum on the electrolyte compartments maintained for some time in order to check that gas would not leak into the electrolyte compartments through possible defects in the membranes or through cross-leaks in the manifold system or through the

side walls of the cell assembly. If gas bubbles appeared in the electrolyte exit manifold, or if electrolyte would flow out of this manifold (indicating internal gas bubble appearance), suitable steps were taken to close off the particular leak in question. All batteries were "bubble-tight" prior to installation on the test rig.

7.2 Humidification

In an actual H_2-O_2 fuel cell system using a Dual-Membrane Fuel Cell Battery, the H_2 and O_2 gases leaving the battery would be recycled. The gases entering the battery (consisting of make-up feed gases and recycle gases) would thus not be bone-dry but would contain water vapor. The test system used during this study did not involve gas recycle: initially bone-dry gases were fed to the fuel cells and the gases leaving were discarded. During the study, it was decided that a better simulation of an actual operation could be obtained if the entering gases were humidified so that they would also contain water vapor. Thus runs made on Battery 3 and thereafter (and some earlier runs) used humidified gases. The gases were passed through flasks containing 3N sulfuric acid at the temperature of the cell. Sufficient disengaging space was available to prevent spray from being carried into the cell.

7.3 Results of 5-Cell Battery Tests

The data from all of the 5-cell battery tests have been summarized in three tables. Table 7.1 describes the components of the batteries; Table 7.2 presents the operating conditions during the runs; and Table 7.3 gives the performance of the batteries. In text following, the performance of each battery is discussed separately.

7.3.1 Performance of Battery 1

Battery 1 contained teflon gas and liquid compartments and tantalum pusher and collector plates. The electrodes were made using the standard sintered electrode formulation. The battery was placed in a constant temperature bath at 60°C. Battery 1 performed satisfactorily from the start. A current density of 24

Table 7.1

Description of 5-Cell Battery Components

COMPONENT	BATTERY 1	BATTERY 2	BATTERY 3	BATTERY 4	BATTERY 5
End Plates	3/8" Stainless Steel				
Insulators	60 mil Butyl Rubber				
Pusher and Collector Plates	10 Mil Tantalum	10 Mil Tantalum	10 Mil Niobium	10 Mil Tantalum	10 Mil Zirconium*
Electrodes	Standard Sintered Teflon				
Membranes	61 AZG**	61 AZG	61 AZG	61 AZL***	61 AZL
Gas Compartments	64-65 Mil Teflon	64-65 Mil Teflon	64-65 Mil Teflon	60-65 Mil Penton	64-65 Mil Teflon
Electrolyte Compartments	118-133 Mil Teflon	99-102 Mil Teflon	118-133 Mil Teflon	110-115 Mil Penton	99-102 Mil Teflon
Trilok Filler	Type 6027-1-1				
	2 pc/cell	1 pc/cell	2 pc/cell	2 pc/cell	2 pc/cell
Gaskets and Grommets	8 Mil Dacron-Backed Viton****				

* In Run 58, Tantalum Terminal Collector and Pusher Plates were used (see Text).

** IONICS 8 oz. Glass-Backed Membrane.

*** IONICS Dynel-Backed Membrane

**** Four Grommets used for each Collector Plate.

Table 7.2

Operating Conditions of 5-Cell Battery Tests

RUN NUMBER	1A	1B	1C	2A1	2A2	2B	2C	3A	3B	4A	4B	4C	5A1	5A2	5B
Feed Rates															
H_2 liters/min	2.1	0.55	0.90	2.2	2.2	2.1	2.0	2.1	2.1	2.2	2.1	2.0	1.2	2.1	2.2
O_2 liters/min	1.02	0.21	0.44	1.05	1.05	1.0	1.1	1.1	1.1	1.0	1.2	1.0	0.8	0.65	1.0
Electrolyte ml/min	60	7	7	60	60	8	27	24	10	30	12	8	30	10	11
Pressures															
H_2, psig	5.0	5.0	5.0	2.5	3.0	3.1	5.4	5.1	5.2	5.2	5.5	5.0	4.8	5.2	4.9
O_2, psig	5.0	5.0	5.0	2.1	3.2	3.1	5.2	4.9	4.8	4.7	5.0	5.1	5.0	4.5	4.8
Electrolyte, psig.															
High	5.1	5.1	5.1	5.1	3.0	5.5	5.5	5.2	5.1	5.3	5.4	5.4	5.2	5.2	5.4
Low	4.7	4.7	4.7	4.7	3.0	4.5	4.5	4.4	4.5	4.0	4.5	4.1	4.5	4.5	4.8
Current Load															
Amps/ft^2	24	24	24	24	24	24	24	24	24	24	24	24	24	24	24
Bath Temp.^oC	60	60	60	30	30	60	30	60	30	60	30	60	30	60	30
Duration, Hours	112	24	27	48	52	100	16	133	51	134	17	26	16	20	117
Humidification	No	No	No	No	No	Yes	No	Yes	Yes	Yes	Yes	Yes	Yes	Yes	Yes

Table 7.3

Performance Data From 5-Cell Battery Tests

RUN NUMBER	1A	1B*	1C	2A1	2A2	2B	2C	3A	3B	4A	4B	4C	5A1	5A2	5B
Pressure Drop (mm H_2O)															
H_2	46	15	25	50	50	81	67	125	100	140	53	280	32	27	58
O_2	60	14	30	100	100	142	123	115	140	150	132	172	57	42	66
Electrolyte	175	52	52	--	--	--	--	95	--	--	--	--	--	--	--
Voltage (Ave. @ 24 A/ft^2)															
Cell 1	.670	.684	.684	.670	.678	.680	.648	.790	.728	.712	.710	.702	.614	.632	.695
Cell 2	.745	.760	.753	.795	.785	.742	.728	.820	.765	.694	.694	.661	.722	.727	.720
Cell 3	.715	.728	.726	.670	.690	.717	.704	.804	.764	.718	.698	.633	.701	.708	.704
Cell 4	.700	.718	.716	.790	.770	.764	.722	.802	.747	.681	.670	.653	.716	.721	.710
Cell 5	.730	.740	.726	.658	.650	.712	.672	.789	.744	.700	.691	.690	.627	.640	.682
Total	3.560	3.630	3.605	3.585	3.575	3.615	3.474	4.005	3.748	3.505	3.483	3.339	3.380	3.428	3.511
Conductance (mhos/ft^2															
Cell 1								294		200		223			
Cell 2								415		174		213			
Cell 3								364		200		229			
Cell 4								425		109		223			
Cell 5								375		186		208			
Total								73.7		33.3		43.5			

*Operation unstable, occasional gas surges needed to clear ports.

amps/ft^2 was maintained at better than 3.5 volts throughout the 165 hours that the battery was on test. This may be compared with the 3.4 volts for a 5-cell battery that corresponds to the average cell voltage of 0.68 volts required for the 10-cell Demonstrator Battery. Figure 7.1 shows a plot of individual cell voltages and of battery voltage versus time. The separate data points are not connected as the particular voltage-time histories are quite convoluted.

The gas-side pressure drops were quite low; on the order of 50 mm H_2O at flow rates of 2 liters/min of H_2 and 1 liter/min of O_2. These pressure drops are shown in Figure 7.2.

During the first 113 hours, Battery 1 was run with gas rates of about 12 times the gas consumption rates - flow rates of approximately 2 liters/min. of H_2, 1 liter/min. of O_2 - and a fairly high electrolyte rate of 60 ml/min. (Run 1-A). Thereafter the gas rates were cut down to about 3 times the consumption rate (Run 1-B) and then upped again part way to about 6 times the consumption rate (Run 1-C). For both 1-B and 1-C, the electrolyte rate was reduced to 7 ml/min.

Operation at the low gas rate (1-B) was not stable: every 8 hours or so the voltage developed in one cell would start to drop, apparently due to liquid accumulation in the gas compartment. A sudden short decrease in downstream pressure would result in a rapid discharge of liquid and return of the cell voltage to normal. At the high and intermediate rates (1-A and 1-C) no such instability occurred, apparently the more significant gas compartment pressure drops (60 and 30 mm H_2O vs. 14 mm H_2O in 1-B) were sufficient to ensure adequate purging of liquid from the gas compartments.

The voltages developed showed no trend with time. They were somewhat higher for 1-B and 1-C than for 1-A. This may be due to the higher internal temperature resulting from a decrease in electrolyte flow rate. The pressure drops measured across the gas compartments agreed with those obtained in the single cell made of some of the same components (Cell E1685). The battery voltages and gas pressure drops are shown in Figure 7.3.

The electrolyte pump operation was such that the pump would operate in either one of two modes. It would either operate continuously giving a fairly constant

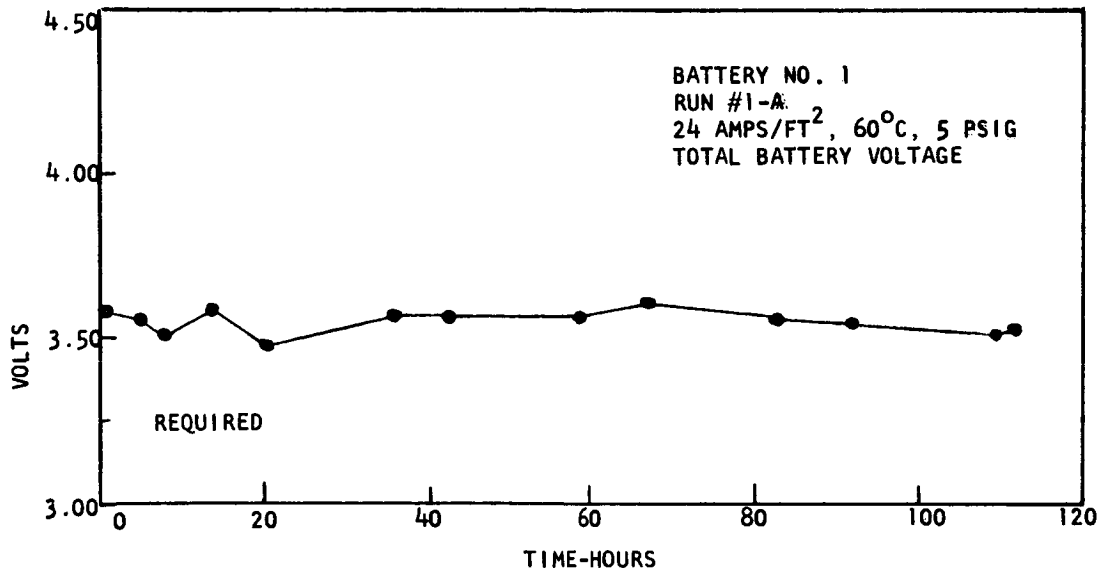

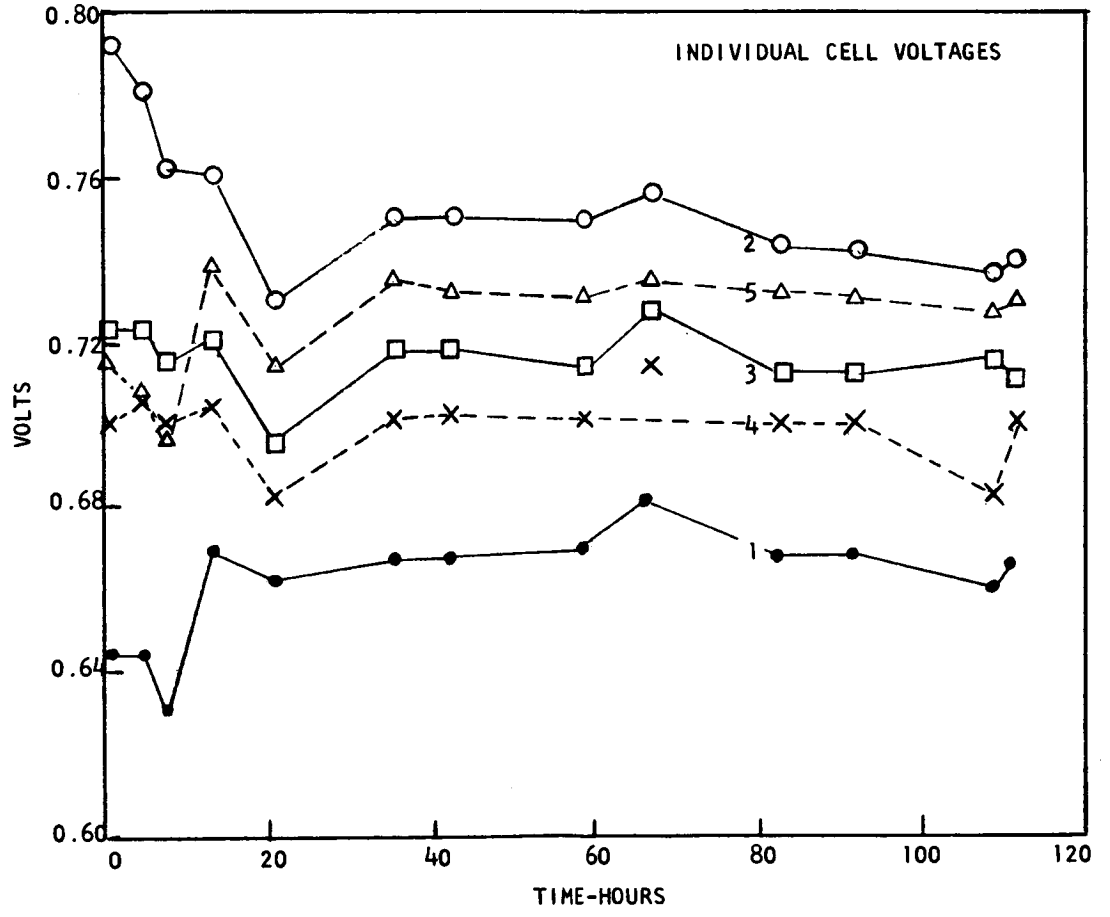

Figure 7.1 Battery 1 Voltages

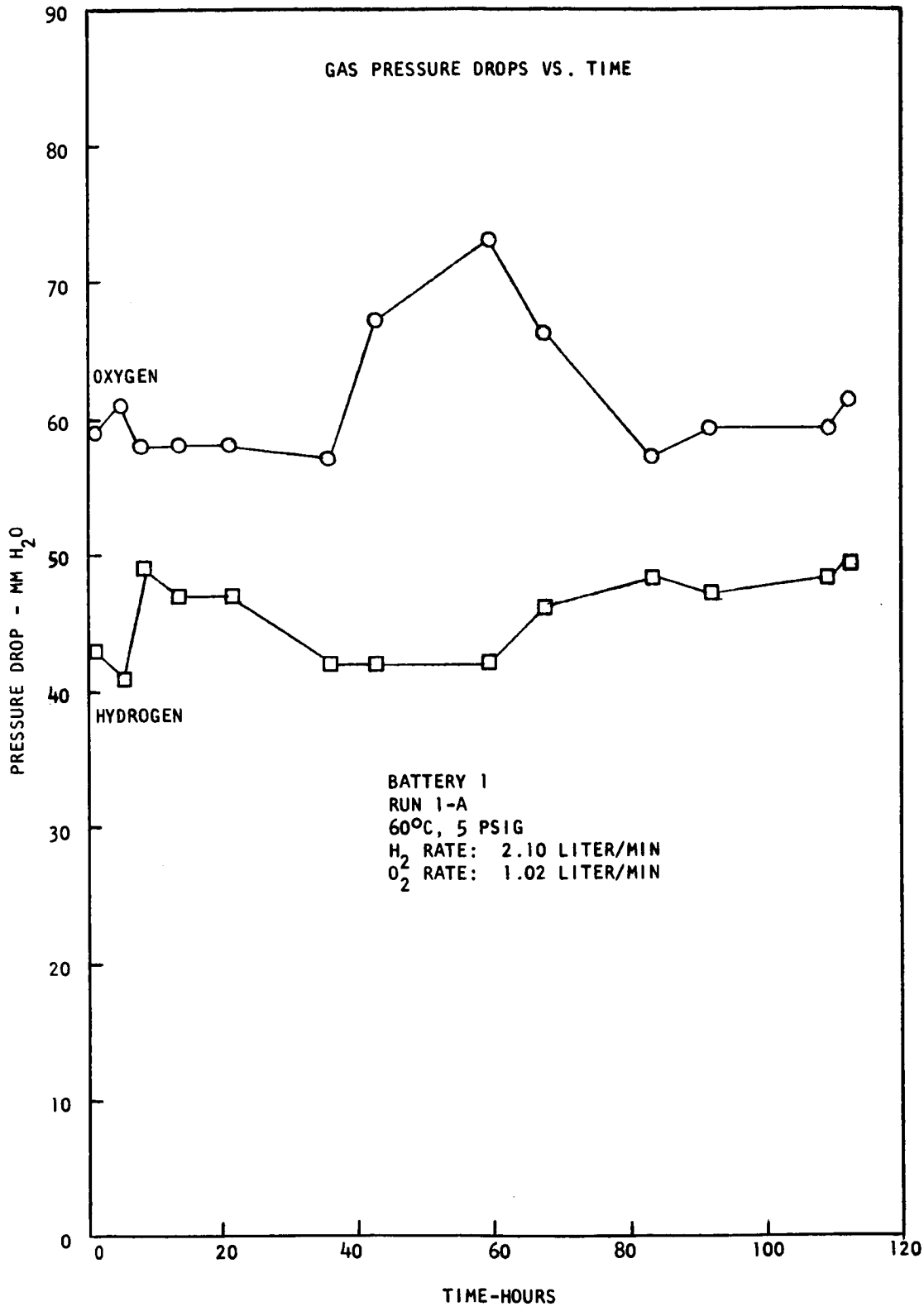

Figure 7.2 Gas Pressure Drops Vs. Time

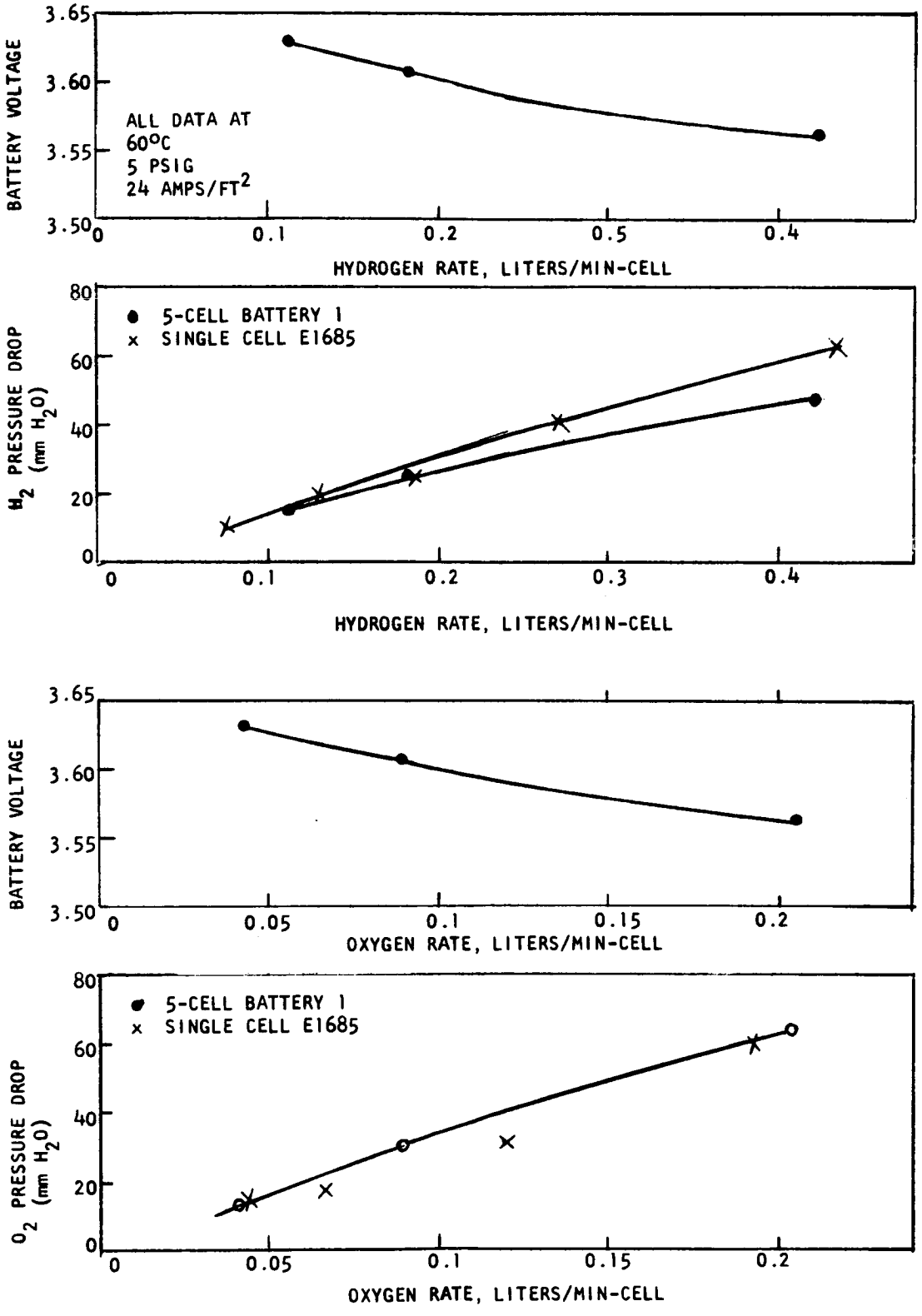

Figure 7.3 Effect of Gas Rates

pressure drop through the battery, or it would pump intermittently, being controlled by high and low pressure relays. This second mode of operation would give a pressure drop cycling in level between high (pump pumping) and low (pump not pumping).

7.3.2 Performance of Battery 2

Battery 2 was similar to Battery 1 except that the electrolyte compartments were thicker in the latter (roughly 1/8" vs. 1/10") and contained two layers of trilok instead of one. The battery was operated in a bath at 30°C.

Battery 2 did not give quite as satisfactory performance. Initially, fairly stable operation could only be obtained by running the electrolyte compartments at a slightly higher pressure than the gas compartments (about 5 psig vs. 2.3 psig). Even so, a slight deterioration in voltage with time was observed. After 48 hours of this sort of operation (Run 2-A-1) performance became erratic for 4 hours but was brought back to an acceptable level by eliminating the deliberate pressure imbalance. The second half of 2A (Run 2-A-2) was then completed. The initial requirement for a pressure imbalance suggests that contact between electrodes and membranes was not as good as it should have been. However, Battery 2 did complete 100 hours at 30°C and a current density of 24 amps/ft^2 while developing a voltage averaging over 3.5 volts. The voltages developed during Run 2A are plotted in Figure 7.4.

Following Run 2A, the temperature on Battery 2 was increased to 60°C. The electrolyte rate was reduced to between 5 to 10 ml/min. This resulted in the pump pumping only intermittently, with its on-off cycling determined by a pressure sensor. The pressure sensor was set to keep the electrolyte stream between 4.5 and 5.5 psig. The gases were humidified. These conditions were maintained for 100 hours and constitute Run 2B.

Finally the cell temperature was dropped to 30°C, the electrolyte flow rate was increased to 27 ml/min., the gas pressures were raised to 5 psig to eliminate the pressure imbalance and the humidifiers were removed from the gas feed system. These conditions, constituting Run 2C, were maintained for another 16 hours. This run was finally terminated to make space for Battery 5.

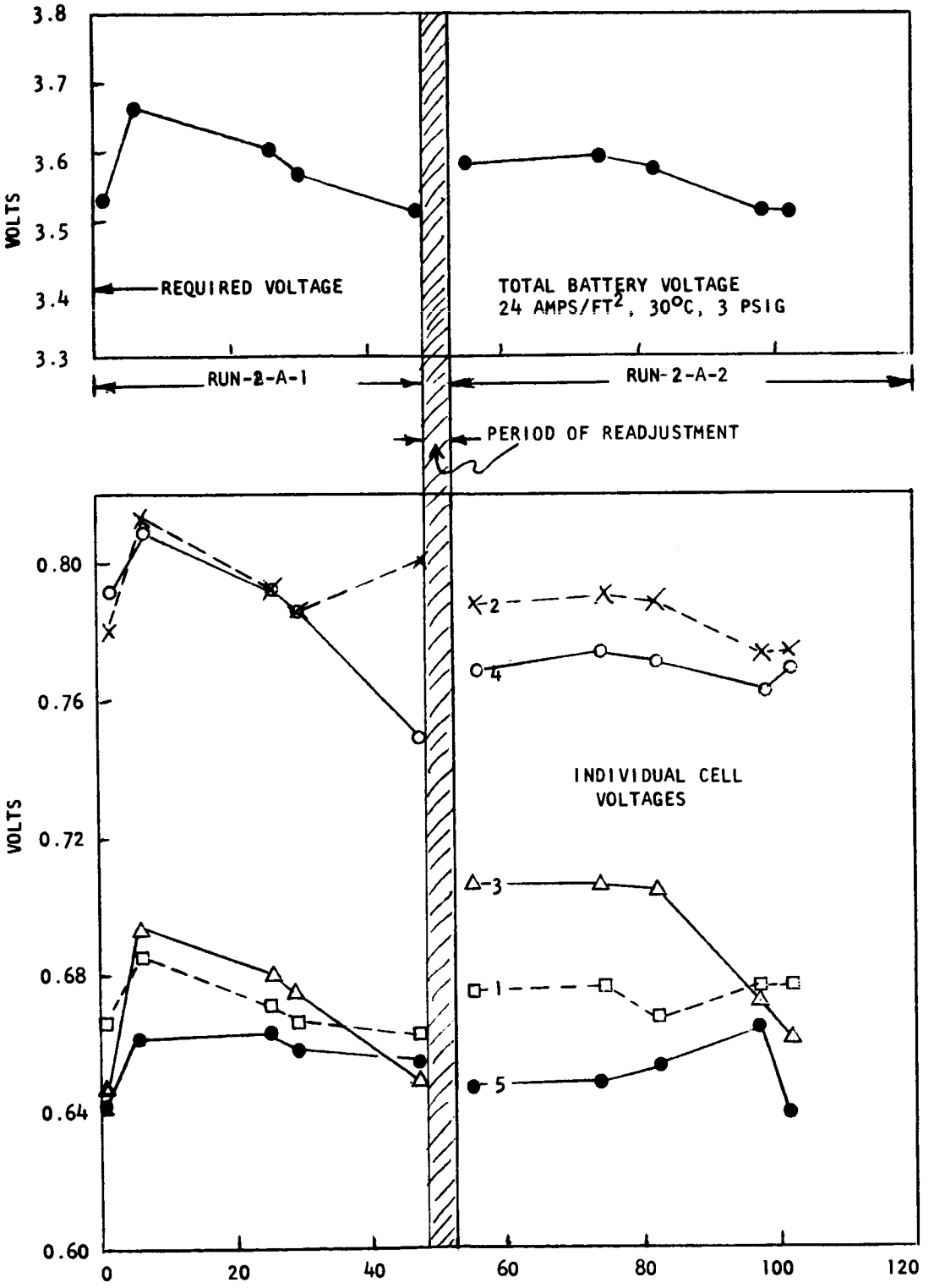

Figure 7.4 Battery 2 Voltages

The average voltage under load produced by the cell in Run 2B was 30 millivolts higher than the voltage maintained in Run 2A. This may be due to the higher bath temperatures or the lower electrolyte rate (i.e., higher internal temperature). However, in contrast to the relatively small and random variation of voltage in 2A, the voltage in 2B drops steadily from a value near 3.9 to just below 3.4 volts at the end of the run. The voltages produced in Run 2B are shown in Figure 7.5.

The voltage in the recapitulation run, 2C, is 100 millivolts below that in 2A. Over the 16 hours that the cell was run at 30°C, the voltage rose slowly, and given time, might have reached the value observed in Run 2A. The gas pressure drops in Run 2B were similar to, but slightly higher than those measured in Runs 2A and 2C.

7.3.3 Performance of Battery 3

Except for Niobium pusher and collector plates, Battery 3 was identical in construction to Battery 1.

This battery was first operated for 133 hours at 60°C (Run 3A). After this, a polarization curve was taken, the cell was leak-tested, and a run at 30°C was begun (Run 3B). After 51 hours of operation, a cell failure forced the termination of the run. The voltages produced in Runs 3A and 3B are given in Figures 7.6 and 7.7.

Two system failures occurred during these runs. In Run 3A, the hydrogen humidifier in the constant temperature bath accidentally upset, sending 3N sulfuric acid through the hydrogen compartments. The cell recovered from this accident rapidly, giving 0.1 volt increase in voltage for a short time after the gas flow was restored.

Run 3B was terminated by a series of events triggered by a failure in the electrolyte circulating system. A leak in the circulating system led to the loss of all of the electrolyte. The loss of electrolyte pressure should have resulted in the shutting-off of the gas feed lines. For an as yet undiscovered reason, the emergency solenoids did not close and gas flow continued. The membranes were no longer kept wet by electrolyte and acted as though they were in a

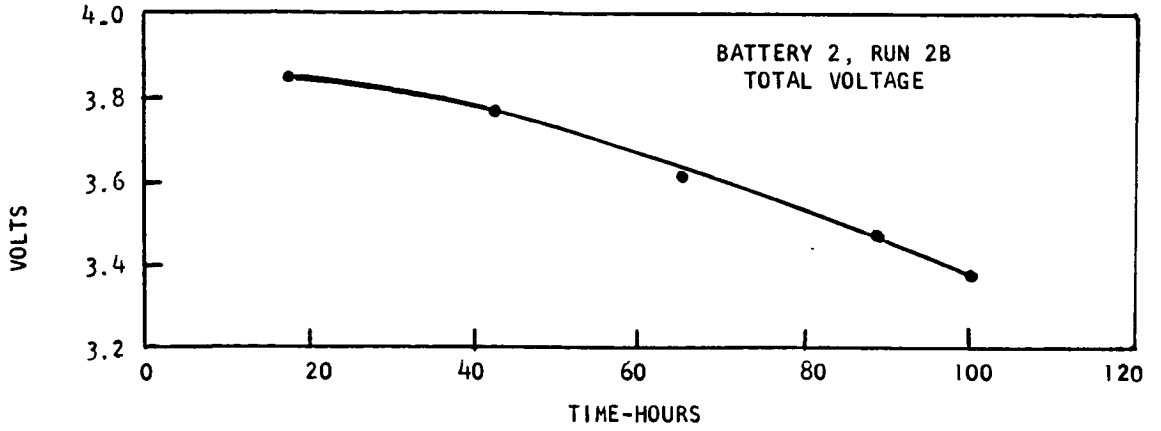

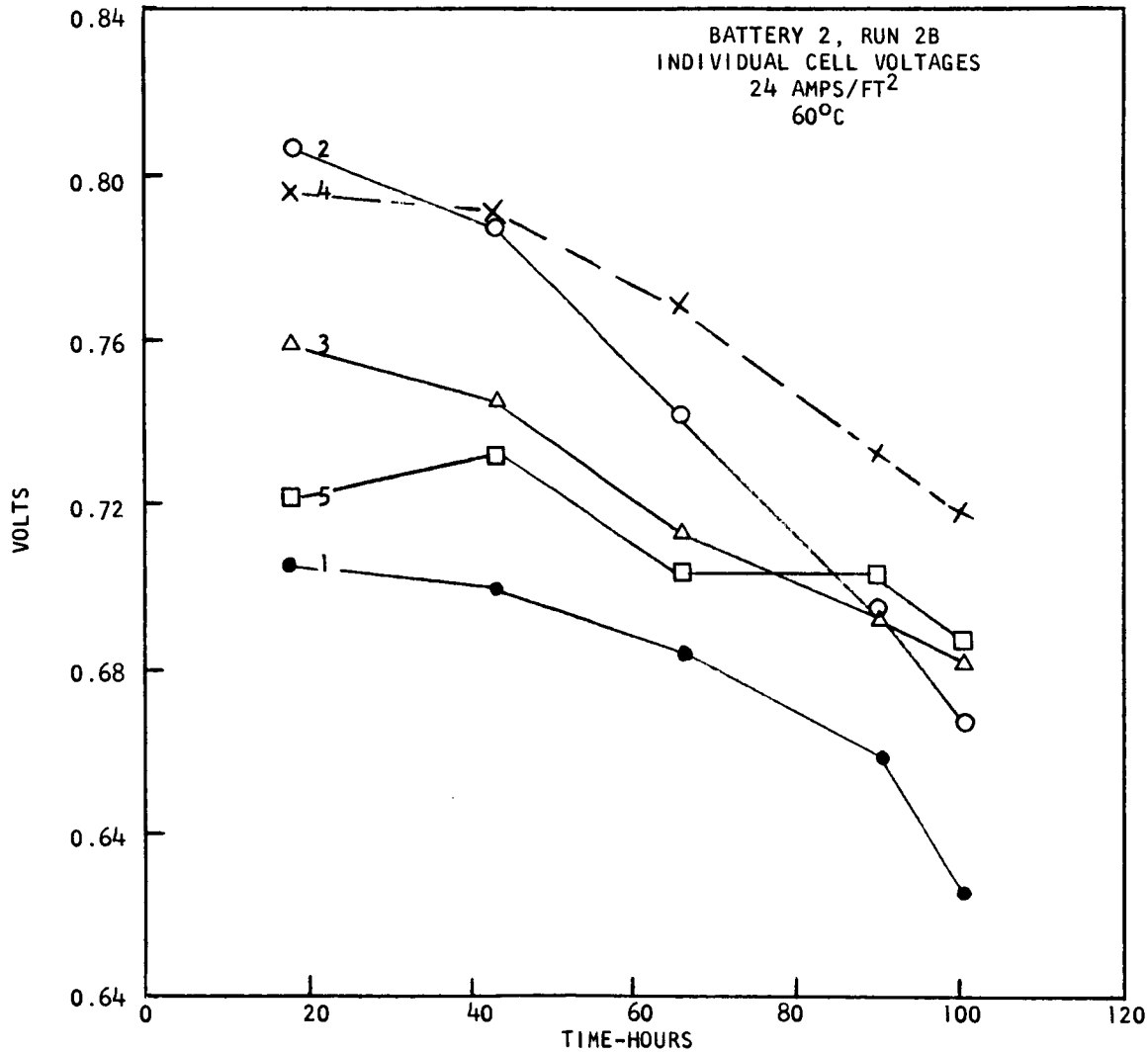

Figure 7.5 Battery 2 Voltages

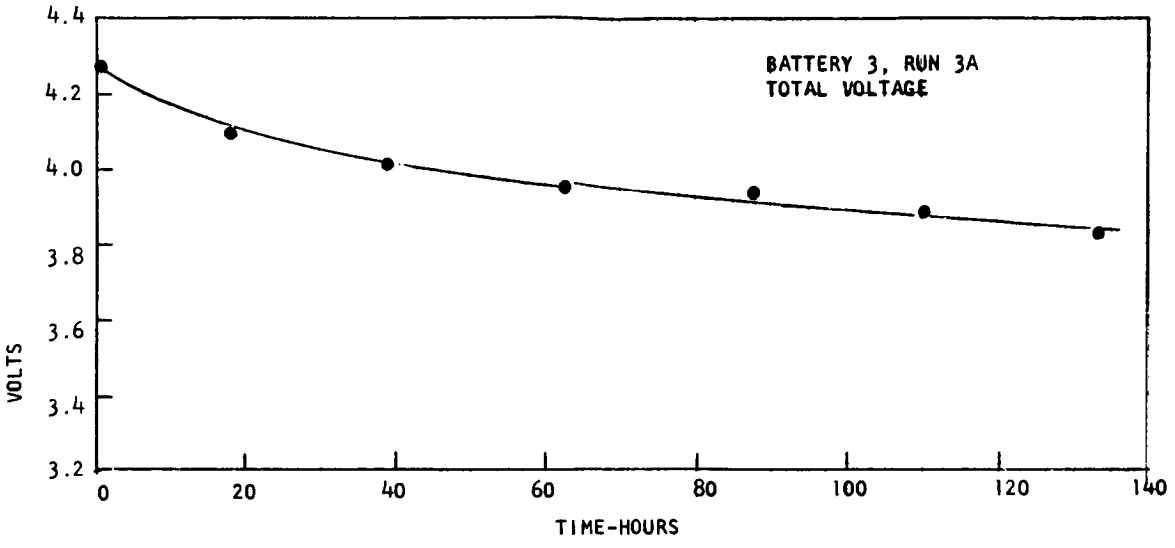

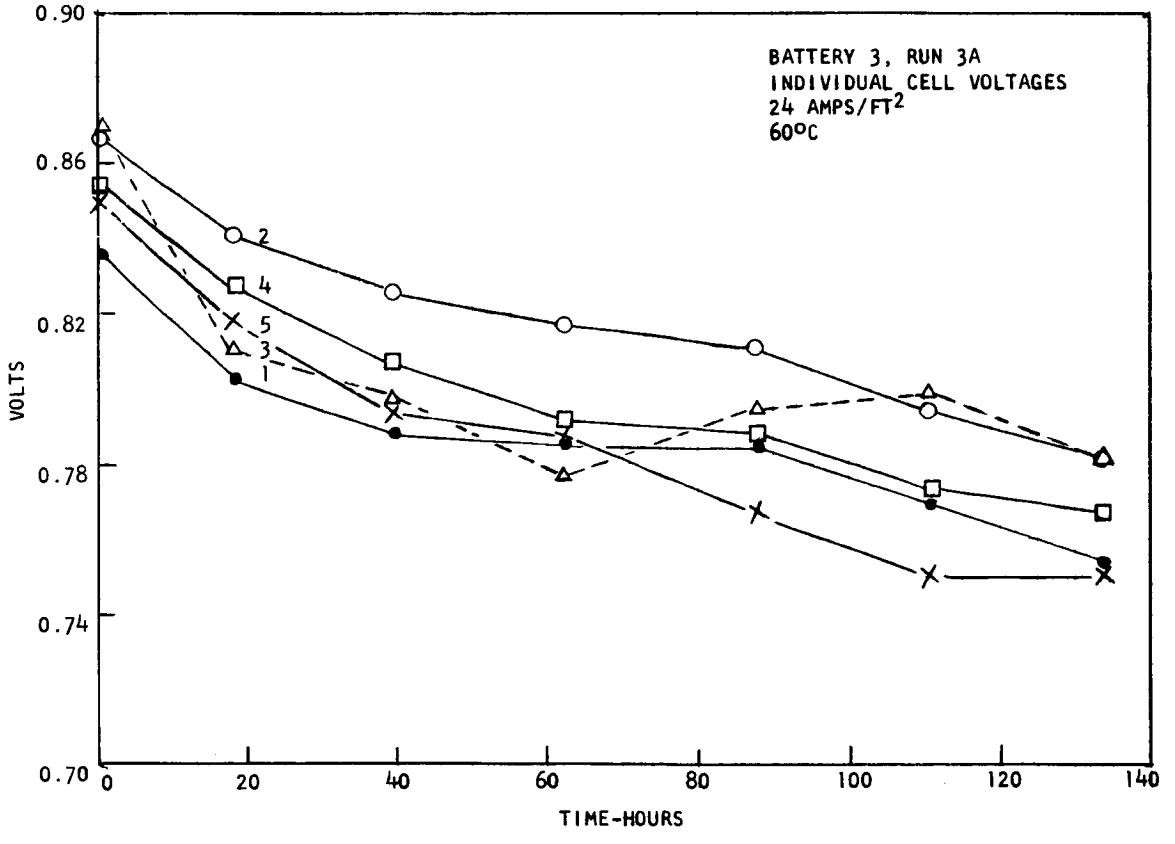

Figure 7.6 Battery 3 Voltages

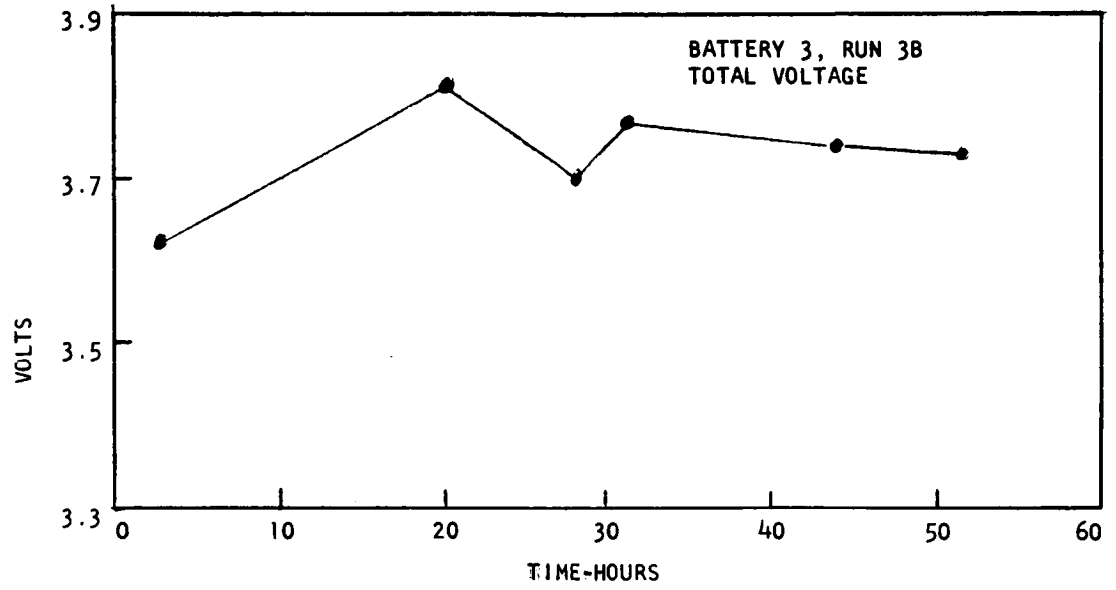

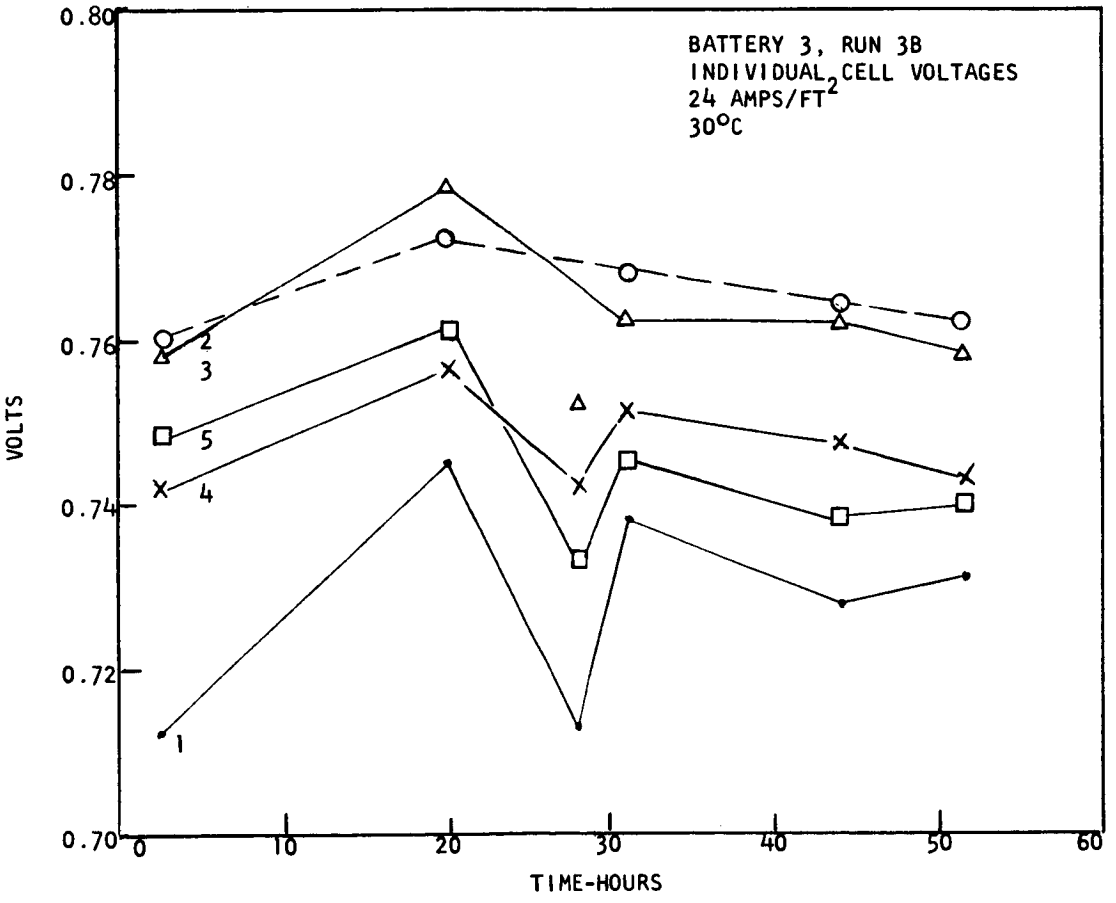

Figure 7.7 Battery 3 Voltages

single membrane fuel cell, i.e., they eventaully dried out and cracked, allowing the hydrogen and oxygen streams to mix in the presence of the platinum black catalyst and burn. The fire within the battery destroyed the membranes and most of the trilok spacer mesh.

The voltage under 24 amps/ft^2 load averaged 4 volts during Run 3A. The voltage showed a slow decline from almost 4.3 volts to 3.84 volts after 133 hours. The polarization curve, Figure 7.8 was measured directly after this run and showed a specific conductance of 73.7 mhos/ft^2. This equals an average of 369 mhos/ft^2 per cell which is considerably higher than had been measured for any single cell. A power density curve is presented in Figure 7.9.

Run 3B, at 30°C, produced a lower, but relatively stable, voltage centering about 3.74 volts.

For a leak test, the cell was submerged in water in the constant temperature bath and carefully observed for leaks. Approximately 2 cc/hr of gas was seen which could not be clearly attributed to electrolysis of the bath water caused by the 4 volts existing between the terminal collector plates.

The gas pressure drops were, on the average, higher than in previous cells. A very marked trend is seen in Run 3A (Figure 7.10) where the oxygen pressure drop increased from 75 to 140 mm water and the hydrogen pressure increased from 95 to 140 mm water over the course of the run. No such relationship existed in Run 3B. (Figure 7.11) The cause for the slowly increasing pressure drop in Run 3A is unknown, as is the cause for the slowly decreasing voltage during that run. It is not known whether the two effects were related.

7.3.4 Performance of Battery 4

This battery used penton compartments and dynel-backed membranes. Battery 4 was first run for 134 hours in a 60°C bath (Run 4A). A polarization curve was recorded and the battery was leak-tested. The battery was then run for 17 hours at 30°C, enough to reach steady-state operation (Run 4B). Then the bath temperature was raised to 60°C, the leak-test was repeated and another polarization curve was recorded. The cell was then run again at 60°C for 26 hours (Run 4C). This test was terminated when some of the components were

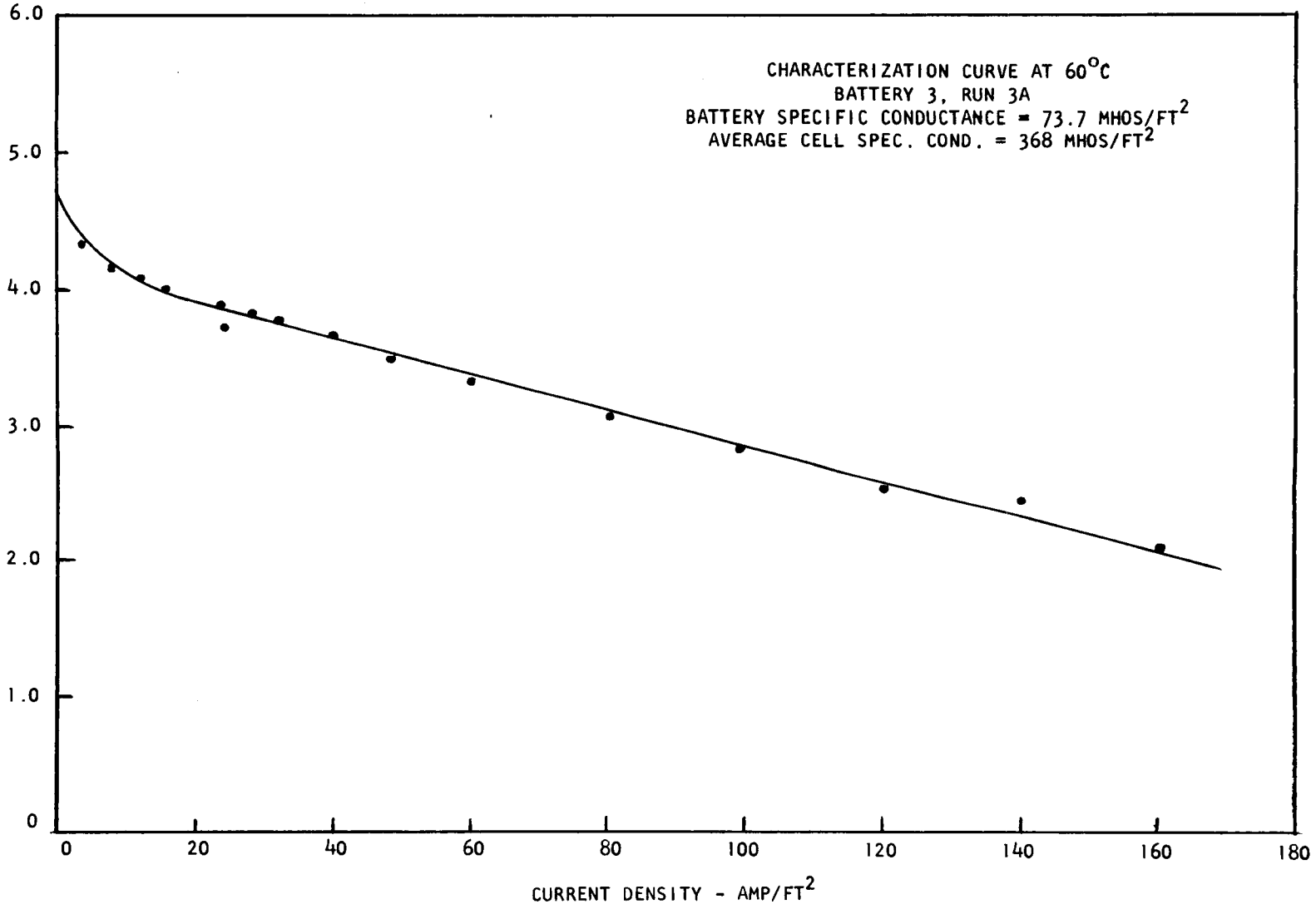

Figure 7.8 Characterization Curve at 60°C

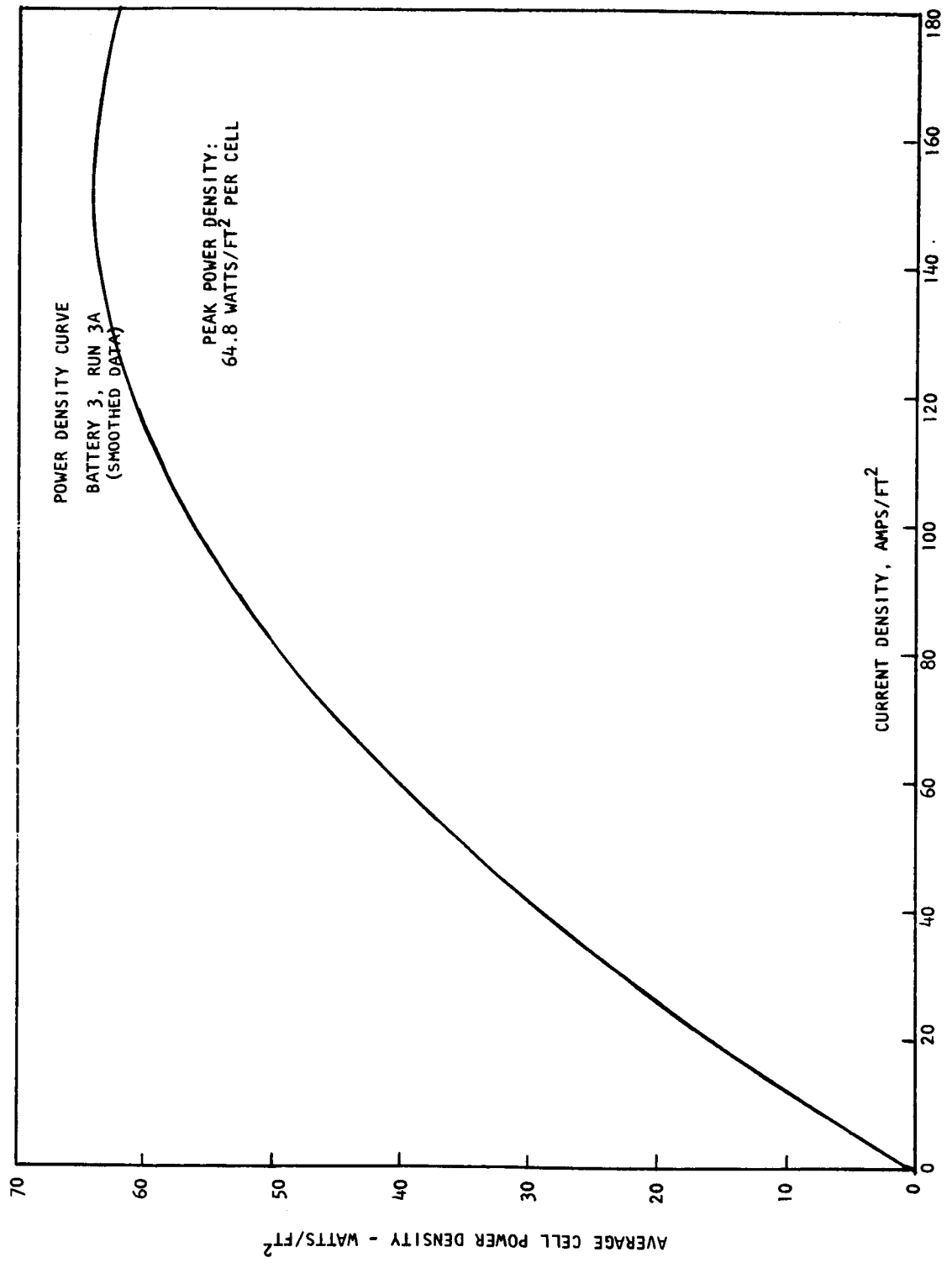

Figure 7.9 Power Density Curve

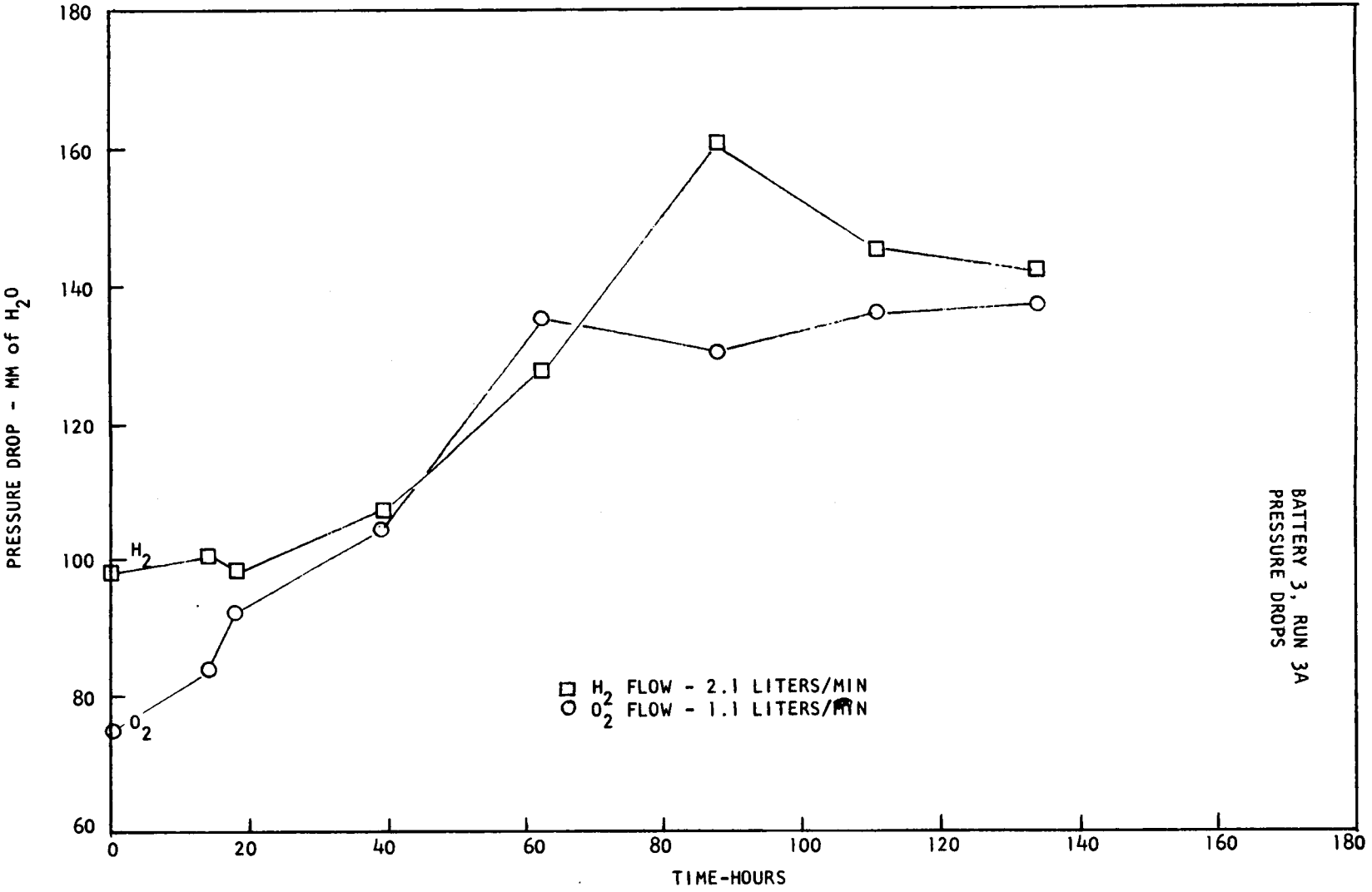

Figure 7.10 Battery 3, Run 3A Pressure Drops

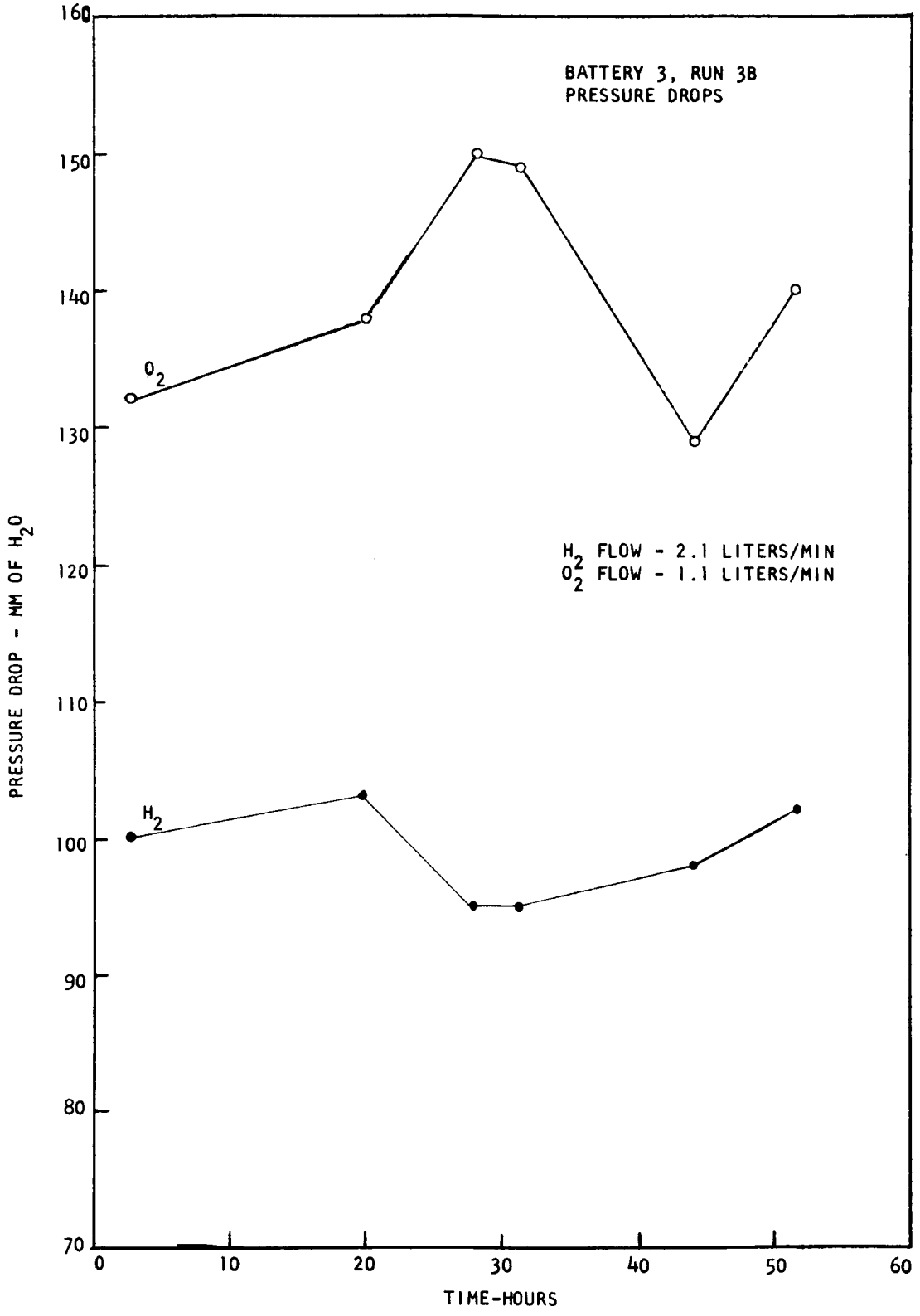

Figure 7.11 Battery 3, Run 3B, Pressure Drops

needed for the assembly of another battery.

The average voltage for the 134 hour Run 4A was 3.5 volts, lower by almost 100 millivolts than Batteries 1 or 2 under similar conditions. (Figure 7.12) Only for a brief period after 100 hours did the voltage drop below 3.4 volts. During the interval at 30°C, the voltage was almost as high, 3.48 volts. However, when the temperature was restored to 60°C, only 3.339 volts were recorded.

Figs.7.13&7.14 show data recorded before and after the 30°C run. These indicate that some significant change occurred in the cell. The first shows a specific conductance of 33.3 mhos/ft^2, the second an increase to 43.5 mhos/ft^2. The voltages on these curves at 24 amps/ft^2 were 3.47 and 3.36 volts respectively. Thus, the polarization curves should cross, which they do at 40 amps/ft^2, indicating that above that current the cell operated better after temperature cycling. The cause of this behavior lies most likely in the position of the electrode-electrolyte interface, which has not been investigated sufficiently to warrant any detailed interpretation.

The leak test consisted, again, of submerging the cell completely in the bath. In both leak tests, a current of 20 amperes reduced the potential between the terminal end plates below that necessary for electrolysis, under which conditions no bubbles were observed rising from the cell.

The gas pressure drops in Run 4A average higher than those of Run 3. In Run 4B, they are almost identical to those of Run 2C. But there is a considerable increase, particularly on the hydrogen side in Run 4C. Upon disassembly, it was found that the gaskets had swelled over the gas inlet channels to the point where these channels appeared to be almost shut off. The swelling probably occurred as a result of heat generated within the cell during the taking of polarization curves. Figure 7.15 shows the log of the experiments carried out with Battery 4.

7.3.5 Performance of Battery 5

Battery 5 was similar to construction to Battery 2 except for the use of zirconium pusher and collector plates and dynel-backed membranes. This battery was intended to have gas and liquid compartments of halon. However, deliveries

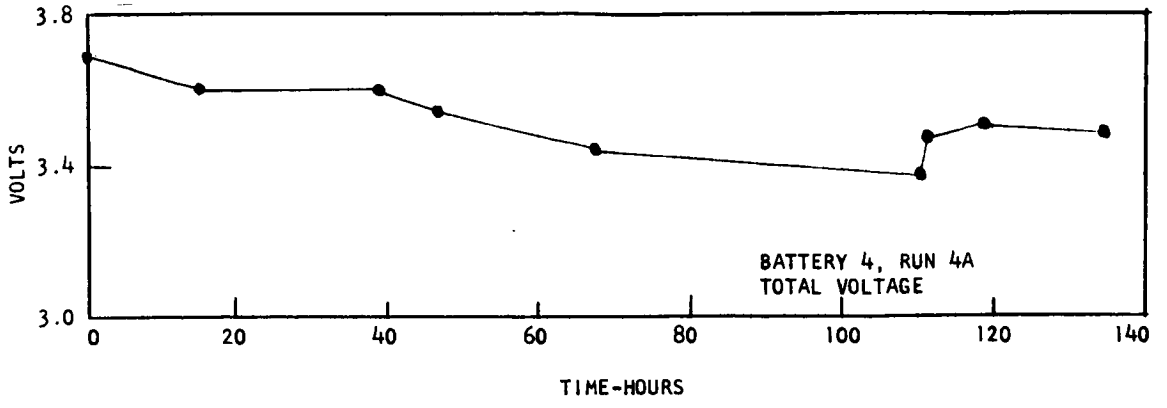

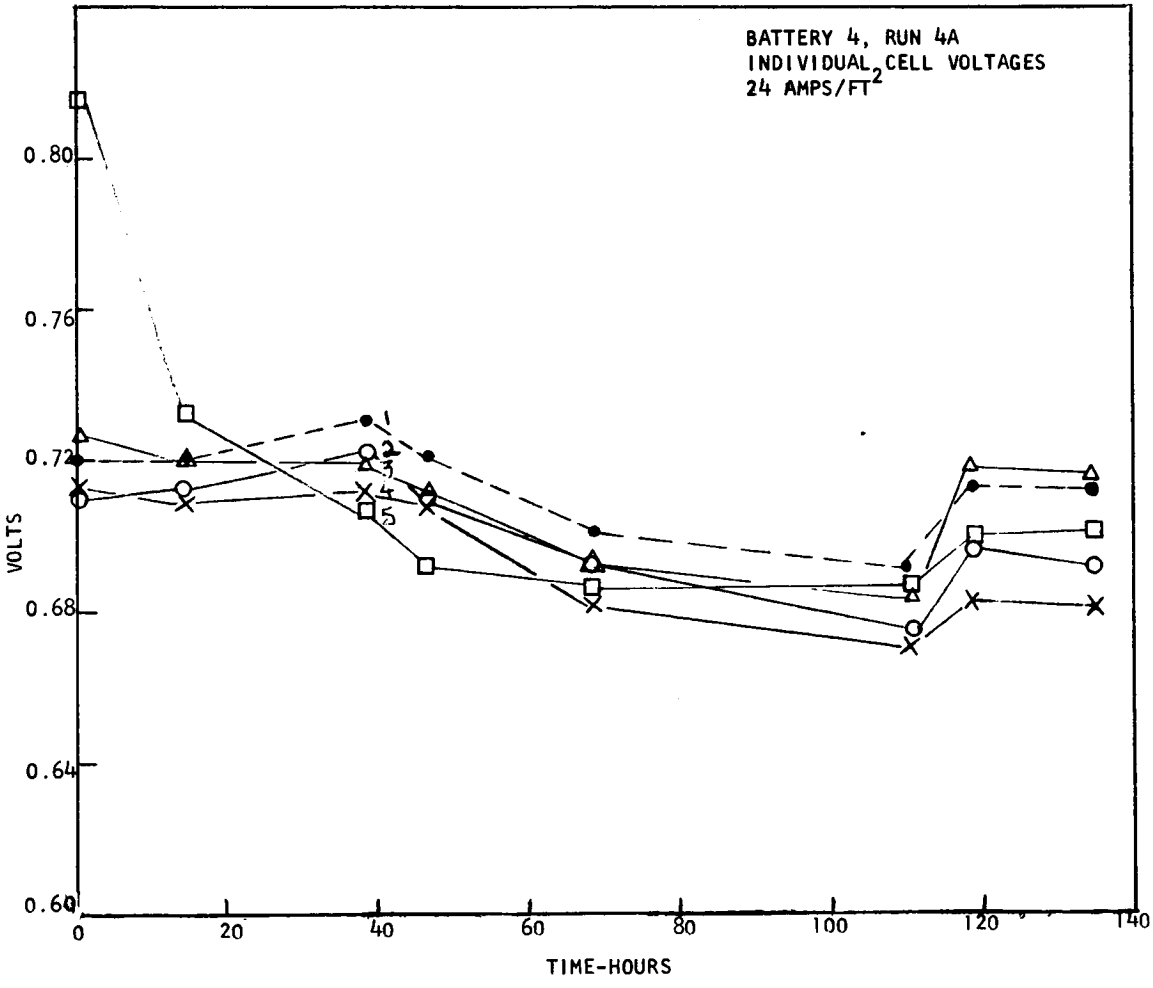

Figure 7.12 Battery 4 Voltages

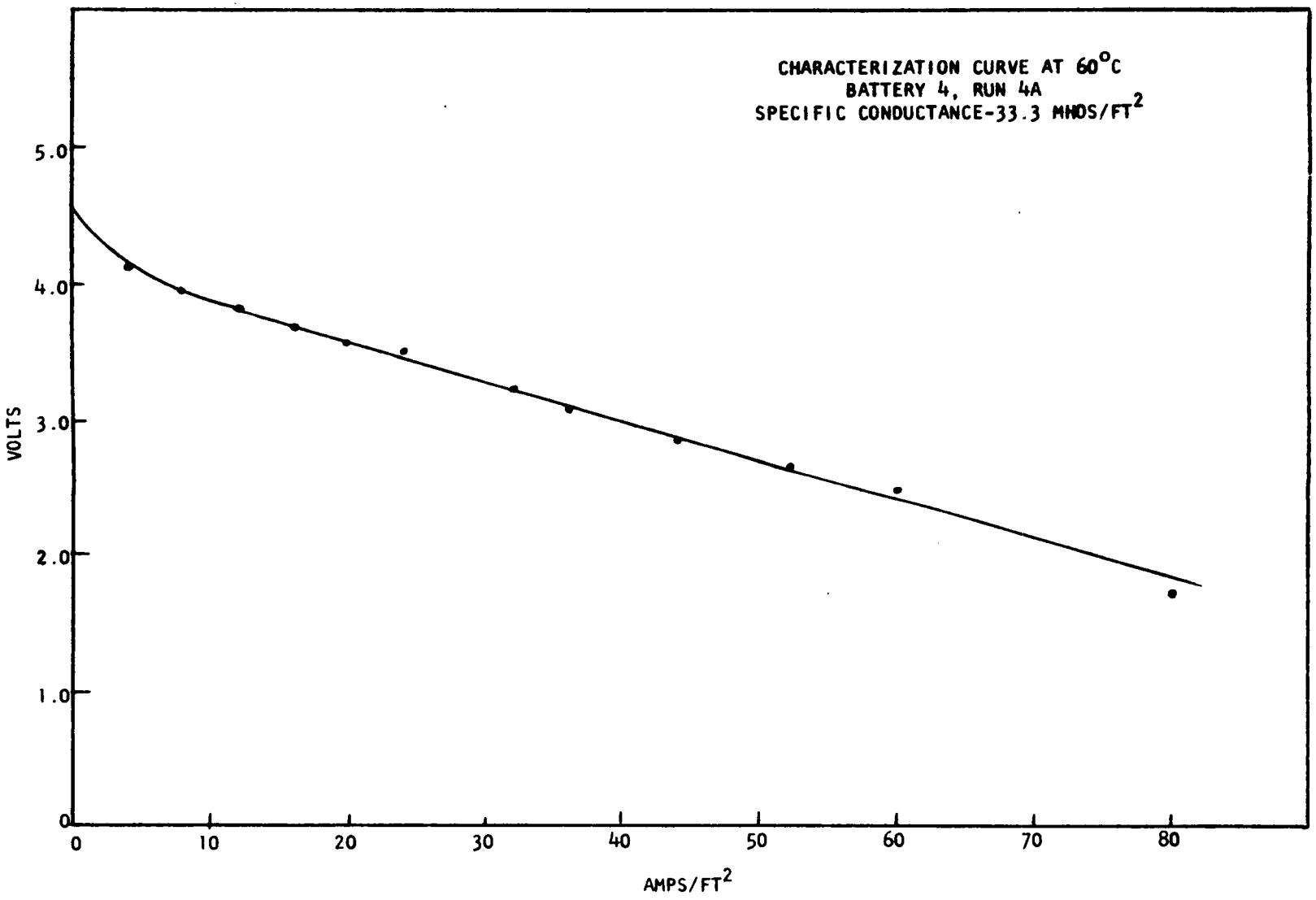

Figure 7.13 Characterization Curve at 60°C

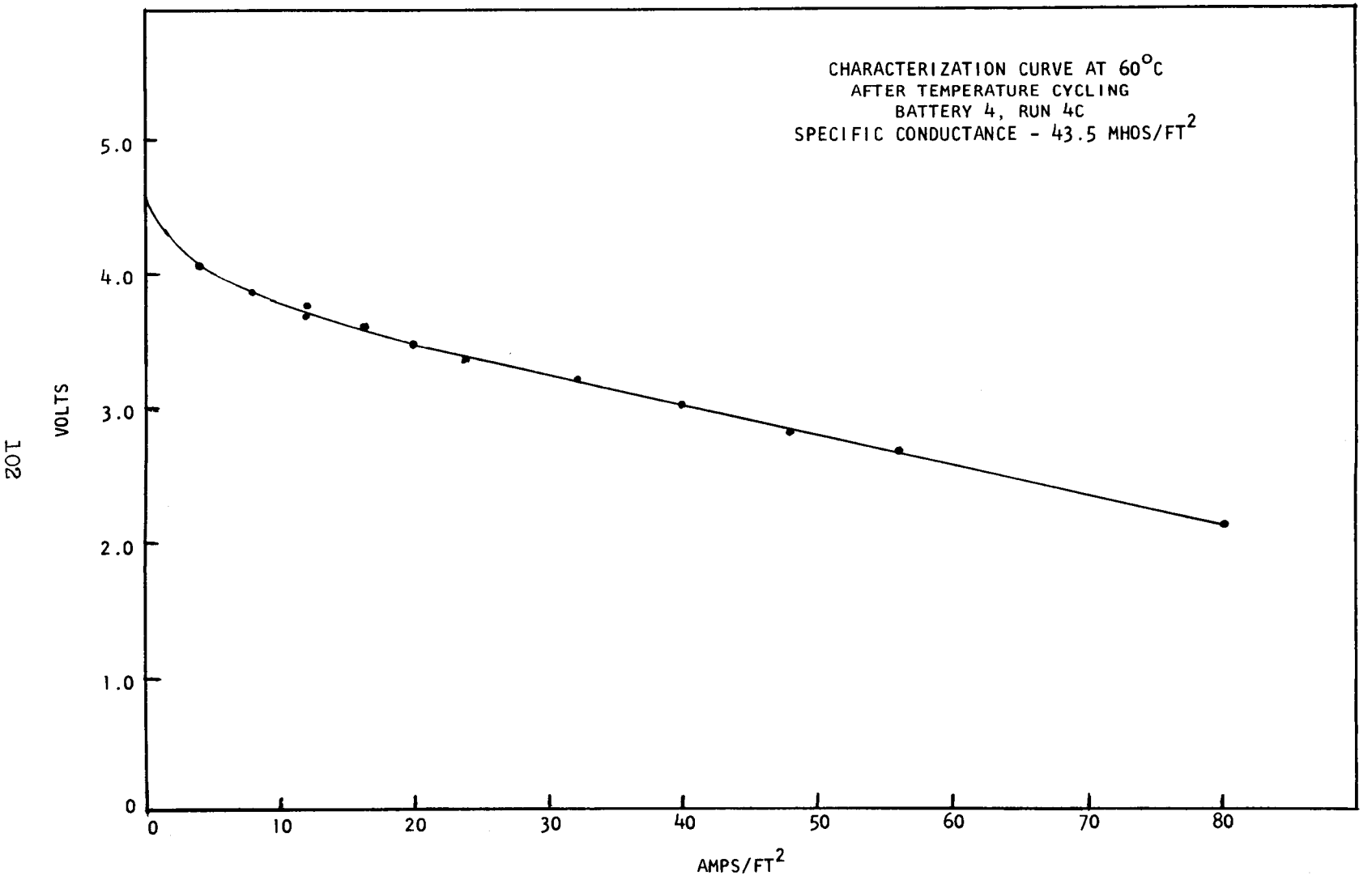

Figure 7.14 Characterization Curve at 60°C

HOURS	EVENT
0 - 134	Run 4A @ 60°C, 24 Amps/Ft^2
139	Polarization Curve @ 60°C
142	Leak Test @ 60°C, no observable leakage rate.
143 - 161	Run 4B @ 30°C, 24 Amps/Ft^2
163	Leak Test @ 60°C, no observable leakage rate.
164 - 168	Polarization Curve @ 60°C
168 - 211	Run 4C @ 60°C, 24 Amps/Ft^2

Figure 7.15 Log of Battery 4

of this material did not meet the quality assurance requirements so teflon components were substituted. Thus, halon compartments were not evaluated.

The first assembly of Battery 5 operated below 3.4 volts from the very beginning at 30°C, Run 5-A-1. To improve the performance, the bath was heated to 60°C. (Run 5-A-2). At this temperature, the cell voltage dropped from a starting high of 3.47 volts to 3.38 volts in 18-1/2 hours. Consequently, the cell was disassembled and two changes were made. The electrodes were shuffled and the oxygen electrodes which had shown the poorest performance were replaced. It has been noticed that the oxygen electrode in a cell exerts considerably more influence over the performance than the hydrogen electrode. Consequently, unsatisfactory oxygen electrodes can be used on the hydrogen side with little bad effect. It was also observed that the zirconium collector plates, because of the relatively higher resistance of zirconium were lowering the voltage of the first and last cells of the battery by about 30 millivolts each. Since the current path in the terminal collector plates is considerably longer than in any interior collector plate, the resistance there is more important; furthermore, considerable electrolysis had occurred along the edges of the collector plates accompanied by noticeable removal of metal. To avoid both of these difficulties, terminal collector and pusher plates of tantalum were substituted. After these adjustments, Run 5B was made, lasting for 117 hours. This run was terminated when the need arose for components for the 10-cell battery.

The electrical performance of Battery 5 was only marginal. (Figure 7.16) While no measurements taken with the calibrated potentiometer were poorer than the criterion of 3.4 volts at 6 amperes, the recorder, a less reliable instrument, showed several points below 3.4 volts. On two occasions surges of electrolyte and gas were used to improve the performance of the battery. A sudden opening and shutting of the exit valves led to a quick drop in pressure and a somewhat slower build up. During the "open" interval, a surge of liquid or gas would leave the battery, presumably carrying any partial obstructions with it.

The pressure drops measured in Run 5B averaged slightly higher on the hydrogen side and considerably lower (66 vs. 100 mm H_2O) on the oxygen side when

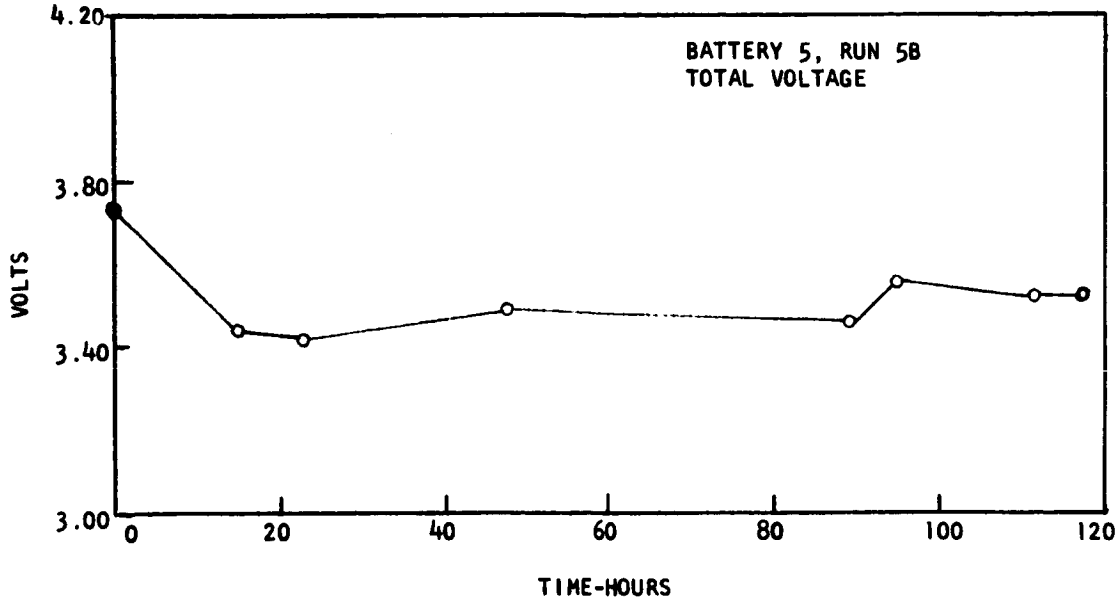

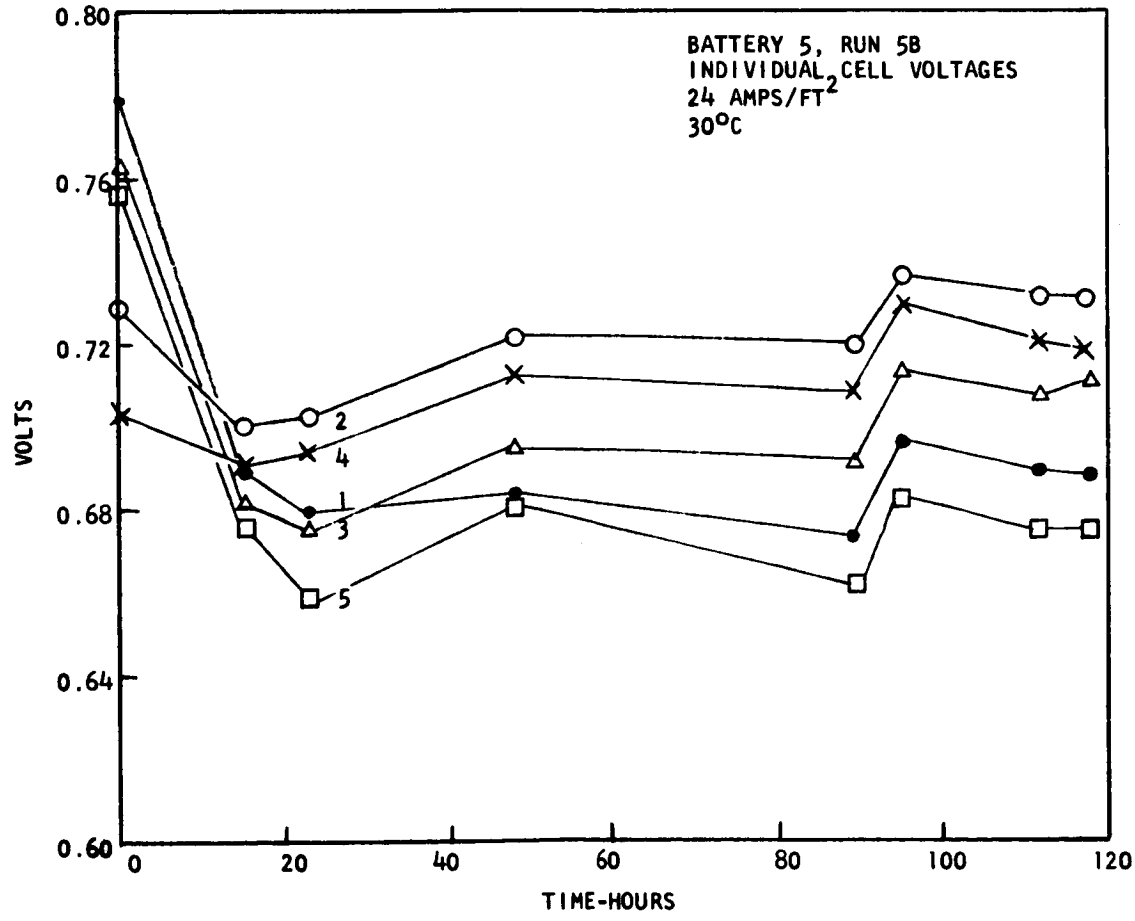

Figure 7.16 Battery 5 Voltages

compared to Run 2A.

.4 Overall Conclusions from 5-Cell Battery Runs

1. Five 5-cell batteries were run for more than 100 hours each while delivering more than 3.4 volts at 24 amps/ft^2.

2. Niobium is the most desirable pusher and collector plate material of those investigated.

3. The voltages produced by the cell using niobium are, on average, higher than any other cell has produced. This is not thought to be due to the internal resistance of the metal but to the surface resistance which is obtained under the conditions of the cell. Note the high specific conductance of the cell measured at the end of Run 3-A.

4. Either Teflon or Penton can be used for gas and electrolyte compartments. No evidence of deterioration of either material during normal testing was observed.

5. Dynel-backed membranes are inferior to glass-backed membranes. No direct comparison can be made since no two batteries differed by only the type of membrane. However, the two poorest batteries both contained dynel-backed membranes.

6. Pressure drops of 25 mm of water are adequate for proper distribution of gases.

7. Improper distribution would leave some cells starved for reactants which results in a steep drop in output voltage from the starved cells. While there have been cases of single cells in a battery performing notably poorer than others in the same battery, the precipitous drop associated with a starved cell occurred only in Run 1B. In that run the gas flow rates were low and the gas pressure drops were only 15 mm of water.

8.0 Ten-Cell Demonstrator Battery

8.1 Introduction

The objective of the test was to run a ten-cell, 36 square inch per cell Ionic's Dual Membrane Fuel Battery for 100 hours at a current density of 24 amperes/ft^2 and to produce a minimum of 40.8 watts or, equivalently, to operate at a minimum of 6.8 volts. The test was completed successfully. During the test the battery produced an average of 46.5 watts with a maximum voltage of 8.7 volts and a minimum of 7.4 volts.

Upon completion of the test, the cell was packed and delivered to TRW.

8.2 Construction of the 10-Cell Battery

Components and materials of construction used in the 10-cell battery are tabulated in Table 8.1. The weight and percentage of total cell weight is tabulated beside each component. The final column gives a percentage weight breakdown for an individual cell.

Little comment is required on most of the components. The selection of niobium for metallic components and glass-backed membranes was obvious in light of the 5-cell battery results. Teflon compartments were used because of the ready availability of teflon.

The only change that was made in the design of the 5-cell batteries was that a part of the gaskets which had covered the gas channels was cut away at a distance of one millimeter from the edges of the channels, thus accounting for the notation "20 cut gaskets". The cuts were made to prevent the possibility of gasket material oozing into the gas channels.

8.3 Data Obtained

8.3.1 Continuous Recording

Over the interval of 120 hours when the battery was on test, thirteen variables were monitored continually:

TABLE 8.1

Descriptive Table of Components

Component	Material	IONICS Dwg. No.	Thickness	Number in 10-Cell Battery	Total Wt., Lbs.	% of Battery Weight	Wt. % of Single Repeating Cell
End Plates	304 Stainless	STD-H-31, Issue 2	3/8"	2	29.10	53.0	-
Insulators	Butyl Rubber	STD-H-22 Original Issue*	60 mil	2	0.44	0.8	-
Collector Plates	Niobium	STD-H-29, Issue 2**	10 mil	11	2.94	5.3	10.85
Grommets	Viton-A on Dacron	-	8 mil	44	0.015	<<0.1	0.05
Gaskets	Viton-A on Dacron	STD-H-28, Issue 2***	8 mil	40 uncut 20 cut	1.27	2.3	5.2
Gas Compartments	Teflon	STD-H-21, Issue 3 Model C	62 mil	20	4.10	7.5	16.75
Pusher Plates	Niobium	STD-H-30, Issue 2**	10 mil	20	2.58	4.7	10.6
Electrodes	Platinum & Teflon	-	7 mil	20	1.67	3.0	6.85
Membranes	IONICS CR61-AZL	STD-H-34 Original Issue	22 mil	20	2.34	4.3	9.55
Electrolyte Compartments	Teflon	STD-H-35, Issue 3 Model C	125 mil	10	4.78	8.7	19.6
Trilok Spacers	Polyethylene & Polypropylene	-	-	20	0.32	0.5	1.3
Electrolyte	25% H_2SO_4	-	-	1100 ml	2.97	5.4	12.15
Bolts	Stainless Steel	-	-	12	1.73	3.2	7.1
Nuts & Washers	Stainless Steel	-	-	24 each	0.63	1.1	-
					54.87 lbs	100.0 %	100.0 %

* except Note 1 - Material: Butyl Rubber; Note 2 - Thickness: .060" ± 0.005"

** except Note 1 - Material: Columbium, unannealed

*** except Note 1 - Material: Viton-A, dacron reinforced; Note 2 - Thickness: .008" ± .001"

1. Battery current
2. Total battery output voltage

3 - 12. Voltage across cells number 1 - 10

13. A reference voltage of 0.4 volts

Each of these variables was recorded every 94 seconds on a self-balancing-potentiometer recorder. The battery current was measured as the potential drop across a 0.05 ohm precision resistance in line with the battery. The total battery voltage was kept on scale on the recorder by means of a 10 to 1 voltage divider. The recorder was set for a full-scale reading of one volt.

8.3.2 Intermittent Recording

Other data were recorded at irregular intervals because they had to be manually recorded. These were:

1. Hydrogen feed rate
2. Oxygen feed rate
3. Electrolyte circulation rate
4. Hydrogen inlet pressure
5. Oxygen inlet pressure
6. Electrolyte inlet pressure
7. Electrolyte outlet pressure
8. Hydrogen side pressure drop
9. Oxygen side pressure drop
10. Electrolyte pressure drop
11. Battery current
12. Individual cell voltages

The last two items appear to be a duplication of the data taken by the recorder. Actually there is a functional difference between the two sets of data. The latter set was taken on instruments which have a calibration* ultimately traceable to the National Bureau of Standards. The current was carefully maintained as close to the desired value as possible while the voltage readings were being taken. Thus these measurements are the best values for cell current and voltage that were obtained. By contrast, the recorder measurements are not sufficiently

* by Alvin S. Mancib Company, Cambridge, Massachusetts

accurate to satisfy the quality assurance requirements of this program. The recorder voltages are fairly consistently 0.01 volts below the values shown by the potentiometer and can be assumed to be correct within 0.02-0.03 volts. These values show behavior of the battery between the potentiometer readings.

The gas feed rates were measured by rotameters which were calibrated at operating pressure with a wet test meter. The electrolyte circulation rotameter was calibrated with a cylinder and stopwatch. The four pressure gauges were set at 5 psi using an Ashcraft dead weight tester. The three pressure drops were measured with polyethylene manometers. The electrolyte manometer gives a considerably more accurate pressure drop than the difference between the inlet and outlet pressure gauges.

8.3.3 Liquid Collections

Liquid appearing in the gas compartments was separated from the gas streams by traps on a lower hydraulic level than the bottom of the cell. After a sufficiently large sample had accumulated in each trap, the quantities were measured and the acid concentration was determined by titration with 0.5N sodium hydroxide. At the same time that the traps were emptied, samples were taken of the electrolyte entering and leaving the battery.

The last six variables measured, then, were:

1. Hydrogen-side liquid accumulation - volume
2. Oxygen-side liquid accumulation - volume
3. Hydrogen-side liquid accumulation - acid normality
4. Oxygen-side liquid accumulation - acid normality
5. Inlet electrolyte normality
6. Outlet electrolyte normality

8.4 Results of Test

8.4.1 Description of Run

The 10-cell battery was subjected to a 120 hour run. The current was maintained at 6 ± 0.02 amperes except for two periods when the cell was deprived of oxygen

for one hour, and for a three hour period when a polarization curve was taken. During the time when the current was 6 amperes, the voltage never dropped below 7.4 volts.

The cell was assembled and connected with the electrolyte system and was free of bubbles and had gases passing through the gas compartments at 11:55 on 5/1/63. After five minutes at open circuit, the current load on the cell was increased stepwise to 6, 12, 16 and 24 amperes/ft^2 over the next 45 minutes. At 12:45 p.m. the current was 24 amps/ft^2 and the voltage 7.66 volts. Between 1700 and 1800 (Run Hour 4.25 and 5.25)*, the high point of almost 8.0 volts was reached. A slow decline to 7.68 volts and 5.8 amps at 0700 (RH 18.25) on 5/21/63. The current was adjusted to 6.0 amps at 0820 (RH 19.58). Following a little run up, the cell operated very steadily (except for some jiggling of the recorder pen) until 1600 (RH 52.25) on 5/3/63 when a slug of fairly concentrated acid was added to the acid reservoir to bring up the concentration of the electrolyte. This caused a severe (almost 0.5 volt) drop in the voltage output. The cell did not entirely recover, but ran along with a slight voltage variations around 7.7 volts until 10:45 (Run Hr 94.00) on 5/5/63 when another addition was made to the reservoir. This time the battery voltage recovered to within 0.1 volt of the voltage before the acid addition.

At 1500 on 5/5/63 (Run Hr 98.25) the oxygen supply to the cell failed because a manifold valve was accidentally left closed and for one hour the cell was deprived of oxygen. When oxygen flow was restored, the battery voltage was considerably higher. A polarization curve was taken and the battery was returned to 24 amps/ft^2 operation at 1815 on 5/5/63. (Run Hr. 101.50). The battery soon reached a peak voltage of 8.35 volts from which it regularly declined to 8.05 volts at 10:00 on 5/6/63 (Run Hr 117.25) when the battery was again deprived of oxygen, this time on purpose. After 65 minutes of oxygen deprivation the battery was again supplied with oxygen to which it responded by producing 8.7 volts at 24 amps/ft^2. The battery was allowed to run until 12:15 on 5/6/63 (Run Hr 120.00) when the run was terminated.

---

* The number enclosed in parentheses represents the hours, written decimally, since the start of the run. This time is used as the abscissa of Figure 8.1 and appears in Table 8.2 under "cumulative hours".

8.4.2 Results and Discussion of Results

8.4.2.1 Current and Voltage

A plot (Figure 8.1) has been made from the battery voltages on the recorder chart using one data point per hour (or more if a maximum or minimum point did not occur near the hour. This shows the general profile of the run described above. The accurate voltages, taken with the calibrated potentiometer, are plotted in Figure 8.2. The points representing the sum total of the cell voltages have been connected along the voltage-time history taken from the recorder chart. It can be seen that direct interpolation between the points would have been incorrect. For this reason the points representing the individual cell voltages have not been connected by smooth lines. Disentangling the separate voltage-time histories of the individual cells from the cells from the recorder chart does not appear to be of significant value. Because of the periodic nature of the readings, the set of points representing one cell are not connected. The plotted values are also listed in Table 8.2. The difference between cells is most likely due to slight differences in the quality of the membrane-electrode contact and possibly to unknown differences in the electrodes themselves.

Two points are particularly noteworthy in the electrical behavior of the cell. The first is the dip in the curve caused by the addition of concentrated acid to the reservoir. Not much mixing occurs within the electrolyte circulation system. Consequently shortly after the concentration of acid in the reservoir is increased, each lateral section of membrane, in turn, is faced with an abrupt rise in acid concentration. This throws the osmotic equilibium out of balance with the probable result that water (or dilute acid) is sucked from the membrane or from the liquid layer between the electrode and the membrane into the electrolyte compartment. This dislocation is sufficiently severe to cause a drop in potential of approximately 0.05 volt per cell.

In a system where the water was continuously removed, i.e., where the electrolyte concentration was maintained at a constant value, this abrupt change of concentration would never occur. However, this effect does suggest that limits must be set on the allowable rate of concentration change.

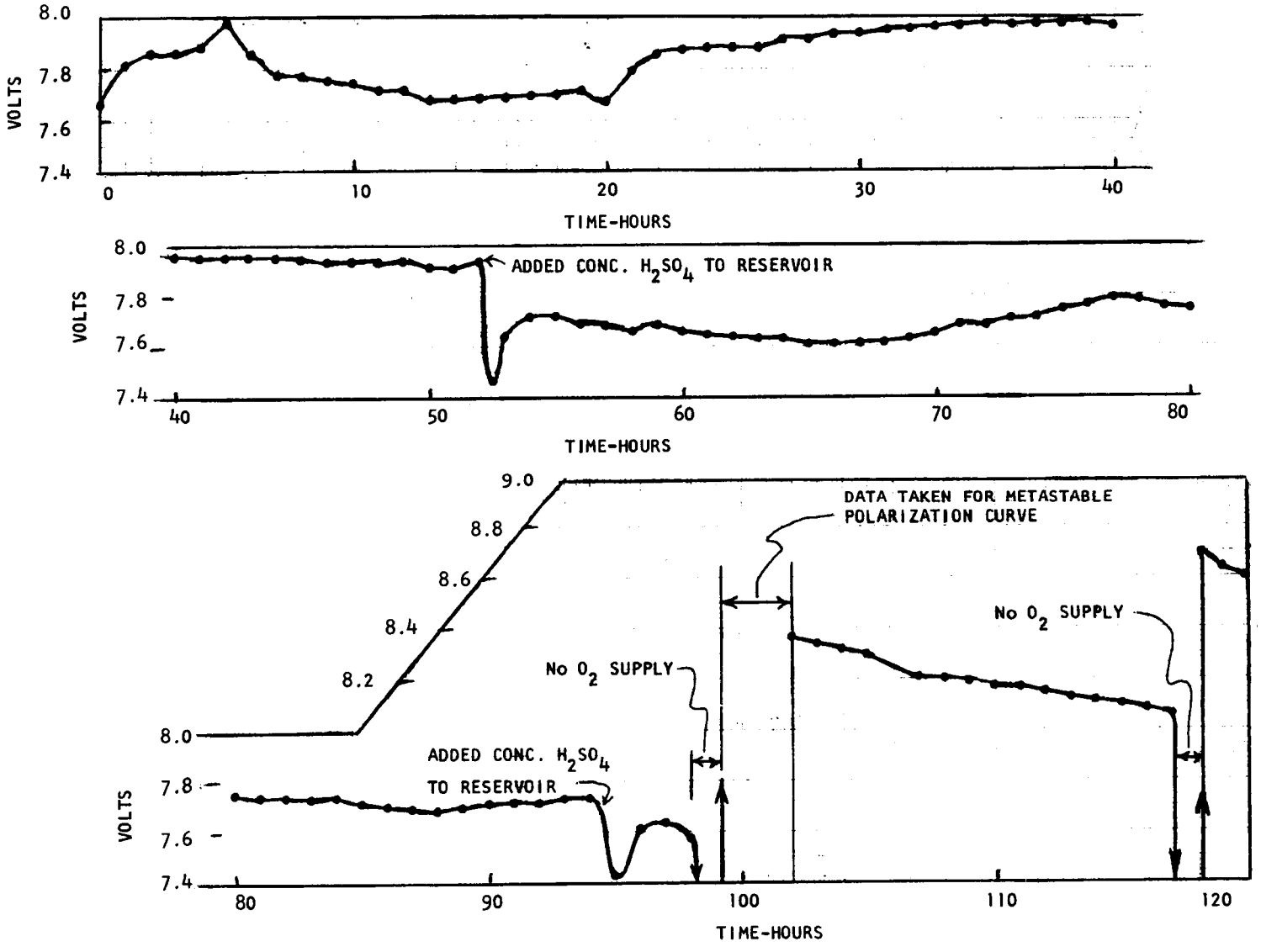

Figure 8.1 Voltage Vs. Time

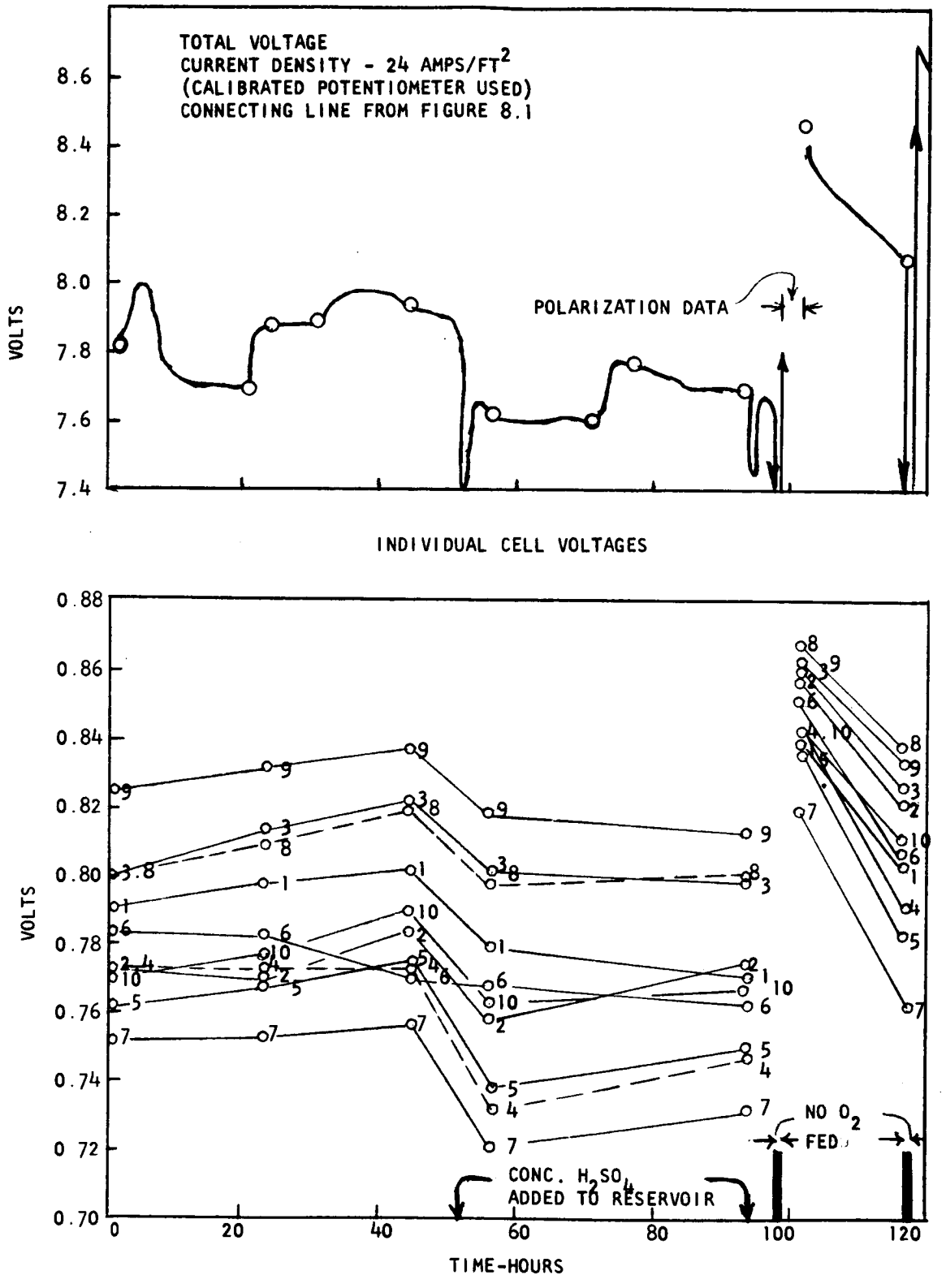

Figure 8.2 10-Cell Battery Voltages

TABLE 8.2

Operational Data from 10-Cell Battery Acceptance Test

Date	5/1/63	5/1/63	5/2/63	5/2/63	5/2/63
Time	1245	1400	0900	1200	1700
Cumulative Hours	0	1.25	20.25	23.25	28.25
H_2 Feed Rate liters/hr.	4.0	4.0	4.0	4.0	-
O_2 Feed Rate liters/hr.	2.0	2.1	1.9	1.9	-
Electrolyte Circulation Rate, l/hr.	1.8	2.0	1.9	1.6	-
H_2 Inlet Pressure, psig	-	4.9	4.8	4.8	-
O_2 Inlet Pressure, psig	-	5.0	4.8	4.7	-
Electrolyte Inlet Pressure, psig	-	5.2	5.4	5.6	-
Electrolyte Outlet Pressure, psig	-	5.0	5.2	5.4	-
H_2 Side Pressure Drop, mm H_2O	-	23	16	14	-
O_2 Side Pressure Drop, mm H_2O	-	23	20	21	-
Electrolyte Pressure Drop, mm H_2O	-	160	187	156	-
Electrolyte Normality	9.07	7.92	-	7.71	7.50
Current	-	6	6	6	-
VOLTAGES:					
Total	-	7.828	7.690	7.871	-
Cell 1		.790	.781	.796	-
Cell 2	-	.772	.758	.770	-
Cell 3	-	.800	.790	.813	-
Cell 4	-	.772	.748	.772	-
Cell 5	-	.762	.749	.767	-
Cell 6	-	.784	.770	.782	-
Cell 7	-	.752	.735	.753	-
Cell 8	-	.800	.789	.809	-
Cell 9	-	.825	.817	.832	-
Cell 10	-	.771	.753	.777	

TABLE 8.2 (Cont'd)

Date	5/2/63	5/3/63	5/3/63	5/3/63	5/4/63	5/4/63	5/5/63***	5/5/63	5/6/63
Time	1960	0840	0900	2130	1100	1715	1015	1740	0900
Cumulative Hours	30.25	43.92	44.25	56.75	70.25	76.50	93.50	100.92	116.25
H_2 Feed Rate liters/hr.	4.0	-	4.0	4.8	-	4.0	4.0	-	4.3
O_2 Feed Rate liters/hr.	1.9	-	2.0	2.0	-	2.0	2.0**	-	2.0**
Electrolyte Circulation Rate, l/hr.	1.8	-	1.6	2.0	1.7	-	1.7	-	1.4
H_2 Inlet Pressure, psig	4.9	-	5.0	5.1	4.6	4.9	4.9	-	4.9
O_2 Inlet Pressure, psig	5.0	-	5.0	5.0	4.9	5.0	5.0	-	5.0
Electrolyte Inlet Pressure, psig	5.4	-	5.3	5.7	6.0	6.0	6.1	-	5.9
Electrolyte Outlet Pressure, psig	5.1	-	5.0	5.3	5.5	5.6	5.8	-	5.6
H_2 Side Pressure Drop, mm H_2O	20	-	20	22	22	-	23	-	23
O_2 Side Pressure Drop, mm H_2O	23	-	20	23	18	-	19	-	19
Electrolyte Pressure Drop, mm H_2O	173	-	164	204	183	-	165	-	142
Electrolyte Normality	-	6.65	-	-*	6.62	-	5.70	-	5.95
Current	6	-	6	6	6	6.1	6	6	6
VOLTAGES: Total	7.885		7.942	7.625	7.60	7.78	7.709	8.470	8.072
Cell 1	.800		.801	.779			.770	.838	.804
Cell 2	.776		.783	.759			.772	.857	.820
Cell 3	.814		.821	.800			.798	.858	.826
Cell 4	.769		.772	.732			.747	.842	.791
Cell 5	.763		.773	.738			.748	.837	.783
Cell 6	.786		.791	.768			.762	.850	.805
Cell 7	.749		.757	.720			.732	.819	.762
Cell 8	.812		.819	.798			.799	.866	.837
Cell 9	.835		.836	.819			.813	.861	.834
Cell 10	.781		.789	.762			.768	.842	.810

* Acid addition at 51.25 hours and 94.00 hours.

** Oxygen feed rate zero from 98 to 99 hours and 117 to 118 hours.

*** Polarization curve taken from 99 to 102 hours (1730) at an electrolyte normality of 6.67.

The second and more important point is the increase in voltage obtained by depriving the cell of oxygen for a period. This gain was quite large: About 75 mV/cell at 24 amps/ft^2. Two possible explanations are available for this phenomenon. First, the overvoltage on the oxygen electrode is increased so much (by 0.7 volt) that all reactable materials (low-energy absorbed molecules, intermediates, impurities) are reacted leaving the electrode in a much higher active state. Or, second, the changes in pressure and electrocapillarity cause the position of the liquid-gas interface to shift exposing relatively fresh catalyst. The effect is not permanent: the voltage delivered by each cell slowly declines toward the original value at about 2 mV/hr.

The second oxygen deprivation is an indication of the reproducibility of the effect. A polarization curve was taken while the cell was in the improved condition. This is reproduced in Figure 8.3. It can be seen that the voltage at 24 amps/ft^2, 8.5 volts is considerably higher than any that was produced by this battery previously. At the highest current density, the two cells next to the end plates showed considerably lower voltages than the other cells which was thought to be due to IR-losses in the terminal collector plates. Consequently, two points are plotted at the highest current density (80 amps/ft^2): The lower is the measured voltage, the higher voltage is calculated assuming that the two end cells should produce a voltage equal to the average of the other eight cells. The two slopes of this polarization curve correspond to specific conductances of 340 and 400 mhos/ft^2. These are quite similar to the conductance of 369 mhos/ft^2 calculated for Battery 3, which also had niobium collector and pusher plates. As a conservative estimate a value for the cell conductivity of 360 mhos/ft^2 will be used in the design of the 2 KW battery.

8.4.2.2 Power

From the data in Figure 8.3, the performance of the battery under other conditions than constant current of 6 amperes can be investigated. A plot of battery power against voltage, shown in Figure 8.4, is a convenient field upon which to work. When the lower curve of Figure 8.3 is plotted as power versus voltage, the solid line curve marked "Demonstrated Performance in 'Metastable' Condition" is obtained. The slope of a straight line between any point and the origin is the

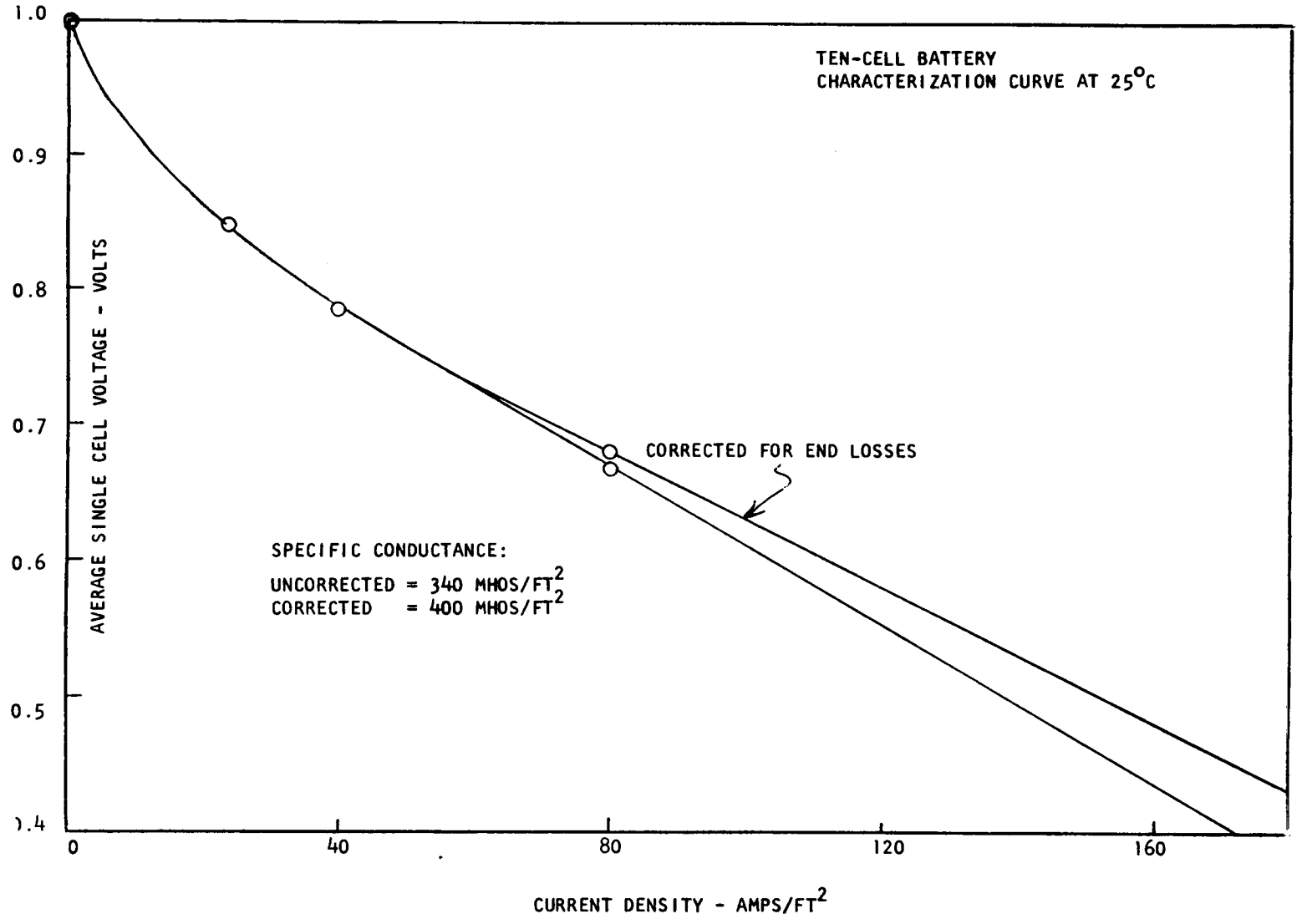

Figure 8.3 10-Cell Battery Characterization Curve at 25°C

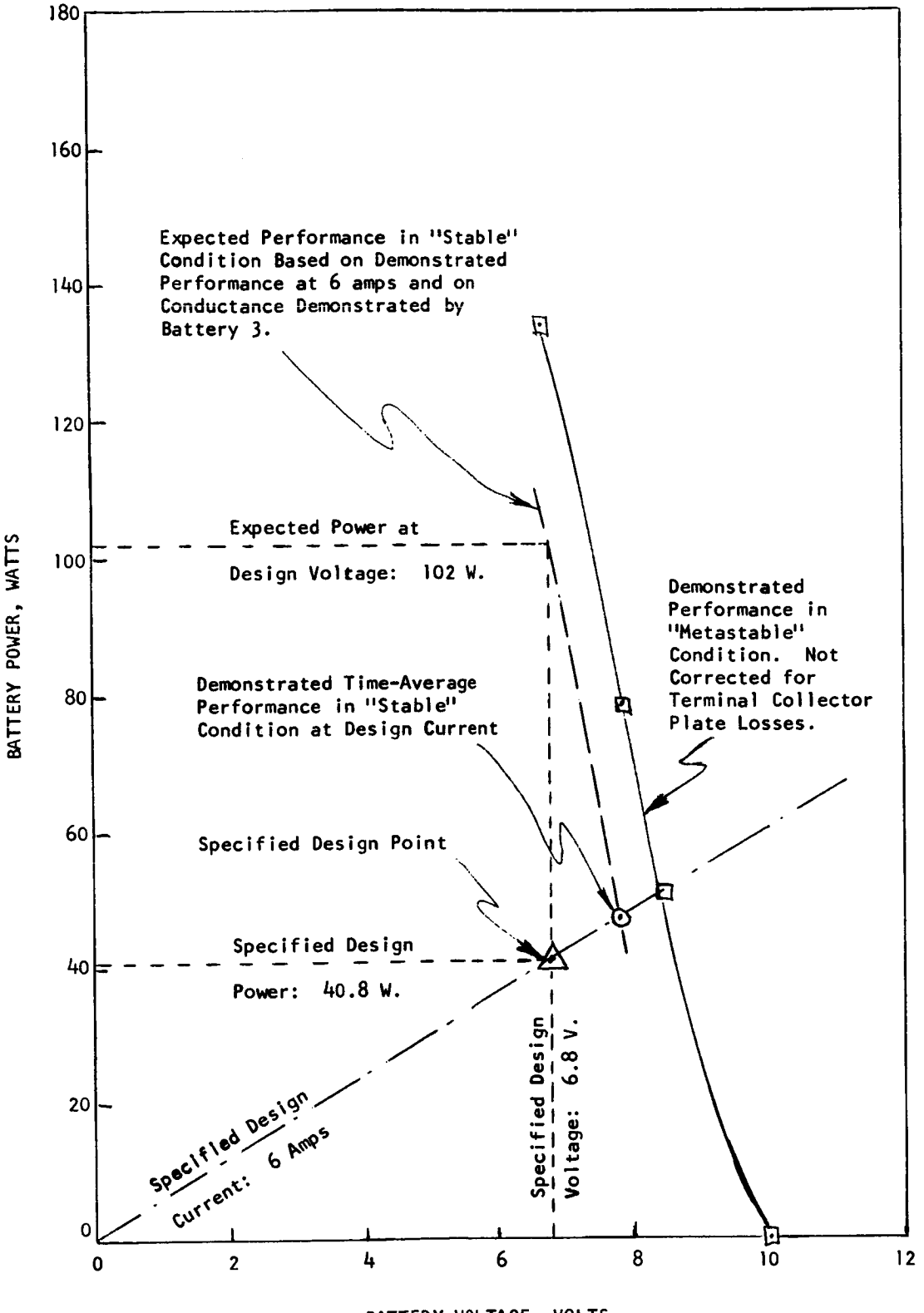

Figure 8.4 Performance of Ten-Cell Battery

battery current corresponding to the conditions at that point. The line representing 6 amperes (this is current, not current density) has been drawn with a dot-dash line labeled "specified design current". This line passes through the specified design point at 6.8 volts (triangle) and the "metastable" curve (square) at 8.4 volts.

The time-average voltage of 7.78 volts obtained over the first 98 hours of operation, i.e., before any oxygen deprivations, is also shown on the 6 ampere line (circle). A power-voltage line was calculated using this point and the conductance demonstrated by the 5-cell Battery 3. This line is shown as the dashed line labeled "Expected Performance in 'Stable' Condition". Now, the criteria of battery operation of a current of at least 6 amperes and a minimum voltage of 6.8 volts leave considerable latitude in selection of operating conditions. In terms of power output, the most desirable is a voltage of 6.8 volts which produces a battery power of 102 watts at a current of 15 amperes. Based on the results of the 120 hour run, we would expect this battery to be capable of producing 100 watts at a voltage of 6.8 volts; however, the service life under this load remains to be demonstrated.

8.4.2.3 Pressure Drops

As a result of the cut-away gaskets, gas side pressure drops were considerably lower than in most of the 5-cell battery runs. These measurements are plotted in Figure 8.5 and tabulated in Table 8.2 along with the measured gas flow rates. Hydrogen pressure drops ranged from 14 to 24 mm of water compared to 18 to 24 mm of water on the oxygen side. There was no noticeable trend with time on either side. These pressure drops appeared to be sufficient for distribution of gases.

The electrolyte pressure drop ranged from 156 to 204 mm of water. Again there was no trend in the variation with time. Values of electrolyte circulation rate and electrolyte pressure drop are tabulated in Table 8.2.

8.4.2.4 Liquid Accumulation

Liquid was disengaged from the existing hydrogen and oxygen streams in measuring cylinders. The amount of liquid collected was recorded periodically. The amount collected between readings was converted into an average rate for the

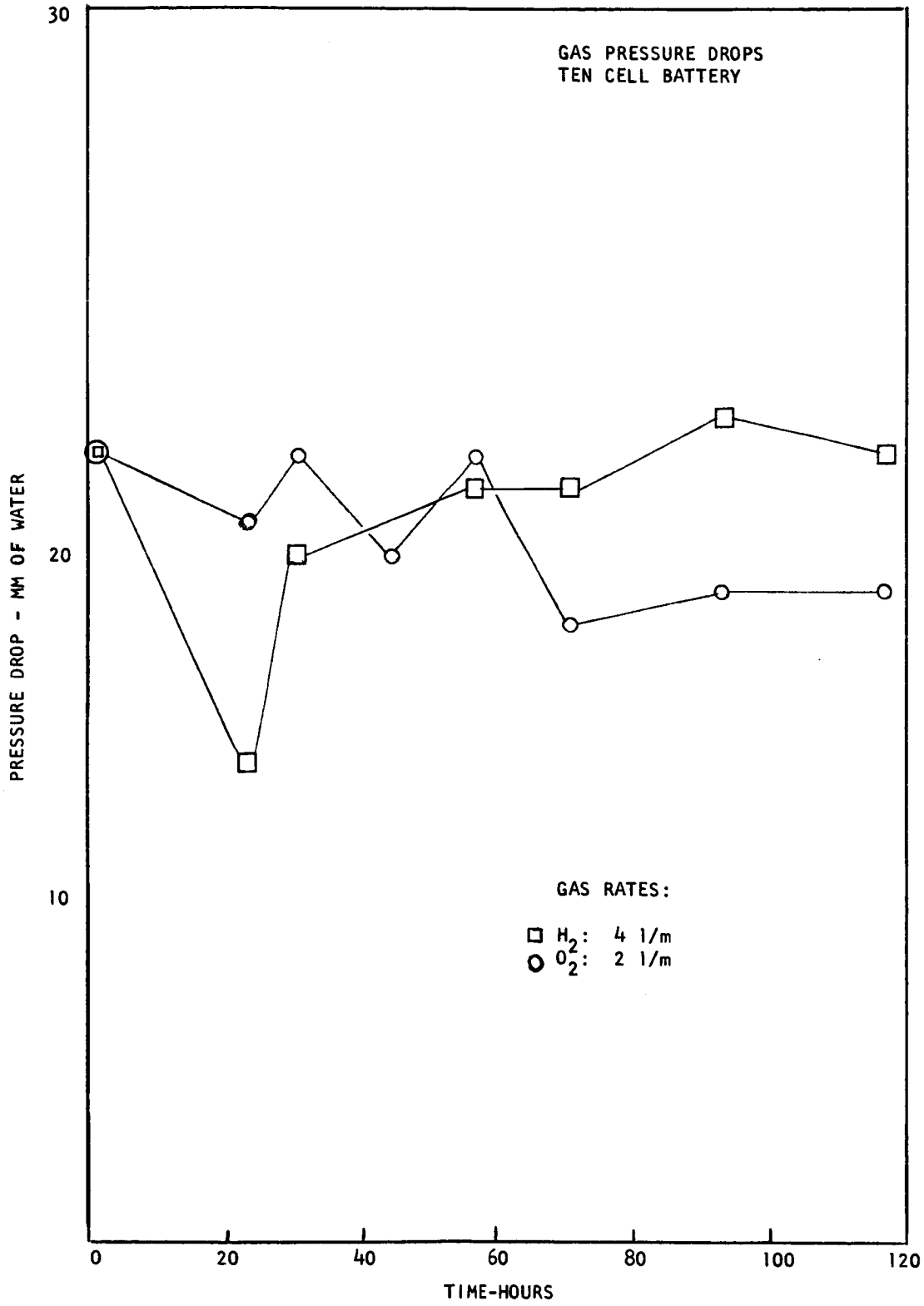

Figure 8.5 Gas Pressure Drops, Ten-Cell Battery

time interval involved. Rates were expressed in milliliters per ampere-hour per cell. Whenever the contents of a cylinder were removed, the normality of the liquid was determined. The results are shown plotted versus time in Figure 8.6(Hydrogen Side) and Figure 8.7(Oxygen Side). The normality of the acid present in the battery is also shown. Rough lines dashed through the data bars indicate where it is expected the instantaneous values of liquid rate and normality would have been.

The normality of the liquid collected on the hydrogen side closely approaches that of the battery acid. However, this is not considered to represent a mechanical "leak". Detailed studies undertaken in other phases of this contract showed that the hydrogen-side liquid always approaches battery acid normality but that the rate of accumulation (ml/hr-cell) is proportional to the current density and approximately to the square of the battery acid normality. Neither variable would be expected to have any significant influence if just a mechanical leakage were involved. Transfer occurs apparently due to the transport of some of the current by solvated acid anions instead of hydrogen ions. The percentage of current carried through the hydrogen-side membrane by acid anions was low.

For 6N acid:
(0.085 ml/amp-hr) (6 meq acid/ml) (0.0267 amp hr/total meq)
= .014 meq acid/total meq = 1.4%

On the oxygen side, the normality of the liquid parallels that of the acid in the battery but is always lower (Figure 8.7). This is due to the formation of water at the oxygen electrode. The more concentrated acid on the electrolyte side of the membrane tends to pull water into the electrolyte stream. The hydrogen ions passing through the membrane to the oxygen electrode tend to be solvated and thus carry H_2SO_4 and H_2O out. Some of the current will carry acid anions back into the electrolyte stream. On balance, at the battery concentrations used here, most of the water formed was pulled back into the electrolyte stream.

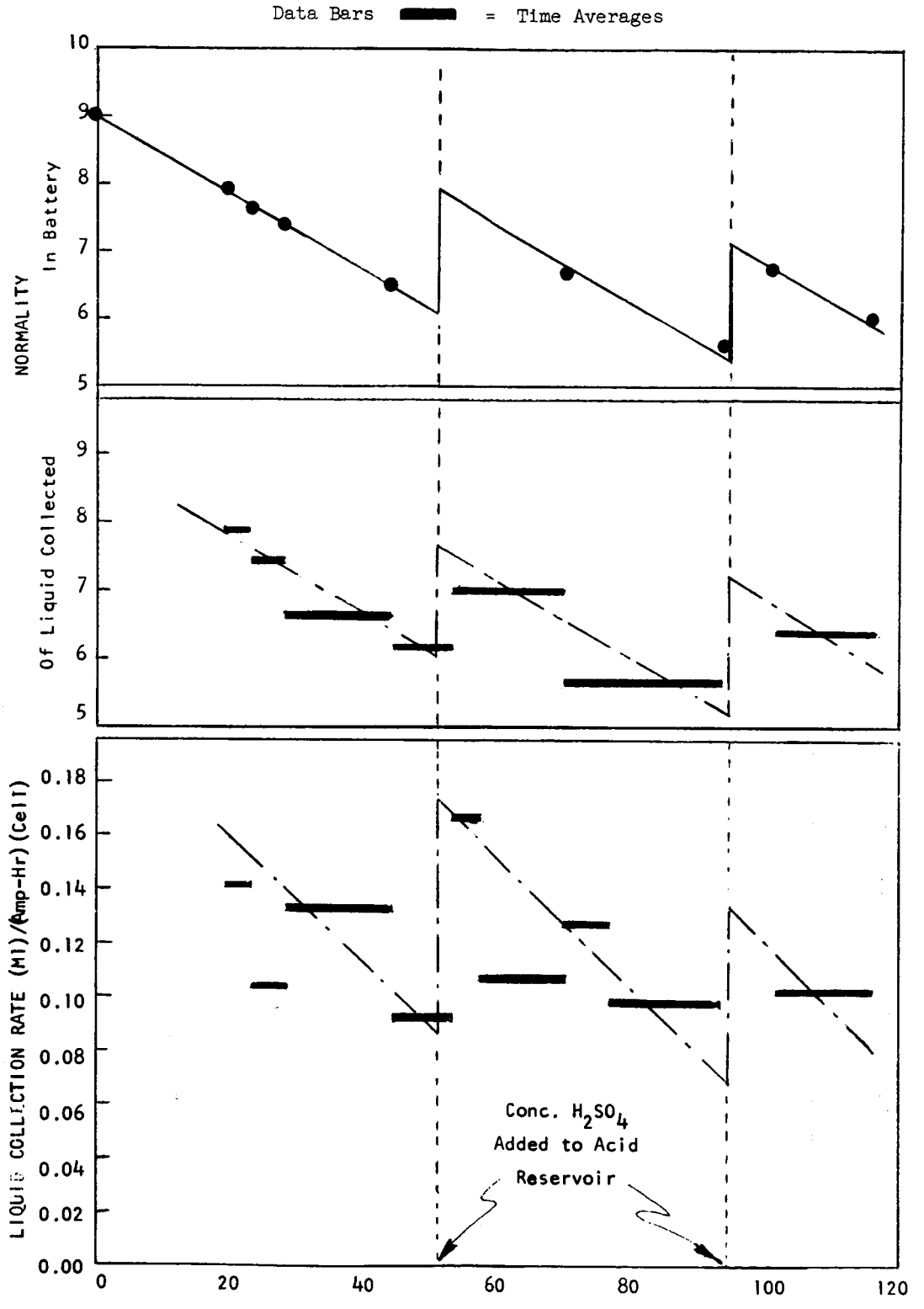

Figure 8.6 Liquid Collection, Hydrogen Side

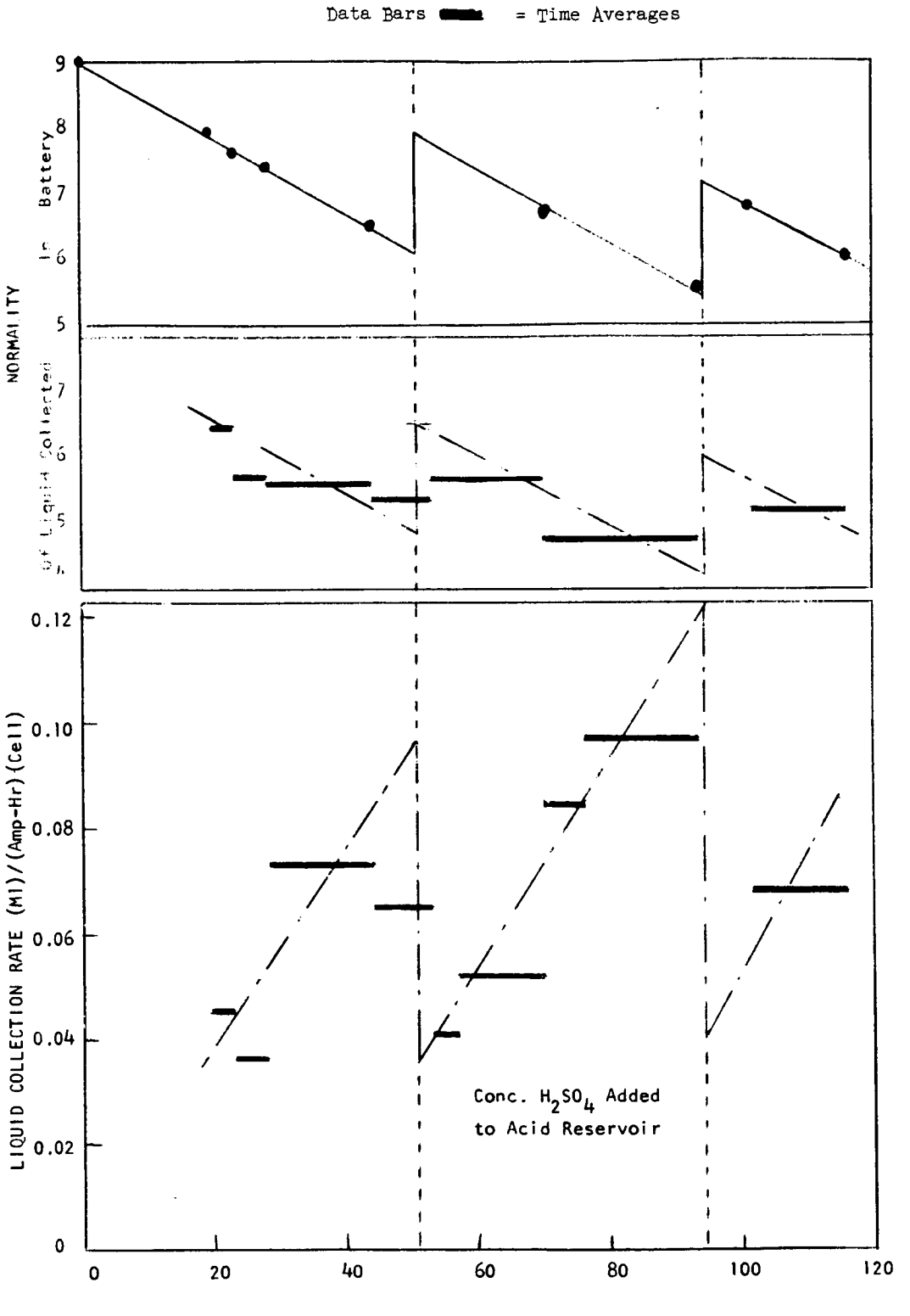

Figure 8.7 Liquid Collection, Oxygen Side

Typical flow streams leaving a cell when the battery acid was 6N were:

	Meq/Amp-hr-cell
Electrochemical Equivalent of Current	37.5
H_2SO_4 out with H_2 gas	0.51
H_2O out with H_2 gas	8.35
H_2SO_4 out with O_2 gas	0.47
H_2O out with O_2 gas	9.85
H_2SO_4 out with electrolyte	200
H_2O out with electrolyte	3280

The large electrolyte rate precludes accurate determination of current efficiency by measuring the electrolyte composition and rate both on entering and leaving the battery. No attempt was made to determine current efficiency by measuring the change in gas composition and rate in passing through the battery.

8.5. Conclusions

The 10-cell battery successfully ran for 115 hours at 24 amps/ft^2 and above the required 6.8 volts. During the entire 120 hour test, the voltage was above 7.4 volts except during:

1. Two one-hour stretches when oxygen feed was cut out, once accidentally (Run Hr 99) and once on purpose (Run Hr 117).

2. Parts of a 3-hour period (Run Hr 100-102) when higher currents were drawn during the determination of a polarization curve.

The average voltage during the first 98 hours was 7.78 volts at 24 amps/ft^2. The average voltage during the 17 hours in the metastable state following oxygen deprivation was 8.25 volts at 24 amps/ft^2.

The battery was crated and delivered to TRW. A photograph of the 10-cell battery after completion of the 120 hour test is shown in Figure 8.8.

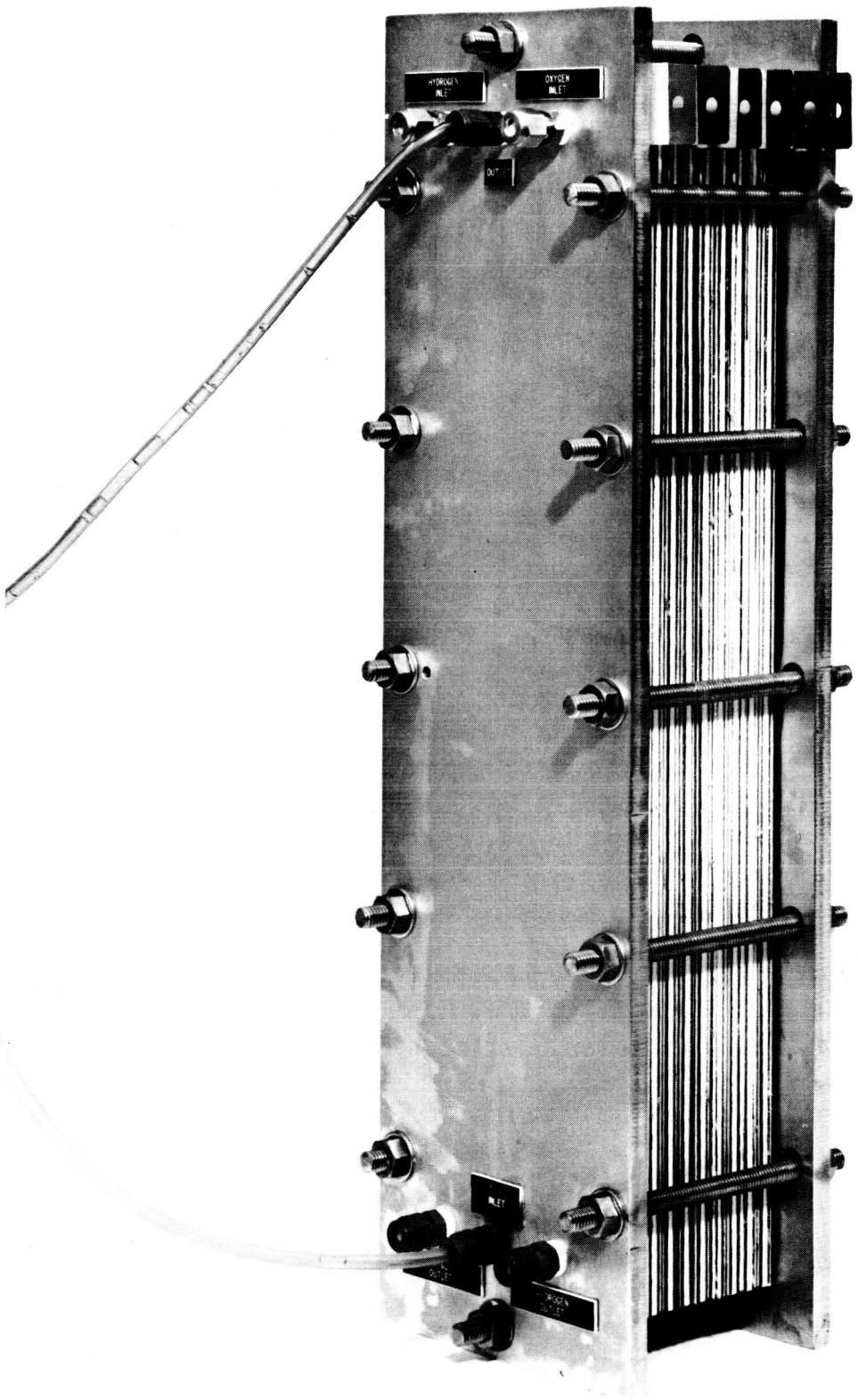

Figure 8.8 Photo of 10-Cell Battery After 120 Hour Test

9.0 2 KW Battery Design

9.1 Design Philosophy

The design is conservative. The expected electrical performance characteristics have all been demonstrated in dual-membrane fuel cell batteries. The mechanical design of the various components closely follows that of components proven in over 10,000 cell-hours of battery performance during this contract alone. Changes in electrolyte porting arrangements and in component thickness which both would lead to substantial weight savings, have not been incorporated in the design as such changes have not been checked out experimentally.

The materials of construction specified in the design are nearly all identical to those used in the 10-cell battery constructed in Task V of this program. The only difference is in the end plates: the previous stainless steel end plates have been replaced by a lighter combination of PVC endblocks and tatanium endframes, closely paralleling the block and frame construction of Ionics' commercial electrodialysis stacks.

As an added conservative feature, the design specified 10% more cells than called for by strict reliance on achieving previously demonstrated electrical performance. There is thus every reason to believe a battery built according to this design will perform satisfactorily, i.e., deliver at least 2000 net watts at least 28.0 volts.

9.2 Overall Design Concepts

The cell design follows that of the dual-membrane, electrolyte-cooled, hydrogen-oxygen fuel cells used in the previous batteries constructed under this contract. Figure 9.1 shows an exploded view of the assembly of the various components. Metallic pusher plates press sintered platinum-black electrodes against pairs of cation-exchange membranes. Sulfuric acid electrolyte-coolant flows between the dual membranes which are held apart by plastic filler mesh. Solid metallic "collector plates" serve to collect current from the pusher plates and to isolate the oxygen compartment of one cell from the hydrogen compartment of the next cell. Hydrogen, oxygen, and electrolyte-coolant streams are fed to and removed from the appropriate compartments through manifold ports leading to internal headers.

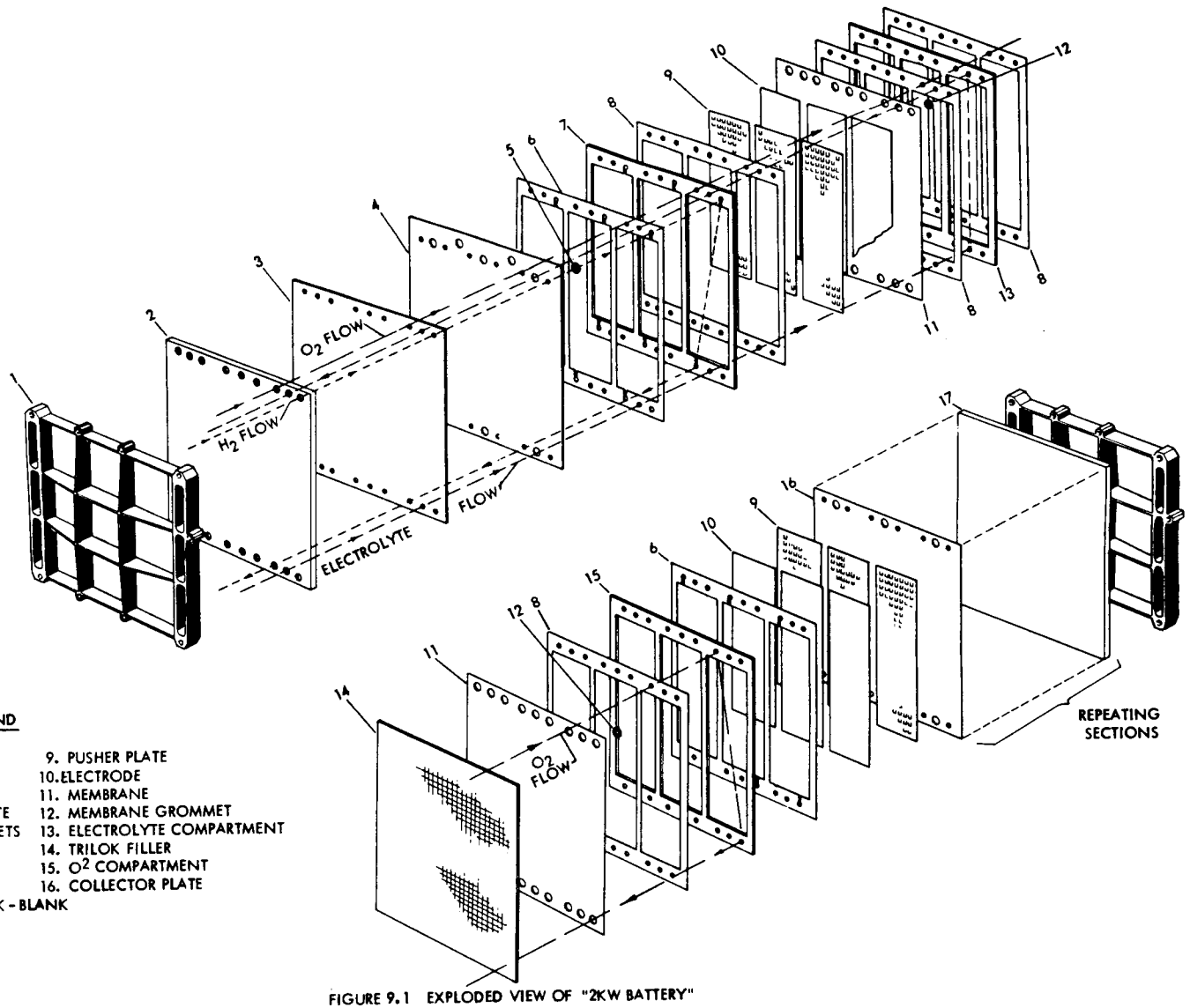

LEGEND

1. END FRAME
2. END BLOCK
3. INSULATOR
4. TERMINAL COLLECTOR PLATE
5. COLLECTOR PLATE GROMMETS
6. CUT GASKET
7. H_2 COMPARTMENT
8. UNCUT GASKET
9. PUSHER PLATE
10. ELECTRODE
11. MEMBRANE
12. MEMBRANE GROMMET
13. ELECTROLYTE COMPARTMENT
14. TRILOK FILLER
15. O^2 COMPARTMENT
16. COLLECTOR PLATE
17. END BLOCK - BLANK

FIGURE 9.1 EXPLODED VIEW OF "2KW BATTERY"

The components for the desired number of cells are "stacked" between a pair of end blocks. The assemblage is held together by tie bolts bearing against end frames which in turn bear against the endblocks.

The flow in the electrolyte compartments is upwards to facilitate removal of gas bubbles during the filling operation which will occur in a positive 1-g environment. The flow in the gas compartments is downward to facilitate liquid removal during the run-in and checkout operations occurring in a positive 1-g environment.

The battery is designed to produce at least two kilowatts, net, of electrical power at 28 volts. Two hundred additional watts have been allowed for auxiliary power. The value of 200 watts for the auxiliary power requirement was arrived at after discussions between TRW and Ionics Incorporated. This battery with a gross power output of at least 2200 watts at 28 volts will be referred to as the "2-KW battery".

9.2.1 Expected Single Cell Characteristics

Niobium metallics produced the highest specific conductances in the 5-cell battery tests and have been specified in the 2-KW design. The average characterization curve for cells from the niobium containing Battery 3 showed a specific conductance of 369 mhos/ft^2. An average of 360 mhos/ft^2 will be considered obtainable.

Most of the data of 5 and 10-cell batteries were obtained at a current density of 24 amps/ft^2. At that current density, good cells provided 0.8 volts or better. It is felt that by careful manufacture and selection of electrodes for the 2-KW battery, the cells of that battery will provide an average of at least 0.8 volts at 24 amps/ft^2. Using this base point and a specific conductance of 360 mhos/ft^2, the expected average single-cell characterization curve shown in Figure 9.2 can be drawn. It passes through 0.8 volts with a reciprocal slope of 360 amps/ft^2 per volt. It extrapolates back to 0.867 volts at zero current density.

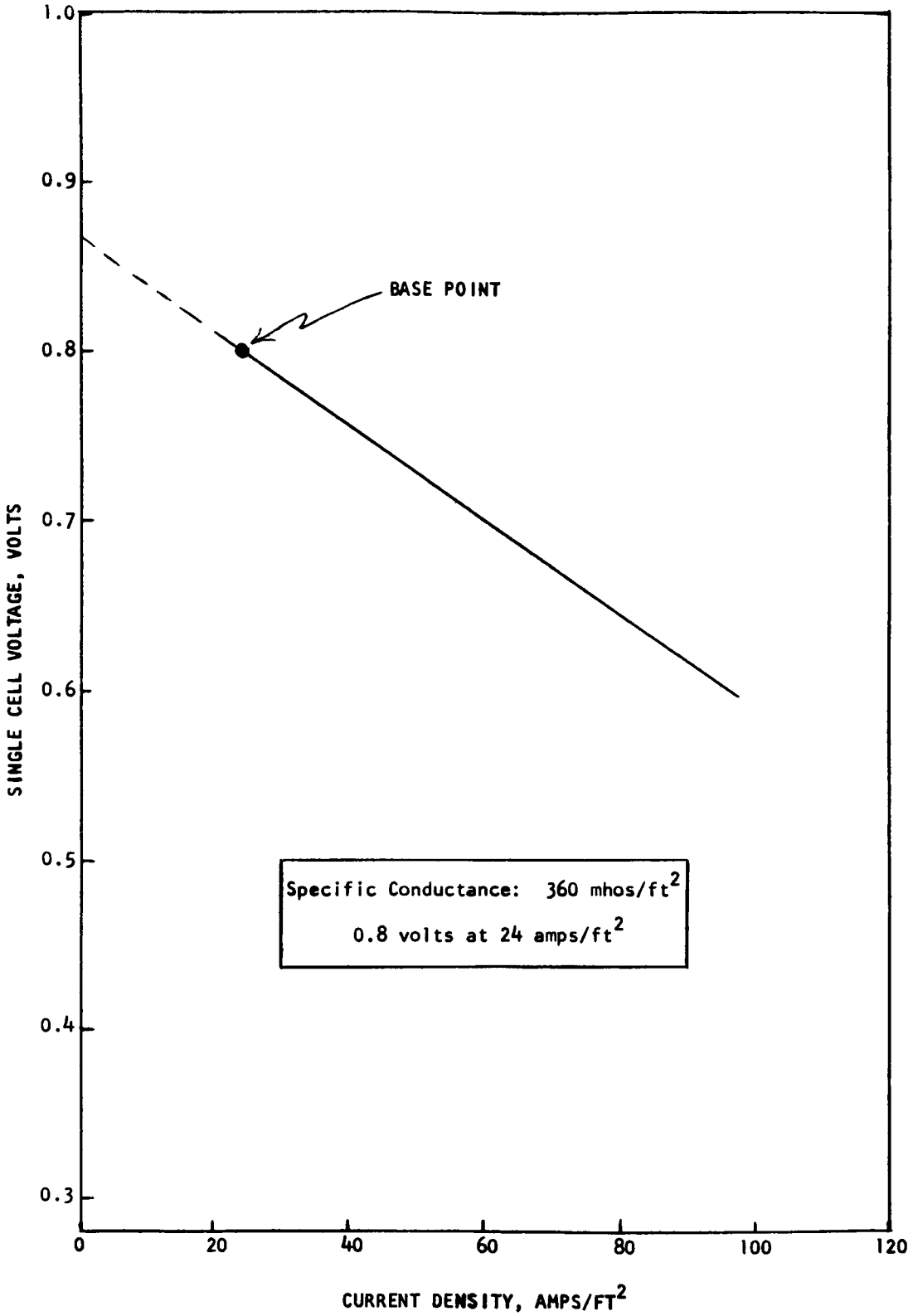

Figure 9.2 Design Polarization Curve

9.2.2 First-Pass Design

The battery is to provide 2200 watts at 28 volts. This calls for a current of 2200/28 = 78.6 amps. An operating voltage of 0.7 volts/cell is desired in order to get reasonable fuel efficiency. The expected cell characterization curve (Figure 9.2) indicates that a cell should maintain 0.7 volts at a current density of 60 amps/ft^2. A current of 78.6 amps at 60 amps/ft^2 calls for 78.6/60 = 1.3 ft^2 of active area per cell. At 0.7 volts/cell the required 28 volts could be provided by 29/0.7 = 40 cells in series.

The first pass design would thus be:

1. 40 cells
2. 0.7 volts/cell (28 volts total)
3. 1.31 ft^2/cell
4. 60 amps/ft^2 (78.6 amps total)
5. 2200 watts at 28 volts

9.2.3 Actual Conservative Design

There is a possibility that the average performance of the cells will not be quite as good as the expected average performance. To guard against this, four extra cells have been added to the first pass design. These cells provide a contingency assurance. If, however, all the 44 cells now in the design perform as expected, the battery will be capable of more than required performance.

The battery is expected to have an internal resistance of

$$\frac{(44)}{(1.31)\ (360)} = 0.0933 \text{ ohms}$$

and an extrapolated zero-current voltage of (44) (0.867) = 38.1 volts. The additional contingency assurance in the design is expected to permit operation either at 2200 watts but higher than required voltage or at 28 volts but higher than required power. Thus it is expected that 2200 watts can be obtained at a higher per-cell voltage (0.720 volts) and a lower current density (53.1 amps/ft^2) than in the first pass design. This results in improved fuel efficiency. Again, the contingency assurance in the design is expected to permit drawing

considerably more than 2200 watts at 28 volts as the 4 extra cells should allow operation at 28/44 = 0.636 volts/cell which is expected to correspond to a current density of 82.9 amps/ft^2 and a total gross power output of 3040 watts.

The contingency allowance in the design basically, however, is intended to permit satisfactory performance (i.e., 2200 watts at 28.0 volts) even if the battery characteristics do not come up to expectations. It is possible, for example, that the specific conductance will be lower than the expected 360 mhos/ft^2 leading to a higher internal battery resistance, or else the electrode polarization may be higher than expected, leading to an extrapolated zero-current voltage of less than 0.867 volts/cell, i.e. less than 38.1 volts for the battery.

The 4 extra cells permit the battery to provide 2200 watts at 28 volts even if the internal resistance is as much as 38% higher than expected (0.1285 ohms instead of 0.0933) or if the electrode polarization is up to 64 mv higher per cell than expected-extrapolate zero-current voltage of 0.803 volts/cell or 35.3 volts/battery.

The various cases discussed above can be summarized as follows:

1. First Pass Design: 40 cells
   (a) Required Performance: 2200 watts at 28.0 volts

2. Actual Conservative Design: 44 cells
   (b) Expected Performance - High Voltage: 2200 watts at 31.7 volts
   (c) Expected Performance - High Power: 3040 watts at 28.0 volts
   (d) Acceptable Performance - High Resistance: 2200 watts at 28.0 volts
   (e) Acceptable Performance - High Polarization: 2200 watts at 28.0 volts

Table 9.1 presents some further details.

Figures 9.3 and 9.4 show the voltage-current and power-voltage characteristics corresponding to the four actual conservative design cases discussed. The first of these four cases, 2200 watts, 31.7 volts (0.72 volts/cell and 69.6 amps (53.1 amps/ft^2) is taken as the expected "design point" for the further process parameter calculations presented in Section 9.7.

TABLE 9.1

Performance Characteristics of Battery Designs

	First Pass Design	Actual Conservative Design			
		Expected Performance		Minimum Acceptable Performance	
		High Volts	High Watts	High Resis.	High Polar.
No. of Cells	40	44	44	44	44
Internal Battery Resistance, ohms	0.0848	0.0933	0.0933	0.1285	0.0933
Extrapolated Zero-Current Voltage	34.7	38.1	38.1	38.1	35.3
Total Voltage	28.0	31.7	28.0	28.0	28.0
Voltage/Cell	0.700	0.720	0.636	0.636	0.636
Amps/Ft^2	60.0	53.1	82.9	60.0	60.0
Total Amps	78.6	69.6	108.6	78.6	78.6
Total Watts	2200	2200	3040	2200	2200
Gms Reacted/KWH*	480	466	522	522	522

*Assuming 100% Current Efficiency

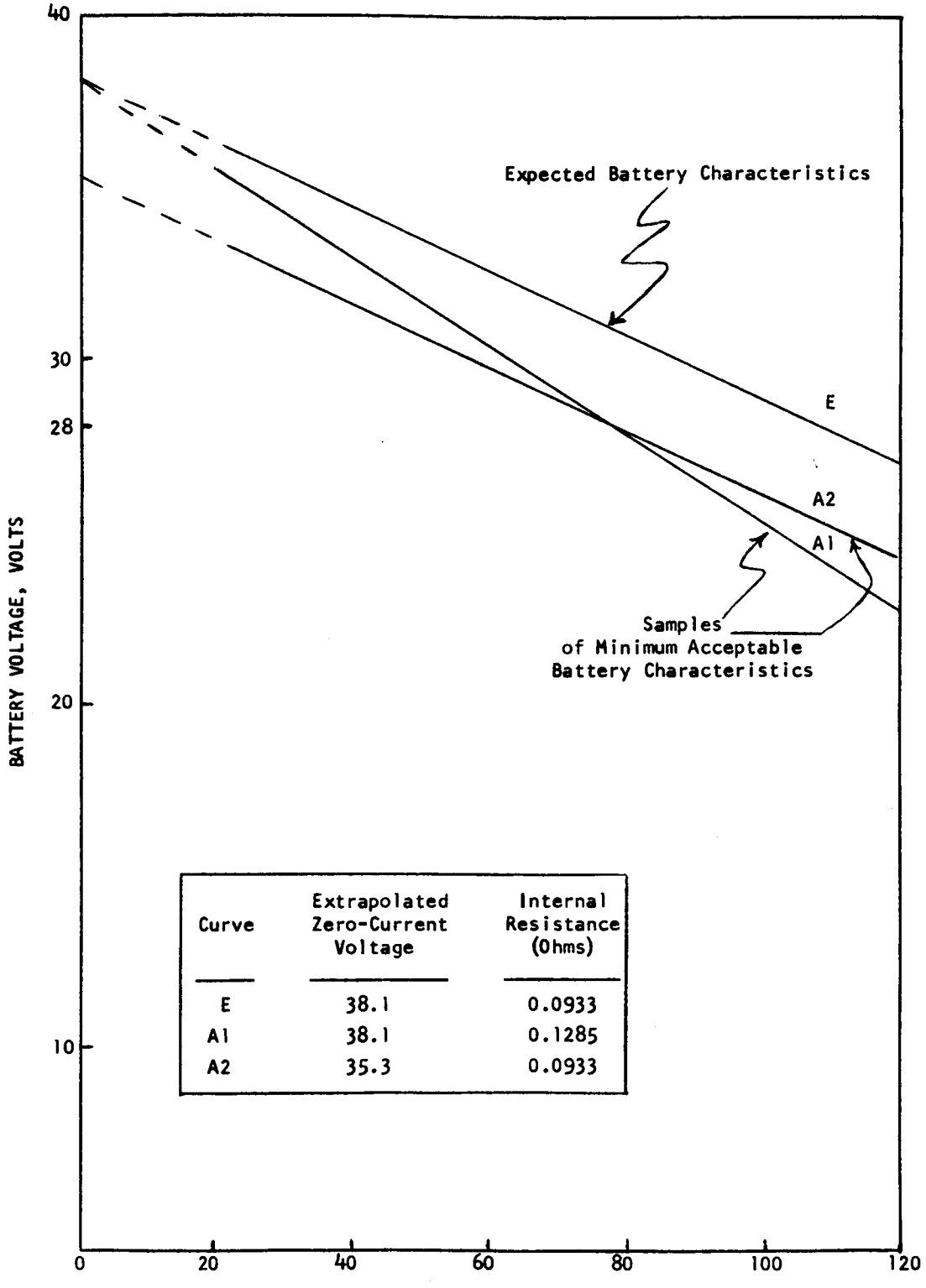

Curve	Extrapolated Zero-Current Voltage	Internal Resistance (Ohms)
E	38.1	0.0933
A1	38.1	0.1285
A2	35.3	0.0933

Figure 9.3 Battery Characteristics

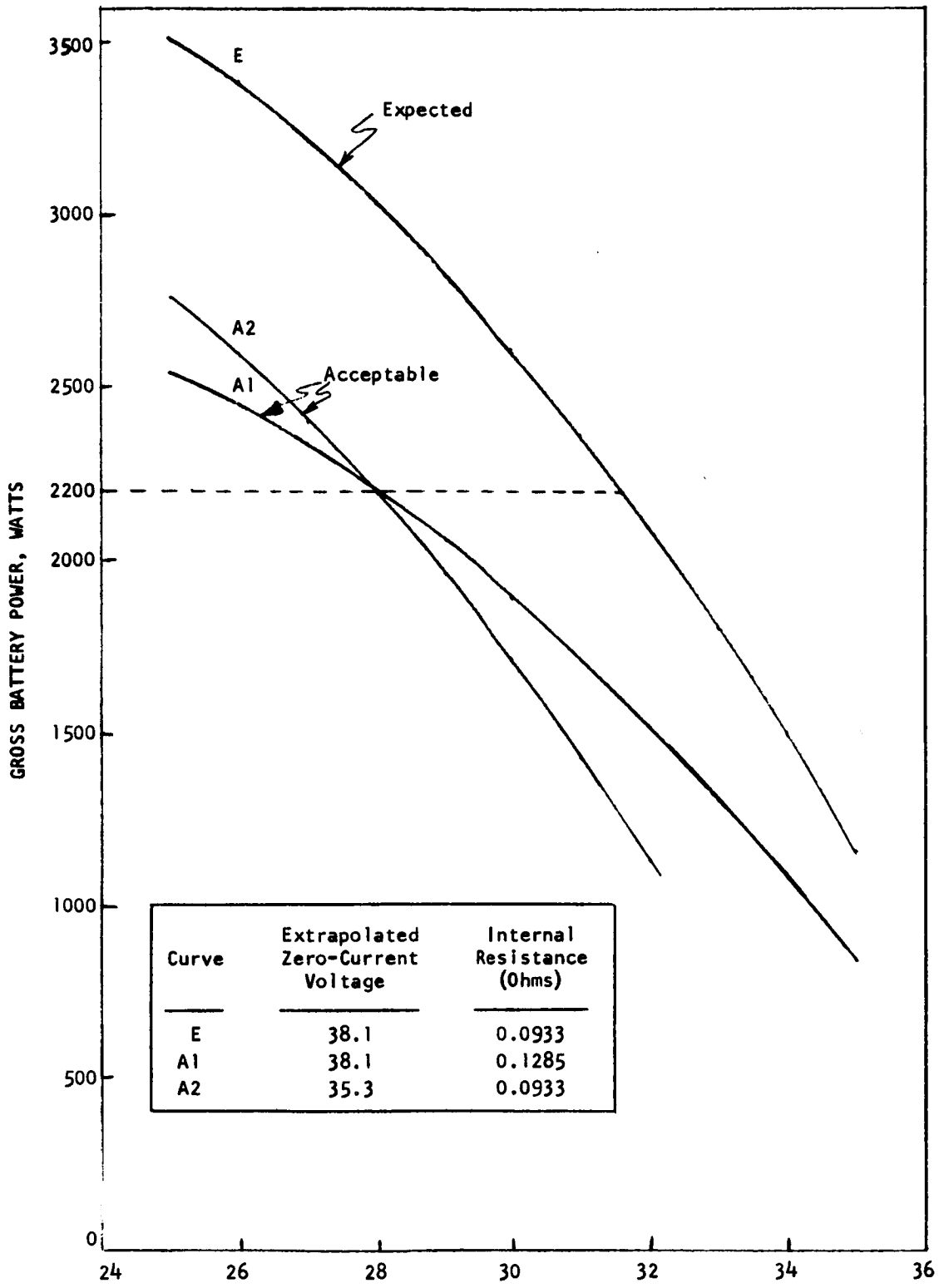

Curve	Extrapolated Zero-Current Voltage	Internal Resistance (Ohms)
E	38.1	0.0933
A1	38.1	0.1285
A2	35.3	0.0933

Figure 9.4 Battery Power-Voltage Curves

9.3 Battery Configuration

It would be relatively simple to build a stack of 44 single cells, each with 1.31 ft^2 of active area. A considerable increase in system reliability can, however, be made by separating the battery into three semi-independent stacks in parallel, each with 0.437 ft^2 of the active area. Each of these stacks has a separate gas and electrolyte manifold. The 0.437 ft^2 of active area per cell in each stack is less than double the 0.25 ft^2 of active area per cell in the 10-cell battery built under the present contract. Scale-up problems should thereby be inconsequential. The stacks of the 2-KW battery are not fully independent because a further increase in reliability is obtained by joining the equivalent collector plates of the three stacks.

The advantage of using joint collector plates can be seen by considering an example. Say Cell 6 of Stack A has failed for some reason and now presents a high resistance to current flow. If the three stacks were independent (i.e., without joint collector plates), this would effectively eliminate Stack A which represents one third of the battery as a power-producting device. However, the joint collector plates permit current to flow from Cell A-5 through Cells B-6 and C-6 and back to Cell A-7. Thus, only Cell A-6, representing less than 1% of the battery, is lost. There are additional slight debits, of course, in that the increased current density now in Cells B-6 and C-6 will result in a somewhat lower output voltage for these cells and in that there will be an IR loss as the current flows down the collector plates from A-5 to B-6 and C-6 and back to A-7*.

---

*Exact calculation of the debits incurred is unwarranted at this time as they would depend, inter alia, on:

1. The type and extent of the cell failure as affecting local electrolyte flow.
2. The exact individual electrical characteristics of the failed cell, and of its two parallel neighbors.
3. The exact electrical characteristics of the six assemblages of cells preceding and following the failed cell and its neighbors.
4. The exact electrical characteristic of the battery load and its voltage regulation system, if any.

However, it is felt that the debits do not outweigh the advantages in system reliability gained by using three semi-independent stacks with separate flow manifolds and joint collector plates. The battery design will thus consist of three semi-independent stacks, each with an active are of 0.437 ft^2/cell.

9.4 Individual Component Design and Justification

The various components of the 2-KW battery are listed in Table 9.2. They are discussed separately below.

9.4.1 End Frame

The end frame is designed to exert a pressure of 290 psi over the gasket area. This is an empirical value which was found to be adequate for the 5-cell batteries. Over a gasket area of 69 square inches, this corresponds to a total force of 20,000 lbs. The frame has been designed so that the members lie just over the gaskets in order to minimize the bending moments on the end block. The end frames have the largest overall dimensions of all the components: 16-5/8" x 19-17/32".

The end frames are to be bolted together with 20 inch pieces of 5/16" high tension rod threaded for approximately 4 inches on either end with 5/16" NF thread. Once the battery is assembled approximately 4 inches can be sawed off one end of each of the rods. Elastic stop nuts are to be used to prevent the nuts from vibrating loose while the battery is in transit.

9.4.2 End Block

Based upon experience in the assembly of electrodialysis stacks, end blocks of PVC, 1/2 inch thick, are needed to prevent distortions of the cell when the tie bolts are tightened to the requisite tension. The half-inch thickness is deep enough to hold the 1/2 inch PVC pipes which are to lead into the manifolds. Rubber "insulators" provide elastic gasketing between the PVC end blocks and the terminal collector plates.

The block and frame construction is a relatively simple straight-forward technique for obtaining strength at low weight.

TABLE 9.2

Descriptive List of Battery Components

Component	Material	Drawing Number	Thickness Mils	Weight Lbs.	Number Req'd	Total Wt., Lbs.	% of Total Wt.
End Frame	Titanium	STD-F-96	2000	13.25	2	26.5	8.48
End Block (less fittings)	PVC	STD-F-97,A,B	500	6.5	2	13.0	4.16
Tie Bolts	High Tensile Rod	-	-	0.482	12	5.79	1.86
Nuts	Elastic Stop Nuts	-	-	0.0264	24	0.63	0.20
Insulators	Butyl Rubber	STD-F-97C	60	0.68	2	1.36	0.44
Collector Plates, Terminal	Niobium	STD-F-100B	20	1.8	2	3.6	1.15
Current Bus Bars	Aluminum	-	-	0.10	2	0.20	0.07
Collector Plates, Internal	Niobium	STD-F-100A	10	0.84	43	36.2	11.60
Collector Plate Grommets	Viton/Dacron	STD-F-98D	12	0.000335	270	0.09	0.03
Pusher Plates	Niobium	STD-F-100C	10	0.21	264	55.5	17.75
Gaskets, Cut	Viton/Dacron	STD-F-99B	8	0.033	88	2.93	0.94
Gaskets, Uncut	Viton/Dacron	STD-F-99A	8	0.033	176	5.85	1.88
Gas Compartments	Teflon	STD-F-98B	31	0.166	88	14.6	4.67
Electrodes	Pt-Teflon	STD-F-99C	8	0.14	264	37.0	11.85
Membranes	IONICS CR-61-AZG	STD-F-98C	22	0.385	88	33.9	10.85
Membrane Grommets	Viton/Dacron	STD-F-98D	26	0.000725	1584	1.15	0.37
Electrolyte Compartments	Teflon	STD-F-98A	100	0.833	44	36.7	11.75
Trilok Mesh Filler	Polyethylene & Polypropylene	-	-	0.028	264	7.37	2.36
Electrolyte	25% H_2SO_4	-	-	-	-	30.0	9.60

TOTAL BATTERY WEIGHT: 312.37 Lbs

9.4.3 Collector Plates

As in the 10-cell battery, the pusher and collector plates are to be made of niobium, also known as columbium. The voltages produced by cells with niobium metallics were on the average about 2% higher than those produced by other cells. This is not thought to be due to any difference in ohmic resistance of the metal, but to the surface or contact resistance which is present during cell operation.

To minimize the IR drop which appears at a current density of 53 amps/ft^2 in the terminal cells, the terminal collector plates are to be made of 20 mil instead of 10 mil stock. This will halve the IR drop to an estimated 80 mv. Also, the current is to be collected in a 1/4" x 1/4" aluminum bar running the width of the collector plate instead of using a corner tab contact which has been sufficient in lower current devices.

9.4.4 Gaskets

The structure of the cell was arranged to keep gasket area to a minimum. This is to limit the force necessary to seal the battery against leaks and thus to simplify and lighten the end plate and frame construction. The total gasket area of 69 in^2 for 1.31 ft^2 of active area can be compared with a gasket area of 42 in^2 for 0.25 ft^2 of active area in the design of the 5 and 10-cell batteries.

In the 5-cell and 10-cell batteries, 8 mil Viton-A with Dacron backing proved entirely satisfactory with regard to dimensional stability and resistance to acid attack, and will be used here.

The gaskets between the gas compartments and the collector plates are to be cut away to a distance of one millimeter from the sides of the gas inlet and outlet channels. This precautionary measure was taken after one of the 5-cell batteries showed abnormally high gas pressure drops presumably as a result of being operated a high temperatures during the taking of a polarization curve. The gasketing material was found to have expanded into the gas channels, almost completely blocking them.

To avoid blocking the manifolds, the holes through the gaskets are to be made slightly larger than the manifold holes in the collector plates.

9.4.5 Gas Compartments

The materials study suggested three plastics for use in the compartment manufacture; Halon, Penton and Teflon. Halon was never evaluated because of the inordinately long delays in manufacture of acceptable sheet stock. Penton and Teflon both proved entirely satisfactory in testing. Teflon was selected as the compartment material because of its availability and better machining characteristics.

The thickness of the gas compartment is to be reduced to the readily available 31 mils (1/32") from 62 mils (1/16"). For a battery containing 88 gas compartments, this results in the battery being thinner by 2.7 inches which is a substantial saving, and reduces the weight by 14.6 lbs.

The inlet channels have been dimensioned to give a pressure drop at rated gas flow of 40 mm of water on the hydrogen side and 50 mm of water on the oxygen side. These numbers are twice the experimentally determined pressure drops necessary to insure good gas distribution.

9.4.6 Electrodes

The standard sintered Teflon formulation is to be used. The recipe for a 15-5/32" x 4-1/2" electrode is given below:

> Mix 34 grams of platinum black* with 2.37 grams to Teflon dispersion** in water. Add 3.4 grams of reagent grade magnesium oxide (MgO) and stir. Add distilled (or deionized) water to make a workable paste. Spread on 90% platinum-10% rhodium mesh.*** Dust with MgO, wrap in aluminum foil and press at 5,000 psi and 650-700°F for 5 minutes. Remove electrode from aluminum foil with care and place in warm sulfuric acid to dissolve MgO. Rinse electrode in distilled water and dry at 110°C.

---

* J. Bishop & Company, Malvery, Pennsylvania, supplier

** American Durafilm, Newon, Massachusetts, Type 852-201

*** J. Bishop & Company, 80 mesh, 3 mil wire

Before the cell can be assembled, the electrodes are to be tested in a single cell. Only those electrodes meeting a minimum cell performance of 0.636 volts @ 60.0 amps/sq. ft. should be used in the battery. (See Table 9.1). An electrode that has performed poorly on the oxygen side, however, is usually a satisfactory hydrogen electrode.

The present plan is to use a three or five-cell battery in which to run the electrodes for a period of 24-28 hours. During this time the operating voltage is to be recorded. After this test the hydrogen and oxygen connections can be reversed and the three or five former hydrogen electrodes can be tested as oxygen electrodes without disassembling the battery. A total of 132 satisfactory oxygen electrodes must be obtained.

9.4.7 Membranes

The membrane study, reported in the Seventh Monthly Report, indicated that of seven different membranes checked for resistance and liquid transport, the Ionics 61-AZG, glass-backed, and 61-AZL, dynel-backed, were most worthy of further consideration. At the end of the 5-cell battery runs, the conclusion was supported by the very good performance of the 10-cell battery.

As a departure from previous practice, the membranes are to be insulated from the manifolds by further grommets. This presents two advantages. The membranes are not in direct contact with the common acid feed system which reduces the current leakage considerably. Second, experience has demonstrated that it is almost impossible to make a clean cut through the membrane particularly with a small radius of curvature. There are invariably small thread ends sticking out into the manifold which represent a hazard in that they may possibly fray loose and then become lodged in an electrolyte port. Grommeting should prevent this ever happening.

9.4.8 Electrolyte Compartments

For reasons mentioned above, the electrolyte compartments are also to be made of Teflon. The 100-mil thickness was retained from the design of the 5 and 10-cell batteries because the compartments are connected to the manifold header by small drilled holes and it is impossible to drill holes of adequate size through material much thinner than 0.100 inches. Development of other reliable means

to connect electrolyte compartments to headers rather than using drilled holes should permit a saving in compartment thickness. However, in keeping with the basic conservative philosophy of this design, proven components have been specified.

The inlet holes have been designed for an electrolyte pressure drop of 200 mm of water. This was found sufficient for adequate liquid distribution in the multiple-cell battery tests.

Since the electrolyte compartments have the smallest open area of the cell compartments, this defines the "active area": 1.31 ft^2 per set of 3 parallel cells in the present design. The height to width ratio of each individual compartment has been reduced in the new design. The width of a single compartment has been almost doubled (to 4-1/4") while the height is almost the same (15"). However, the height is still considerably greater than the width so no significant difficulty is expected due to dead corners".

The arched top in the compartment is to facilitate the removal of gas bubbles during the filling procedure.

9.4.9 Mesh Filler

The filler to be used in the electrolyte compartments is type 6027-1-1 Trilok (73% polypropylene, 27% polyethylene). The configuration will be analagous to that used in the 10-cell battery. Two rectangular pieces, 1/8" smaller than the inside dimensions of the compartment, are placed back to back after the blue threads have been removed to improve flow distribution.

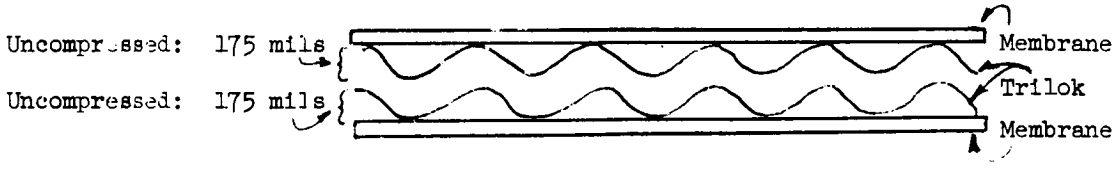

The sketch above showing an end view suggests the support which this offers to the membranes. Considerable force is required to compress the two layers of Trilok, each of which has a maximum thickness of 175 mils when uncompressed, to a total thickness of less than the 116 mils occupied by the compartment and gaskets.

9.5 Overall Battery Dimensions

9.5.1 Battery Area

Maximum dimensions of all components except end frames and terminal collector plates:

15-3/8" x 18-9/32" = 281 sqaure inches

Maximum dimensions of terminal collector plates:

15-3/8" x 19-21/32" = 303 square inches

Maximum dimensions of end frames:

16-5/8" x 19-17/32" = 324 square inches

9.5.2 Battery Depth

The thickness of an individual assembled set of three parallel cells can be calculated as follows:

	Mils
Collector Plate	10
Gasket (Compressed)	7
Gas Compartment	31
Gasket (Compressed)	7
Membrane	22
Gasket (Compressed)	7
Electrolyte Compartment	100
Gasket (Compressed)	7
Membrane	22
Gasket (Compressed)	7
Gas Compartment	31
Gasket (Compressed)	7
TOTAL REPEATING UNIT	258 mils

The exact amount of compression occurring will have to be determined experimentally.

Set of 44 cells including terminal collector plates:

$$44(258) + 30 = 11{,}382 \text{ mils}$$

Assembled battery:

	Inches
Cells	11.38
End Blocks	1.00
End Frames	4.00
TOTAL DEPTH	16.38 inches

9.5.3 Battery Volume

The total volume occupied by the cells, end blocks, end frames, nuts, and bolts is approximately 2.12 cubic feet. The exact volume will depend upon the amount of compression actually occurring in the gaskets.

9.5.4 Battery Weight

As detailed in Table 9.1, the filled weight of the battery is approximately 315 lbs.

9.6 Battery Assembly

To facilitate and expedite assembly, it is currently intended to preassemble some of the components. Two "sandwiches" are contemplated for each set of 3 parallel cells. One will be a three-component sandwich consisting of the electrolyte compartment and its two adjacent gaskets. The other will be a seven-component sandwich consisting of a collector plate in the middle flanked on each side by a gasket, a gas compartment and another gasket (four gaskets, two gas compartments and a collector plate in all). These "sandwiches" will each be preassembled by spot-gluing sufficiently to permit handling as a unit during the actual assembly of the battery. A diluted commercially available neoprene cement is currently scheduled to be the gluing agent.

The battery is to be assembled on a jig consisting of four stainless steel

line-up posts which will go through the manifolds in the four corners. The post in the upper right hand corner is to have only a slight clearance. A post of 5/32" diameter will provide 1/32" clearance. The other posts will have 1/16" clearance, i.e., 7/16" diameter.

The bottom end frame and end block will be placed on the rig first, the other components then proceeding in order. A check-off list is to be maintained simultaneously, each part being noted as the assembly proceeds. This technique has been very successful in the past for preventing the omission or misplacement of a component from a many-component assembly.

When the cell is assembled, the bolts will be tightened using a torque wrench. The requisite torque must be determined experimentally; however, it should be on the order of 200 inch-lbs., which has been satisfactory for multi-cell batteries.

9.7 Battery Process Parameters

The process parameters will be based upon the expected battery characteristics shown in Figures 9.3 & 9.4. It is assumed that 2200 watts will be drawn from the battery at 31.6 volts and 69.6 amps, i.e., at a current density of 53.1 amps/ft^2.

9.7.1 Gas Rates

$$\text{Hydrogen consumed} = \frac{(44 \text{ cells})\ (69.6 \text{ amperes})}{(26.8 \text{ amp-hr/eq})(2 \text{ eq/mol})}$$

$$= 57.2 \text{ mg-mol/hr} = 1280 \text{ STP liters/hr}$$

$$\text{Oxygen consumed} = 28.6 \text{ gm-mol/hr} = 640 \text{ STP liters/hr}$$

Since the accumulation of liquid in the gas compartments precludes "dead-ended" operation of the battery, a choice must be made as to the recycle rate. Recycle rates as low as four times the consumption rate have proven successful. (See Section 6.0&7.0 of this Report). The balance of the calculation is done assuming 25% utilization of feed. In practice adjustment of this parameter is a convenient method of obtaining the desired pressure drop across each cell.

Thus, the inlet and outlet rates are fixed:

Hydrogen inlet rate	-	5120 STP liters/hour
Hydrogen outlet rate	-	3840 STP liters/hour
Oxygen inlet rate	-	2560 STP liters/hour
Oxygen outlet rate	-	1920 STP liters/hour

Battery operation at 20 psia is envisaged, although satisfactory performance should be obtained at pressures anywhere in the range of 10 to 35 psia.

9.7.2 Heat Load

For the reaction, $H_2(g) + 1/2O_2(g) \rightarrow H_2O(l)$, the enthalph change is ΔH° = -68,320 cals per gm-mol H_2 reacted at 25°C. The actual reaction in the battery is to occur at around 60°C and the product water will be dissolved in 6N H_2SO_4. For present purposes corrections to the value of ΔH° given above are not warranted.

Total enthalpy change (57.2) (68,320)	= 3.91×10^6 cals/hr
Electrical work (2,200) (3,600/4.18)	= 1.89×10^6 cals/hr
Heat rejection from reaction	= 2.02×10^6 cals/hr

9.7.3 Electrolyte Circulation Rate and Temperature Rise

The ten-cell stack worked satisfactorily at an electrolyte rate of 30 ml/min. at a current of 6 amperes. The equivalent rate for the 2-KW battery is:

$$(30)\ \left(\frac{(44)}{(10)}\right)\ \left(\frac{(69.6)}{(6)}\right) = 1{,}530 \text{ ml/min}$$

Electrolyte Normality	-	6N
Weight Percent H_2SO_4	-	25%
Specific Gravity 60/60°F	-	1.18
Specific Heat	-	0.81 cal/gm°C

(almost independent of temperature between 30°C and 90°C)

$$\text{Temperature rise: } \frac{(2.02 \times 10^6)}{(1,530)(1.18)(0.81)(60)} = 23.1^\circ C$$

Optimization of electrolyte flow rate will depend on total system considerations.

9.7.4 Liquid Removal Rates

Experiments have shown that at 53.1 amps/ft^2 and 60°C, the hydrogen stream passing through a cell using 6N H_2SO_4 as electrolyte-coolant removes 7.45 ml of 6N H_2SO_4 per hour per square foot of cell while the oxygen stream removes 9.45 ml of 4.3N H_2SO_4 (See Section 6.0 of this Report).

For the 2-KW battery (44 cells of 1.31 ft^2), this corresponds to:

H_2 Stream: (7.45) (44) (1.31)/(60) = 7.1 ml/min 6N H_2SO_4

O_2 Stream: (9.45) (44) (1.31)/(60) = 9.1 ml/min 4.3N H_2SO_4

9.8 Areas for Possible Improvement

This design is based on a very conservative philosophy: the design of all components involves only very minor changes from the present proven state-of-the-art. Considerable improvements in weight, volume and cost should be obtainable after a reasonable amount of further development effort. Some of the possible areas of improvement follow.

9.8.1 Electrolyte Compartments

This design calls for compartments 100 mils thick to permit drilling of inlet and outlet ports. Thinner compartments with milled channels covered with suitable cover plates should be developable. The total thickness should be reducible to 50 mils which would represent a saving of 50% of the weight of electrolyte compartment, electrolyte and mesh filler or a saving of 37 lbs representing 12% of the battery weight.

9.8.2 Electrodes

Present electrodes contain 84 grams of platinum black per square foot giving a total of 21.4 pounds of platinum black for the 2-KW battery. It should be

possible to reduce the platinum content of oxygen electrodes by a factor of at least 2 and of hydrogen electrodes by a factor of at least 6. This would represent a saving of 14.3 pounds of platinum black.

9.8.3 Pusher and Collector Plates

Present plates are 10-mil thick in order to maintain adequate "springiness". The supplier(Kawecki Chemical Company) feels that with suitable mechanical treatment, equivalent springiness can be obtained from 5-mil stock. This change would represent a saving of 45.8 pounds.

These examples of possible weight savings should be cumulative, i.e., amount to 97 pounds or more than 30% of the battery weight.

9.8.4 Performance Improvements

In addition to the weight savings discussed above, it is likely that significant performance credits should be attainable. Preliminary experimental results have shown that temporarily depriving the oxygen electrode of oxygen while under load will decrease the cell electrode polarization by about 70 mv when oxygen feed is restarted. Polarization increases thereafter at approximately 2 mv/hr. (See Test and Inspection Report, 10-Cell Battery, July 17, 1963, submitted as part of this program). It is apparent that intermittent oxygen deprivation, on the order of once every 12 hours or so, would lead to average cell polarization levels well below those listed for the "steady state" case discussed: an average extrapolated zero current voltage of 0.925 volts/cell should be attained instead of 0.867 volts/cell. This would correspond to a gross time-average battery power of 3780 watts for this "2-KW battery". Further systems analysis of the expected power demand profile should show what the optimum schedule of oxygen deprivation either of the entire battery or of one separated module at a time would be.

10.0 Conclusions and Recommendations

10.1 Conclusions

The conclusions drawn from this study have been grouped according to the general aspects of the work performed:

1. Materials Testing
2. Battery Performance and Effect of Operating Parameters
3. Ten-Cell Demonstrator Battery
4. 2-KW Battery Design

10.1.1 Materials Testing

At least one material, and sometimes more than one, was found for each of the fuel cell component requirements. The materials which are satisfactory for service in 6N H_2SO_4 at temperatures up to 95°C are:

1.	Metallic:	platinum, zirconium, niobium
2.	Membrane:	Ionics cation resin 61-AZG
3.	Elastomer:	Dacron-backed Viton A and Butyl rubber
4.	Compartment Plastic:	Teflon, Kel-F, Penton, Halon TVS-500, ADM Arapel-7250, Hetron 92, Hypol 4050, Atlac 382
5.	Spacer Mesh:	Trilok 6027-1-1

No difficulties are therefore expected in meeting the material requirements of dual membrane fuel cells.

10.1.2 Battery Performance and Effect of Operating Parameters

The current Dual Membrane Fuel Cell design for single cells or multiple cell batteries permitted extended operation greater than 1000 hours under constant or variable load. The preferred components are listed below.

1. Electrodes: Platinum black bonded to platinum gauze with the aid of sintered teflon.

2. Membranes: Ionics cation resin 61-AZG glass-backed sulfonated polystyrene

3. Pusher and Collector Plates: Niobium sheet stock suitable stamped.

4. Compartment Frames: Any of the plastics found acceptable in the materials testing program. Teflon has a slight edge on the basis of ready availability and easy machinability.

5. Gaskets: Dacron-backed Viton-A.

Performance at 60°C of a battery containing niobium metallics can be characterized by an average voltage of 0.78 volts/cell at 24 amps/ft^2, a specific conductance of 360 mhos/ft^2-cell and a peak power density of 64 watts/ft^2-cell. Variations existed between cells presumed to be primarily due to oxygen electrode variations. With judicious selection of oxygen electrodes, the average cell voltage should be raised to at least 0.8 volts/cell at 24 amps/ft^2.

Decreasing temperature lowers the voltage attainable at a given current density and increases the specific conductance. Lowering the temperature from 60°C to 20°C decreases the specific conductance by as much as 50 mhos/ft^2 and lowers the extrapolated zero current voltage by 10 to 20 mv.

Electrolyte normality, gas flow rates and small changes in pressure level (5 to 15 psig) have no noticeable effect on battery electric performance. Gas pressure drops can be kept quite low, on the order of 25 mm H_2O, without adversely affecting gas distribution among the cells of a battery.

Electrolyte normality has a pronounced effect on the amount of liquid transported across the ion-exchange membranes. At 20°C, the quantities involved are given by the relations:

Liquid transported across H_2-side membrane = 0.0022 N_e^2 gms/amp-hr-cell

Liquid transported across O_2-side membrane = 2.9 N_m^{-2} gms/amp-hr-cell

where N_e is the electrolyte normality and N_m is the "membrane" normality, i.e., the geometric mean of the liquid normalities on either side of the oxygen-side membrane. For 6N electrolyte and a current density of 24 amps/ft^2, these liquid rates correspond to 1.9 gms/hr-ft^2 of cell on the hydrogen side and 2.3 gms/hr-ft^2 of cell on the oxygen side. Operation at 60°C instead of 20°C approximately doubled these liquid rates.

10.1.3 Ten-Cell Demonstrator Battery

The 10-cell battery built and delivered under this contract maintained an average voltage of 7.78 volts at the required current of 6 amps (24 amps/ft^2) at a temperature of 20°C. Electrode rejuvenation by temporary oxygen deprivation increased the voltage to 8.5 volts at 6 amps but this higher voltage dropped back slowly at the rate of approximately .02 v/hour. At the design voltage of 6.8 volts the battery delivered a current of 18.8 amps and a power output of 128 watts while in the metastable rejuvenated condition. The corresponding values for the stable unrejuvenated condition were calculated to be 15 amps and 102 watts at the design voltage of 6.8 volts.

10.1.4 2-KW Battery Design

The 2-KW (net) Fuel Cell Battery designed under this contract was designed on a very conservative basis. The expected electrical performance characteristics have all been demonstrated in dual membrane fuel cell batteries. The individual cell compartments are less than twice as big as the current cells, holding possible scale-up problems to a minimum. The specification of three semi-independent modular stacks provide for a high degree of reliability.

10.2 Recommendations

Three lines of continued effort appear worthwhile:

1. Construction of the 2-KW Battery designed under this contract.
2. Further engineering development aimed at decreasing the weight and volume of dual membrane fuel cell batteries.

3. Further laboratory development aimed at decreasing oxygen-side electrode polarization, increasing cell specific conductance and decreasing liquid transport across the membranes.

These three lines of effort can be pursued either simultaneously or serially. They are discussed in some further detail below.

10.2.1 Construction of 2-KW Battery

The design presented in Section 9.0 of this report should lead to an excellent, reliable H_2/O_2 fuel cell battery. No technical stumbling blocks to the realization of at least 2000 watts (net) at least 28 volts are foreseen. Construction of the battery would not only provide a working prototype of a fuel cell battery in the important low-kilowatt range but also provide an opportunity to discover and resolve any unforeseen difficulties. The design is sufficiently flexible so that engineering improvements recommended as a result of a possible parallel engineering development program could most probably be incorporated in the battery under construction.

10.2.2 Engineering Development Program

The present 2-KW Battery design is very conservative and relies on components proven in extensive testing. Significant weight, volume, and platinum cost reductions should be achievable after some additional engineering development work. Typical areas of possible improvement are detailed in Section 9.8 of this report.

10.2.3 Laboratory Development Program

Further laboratory investigations of electrode formulations not requiring a high temperature sintering step could lead to oxygen electrodes with lower polarizations. The use of polyethylene instead of teflon as a binding and waterproofing agent is one likely avenue of approach.

The further development of electrodes formed directly on the ion-exchange membrane could conceivable increase the specific conductance of the cells.

A more detailed study of electrode rejuvenation either by oxygen deprivation or by electrical forcing (imposing momentarily a reverse potential on the battery) could lead to large gains in overall battery performance.

Development of separate specific ion-exchange membranes for the hydrogen and the oxygen sides should lead to overall minimizing of the liquid transport across the membranes. The hydrogen side needs a rather thick membrane with very high ion-exchange capacity to present a successful barrier to anion transport. The oxygen side needs a thinner membrane with a lower H_2O diffusion resistance to facilitate the movement of the water formed on the electrode side back into the electrolyte. Such specific membranes are felt to be developable.

PART II

OSMOTIC STILL DEVELOPMENT

1.0 Introduction

The dilution of the acid electrolyte with water during the operation of the dual membrane fuel cell requires that this byproduct water be continuously removed from the circulating electrolyte system. When fuel cells are employed as a source of auxiliary power in manned space vehicles, the water removed must be of a purity suitable for human consumption. Further, the method of removal of water from the electrolyte must be applicable to a zero gravity environment.

Earlier experiments at TRW indicated that the osmotic phenomena of semipermeable membranes could be utilized for water separation at rates sufficiently high for fuel cell applications.

One of primary objectives of the NASA program described in this report was to design and test a water separation unit with the separation capacity equal to that required for a nominal 2 KW fuel cell. The program to accomplish this objective was divided into two major efforts: (1) the experimental study of water removal rates of various types of membranes under controlled conditions of temperature, pressure and acid concentration and (2) the design, fabrication and 100 hour endurance test of an osmotic still unit with a water separation capacity equal to the water generation of a nominal 2 KW H_2 - O_2 fuel cell battery. (Approximately 2 lbs/hr.)

2.0 Summary

An experimental test program was performed to determine the suitability of commercially available ion-exchange membranes and other component materials for incorporation in a water extraction unit (Osmotic Still). A water extraction unit with a water separation capacity from 6N sulfuric acid equal to that required for a nominal 2 KW dual membrane fuel cell (2# H_2O/hr) was designed, fabricated and successfully tested.

Membranes and porous materials tested for water separation performance during the experimental phase of the program were:

1. Ionics Inc. membranes (CR-61) and (AR-111A)
2. American Machine & Foundry membranes (C-60), (C-103-C) and (A-60)
3. Ionac Company membranes (MC-3142), (MA-3148), (XLMC-3235) and (XLMA-3236)
4. E. S. B. Reeves Company porous Teflon and porous polyethelene

Ionics membranes were unsatisfactory due to membrane cracking and subsequent liquid leakage. Ionac membranes and the porous materials were unsatisfactory due to liquid leakage. Good durability was exhibited by all of the American Machine & Foundry membranes and water extraction rates were obtained for these membranes from Sulfuric acid solutions up to 200°F. The AMF C-60 membrane was far superior to the other AMF membranes in that its water extraction performance exceeded the others by more than 2 to 1. Test with this membrane indicated that extraction performance is a strong function of acid concentration; for example, the maximum extraction rate obtained from a 200°F, 15.2% H_2SO_4 concentration was 320 cc/hr/ft^2 compared to 160 cc/hr/ft^2 obtained from a 200°F 25.2% H_2SO_4 concentration.

These membrane performance tests along with related material evaluations led to the selection of the following materials for the 2 KW osmotic still components:

1.	Membranes:	AMF cation C-60
2.	Membrane Supports - Vapor Cavity:	Kel-F coated monel screens
3.	Membrane Supports & Flow Distribution - Acid Cavity:	Trilok Fabric - (Style D-59633-C) (Polypropylene & polyethylene)

4.	End Plates & Cavity Rims	Polyvinyl Dichloride
5.	Gaskets	Viton A- Synthetic Rubber

The 2K Osmotic Still was tested continuously for 100 hours and the design water extraction rate of 2 lbs/hr of pH 5 or above from 6N H_2SO_4 at 195°F was obtained during this test.

Visual inspection of the still component materials at the completion of the 100 hour test found all components intact with little or no evidence of material corrosion or failure which would limit performance or operational life.

3.0 Principles of Operation

3.1 Osmosis & Semipermeability

The basic principle employed in the osmotic still is the phenomena of osmosis and semipermeability. Osmosis may be defined as the spontaneous flow of water into a solution, or from a more dilute to a more concentrated solution, when separated from each other by a suitable membrane. The essential property of these membranes is that they allow free passage of the water or solvent but not of the dissolved substance or solute. Such a membrane is termed a semipermeable membrane.

Although there have been several theories advanced as to mechanisms involved in osmosis and semipermeability, it is generally recognized that there may be no one explanation covering all instances of semipermeability and osmosis. The surface of a solution consisting of a non-volatile solute in a volatile solvent is a semipermeable membrane, since it allows free passage of the solvent molecules from the surface in the form of vapor while the solute is held in the liquid. Yet the mode of operation of this membrane may be considerably different from that of animal and vegetable membranes. However, it is well known that primary variables effecting osmosis are vapor pressure, solution concentration, static pressure, and temperature.

3.2 Method of Water Separation

The method employed for water separation from an acid electrolyte utilizing ion exchange and non-ionic membranes is best described by referring to Figure 3.1.

Figure 3.1-A shows a closed container divided into two cavities by a semipermeable membrane. One cavity contains a sulfuric acid solution and the other cavity contains only water vapor. When the two cavities are in thermal equilibrium the vapor pressure in the water vapor cavity equals the water vapor pressure at the surface of the acid saturated membrane. Ideally, this vapor pressure is the same as the water vapor pressure of the acid solution. When the water vapor pressure is reduced in the vapor cavity by the removal of water vapor as shown in Figure 3.1-B, a vapor pressure gradient is established between the

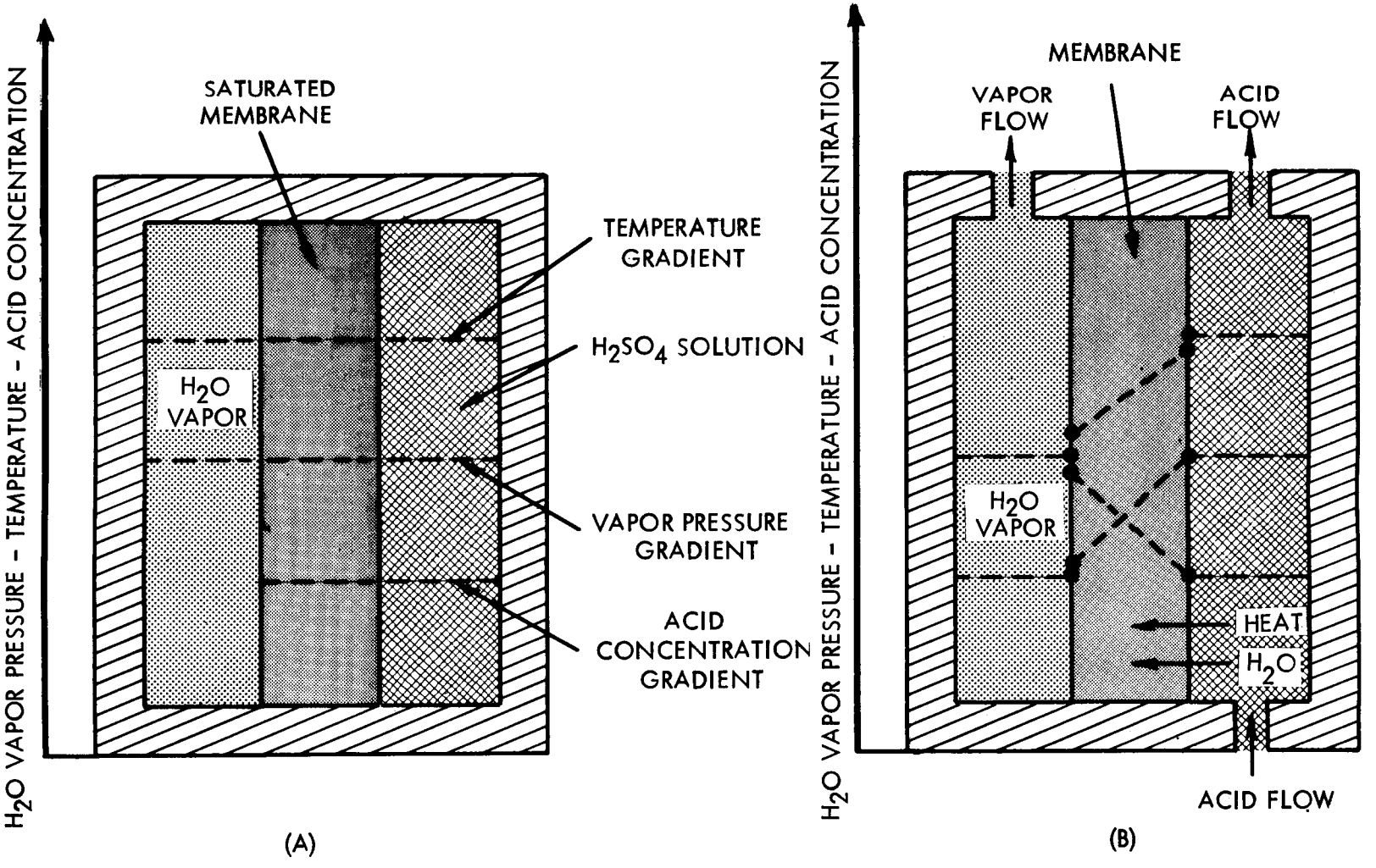

Figure 3.1 Illustration of Water Separation From an Acid Electrolyte

membrane surface and the vapor cavity resulting in water evaporation from the membrane surface. The heat for vaporization is supplied by the acid solution and a temperature gradient is established between the acid bulk and the vapor side of the membrane. Since water is being removed from the vapor side of the membrane an acid concentration gradient is established across the membrane. This concentration gradient across the membrane results in water flow by osmosis through the membrane from the acid solution to the vapor side of the membrane. When water vapor is continuously removed from the vapor cavity at a constant rate and acid, at a given concentration and temperature, is circulated through the acid cavity, the various gradients are established as shown in Figure 3.1-B. The hydrodynamic liquid flow through the membrane by virtue of the static pressure difference between the two cavities is virtually zero due to the extremely small pores in the membrane. Extremely high pressure differences can be tolerated without hydrodynamic leakage.

The membrane then serves as a barrier between the two cavities and is a static liquid-vapor interface independent of gravity.

The liquid-vapor interface imposed by the membrane is of course an imperfect interface since it introduces additional heat and mass transfer resistance between the two cavities.

4.0 Experimental Evaluation of Membranes

4.1 Method of Membrane Testing

Since the heat and mass transfer characteristics of various membranes is unknown, emperical evaluation of the water separation capacity was accomplished by measuring the water separation rate while controlling the temperature, pressure and concentration of the sulfuric acid and controlling the vapor pressure on the vapor side of the membrane.

4.2 Experimental Test Unit

An exploded cross section of the circular experimental test unit used in the evaluation of membranes is shown in Figure 4.1. The single gas cavity is contained by a vapor housing and two membranes with a total separation area of 0.426 ft^2. The gas cavity is flanked on both sides by an acid cavity contained by the acid housing walls of the test unit. This arrangement prevents condensation in the vapor cavity due to external heat loss which would result in uncontrolled vapor pressures.

Since the acid static pressure is at atmospheric pressure or above and the vapor pressure is a partial vacuum, the membranes were supported in the vapor cavity by two perforated plates which were separated by spacers. Between the perforated membrane support plates and the membranes, a screen mesh or matrix was used to achieve maximum effective separation area and to permit lateral vapor flow to the holes in the perforated support plates. The support plates were not anchored to the vapor cavity rim but were floating and held in place only by the membranes. This allowed matrices of various thicknesses to be tested merely by changing the support plate spacers. Hypalon rubber gaskets were used on both sides of each membrane. The entire assembly was bolted together with 1/4" bolts.

The material used for construction of entire test unit, with the exception of the gaskets, membranes, and support matrices was polyvinldichloride. Figures 4.2 and 4.3 are photos of details of the experimental test unit.

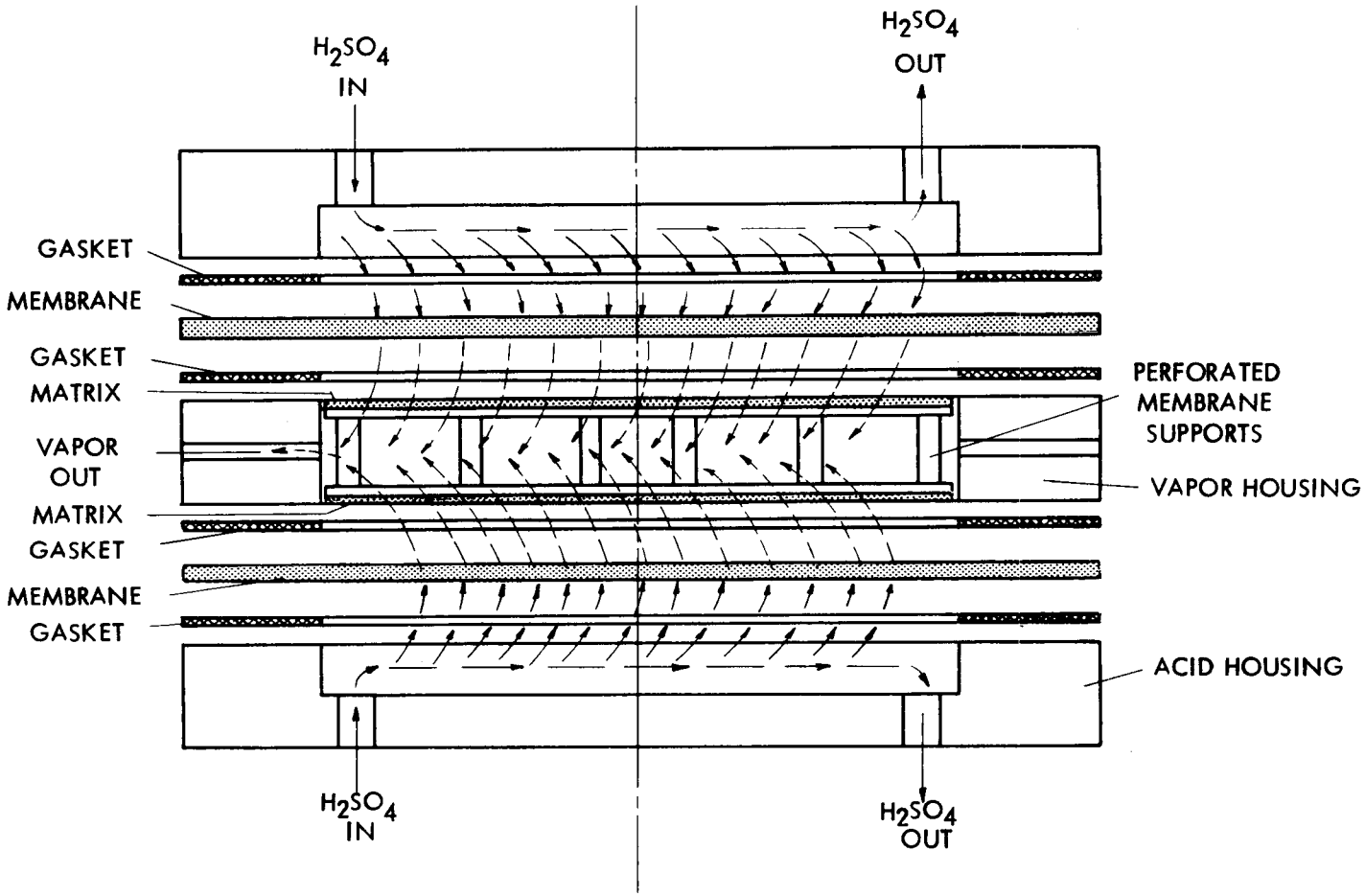

MATERIALS

ACID HOUSING, VAPOR HOUSING & PERFORATED MEMBRANE SUPPORTS - POLYVINYL DICHLORIDE
GASKETS - POLYETHYLENE & POLYPROPYLENE

HOUSING OUTSIDE DIAMETER - 9"
HOUSING INSIDE DIAMETER - 6-3/4"

Figure 4.1 Experimental Test Unit - Osmotic Still

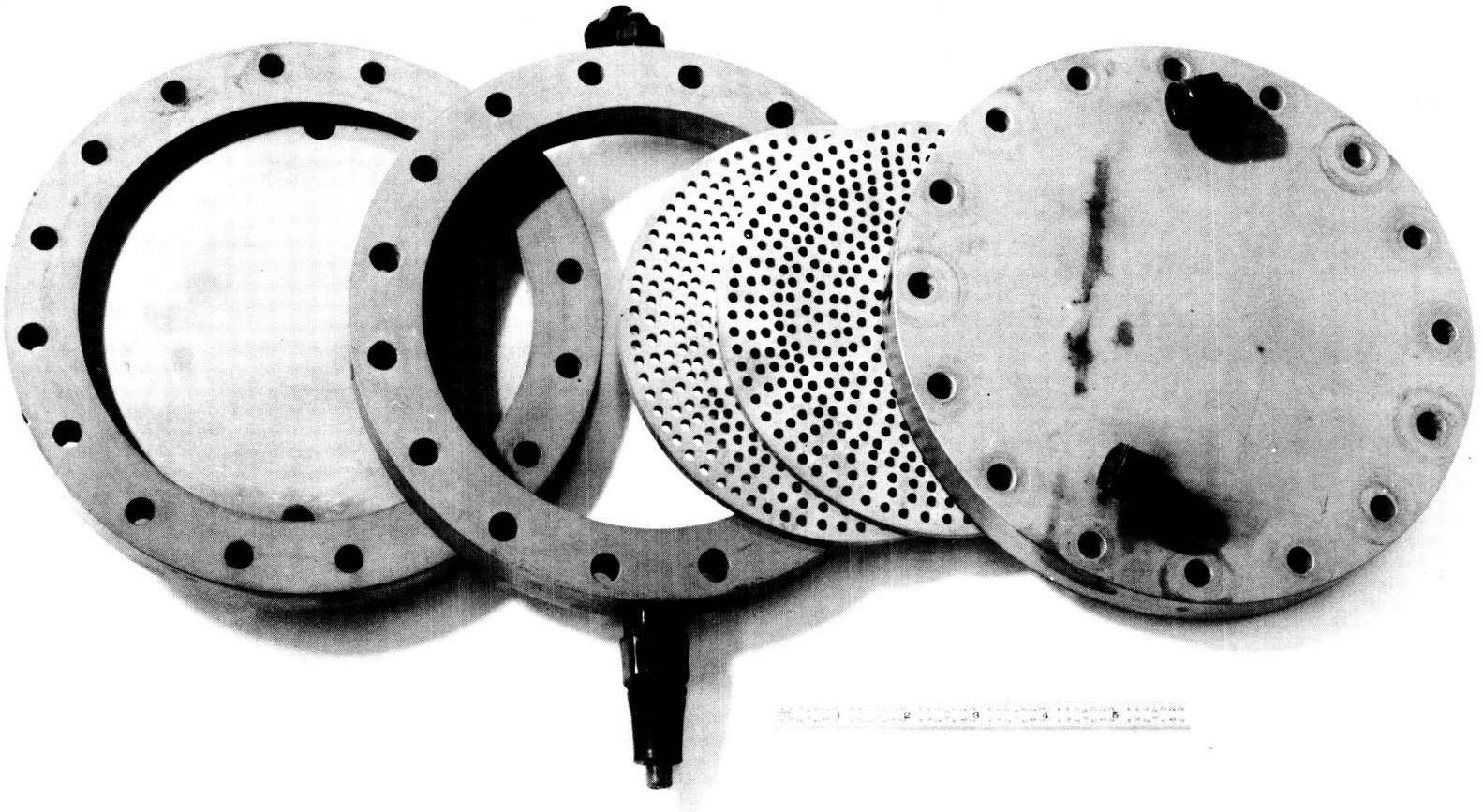

Figure 4.2 Photo of Experimental Test Unit Osmotic Still - Disassembled

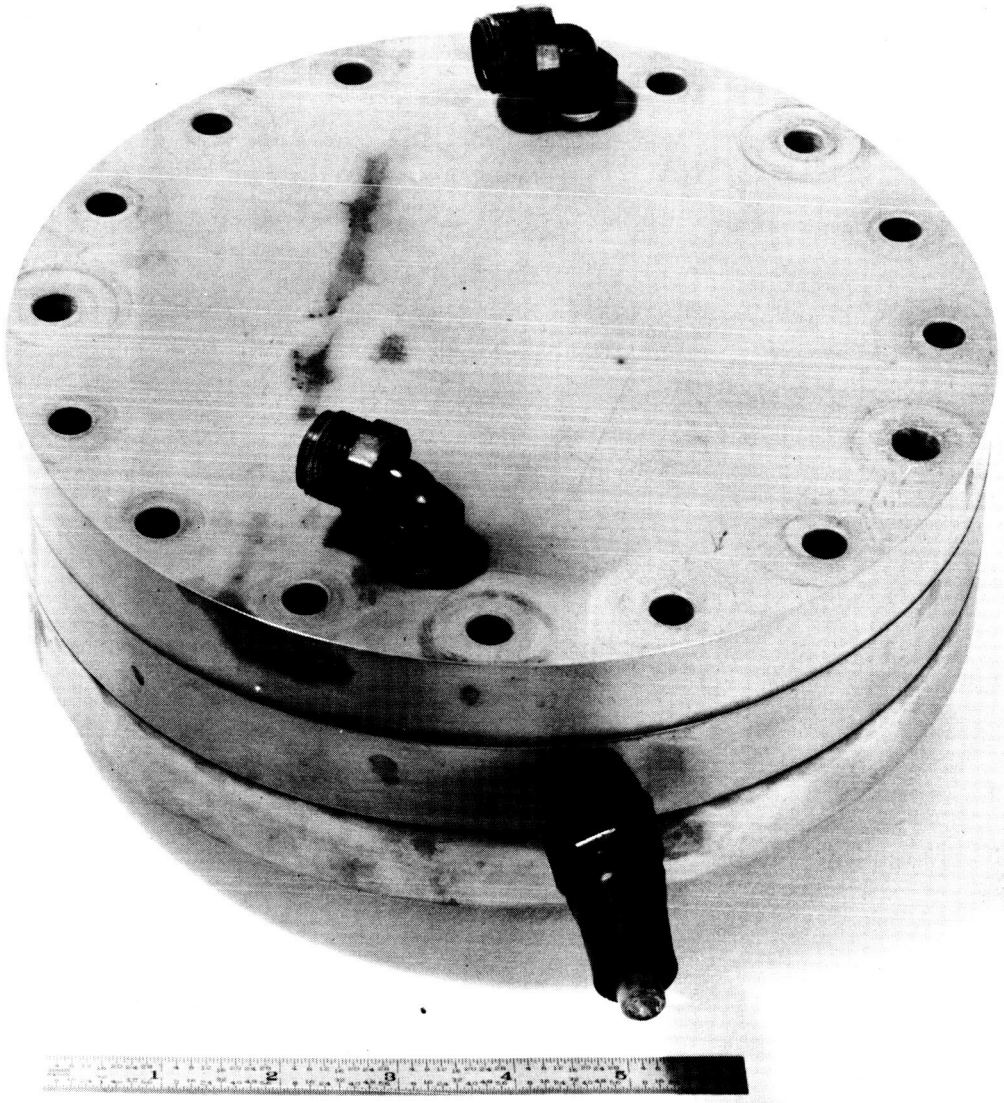

Figure 4.3 Photo of Experimental Test Unit Osmotic Still - Assembled

4.3 Experimental Test Rig

4.3.1 Description and Operation

The test rig used for the experimental testing is shown schematically in Figure 4.4. The acid electrolyte, heated and maintained at test temperature was circulated through the test unit with a parastaltic acid pump. The acid loop was pressurized with argon at the acid reservoir and this pressure (P_2) was measured directly with a standard mercury U tube monometer. The acid flow rate was monitored with a rotometer tube utilizing a tantalum float. Acid concentration was maintained by periodic injection of distilled water into the acid reservoir from the water supply flask. Water vapor leaving the vapor cavity of the test unit was condensed in a water cooled pyrex condenser and drained into a measuring flask. Water vapor pressure (P_1) was measured at the upper end of the test unit with a U-tube mercury manometer. Both the vapor leg of the manometer and the vapor line between the test unit and the condenser was heated above acid temperature to insure that condensation occurs only in the condenser. The water vapor pressure was controlled by controlling the temperature of the circulated cooling water flowing through the condenser jacket. The vapor cavity in the test unit and the vapor side of the system was connected to a vacuum pump for initial removal of noncondensable gases and for periodic purging of non-condensibles. The test unit was mounted with the vapor exit port at the bottom to allow any acid leakage to drain directly into the condenser permitting immediate leak detection. Also, vertical orientation of the membranes demonstrates water separation independent of gravity.

The test unit, heated reservoirs, and all hot lines were insulated to minimize external heat loss.

Acid temperatures T_1 and T_2 and cooling water temperature T_3 were measured with calibrated mercury in glass thermometers immersed in the flowing fluid streams. Temperatures T_4 and T_5 were measured with mercury in glass thermometers intimately attached to the two acid outlets from the test unit. These temperatures were monitored only for detection of unequal flow in the two acid cavities in the test unit.

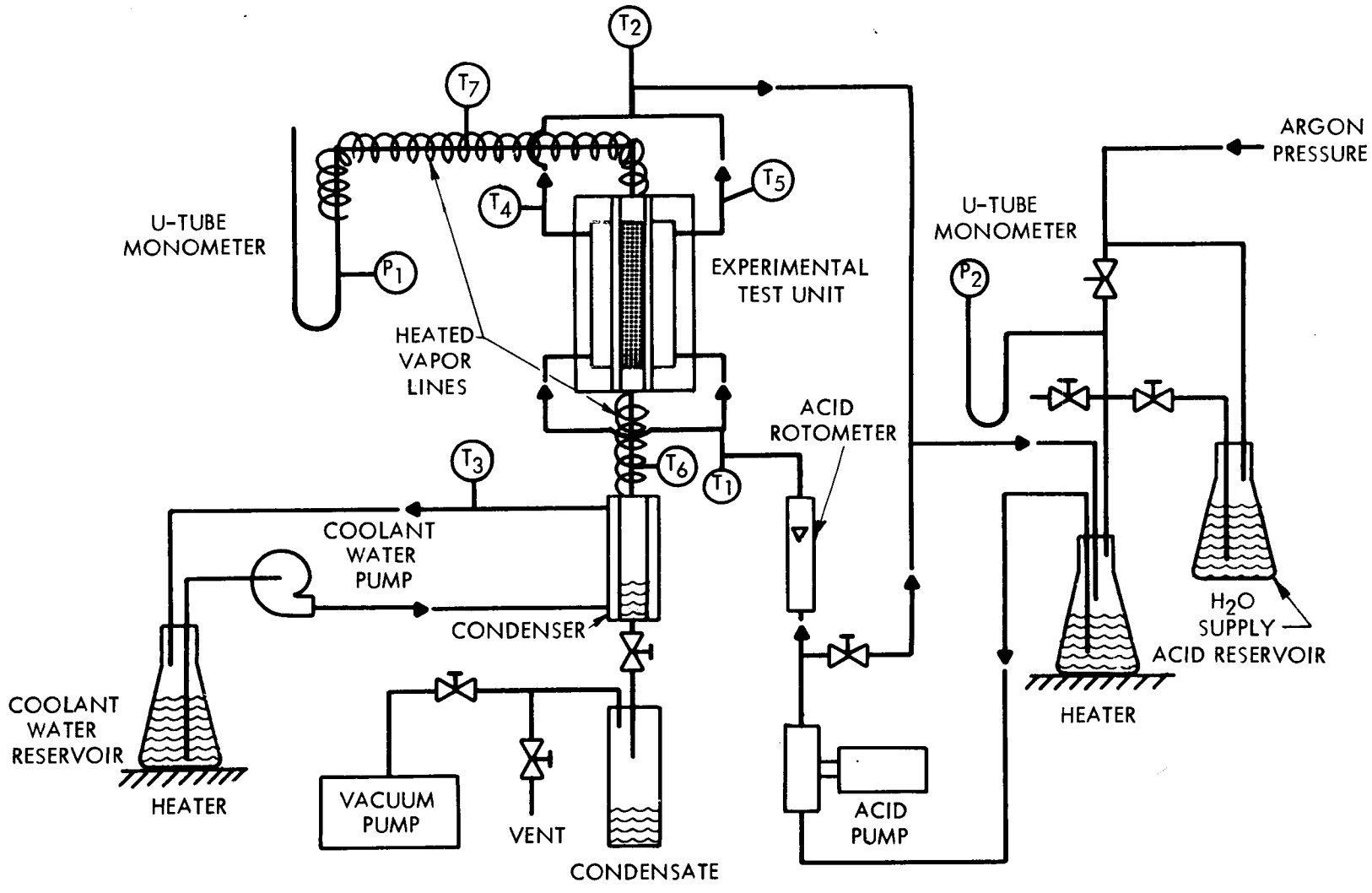

Figure 4.4 Experimental Test Rig Schematic

Temperatures T_6 and T_7 were Weston dial thermometers attached intimately to the heated vapor lines.

Heating of the acid solution and the condenser cooling water was accomplished by variac controlled hot plates. Heating of vapor lines was accomplished by variac controlled strip heaters wrapped around the vapor lines.

4.4 Test Procedures and Results

4.4.1 Membrane Tests

Tests were performed on a total of nine types of commercially available ion exchange membranes from Ionics, Inc., Ionac, and American Machine and Foundry. In addition, tests were conducted on two types of non-ionic porous materials. Table 4.1 lists the ion exchange membranes and their properties as compiled from the manufactures' literature. Test procedures and results of these membranes test are presented in the following subsections.

4.4.1.1 Ionics Inc. Membranes

Several performance tests with Ionics cation CR-61 and anion AR-111A membranes were performed in the test unit. Each of these tests ended in membrane failure due to membrane cracking and subsequent acid leakage.

The initial test was with cation membranes and with water used in place of the H_2SO_4 solution. As a vacuum was slowly drawn on the vapor side of the test unit, periodic leakage of water into the condenser indicated membrane failure at the onset of the test. Inspection of the membranes after dismantling of the test unit revealed excessive cracking along the gasket edge of the membrane and considerable sagging of the membrane towards the vapor cavity as well as cracking under the gaskets. Modifications to test unit prior to the next test included making closer fitting support plates to give better support at gasket edges and also trimming gasket I.D.'s to eliminate interference with the spacer material.

Cation membranes, after soaking in 25% H_2SO_4 for approximately 118 hours, were tested in the test unit for approximately 4-1/2 hours with H_2SO_4 temperature

TABLE 4.1

Membrane Properties

A. American Machine & Foundry Membranes

Property	Strong Acid Type (Cation)		Strong Base Type (Anion)
Manufacturer's No.	C-60	C-103 C	A-60
Resistance (0.6N K Cl)-ohm-cm^2	5 ± 2	7 ± 2	7 ± 2
Permselectivity (0.2N/0 in K Cl)%	92 ± 3	98 ± 1	93 ± 3
Capacity (dry) meq/g	1.6 ± 0.2	1.2 ± 0.2	2.0 ± 0.2
Gel Water (wet basis) %	35 ± 6	15 ± 3	22 ± 5
Mullen burst strength (wet) psig	35 ± 5	55 ± 7	50 ± 5
Thickness (wet) mils	12 ± 1	7.5 ± 0.7	12 ± 1

Note: Values listed are average values for individual production runs. The electrochemical properties listed are measured under the standard specified conditions. As with all ion-permeable materials, the resistance, swelling, and capacity are affected by the ambient solution concentrations and temperatures and by the type of ions present.

TABLE 4.1 (CONT'D)

Membrane Properties

B. Ionac Membranes

Property	Cation Membrane Ionac MC-3142	Anion Membrane Ionac MA-3148	Cation Membrane Ionac XLMC-3235	Anion Membrane Ionac XLMA-3236
Area Resistance (avg):				
in 0.1N NaCl	15 ohms-cm^2	56	18	121
in 1.0N NaCl	11 ohms-cm^2	22	11	38
Thickness (mils):	6	7	12	12
Mullen Burst Strength:	ca 190 psi	ca 190	ca 165	ca 165
Water Permeability (avg):				
$ml/hr/ft^2/10psi$	2.4	0	1.20	0.75
Total Capacity:	0.021 meq/cm^2	0.012	0.045	0.025
Stability:				
Dimensional	Good	Good	Good	Good
Acid	Good	Good	Good	Good
Alkali	Poor	Poor	Good	Good
Drying-Rewetting	Good	Good	Good	Good
Salt	Good	Good	Good	Good
Oxidizing Agents	Good	Good	Good	Good

Note: Ionac MC-3142 and MA-3148 are primarily acid stable. Ionac XLMC-3235 and XLMA-3236 are acid and alkali stable. Some variability in membrane properties should be expected from different manufacturing runs.

TABLE 4.1 (CONT'D)

C. Ionics Membranes

Property	Anion Membrane	Cation Membrane
Manufacturer's No.	AR-111A	CR-61
Resistance-ohm-cm^2	25.0 (Cl-form)	13.0 (Na-form)
Permselectivity (0.in NaCl)%	98.0	98.0
Backing by Weight %	33.0	32.0
Salt Splitting Capacity-meq/gn	1.0	1.0
Thickness - mm	0.7	0.7

Stability of Resin: All media except concentrated caustic and oxidizing agents.

held at 175°F and the vacuum on the vapor side held at 48 cm Hg. Water condensed had a pH of 1 indicating leaks. Inspection of membrane showed membrane sagging towards the vapor cavity with small cracks in the center. The membranes also had cracks under the gaskets with bolts tightened to a torque of 50 inch-pounds.

Anion membranes were installed in the test unit and tested under the same test conditions as above, except bolt torque was reduced to 35 inch-pounds. Again, these tests were unsuccessful due to the same type of membrane failure as in the previous tests.

Modifications in the test unit included replacement of Trilox spacer material with Monel screens (12 mesh .032 in. D. wire). Cation membranes were installed with bolts tightened to 25 inch-pounds.

Testing of cation membranes with H_2SO_4 temperatures of only 78°F resulted in acid leakage into the condenser with up to 72.6 cm Hg vacuum on vapor side of membranes.

Inspection of membranes indicated no sagging at all in the membrane surfaces but cracks were visible.

Previous tests were run with the membranes either soaked in 25% H_2SO_4 prior to installation or installed with only water soaking. Two more membrane tests were conducted but membranes were first progressively soaked in 10%, 20% and 25% H_2SO_4 for approximately 30 minutes in each solution to eliminate possibility of cracks due to rapid shrinking of the membrane upon exposure to more concentrated solutions. Both membrane tests produced water with a pH of 1 and upon removal of membranes from the test unit, inspection showed small cracks in the center of the membranes.

Due to the fact that membrane cracking and subsequent leakage could not be eliminated, testing with Ionics membranes was discontinued.

4.4.1.2 American Machine & Foundry Membranes

Initial tests with three sets of AMF C-60 cation membranes were made at acid temperatures ranging from 70°F to 200°F and with a maximum test duration of

13 hours over a period of three days. Throughout these tests condensate samples were taken each hour. In each test condensate samples had a pH 2 or less indicating acid contamination of the condensate. Upon examination of the membranes after the tests, no cracks or defects were found by visual inspection or by leak detection tests with a cationic dye. The membranes were in excellent condition and appeared to be extremely flexible and durable.

The failures of tests to obtain water with a pH rating above 4 without evidence of membrane leakage lead to suspicion that an unknown membrane behavior was taking place which resulted in contamination of the condensate water with acid. Therefore, a test was set up with an AMF cation membrane such that a visual observation of the membrane was possible during operation. This test revealed that upon introduction of acid at room temperature in the acid cavity of the test rig, the exposed face of membrane started to evolve liquid droplets of pH 1. The evolution of droplets was excessive enough to cause vertical liquid runs on the membrane surface and collection of liquid at the bottom of a test unit. Increasing acid temperature produced a drying effect on the entire surface of the membrane. Once the surface was dry, the application of acid solution to the membrane on the vapor side induced this "sweating" in the area around the point of application. Application of pure water on the dry membrane surface produced no "sweating" but in a short time drying would result at the point of application.

As a result of this test, it was hypothesized that the failure of the previous tests to produce water of higher purity was due to the wet surface of the membrane on the vapor side upon installation in the test unit. Upon installation, the acid on the vapor side of the membrane "wetted" the bare monel screen support and upon acid introduction to the test unit, sweating occurred at the membrane surface and the acid accumulated in the wetted screen matrix. This acid continuously migrated to the condenser resulting in contamination of the condensate.

To prevent the occurrence of this sweating phenomena, the monel screen supports were coated with a non-wetting material (described later in Section 5.0) to provide a non-wetting surface on the screen support and to protect the support

screens from acid attack. Also, before membrane installation, the vapor side of the membrane was thoroughly wiped with an absorbent cloth to remove all liquid from the membrane surface.

Subsequent performance tests with A-60, C-60 and C-103 membranes were completed with 25% acid temperatures ranging from 125°F to 200°F and with various vapor pressures.

Performance comparison indicated that the C-103 and A-60 membranes were inferior in water extraction rates to the C-60 membrane and testing of the C-103 and A-60 membranes was discontinued.

Performance tests with the C-60 membrane were concluded with several tests at 15%, 25%, 40% and 60% acid concentrations and with acid pressures of 0, 26, and 32 psia.

Figure 4.5 shows the performance test results of all the AMF membrane tests. The data is plotted with water extraction rate versus the vapor pressure difference between the vapor pressure of the acid solution at the test temperature and the vapor pressure maintained in the test unit. The data is presented in this manner to permit a simple comparison that includes all of the pertinent test variables. These results are listed in tabular form in Table 4.2.

4.4.1.3 Ionac Membranes

The initial test with the Ionac MC 3142 membrane material was made in the test unit after the membranes had been soaked in 180°F water for four hours as recommended by the Ionac representative. Upon initial evacuation of the vapor chamber prior to acid heatup, the membrane leaked acid excessively with a vacuum of only 20 cm of mercury. Upon removal of the membrane from the test unit, inspection showed no rupture in the membrane. It was therefore decided to perform leakage tests outside the test unit on all the Ionac membranes before cutting and installing membranes in the test unit. These tests were made by securing the membrane over a 3/8" diameter hole and exposing one side of the membrane to pressurized water and the other side to atmospheric air. Leakage was determined by visual observation. The water pressure was gradually increased to determine where leakage was visible. Table 4.3 tabulates the results

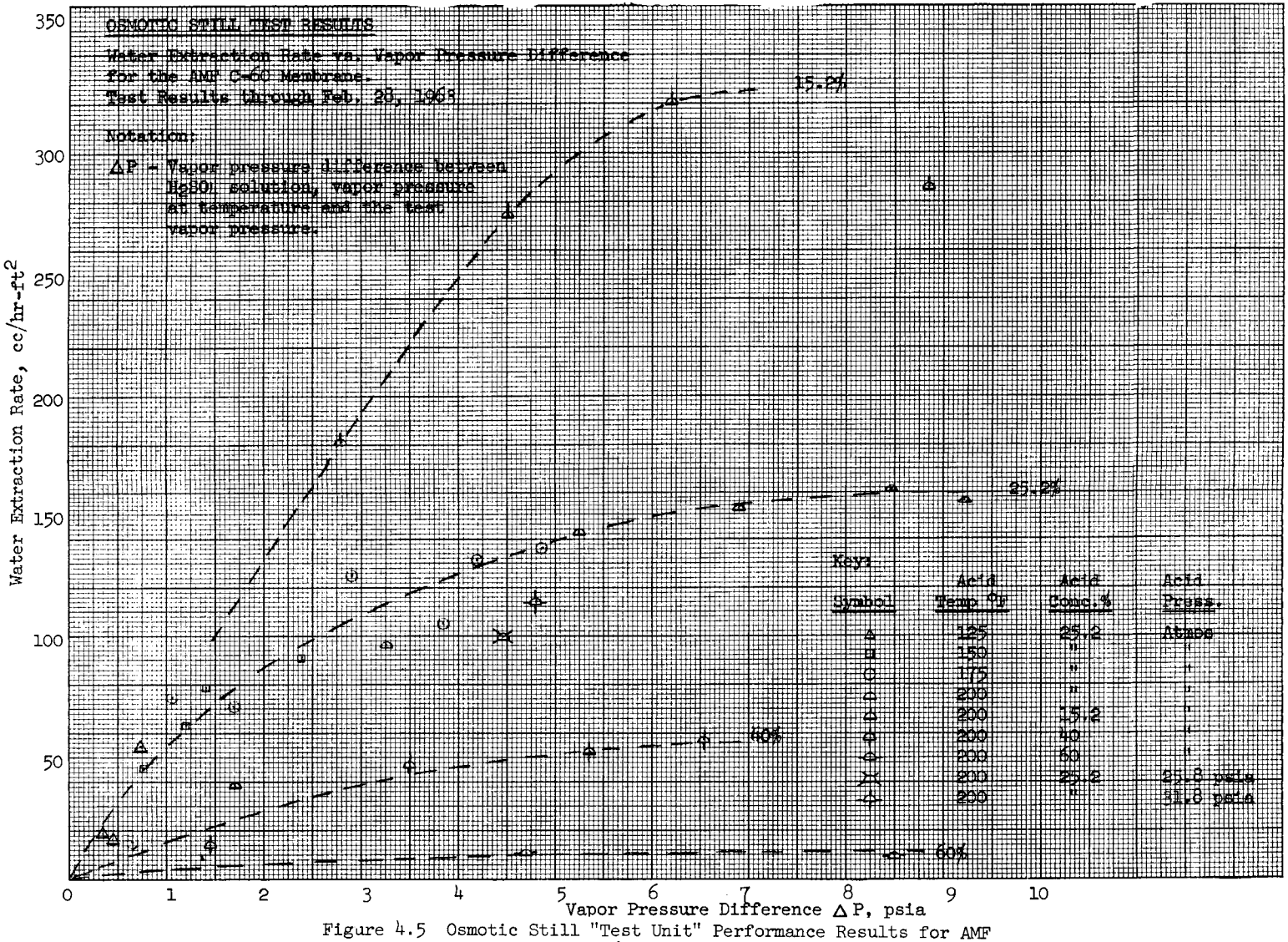

Figure 4.5 Osmotic Still "Test Unit" Performance Results for AMF C-60 Membrane

Test Results - AMF Membranes

TABLE 4.2

Date Tested	Membrane Number	Membrane Type	Avg H_2SO_4 Temp. in Test Unit °F	H_2SO_4 Conc. %	H_2SO_4 Pressure psia	H_2SO_4 Vapor Pressure @ Avg. Temp. psia	H_2O Vapor Pressure psia	Vapor Pressure Diff. psia	Total H_2O Extracted cc	Total Test Time Hr	H_2O Extraction Rate $cc/hr\ ft^2$	H_2O pH
1-29-63	16	AMF C-60	199.5	25.2		9.56	6.30	3.26	82.0	2.00	96.24	4.0
1-29-63	16		199.3			9.56	4.31	5.25	91.0	1.50	142.4	4.2
1-30-63	16		199.4			9.56	2.67	6.89	130.0	2.00	152.5	4.1
1-31-63	16		200.6			9.66	7.96	1.70	32.5	2.00	38.14	4.0
2-11-63	16		199.5			9.56	1.10	8.46	137.5	2.00	161.3	4.5
2-12-63	16		199.9			9.66	.45	9.21	133.0	2.00	156.1	4.6
2-27-63	16		198.2		25.8	9.24	4.77	4.47	85.0	2.00	99.8	5.0
2-28-63	16		199.2		31.8	9.56	4.74	4.82	29.0	.6	114.5	5.0
3-4-63	16		200.9		9.0	9.74	4.36	5.39	116.0	2.00	136.1	5.0
2-12-63	16		175.2			5.50	.63	4.87	116.0	2.00	136.1	4.7
1-28-63	16		175.2			5.50	3.82	1.68	60.5	2.00	71.0	4.1
1-29-63	16		174.7			5.50	1.66	3.84	89.5	2.00	105.0	4.1
2-11-63	16		175.5			5.41	1.23	4.18	112.0	2.00	131.4	4.3
1-25-63	16		148.2			2.99	1.58	1.41	67.5	2.00	79.22	4.3
1-25-63	16		150.5			3.09	2.33	.76	39.0	2.00	45.77	4.1
1-28-63	16		149.2			3.05	1.85	1.20	54.5	2.00	63.96	4.3
2-12-63	16		150.5			3.09	.71	2.38	77.5	2.00	90.96	4.5
1-22-63	16		125.1			1.62	.88	1.62	52.0	2.25	54.25	3.9
1-23-63	16		126.5			1.67	1.33	.34	4.0	.50	18.77	5.0
1-24-63	16		124.3			1.57	1.12	.45	7.0	1.00	16.43	5.0
2-14-63	16		197.9	15.2		10.14	1.29	8.85	244.0	2.00	286.3	4.7
2-15-63	16		198.2			10.24	4.03	6.21	273.0	2.00	320.4	4.3

Date Tested	Membrane Number	Membrane Type	Avg H_2SO_4 Temp. in Test Unit °F	H_2SO_4 Conc. %	H_2SO_4 Pressure psia	H_2SO_4 Vapor Pressure @ Avg. Temp. psia	H_2O Vapor Pressure psia	Vapor Pressure Diff. psia	Total H_2O Extracted cc	Total Test Time Hr	H_2O Extraction Rate cc/hr ft^2	H_2O pH
2-15-63	16	AMF C-60	199.6	15.2		10.53	6.02	4.51	234.0	2.00	274.6	4.5
2-15-63	16		201.2	15.2		10.92	8.14	2.78	154.0	2.00	180.7	4.3
2-20-63	16		201.2	40		7.15	.61	7.15	49.0	2.00	57.51	4.0
2-20-63	16		202.9	40		7.53	2.17	5.36	44.5	2.00	52.23	4.3
2-21-63	16		202.9	40		7.53	4.03	3.50	40.5	2.00	47.53	4.0
2-21-63	16		202.6	40		7.44	5.99	1.45	12.0	2.00	14.08	5.0
2-18-63	16		199.9	60		2.60	.67	1.93	4.7	1.00	11.03	5.0
2-19-63	16		201.0	60		2.66	.48	2.18	8.5	2.00	9.97	5.0
1-9-63	14		173.8	25.2		5.41	4.77	.64	13.3	2.00	15.61	5.0
1-9-63	14		174.7			5.09	4.03	1.06	58.0	1.23	74.40	5.0
1-10-63	14		174.0			5.45	2.54	2.91	71.0	1.33	125.3	3.5
1-15-63	15	AMF C-103	174.3			5.45	1.41	4.04	37.5	2.25	39.12	3.8
1-16-63	15		176.0			5.60	1.41	4.19	15.0	1.00	35.21	3.8
1-17-63	15		175.4			5.56	.53	5.03	19.5	1.50	30.51	3.9
12-17-62	13	AMF A-60	197.9			9.18	8.10	1.08	2.0	1.28	3.67	4.5
12-14-62	13		174.3			5.45	1.96	3.49	4.5	1.00	10.55	5.0
12-13-62	13		174.8			5.56	3.12	2.44	12.2	4.05	7.07	3.8
10-15-63			189.5			7.58	4.91	3.17	870.0	1.00	123.7	5.0
10-15-63			186.5			6.92	3.49	3.43	1805.0	2.00	128.3	5.0
10-16-63			184.5			6.83	4.05	2.78	1785.0	2.00	126.9	
10-16-63			187.5			7.56	4.03	3.53	1845.0	2.00	131.2	
10-17-63			187.5			7.57	3.90	3.67	1830.0	2.00	130.1	
10-17-63			197.2			8.83	3.85	4.98	1875.0	2.00	133.3	
10-18-63			198.3			9.22	5.67	3.55	1820.0	2.00	129.4	5.8
10-18-63			199.2			9.31	6.09	3.22	1815.0	2.00	129.0	
10-19-63			197.2			8.83	5.89	2.94	1810.0	2.00	128.7	
10-19-63			197.2			8.83	5.80	3.03	1820.0	2.00	129.4	5.8

TABLE 4.3

LEAKAGE TEST RESULTS

Ionac Membranes After Soaking In
Room Temperature Water for 16 Hours

Membrane	Water Pressure	Pressure Duration	Results
MC 3142	16 psig	16 hrs	No leakage
MA 3148	16 psig	1 hr	No leakage
XLMA 3236	16 psig	1 hr	No leakage
XLMC 3235	15 psig	1 hr	Small leakage at first but increased with time

Ionac Membranes After Soaking In
180°F Water for Four Hours

Membrane	Water Pressure	Results
MC 3142	2 psig	Rapid leakage
MA 3148	10 psig	Small leakage
XLMA 3236	8 psig	Rapid leakage
XLMC 3235	3 psig	Rapid leakage

NON WETTING POROUS MATERIALS

	Sample	Results
ESB Reeves Corp.	Porous Kel-F (Pore size under 7 microns)	Leaked at 7 psig
ESB Reeves Corp.	Porous Polyethylene 13-CN (Pore size under 2 microns)	Leakaed at 3.5 psig

of these leakage tests. Since the Ionac MA 3148 membrane showed very small leakage, a set of membranes were prepared for installation in the test unit. This membrane was run for approximately four hours at acid temperatures of 125°F and 140°F, but extremely small amounts of liquid were extracted during this period and a pH 1 was never exceeded. Thus the Ionac Membranes listed in Table 4.3 were determined unsuitable for the intended application and testing of these membranes was discontinued.

4.4.2 Porous Material Tests

Two samples of non-wetting porous sheets were obtained from the ESB Reeves Corporation to determine the suitability of their use in a water extraction unit. A sample of porous Kel-F sheet, with pore size under 7 microns and a sample of porous polyethylene sheet with pore size under 2 microns were leak tested in the same manner as the Ionac membranes. The tests were made with water at room temperature. Leakage through the Kel-F material occurred at 7 psig and leakage through the polyethylene material occurred at 3.5 psig. These materials were considered unsatisfactory for acid-water separation.

5.0 Materials Compatability Tests

5.1 Membrane Support Matrices

During initial membrane performance tests, a Trilox spacer matrix was used between the membrane and the perforated support plates. It was found that after this material had been subjected to 200°F acid and 15 psi pressure for six hours the material had suffered a permanent deformation of 25% of the original thickness of 0.1 inch. The compression of this material was considered unsatisfactory for this purpose as it would result in membrane stretching as well as constrict the flow of vapor from the membrane surface to the holes in the perforated plate. However, the exposure of this material to 200°F acid appeared not to effect the material in any other manner.

Twelve mesh x 0.032" wire Monel screens were substituted for the Trilox material to give rigid support to the membranes and to prevent constriction of the lateral vapor flow. However, the bare Monel metal screens were severely corroded upon exposure to the acid saturated membrane at high temperatures.

To prevent acid attack on the Monel metal and to provide a non-wetting support for the membranes the screens were coated with a teflon film. This was accomplished by dipping the screens in a Teflon dispersion solution of 12% TFE and 88% water by weight and sintering at 200°F for 30 seconds. Two coats were applied in this manner. Further membrane testing resulted in the flaking off of the teflon coating and severe corrosion of the Monel screens. The screens were coated again after cleaning with a solution of 20% chromium trioxide 10% sulfuric acid and 70% water. The coating was applied in the same manner as before but with a TFE dispersion of 20% TFE and 80% water. Further testing resulted again in the flaking off of the coating and severe corrosion of the metal.

The Monel screens were then coated with a thin film of Kel-F. The coating was applied to the screens by dipping them in a full strength KX-633 Kel-F dispersion and the excess blown off with an argon gas stream. The screens were allowed to air dry and then were placed in a 500°F oven for 20 minutes. Three coatings were applied in this manner. Subsequent testing with these screens

included all of the tests with the AMF C-60 membrane. Visual observation at the completion of membrane tests revealed only a slight discoloration on the metal at a few spots beneath the coating. The coating however appeared to be in excellent condition.

5.2 Materials of Construction

Early in the program, precautionary compatibility tests on materials of construction used in the "Osmotic Still" test unit and test rig were made. These tests consisted of immersing two samples of material in the same 25 per cent sulphuric acid bath for a continuous 31 day test. One sample of Polyvinyl Dichloride (2.905 grams) and one sample of Cast Methyl Methacrylate (2.462 grams) were used for testing purposes. During the period of 31 days, the acid bath was heated to a temperature of 200^{o}F and was kept at that temperature for the remainder of the time. Visual inspection after this elapsed time showed no deterioration of the samples. It was intended to weigh these samples at the end of the test, but the samples were accidentally destroyed due to overheating of the acid bath.

Since this test was strictly qualitative and since the test unit and some of the other test rig components were fabricated from uncertified materials, quantitative tests on samples made from both uncertified stock and from certified stock were conducted. The results of a 30 day test on Polyvinyl Dichloride (PVDC) and Polymethyl Methacrylate materials after being exposed to a 30% solution of sulfuric acid at 200^{o}F in a reflux condenser are presented in Table 5.1 A total of eight samples were tested. Two duplicate samples each of Polyvinyl Dichloride and Polymethyl Methacrylate prepared from "Still Test Unit" material stock, and two samples each of subsequently purchased "certified" material were tested. The weight, hardness, and dimension of each sample was determined before and after the test.

TABLE 5.1

Plastic Material Compatibility Test With 30% H_2SO_4 at 200°F

Sample Description	Dimensions (Inches) Before	Dimensions (Inches) After	Hardness (Barcol) Before	Hardness (Barcol) After	Weight (Grams) Before	Weight (Grams) After	Remarks
Polymethyl Methacrylate							
Uncertified Sample A-1	0.9975 x 1.002 x 0.247	0.999 x 1.025 x 0.244	49	42	4.6773	4.7197	Thickness ranged from 0.241 to 0.246
Uncertified Sample A-2	0.9980 x 1.003 x 0.247	0.984 x 1.040 x 0.241	49	42	4.6799	4.7233	Thickness ranged from 0.239 to 0.243
Certified Sample B-1	0.999 x 1.002 x 0.226	0.999 x 1.0025 x 0.226	50	42	4.3550	4.3904	
Certified Dample B-2	0.999 x 1.002 x 0.224	1.000 x 1.002 x 0.225	49	41	4.3292	4.3628	
Polyvinyl Dichloride							
Certified Sample C-1	0.999 x 1.005 x 0.126	0.999 x 1.005 x 0.127	3	4	3.1662	3.1855	
Certified Sample C-2	0.998 x 1.005 x 0.126	0.998 x 1.002 x 0.127	5	6	3.1593	3.1765	
Uncertified Sample D-1	0.983 x 0.996 x 0.123	0.990 x 0.986 x 0.121	5	5	2.9733	2.9920	Thickness ranged from 0.119 to 0.123
Uncertified Sample D-2	0.984 x 1.004 x 0.123	0.989 x 1.004 x 0.121	8	8	3.0026	3.0191	Thickness ranged from 0.121 to 0.126

6.0 Conclusions of Experimental Test Program

The following major conclusions were drawn as a result of the experimental test program.

1. The only membranes of those tested, which are suitable for the osmotic still application, are the American Machine and Foundry membranes. Of these the C-60 cation membrane exhibited the highest water extraction rate and operated satisfactorily up to 200°F. Further, this membrane exhibited high strength and extreme flexibility which permitted ease of fabrication and subsequent handling.

2. The AMF C-60 membrane material as received is water saturated. Before membrane cutting and installation, the membrane material must be saturated in an acid solution of the concentration used in the still (6 $\underline{N}$ H_2SO_4). This treatment preshrinks the membrane material, preventing subsequent shrinking during operation of the still.

3. During assembly of the C-60 membranes into the still test unit, the vapor side of the membrane must be wiped dry to prevent induced "weepage" as discussed in Section 4.4.1.2.

4. The Polyvinyl Dichloride was determined to be a suitable material for still component construction.

5. Rigid Monel screens coated with Kel-F as described in Section 5.0 was determined to be suitable as a vapor-cavity membrane support element.

6. It was determined that the Trilox Fabric (Style D-59633-C) is a suitable material for use in a 200°F acid environment.

7.0 2KW Osmotic Still

7.1 Design Specifications

An osmotic still was designed to have a water separation capacity equal to the water generation of a nominal 2KW fuel cell. The unit designed to provide this capacity has the following specifications:

H_2O Extraction Rate = 2 lb/hr = 908 cc/hr
H_2SO_4 Concentration = 6N or 25%
Average H_2SO_4 Temperature = 200°F
Total Active Membrane Area = 7 Ft^2
Number of Membranes = 14
Active Membrane Diameter = 9.6"
Number of Electrolyte Cavities = 8
Number of Vapor Cavities = 7

7.2 Unit Description

Figure 7.1 shows an exploded view of the "2 KW Osmotic Still". The unit consists of 7 vapor cavities and 8 acid cavities separated by 14 AMF C-60 membranes. The membranes are supported on the vapor side by two Kel-F coated monel screens shown in Figure 7.2 to allow vapor to flow laterally through the vapor cavity to the internal vapor manifolds in the unit rim. The vapor cavity recess in the vapor cavity rim shown in Figure 7.3 allows vapor flow around the screen matrix to the vapor manifold with a minimum vapor pressure drop. The acid, entering at the bottom of the unit flows through each of the electrolyte cavities in succession (a series arrangement) and leaves the unit at the top. The pressure drop in the acid flow stream results in a net force from the bottom acid cavity to the top acid cavity. This force created by the series flow arrangement of the acid, required that the membranes be also supported in the acid cavity. These supports are Trilox spacer fabric oriented to provide good flow distribution of the acid over the membranes. The membranes are gasketed on both sides with Viton rubber gaskets. Gaskets are provided on both sides of the bolt hole and manifold circle, the inner gaskets provide the seal while the outer gaskets merely act as spacers to prevent bending moments about the inner gaskets. The acid and vapor internal manifolds are sealed with Viton rubber gaskets between

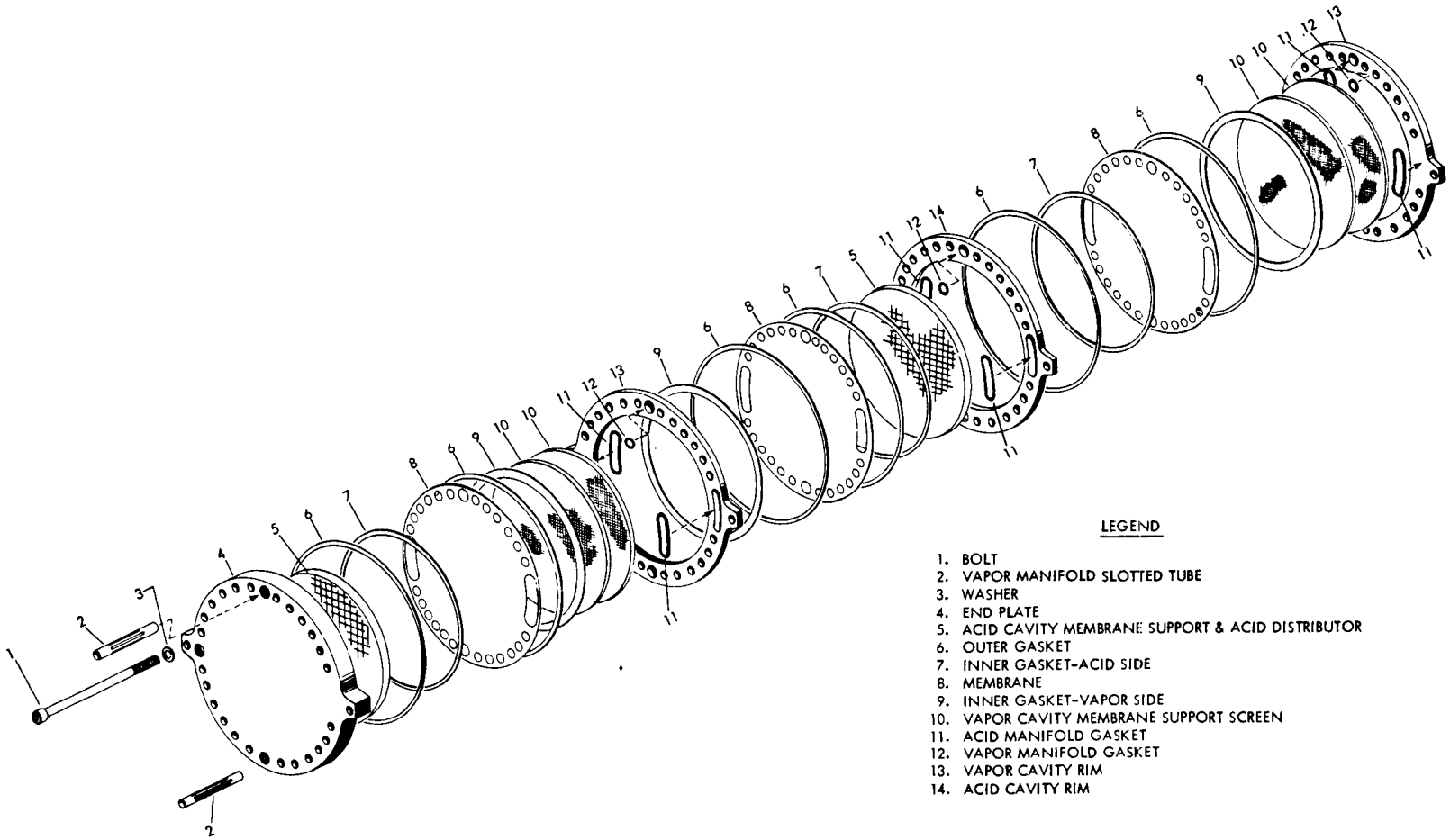

LEGEND

1. BOLT
2. VAPOR MANIFOLD SLOTTED TUBE
3. WASHER
4. END PLATE
5. ACID CAVITY MEMBRANE SUPPORT & ACID DISTRIBUTOR
6. OUTER GASKET
7. INNER GASKET-ACID SIDE
8. MEMBRANE
9. INNER GASKET-VAPOR SIDE
10. VAPOR CAVITY MEMBRANE SUPPORT SCREEN
11. ACID MANIFOLD GASKET
12. VAPOR MANIFOLD GASKET
13. VAPOR CAVITY RIM
14. ACID CAVITY RIM

FIGURE 7.1 EXPLODED VIEW OF "2KW OSMOTIC STILL"

Figure 7.2 Photo of Electrolyte Cavity for "2 KW Osmotic Still" - Trilox Mesh & Membrane Removed to Show Kel-F Coated Monel Support Screen

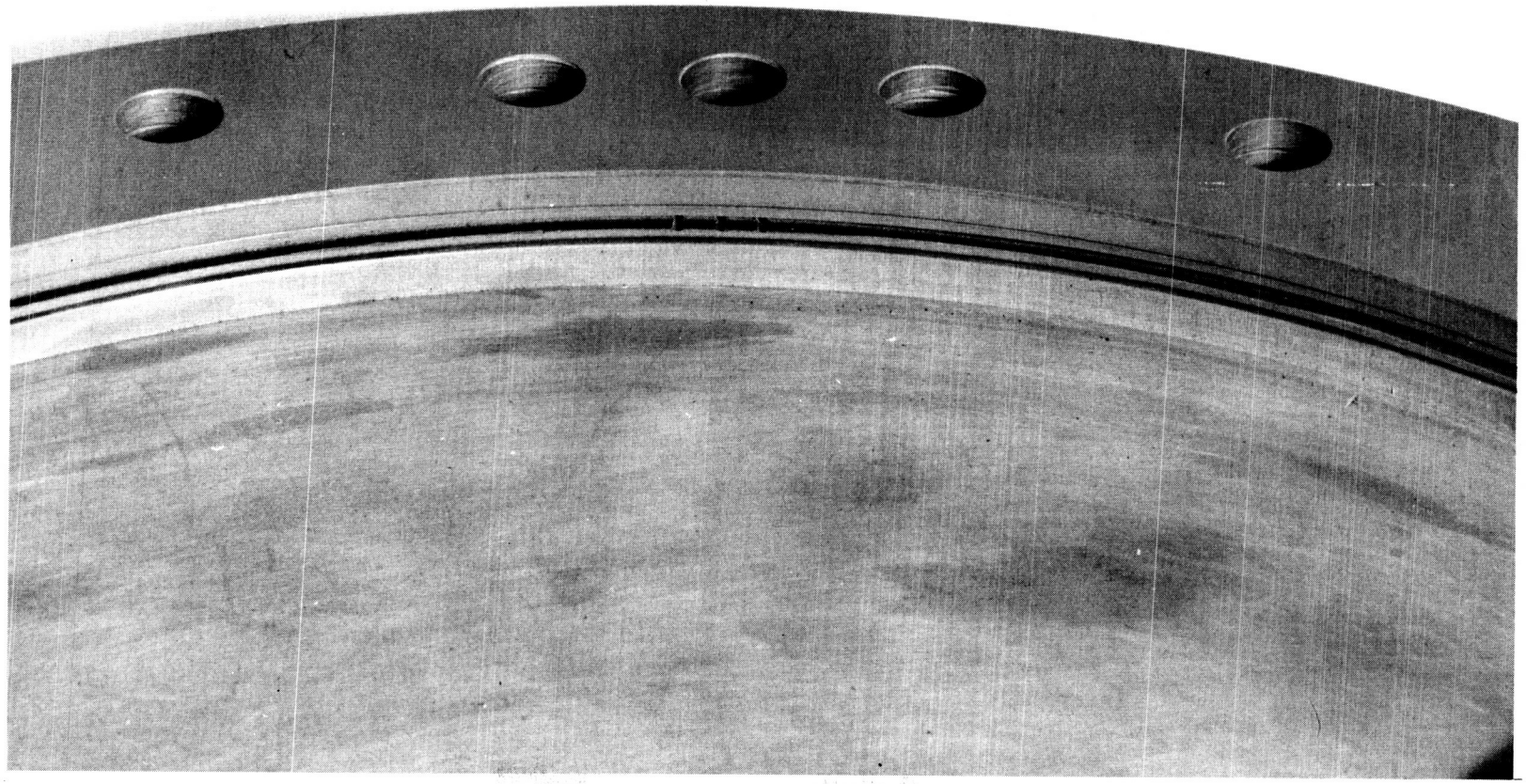

Figure 7.3 Photo of Vapor Cavity Rim Recess - Monel Screen Removed

the acid and vapor cavity rims. Since the vapor manifolds are below atmospheric pressure, slotted stainless steel tubes are inserted in the vapor manifolds to prevent the manifold gaskets from collapsing into the manifold. The lapping of the Viton gasket over the monel screen on the vapor sides of the membranes protects the membrane from the wire ends of the monel screen supports preventing membrane puncture.

Figures 7.4 and 7.5 show two photos of the "2K Osmotic Still". These photographs were taken after the successful completion of the 100 hr test.

7.2.1 Materials of Construction

The materials of construction used for the various components of the 2 KW unit are described herein.

1. The end supports and the acid and vapor cavity rims are Polyvinyl Dichloride.

2. The membrane gaskets are Viton rubber 0.016" thick.

3. The acid and vapor manifolds are Viton rubber 0.048" thick.

4. The acid side support matrix is polyethelene-polypropolene (U. S. Rubber Trilox Fabric style D-59633C)

5. The vapor side support screens are 10 mesh x .032" wire monel screens coated with Kel-F as described in Section 5.1.

6. The slotted tube in the vapor cavities is 3/8" x 0.038" wall 316 stainless steel.

7.3 Test Rig Description and Operation

The test rig used for the 100 Hr test of the "2 KW Osmotic Still" unit is shown schematically in Figure 7.6. A photograph of this rig is shown in Figure 7.7.

The acid electrolyte is circulated through the unit with a positive displacement Vanton Flexiliner sealess pump with a hypalon liner. The acid is heated

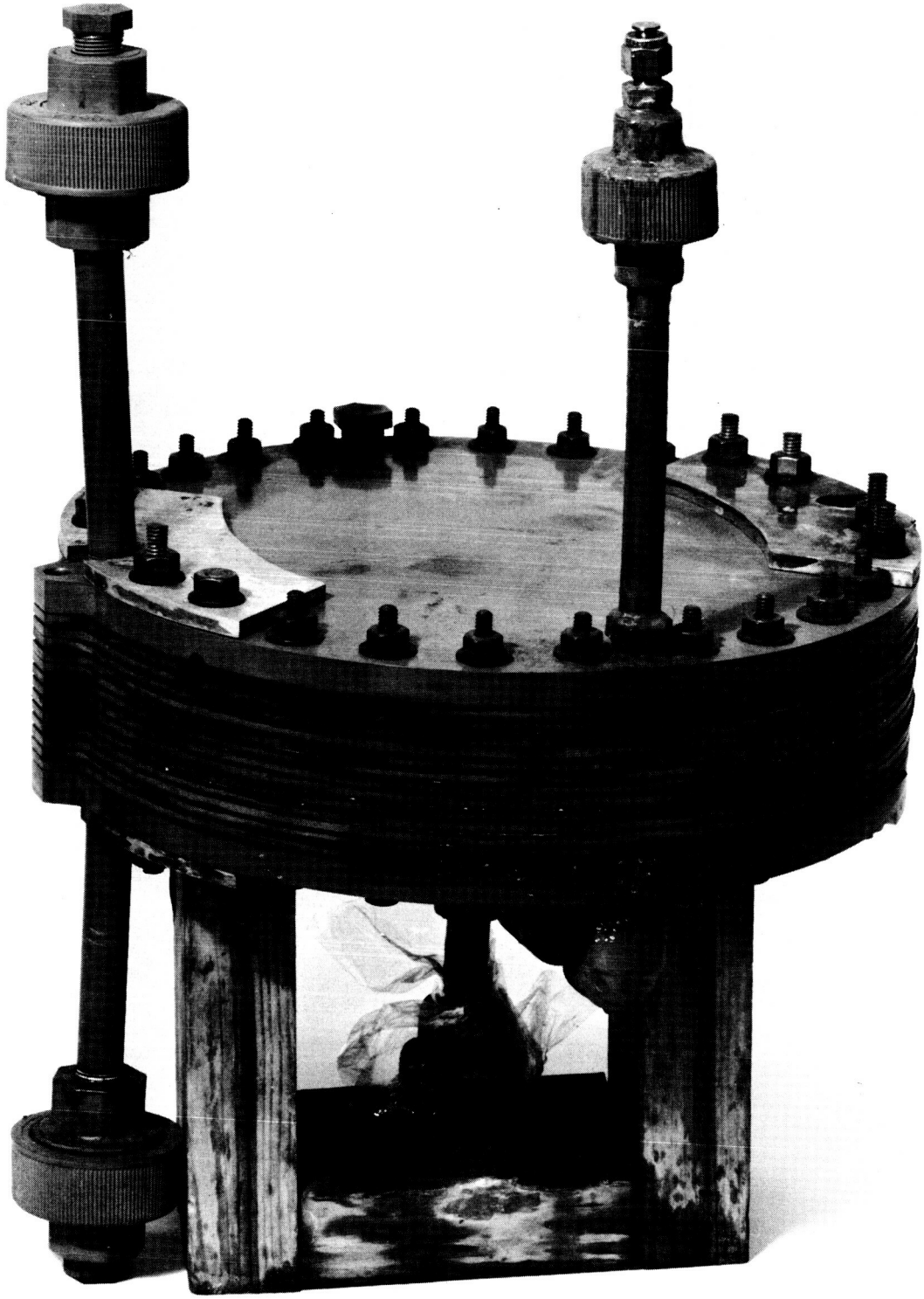

Figure 7.4 "2 KW Osmotic Still" Assembly Showing "Acid Outlet Line" (top left) and "H_2O Vapor Line" to Monometer (top right)

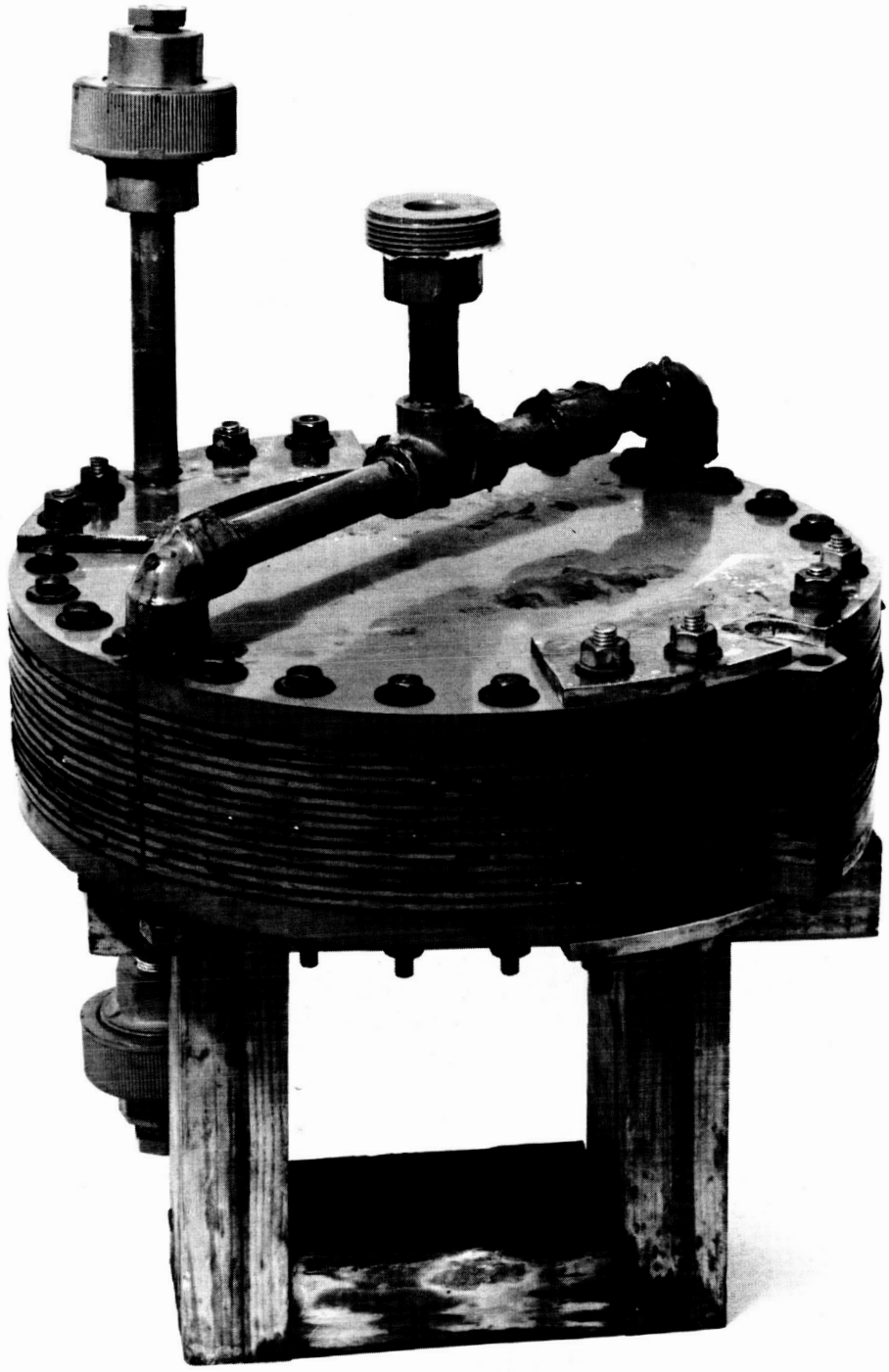

Figure 7.5 "2 KW Osmotic Still" Assembly Showing Acid Inlet Line (top left) and H_2O Vapor Outlet Line (top right - bridged)

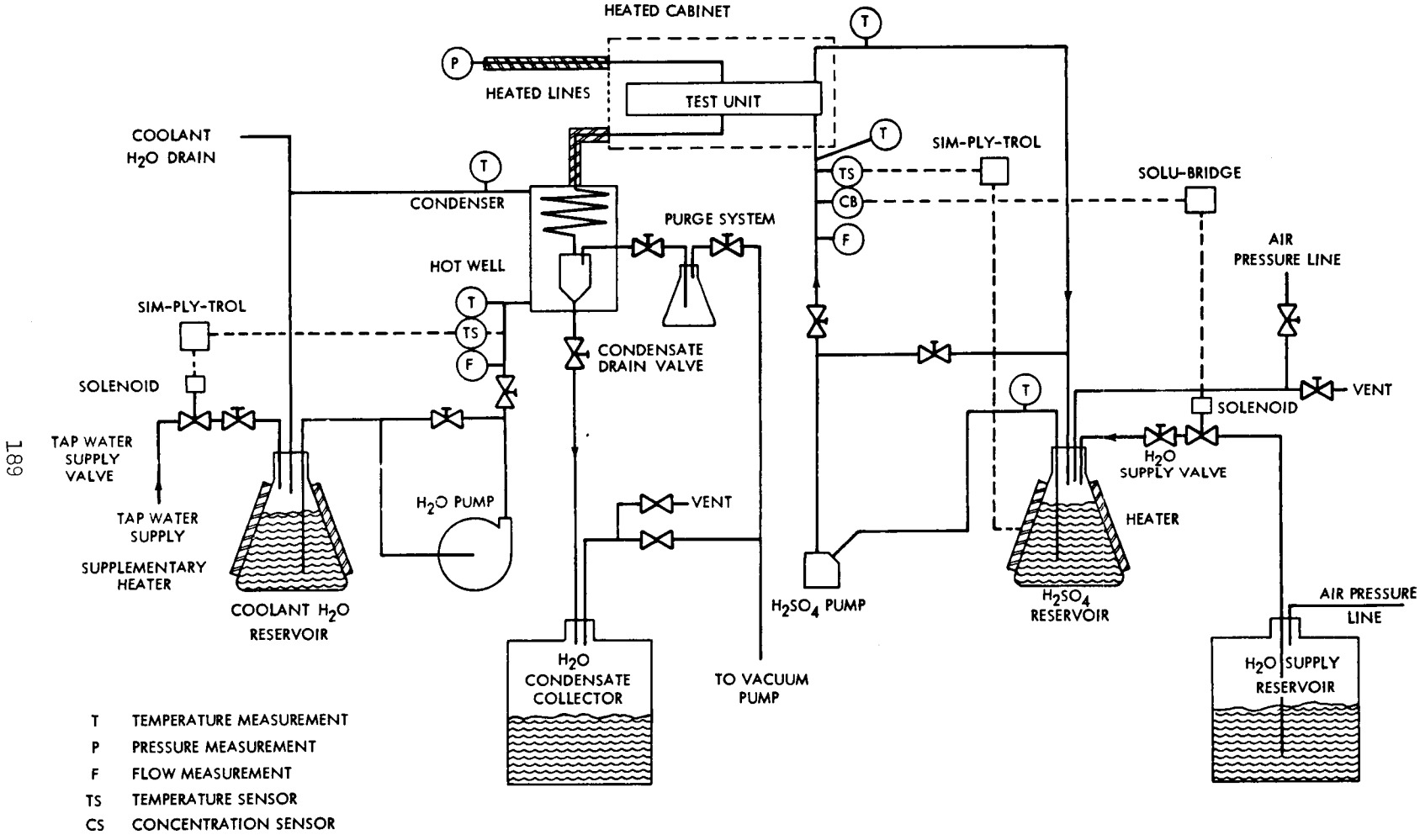

FIGURE 7.6 TEST RIG SCHEMATIC (2KW OSMOTIC STILL)

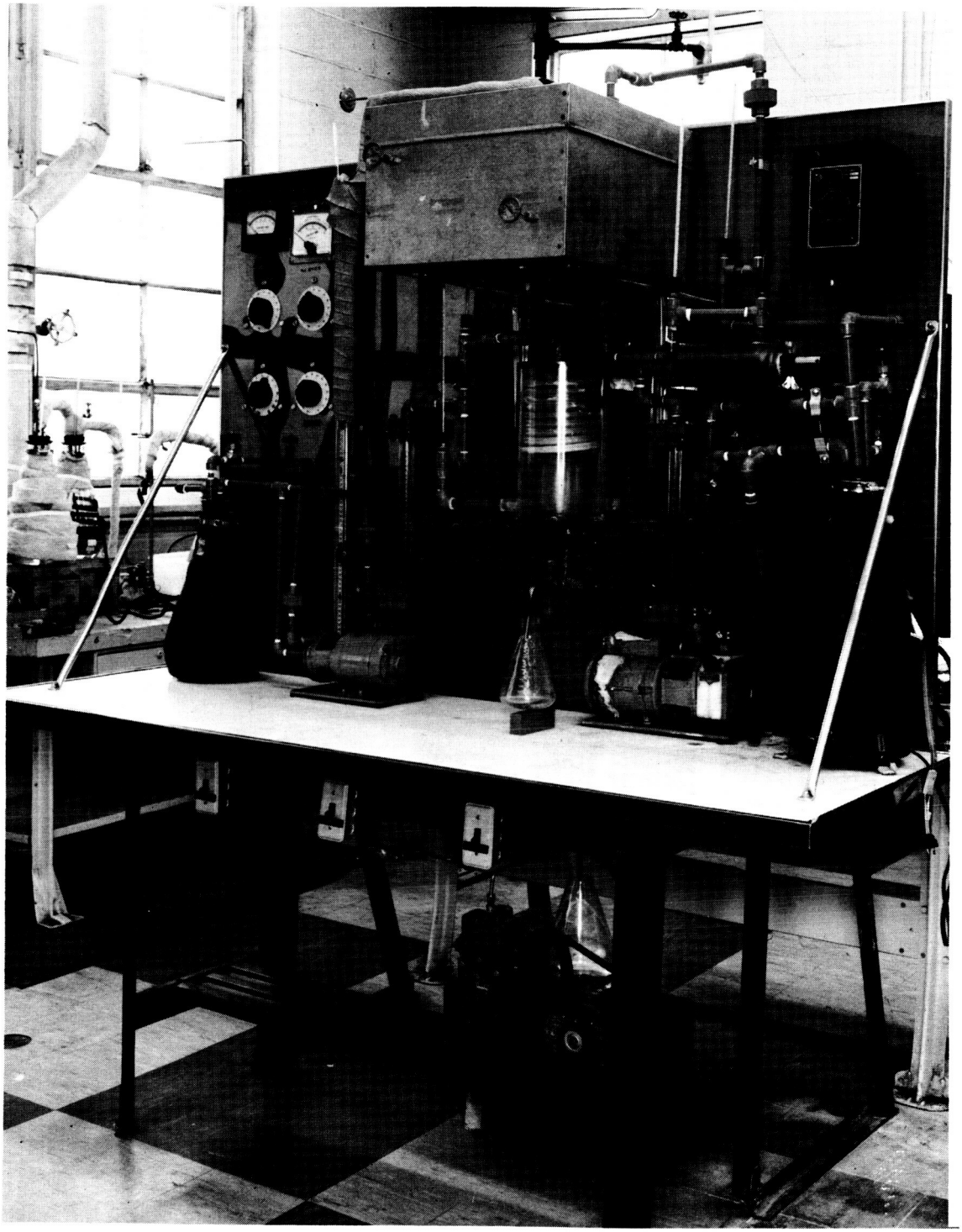

Figure 7.7 Photo of Test Rig for 100 Hour Performance Test of "2 KW Osmotic Still"

in the acid reservoir and the test temperature is maintained either by manual voltage control of the reservoir heater or by the on-off controller with the sensor immersed in the acid inlet line. The acid concentration is maintained by supplying distilled water to the acid reservoir from the pressurized H_2O supply reservoir. The concentration is maintained either by manual operation of the H_2O supply value or by the on-off controller activating a solenoid value in the H_2O supply line. The concentration sensor for the controller is a conductivity cell immersed in the acid inlet line. The acid loop may be pressurized with air at the acid reservoir.

Water vapor leaving the vapor cavities of the test unit is condensed in the plexiglass water jacketed condenser and periodically drained from the condenser hot well to the condensate collector. The condensate collector and the entire vapor system is connected to a vacuum pump for evacuation of the vapor system and for periodic non-condensable purges. The condenser is cooled by circulating coolant water from the coolant water reservoir through the water jacket of the condenser with a centrifugal pump. The water vapor pressure is controlled by controlling the water coolant temperature and flow to the condenser. The condenser coolant temperature is maintained by the controlled addition of cold tap water to the coolant reservoir and allowing hot coolant to drain out of the coolant system. The addition of the tap water to the coolant system is controlled either by manual control of the tap water supply valve or by the on-off controller which actuates the solenoid valve in the tap water supply line. This controller has a temperature sensor immersed in the coolant line to the condenser. The 2 KW unit is mounted in a heated cabinet to prevent excessive heat loss during operation. The vapor pressure is measured with a standard U tube monometer. The vapor leg of the monometer and the vapor line between the monometer and the heated cabinet is heated with a wrap-on strip heater to prevent condensation. Temperatures of the acid entering and leaving the 2 KW unit and temperatures of the condenser coolant water entering and leaving the condenser are measured with calibrated mercury in glass thermometers immersed directly in the fluid streams.

All the acid, vapor, and condenser coolant lines are Polyvinyl Dichloride pipe. The valves in the acid lines and the condensate drain valves are Vanton flex-plug gate valves with penton bodies and hypalon stem caps.

7.4 Test Procedure and Results

7.4.1 Preliminary Tests

Initially, acid flow distribution tests were conducted to test various methods of obtaining good flow distribution in the acid cavity. These tests were performed by placing an acid cavity rim between two transparent plexiglass plates and flowing water through the cavity. Flow distribution was determined visually by injecting dye into the cavity at various points. Two types of flow distributors were determined to be satisfactory. One type, shown in Figure 7.8, was used initially in the 2 KW unit but this type of distributor caused puncturing of the membranes. The other type which was used successfully in the 2 KW unit is shown in Figure 7.9.

Preliminary leak tests of the assembled 2 KW unit were performed by evacuating the vapor side of the unit while applying 10 psig air on the acid side and sealing the unit. Leakage was then detected by the inability of the sealed unit to hold the vacuum and the positive pressure. Initial leak tests on the unit indicated no leakage from the acid side of the unit but gasket failures in the vapor manifold resulted in loss of vacuum on the vapor side. This failure was due to the ability of the gasket to move into the evacuated manifold under the influence of compression and pressure difference. Introduction of the slotted stainless steel tube prevented this gasket failure and all leakage was eliminated.

7.4.2 100 Hr Test Procedure

Upon installation of the assembled unit in the test rig, the vapor side of the system was evacuated. Acid and condenser coolant were circulated and heated from room temperature to operating temperature. The acid reservoir was maintained at atmospheric pressure. The vapor pressure was varied by adjustment of the condenser coolant temperature until the design water extraction rate of 908 cc/hr was obtained. After approximately 5 1/2 hrs from the initial evacuation of the vapor system, the design extraction rate was attained and the 100 hr test was started. All test variables were recorded and appropriate adjustments were made every 15 minutes for the first 5 hours of the test

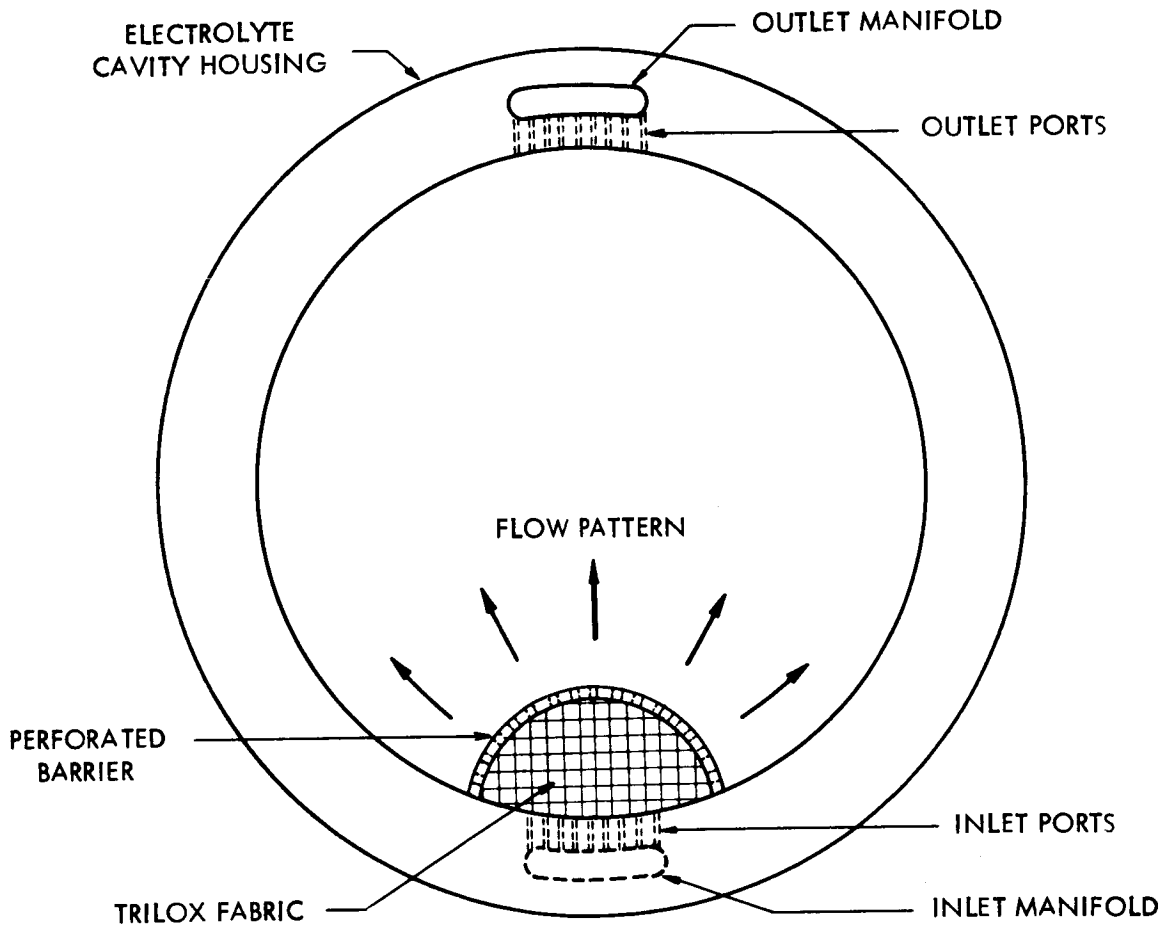

FIGURE 7.8 ELECTROLYTE FLOW DISTRIBUTION ARRANGEMENT USING PERFORATED BARRIER SURROUNDING INLET PORTS

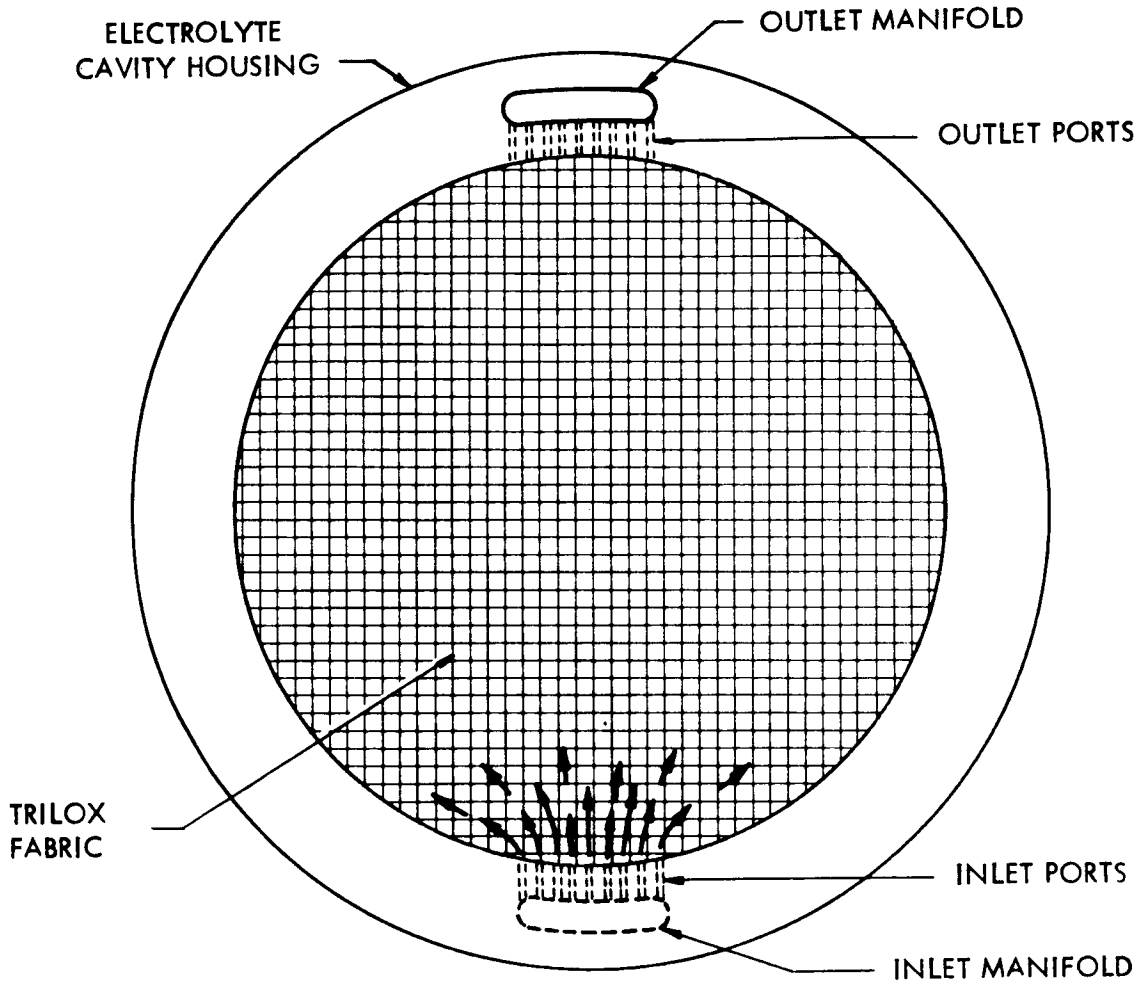

FIGURE 7.9 ELECTROLYTE FLOW DISTRIBUTION ARRANGEMENT USING TRILOX FABRIC THROUGHOUT ELECTROLYTE CAVITY

and every 30 minutes for the remainder of the test. The vapor system was purged through the condenser approximately every 15 minutes.

During the first 40 hrs of the test, the average acid temperature in the test unit was maintained only between 185°F and 187°F due to excessive heat loss in the acid lines and reservoir as well as to insufficient contact between the heater and the glass reservoir. The average acid temperature in the unit was approximately between 195°F and 199°F for the remaining 60 hours of the test after an additional heater was installed at the acid reservoir and additional insulation was added. Condensed water vapor was removed from the condensate collector every 2 hours and measured. Periodic nominal measurements of the water pH were made throughout the tests with pH indicator paper and with a Taylor pH meter.

During the entire test there were no failures and the 100 hrs test was continuous.

7.4.3 Test Results

The 100 hr continuous endurance test run on the 2 KW unit was successfully completed. A total of 91,121 cc of water was removed from the test unit during the 100 hrs. An average removal rate of 911 cc/hr was attained, meeting the design removal rate of 908 cc/hr (2 lb/hr). The average acid temperature in the test unit was 185 - 187°F during the first 40 hours and 195 - 199°F during the remainder of the test. Table 7.1 lists average test variables for the entire 100 hrs. Table 7.2 lists condensate pH of samples taken from water storage bottles at the termination of the test. These measurements indicate an increase of water purity with test time. Table 7.3 lists pertinent reduced test values taken at various times throughout the 100 hrs.

A comparison of performance of the still is made in Figure 7.10. Table 7.3 vapor pressure difference data is compared to the vapor pressure difference predicted from Figure 4.5 for the average H_2O extraction rate of the test points. This comparison indicates no decrease in still performance during the 100 hour test. In addition it can be seen that the operating vapor difference was 22% less than that shown in Figure 4.5 for the average water extraction rate of 129.5 cc/hr ft^2.

TABLE 7.1

100 Hr Test Data

Electrolyte - Sulfuric Acid Solution

Acid Concentration - 25.2 % (6N)

Average Acid Temperature - 185 - 187°F During first 40 Hrs

- 195 - 199°F During last 60 Hrs

Total Water Removed During 100 Hrs - 91121 cc

Average Water Removal Rate - 911 cc/hr - 130 cc/hr ft^2 membrane

Acid Flow Rate - Approximately 3.5 - 4.1 lbs/hr

Condenser Water Flow Rate - Approximately 7 - 9.5 lbs/hr

TABLE 7.2

pH* of Collected Water

Container No	Water Quantity Gallons	Test Time Duration Hrs	Water pH
1	5	Q-21	4.8
2	5	21-42	5.0
3	5	42-63	5.1
4	5	63-84	5.4
5	4	24-100	5.6

*Measurements taken with Taylor pH meter

TABLE 7.3

2 KW Osmotic Still 100 Hr Test Results

Test Duration Hr.	H_2SO_4 Temp Ent Unit °F	H_2SO_4 Temp Lv Unit °F	H_2SO_4 Ave Temp In Unit °F	H_2SO_4 Vapor Press @ Ave Temp psia	H_2O Vapor Press psia	Vapor Press Diff psia	H_2O Extraction Rate cc/hr	H_2O Extraction Rate cc/hr ft^2	Test Point Duration Hrs
1	193.5	185.0	198.5	7.52	4.41	3.11	870	124	1
7	191.0	182.0	186.5	7.14	3.49	3.65	903	129	2
15	189.0	180.0	184.5	6.85	4.05	2.80	893	127	2
27	192.0	183.0	187.5	7.34	4.03	3.31	923	132	2
39	191.7	183.2	187.5	7.34	3.90	3.44	915	131	2
53	201.0	192.5	197.2	9.00	5.31	3.69	938	134	2
61	202.0	193.5	197.7	9.06	5.71	3.35	920	131	2
65	202.5	194.2	198.3	9/25	5.67	3.58	910	130	2
77	203.5	195.0	199.2	9.35	6.09	3.26	908	130	2
83	202.0	194.5	197.2	9.0	5.89	3.11	905	129	2
95	202.5	194.0	197.2	9.0	5.80	3.20	910	130	2
					Average	3.32	908.6	129.5	

NOTE: See Figure 7.10 for Vapor Pressure Difference Vs Time Plot

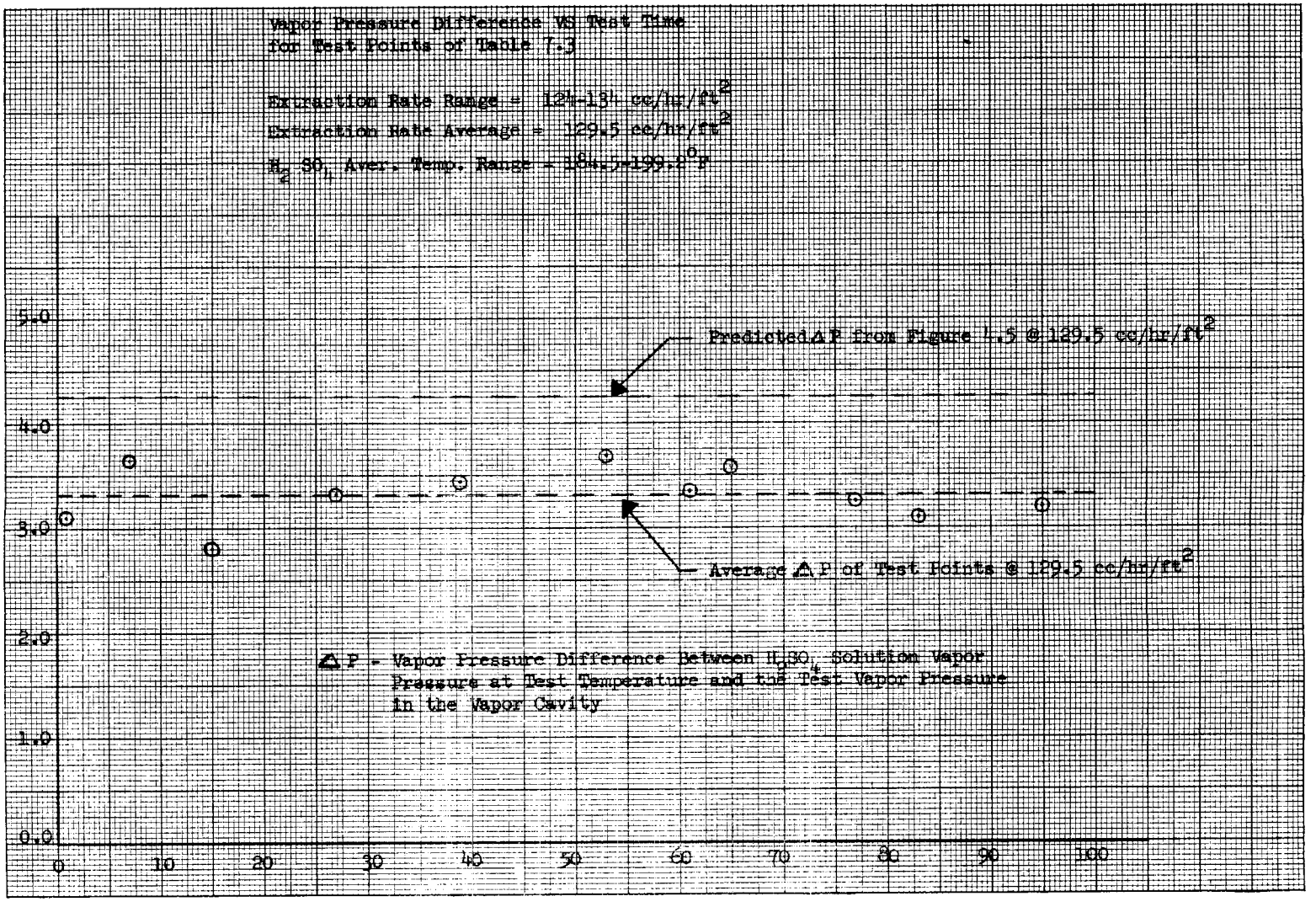

Figure 7.10 "2 KW Osmotic Still" 100 Hour Performance Test Results

Visual examination of the still components upon still disassembly after the test indicated that all the components of the still were in excellent condition and that the coated monel screens showed only a slight discoloration under the Kel-F film in a few areas.

III. CONCLUSIONS

This report has defined and presented the methods used in constructing and testing the dual membrane fuel cell and the osmotic still, two major components of the TRW space vehicle power supply. Both units were found to perform better than required by program design goals.

The results of the program have verified the safety of dual membrane fuel cells and the loose controls permitted in their operation. The circulating electrolyte serves ideally as a heat and moisture removal medium which, when coupled with the osmotic still, permits zero gravity water separation with no free liquid surface.

Contrary to typical fuel cell technology each scale-up in design resulted in an improvement in cell performance. Because the approach taken to the 2 KW Battery Design was based upon demonstrated performance and because the component sizes were not optimized, the construction of such a battery is very conservative.

The general conclusion is that the power system remains very attractive. Additional effort should be spent in optimizing the component geometries, e.g., electrolyte compartment thickness, which would considerably decrease battery weight and volume. The system is inherently rugged and reliable. Additional experimental development should be aimed at decreasing oxygen-side polarization and liquid transport through the membranes. Subsequent to that part of the program which was related to electrode fabrication much progress has been made on other government sponsored programs which indicate that electrodes, applicable to dual membrane cells are available commercially and would not represent a cell limitation.

An evaluation of the test results obtained during the 100 hour test of the osmotic still indicates the adequacy of performance of this unit for application in the dual membrane fuel cell system. Since a reduced electrolyte normality substantially increases the water extraction rate of the osmotic still while exhibiting little or no effect on the fuel cell performance, it can be concluded that further optimization can be accomplished in matching fuel cell and osmotic still performance characteristics. Such optimization should result in a substantial size and weight reduction of the osmotic still.

APPENDIX

TO

PART I

TABLES

Table A1

Summary of Single 36 Sq. In. Cell Tests

Cell No.	Components	Bath Temp.	Pressure, Psig		Current Amperes	Voltage Volts	Specific Conductivity Mhos/Ft^2	Test Time Hours	Remarks
			Gas	Electrolyte					
D9716	Paste electrodes Titanium metallics* 61-AZG Membranes	30°C	15	20	4.0	0.72	--	12	Cell Operation stopped overnight. Disassembled when voltage did not recover upon startup.
D9718	Paste electrodes Titanium metallics 61-AZG membranes	30°C	15	20	4.0	0.78 0.78 0.72 0.68 0.64 0.64 0.68 0.68 0.65 0.741 0.718 0.702 0.658	-- -- -- -- -- -- -- -- -- 81 83 -- 68	12 21 72 118 143 192 210 256 288 384 408 552 696	Run terminated due to membrane drying at top of cell.
D9719	Paste electrodes Titanium metallics 61-AZG membranes	30°C	15	20	4.0	0.63 0.59 0.59 0.46 0.588 0.498	-- -- -- -- -- --	1 44 75 146 224 277	Run terminated due to membrane drying at top of cell.
D9723	Sintered Teflon electrodes Titanium metallics 61-AZG membranes	30°C	15	20	4.0	0.76 0.74 0.72 0.71 0.72 0.64 0.71 0.65 0.64	-- 116 -- -- 99 65 53 54 62	20 108 252 348 396 624 720 936 960	Discontinued due to blockage of gas inlets. Pinholes found in membranes

* Unless otherwise specified titanium metallics have been thermally platinized.

Table A1 (continued)

D9723						0.58 0.52 0.59 0.59	-- 40 45 54	1104 1128 1176 1344	
D9725	Sintered Teflon electrodes Gold plated mettalics 61-AZG membranes Epoxyglass compartments Bunan. gaskets	90°C	15	20	4.0	0 725	--	1	Discontinued one day after start due to cross leak. Most components had been affected by acid.
D9728	Sintered Teflon electrodes Titanium metallics 61-AZG membranes	30°C	15	20	4.0	0.648	90	20	Run terminated when acid inlet tubing broke causing electrolyte to flow out of the cell. Membrane dried at top.
D9734	Paste electrodes Titanium metallics 61-AZG membranes	60°C	15 20	20 28	4.0	0.748 0.568	74 91	1.5 3	Terminated when connection snapped causing a gas compartment to become flooded.
D9734 (a)	Same components as 9734. Electrodes dried before reassembly.	60°C	15	20	4.0	0.760 0.712	121 72	0.5 5.5	Terminated when connection snapped again.
D9735	Paste electrodes Titanium metallics 61-AZG membranes	60°C	15 20	20 28	4.0	0.722 0.748	71 140	1.5 3	Terminated when connection snapped again.
D9735 (a)	Same components as 9735. Electrodes dried before reassembly.	60°C	15	20	4.0	0.832 0.786	134 96	1.5 6	Terminated when connection snapped again.

Table A1 (continued)

D9739	Paste electrodes Titanium metallics 61-AZG membranes	60°C	15	20	4.0	0.558	47	1	Both cells discontinued after failure of thermostatic switch to open caused fire in tank.
D9740	Paste electrodes Titanium metallics 61-AZG membranes	60°C	15	20	4.0	0.822	154	1	" " "
D9743	Sintered Teflon electrodes Titanium metallics 61-AZG membranes	60°C	15	20	2.0	0.100 0.48 0.100 0.238	-- -- -- --	6 78 102 192	Gas fed from bottom of compartment. Discontinued because of low voltage output.
D9744	Sintered teflon electrodes Titanium metallics 61-DYG membranes	60°C	15	20	4.0	0.618 0.740 0.618 0.232	75 71 72 --	6 96 120 192	" " "
D9745	Sintered teflon electrodes Titanium metallics 61-DYG membranes	60°C	15	20	4.0	0.310	--	120	" " "
D9745 (a)	Same as D9745	60°C	15	20	4.0	0.763 0.770 0.768	102 96 100	2 24 48	Gas feed tubes switched to top. Discontinued following fire in oxygen supply tube.
D9746	Sintered Kel-F Titanium metallics 61-AZG membranes	60°C	15	20	4.0 2.0	0.112 0.160	-- --	120 168	" " "
D9749	Sintered Kel-F electrodes Titanium metallics 61-DYG membranes	30°C	16	20	4.0 2.0	0.503 0.562 0.272 0.382 0.312 0.490	65 61 27 13 22 --	24 120 144 168 192 264	Discontinued because of low voltage readings.

Table A1 (continued)

D9750	Sintered Kel-F elec. Titanium metallics 61-DYG membranes	30°C	16	20	4.0	0.313 0.598 0.300 0.568 0.512 0.618 0.596 0.652 0.610 0.608 -----	66 76 --- --- 47 --- 74 --- 74 --- ---	24 120 144 168 192 264 288 312 336 360 432	This cell is similar to Cell D9749 except that pieces of expanded titanium were placed between electrodes and pusher plates to avoid electrode shadowing.
E1259	Sintered Teflon electrodes Titanium metallics 61-AZG membranes	60°C	16	15	4.0	0.822 0.837 0.808 0.808 0.738 0.691 0.768 0.651 0.702	--- 167 --- --- --- 66 --- 72 ---	4 24 48 72 96 144 168 192 216	Discontinued due to large quantities of liquid in gas compartments.
E1263	Paste electrodes Titanium metallics 61-AZG membranes	60°C	15	15	4.0	-----	---	---	Cell contained gasket of less width than normal. No data taken due to failure of gasket. Severe cross leaks noticed.
E1268	Paste electrodes Titanium metallics 61-AZG membranes	60°C	16	16	9.0	0.792 0.758 0.698 0.672 0.632	156 102 95 80 60	4 24 48 96 120	Discontinued after 120 hours of operation.
E1273	Sintered Kel-F Titanium Metallics 61-AZG membranes	60°C	15	15	4.0	-----	---	---	Discontinued following fire in oxygen line.
E1279	Sintered Kel-F electrodes Titanium metallics 61-AZG membranes	60°C	16	15	4.0	0.548 0.602 0.602 0.712 0.510	84 105 95 70 42	4 24 48 66* 87**	*Cell was shut down for 140 hours due to malfunction of control system. **Recorded after cell had been off test 144 hours and

Table A1 (continued)

E1279	(continued)								restarted. Run discontinued due to poor performance.
E1282	Paste electrodes Titanium metallics 61-AZG membranes	60°C	5	5	4.0	0.772 0.782 0.762 0.755 0.755 0.740 *0.780 0.780 0.758 0.744 0.728 0.748 0.700 -----	145 --- --- --- --- 123 --- --- 109 --- 109 --- 79 ---	5 24 46 72 96 120 123 144 216 240 264 288 312 384	*Taken after cell had been off for 72 hours. Cell discontinued due to blockage
E1284	Paste electrodes Titanium metallics 61-AZG membranes	30°C	16	15	4.0	0.733	129	4	Discontinued due to mal-function in control system.
E1288	Sintered Teflon electrodes Titanium metallics 61-AZG membranes	60°C	16	15	4.0	0.752	80	4	" " "
E1290	Paste electrodes Titanium Metallics 61-AZG membranes	30°C	16	15	4.0	0.766 0.780 0.760 0.598* 0.340	114 110 102 60 24	20 48 96 120 144	*Recorded after cell had been off test for 72 hours. Discontinued due to low voltage.
E1292	Sintered Kel-F electrodes	30°C	16	15	4.0	0.762 0.780 0.702 0.598* 0.638	4 24 48 72 144	121 160 125 52 65	*Taken after cell was off test 72 hours and restarted.

Table A1 (continued)

E1297	No electrodes Titanium metallics Buna-N rubber sheets in place of membranes.	60°C	16	14	none	---	---	---	This cell was run with normal gas and liquid pressures and flow rates to determine whether liquid leakage was through membrane or around it.
E1651	Sintered Teflon electrodes. Tantalum metallics 61-AZG membranes	60°C	6	5	4 4 4 4 4 4 4 4 6 6 0 0 41 36 4 4	0.782 0.782 0.808 0.735 0.828 0.825 0.830 0.818 0.815 0.775 0.778 1.04 1.05 0.21 0.19 0.81 0.81	121 --- --- 200 --- 167 --- --- 226 --- --- --- --- --- --- --- ---	504 552 600 672 744 840 888 1008 1032 1032 1080 1080 1104 1104 1126 1126 1152	Removed from Rig.
E1652	Sintered Teflon electrodes Titanium metallics 61-AZG membranes Externally fed PVC electrolyte compartment	60°C	1	1	4 2 4 4 4 4 4 4 4 4 4 4	0.648 0.382 0.288 0.578 0.538 0.692 0.632 0.768 0.738 0.607 0.728 0.738	--- --- --- --- --- --- --- --- --- --- --- ---	8 10 20 28 46 64 70 76 84 92 100 108	Companion to Cell E1297. Run only during day.
D9228	Sintered Teflon electrodes Tantalum metallics 61-AZG membranes	25°C	5	5	4	0.728 0.760 0.752 0.740	102 187 184 140	264 360 384 432	Removed from rig.

Table A1 (continued)

D9228	(continued)					0.758	135	456	
						0.740	133	480	
						0.758	147	504	
						0.760	178	528	
					4	-----	---	554	
					16	0.36	---	554	
					12	0.52	---	554	
					12	-----	---	603	
					4	0.742	---	603	
					4	0.750	---	627	
E1679	Sintered Teflon electrodes. O_2 electrode had 4 times normal Teflon Gold plated titanium metallics 61-AZG membranes	60°C	5	5	4.0	0.632	---	5	Discontinued due to poor performance.
						0.635	51	102	
E1685	Sintered Teflon electrodes Tantalum metallics 61-AZG membranes Teflon compartments Viton gaskets	60°C	5	5	4.0	0.782	---	16	To test new components for Battery 1. Removed from rig after one day.
					6.0	0.70	99	16	

Table A2

Summary of Electrode Studies in 4 Sq. In. Cells

($20^{o}C$; 1 atm; 61 AZG Membrane)

Cell No.	Electrodes	Voltage at 14.4 Amps/Ft^2	Specific Conductance Mhos/Ft^2
E0223	Platinum gauze sprayed with platinum black in solution of polyethylene in benzene.	0.70	95
D9708	Standard Sintered with 0.26 gm Teflon.	0.73	135
E0224	Sintered electrodes fabricated by Clevite Corporation.	0.74	116
E1305	Platinum gauze mixture of platinum black and solution of polyethylene in benzene sprayed on membrane.	0.66	105
E1308	Sintered electrodes using 0.28 gm Kel-F dispersion in place of Teflon dispersion. Without MgO.	0.72	145
E1312	Sintered electrodes as above with 0.4 gm MgO.	0.55	67
E1310	Platinum gauze sprayed with platinized carbon in solution of polyethylene in benzene.	0.420	55
E1302	Platinum gauze electrolytically coated with platinum.	0.38	---
E1313	Standard sintered electrodes but with 0.13 grams Teflon.	0.72	---
E1314	Standard sintered electrodes but with 0.52 grams Teflon.	0.68	100
E1315	Standard sintered electrodes but with 1.06 grams Teflon.	0.74	125
E1318	Standard sintered electrodes but without MgO.	0.69	115
E1320	Standard sintered electrodes but with 2.0 grams Teflon.	0.44	64
E1324	Sintered electrodes pressed at 10,000 psi made by Clevite Corp.	0.41	100

Table A2 (continued)

Cell No.	Electrodes	Voltage at 14.4 Amps/Ft^2	Specific Conductance Mhos/Ft^2
E1332	Sintered platinum black electrodes made by MOTT Metallurgical Corp.	0.41	95
E1317	Hydrogen Electrode as E1313 Oxygen Electrode as E1315	0.76	--
ADL-1	Standard sintered.	0.74	135
ADL-2	A thin layer of platinum black was sandwiched between membranes and platinum gauzes well coated with electrochemically deposited platinum black.	0.76	95
ADL-3	Platinized carbon electrodes.	0.34	--

Table A3

Effect of Time and Temperature

(4 Sq. In. Cells)

Cell Number	Time Hours	Temperature ^{o}C	Voltage at 14.4 Amps/Ft^2
D9204	0	20	0.78
	24	"	0.83
	408	"	0.72
	864	"	0.68
D9209	2	24.0	0.76
	5	35.0	0.797
	8	36.3	0.80
	26	39.5	0.805
	28	41.5	0.81
	30	44.0	0.818

NASA-Langley, 1964 E-2561